中國醫藥大學中醫學系博士論文

指　導　教　授：謝慶良 教　授

論文題目

牡丹皮及其主要純化物-丹皮酚對內毒素所致急性肺損傷大鼠之效用評估及探討

The evaluation of treatment effects and mechanisms of *Moutan Cortex* Radicis and Paeonol on LPS-induced acute lung injury in rats

研究生：傅彬貴

中華民國一百零一年十月

中國醫藥大學博士班研究生
論文指導教授推薦書

中醫學系博士班，傅　彬　貴君所提之論文牡丹皮及其主要純化物-丹皮酚對內毒素所致急性肺損傷大鼠之效用評估及探討，係由本人指導撰述，同意提付審查。

指導教授謝慶良（簽章）

中華民國 101 年 10 月 05 日

中國醫藥大學博士班研究生
論文口試委員審定書

中醫學系博士班，傅　彬　貴君所提之論文
牡丹皮及其主要純化物-丹皮酚對內毒素所致急性肺損傷大鼠之效用評估及探討
，經本委員會審議，認為符合博士資格標準。

論文口試委員會　　委員＿＿＿＿＿＿（簽章）

＿＿＿＿＿＿

＿＿＿＿＿＿

＿＿＿＿＿＿

＿＿＿＿＿＿

主任＿＿＿＿＿＿

中華民國 101 年 10 月 05 日

目錄

圖目錄

表目錄

縮寫對照表

1. **AECC: American-European Consensus Conference**
2. **ALI: Acute lung injury**
3. **ARDS: Acute respiratory distress syndrome**
4. **BAL: bronchoalveolar lavage**
5. **CARS: Compensatory Anti-inflammatory Response syndrome**
6. **DIC: Disseminated intravascular coagulation**
7. **ELISA: enzyme-linked immunosorbent assay**
8. **ERK: extracellular signal-regulated kinase**
9. **HPLC: High-performance liquid chromatography**
10. **ICAM-1: intercellular adhesion molecule-1**
11. **iNOS: inducible nitric oxide synthase**
12. **IFN-γ: interferon-γ**
13. **JNK: Jun N-terminal kinase**
14. **KC: Keratinocyte Chemoattractant**
15. **LPS: lipopolysaccharide**
16. **LWG: Lung Weight Gain**
17. **MAO: monoamine oxidase**
18. **MAPK: mitogen-activated protein kinas**
19. **MCP-1: chemoattractant protein-1**
20. **M-CSF: macrophage colony stimulating factor**
21. **MCR: Moutan Cortex Radicis**
22. **MIP: macrophage inflammatory protein**
23. **MMPs: matrix metalloproteinases**
24. **MODS: Multiple organ dysfunction syndrome**
25. **MPO: myeloperoxidase**
26. **MTT: 3-(4,5-Dimethylthiazol-2-yl)-2,5-diphenyltetrazolium bromide**
27. **NADPH: nicotinamide adenine dinucleotide phosphate**

28. **Na^+ -K^+-ATPase: Na^+-K^+ adenosine triphosphatase**
29. **NF-κB: nuclear factor-kappaB**
30. **OA: oleic acid**
31. **PAF: platelet activating factor**
32. **PAWP: pulmonary artery wedge pressure**
33. **PAI-1: Plasminogen activators inhibitors-1**
34. **PEEP: positive end-expiratory pressure**
35. **PMN: polymorphonuclear neutrophils**
36. **RANKL: receptor activator of nuclear factor kappa B ligand**
37. **ROS: reactive oxygen species**
38. **SDS-PAGE: sodium dodecyl sulfate-polyacrylamide gel electrophoresis**
39. **SIRS: systemic inflammatory response syndrome**
40. **SOD: superoxidase dismutase**
41. **TF: Tissue factor**
42. **TGF-β: transforming growth factor-β**
43. **TLR-4: toll-like receptor 4**
44. **TNF-α: tumor necrosis factor-α**
45. **VCAM-1: vascular cell adhesion molecule-1**
46. **VILI: Ventilator-induced lung injury**

牡丹皮及其主要純化物-丹皮酚對內毒素所致急性肺損傷大鼠之效用評估及探討

研 究 生 ：傅彬貴

指導教授 ：謝慶良教授

單　　位 ：中醫學系博士班

中文摘要

急性肺損傷(Acute lung injury; ALI)以及急性呼吸窘迫症(Acute respiratory distress syndrome; ARDS)是造成急重症患者的多器官衰竭甚至死亡的主要原因，至今仍未有特殊的治療藥物。本研究目的是探討具有活血化瘀功能的牡丹皮(*Moutan Cortex* Radicis; MCR)以及其主要的成分-丹皮酚(Paeonol)是否能改善由高劑量內毒素所誘發急性大鼠肺損傷模型，並探討其治療效果與發炎反應以及凝血功能紊亂之間的關聯性。

首先，我們模擬人類在肺炎所致急性肺損傷之病理生理反應，建立了實驗動物模型，並進行時序性的研究，包括肺泡液細胞計數、肺泡液細胞激素的分析及肺部病理組織切片之肺損傷程度的判定等，以作為選擇誘發肺損傷後第 16 小時為觀測時間點的依據；第二：進行活血化瘀藥—牡丹皮之療效評估，比較“誘發前”以及“誘發後”給藥的效果。我們發現在“誘發肺損傷前”給予口服牡丹皮，具有保護作用，其作用可能與抑制肺部發

炎反應細胞激素如 IL-6、IL-1β以及 MIP-2 的表現量有關。不論是誘發前或誘發後給藥，牡丹皮均有調節體溫、抑制 MPO 表現量的作用；第三：丹皮酚為牡丹皮的主要有效化學物質，具有良好的抗發炎作用。在 LPS 誘發急性肺損傷後，給予大鼠經腹腔注射丹皮酚，具有顯著抑制肺部發炎反應的效果，其機轉可能與抑制 TNF-α、IL-1β、IL-6 以及 MPO 和 iNOS 的表現量有關。丹皮酚注射也可以抑制大鼠肺泡液中 PAI-1 的表現量，以降低凝血功能紊亂。這個實驗顯示，丹皮酚具有顯著的抗發炎以及部份的抗凝血作用；第四個部分，使用不同濃度的丹皮酚與大鼠中性球作用，結果發現丹皮酚具有顯著抑制中性球移行的能力，同時促進中性球的吞噬能力。

本研究為選擇一目前現代醫學治療上有瓶頸之臨床疾病，經由實驗動物模型的建立，來進行篩選及驗證潛在具有治療效果之中草藥，並探討其可能的作用機轉。本研究結果，後續可深入探討：關於活血化瘀類中草藥是否均可透過抑制發炎和凝血功能紊亂來改善急性肺損傷，及可能涉及的治療靶點，以此做為中西醫臨床理論結合及應用的依據，及新藥開發、臨床試驗的起點。

關鍵詞：牡丹皮；丹皮酚；內毒素；急性肺損傷；抗發炎；抗凝血

第一章 前言

1-1. 選擇急性肺損傷/急性呼吸窘迫症(ALI/ARDS)為研究主題的原因

急性肺損傷(Acute lung injury, ALI)以及急性呼吸窘迫症(Acute respiratory distress syndrome, ARDS) 屬於嚴重的肺部發炎反應，往往是造成急重症患者的多器官衰竭甚至死亡的主要原因。根據統計，即便在美國等醫療先進國家，急性肺損傷的年發生率大約有 190,000 個病案/年，造成的死亡人數為 74,500 人/年[(1)]。ALI 的住院病患死亡率大約為 38.5%，ARDS 則是更為嚴重的肺部發炎反應，其死亡率可以高達 41.1%[(1)]。造成罹患 ALI/ARDS 病患死亡的主要原因，通常不只是源於單純的呼吸衰竭，而是與敗血症(sepsis)所產生的瀰漫性溶血(Disseminated intravascular coagulation; DIC)及多重器官衰竭(Multiple organ dysfunction syndrome; MODS)有關[(2-4)]。對於 ALI 的歸納及描述，最先是由 Ashbaugh 等(1967 年)根據 12 位病患的臨床表現、血氧狀況及 X 光片的變化而來[(5)]，但醫學界直到 1994 年才對這個疾病開始有了臨床定義及診斷標準[(6)]。經過近 20 年的發展與研究，學界對於 ALI/ARDS 的發生原因、病理變化日益瞭解，然而，在治療上，除了呼吸器的設定採取較小的潮氣容積進行保護性肺臟通氣策略(Lung-protective ventilator strategy)[(7-9)]、輸液及支持性的治療外[(10-12)]，其他有效藥物的進展，仍十分有限。因此，我們選擇這個疾病來作為研究主題，建立實驗動物平台，並探討中醫藥在

急性肺損傷的治療上是否具有療效及發展潛力。

1-2. 使用活血化瘀藥治療 ALI/ARDS 的理論基礎

造成 ALI/ARDS 的原因，可以是肺部的直接損傷，如肺炎、嗆入胃酸物質、溺水、肺挫傷等；或是間接產生的肺部傷害，如敗血症引起的全身性發炎反應、嚴重外傷引起的休克、急性胰臟炎等[3, 4, 13]。在病理生理學方面，ALI/ARDS 主要發生於肺泡上皮以及微血管內皮(alveolar-capillary membrane)，呈現如瀑布效應的發炎反應(inflammatory cascades)，依時序之進展如下：在細菌所釋放的內毒素攻擊肺泡後的數小時至數天內，肺泡內的巨噬細胞會分泌大量的發炎物質，驅使中性球(polymorphonuclear neutrophils; PMN)從周邊血液聚集至肺部[14-17]，造成肺間質水腫、肺泡上皮細胞屏障破壞以及大量蛋白質滲漏(protein leakage)至肺泡內、透明膜形成，最後產生嚴重的肺損傷[13, 18, 19]；在第 7-14 天後，會進入增生期，第二型肺泡上皮細胞增生，肺泡內的水分及蛋白質開始吸收[20, 21]；在第 14 天以後，會進展到纖維化期，肺泡內纖維組織開始增生，肺部纖維化形成[22-24]。除了肺部的發炎反應外，在 ALI/ARDS 中所產生的凝血功能障礙或者纖維溶解功能紊亂，也是研究人員逐漸重視的區塊，甚至認為改善肺部凝血功能障礙(pulmonary coagulopathy)是一個治療 ALI/ARDS 的新契機[2, 25-27]。因此，能夠同時抑

制肺部的發炎反應以及改善凝血功能紊亂的藥物，將具有發展潛力成為治療 ALI/ARDS 的新藥物。

1-3. 過去文獻在探討使用中草藥治療 ALI/ARDS 之實驗設計侷限

文獻報導，許多中草藥及方劑甚至中成藥，已在動物實驗中證實具有急性肺損傷的保護效用。例如：Xu 等(2005 年)的研究顯示，活血化瘀藥槐花(Oxymatrine)可以抑制 p38 絲裂原活化蛋白基腖(mitogen-activated protein kinas; MAPK)的磷酸化，從而降低小鼠急性肺損傷(ALI)[28]；Tajima 等(2006 年)發現，將小鼠餵食補中益氣湯(Hochu-ekki-to) 1g/Kg/day 連續八周，可以對內毒素(lipopolysaccharide; LPS)所致急性肺損傷(ALI)產生保護效用[29]；Yeh 等(2006 年)發現使用瀉白散(Xia-Bai-San) 1 mg/kg 術前餵食小鼠，具有降低肺部發炎反應，對急性肺損傷具有保護作用[30]；Yeh 等(2007 年)發現給予小鼠口服餵食銀翹散(Gingyo-san)，可以降低肺泡中性球數目及肺部發炎反應，進而達到急性肺損傷之保護作用[31]。從中藥萃取出來具有抗氧化效用的純化物，也被用來進行評估是否對 ALI/ARDS 具有保護效果。例如：Yeh 等(2007 年)使用自陳皮萃取出的橙皮苷(hesperidin) 200 mg/kg，在術前餵食小鼠，結果發現，橙皮苷(hesperidin)對急性肺損傷具有保護作用，可以降低肺部發炎反應[32]；Luo 等(2011 年)使用自五味子萃取出的活性化學物質-雙環醇(bicyclol)，

在誘發 ALI 之前給予小鼠餵食，結果也發現具有抗氧化及肺部保護作用[33]。近年來，中成藥製劑—血必淨(Xuebijing)，由於含有赤芍藥、紅花、川芎以及丹蔘和當歸等成分，所以具有活血化瘀、抗發炎及抗氧化的作用。Sun 等(2010 年)研究顯示，使用血必淨(Xuebijing)注射至實驗用兔，對 LPS 注射所引發之 ALI 具有保護作用[34]。這些利用中醫藥單方或方劑來進行 ALI 效用之相關研究，雖然為這個具有高度死亡率的疾病開啟治療的新契機，但分析這些文獻的實驗設計、給藥模式，卻發現當中存在許多與臨床狀況差距甚大的情況。首先，所有的文獻都採取“術前給藥”，所以得到的結果是“具有保護效果”。然而，ALI/ARDS 既不能事先知道而給予預防性投藥，也不像糖尿病及高血壓等慢性病需要長期服藥，所以這些實驗結果顯示的“保護效用”事實上在臨床診治病患是不可行的。其次，許多實驗設計採取的 ALI 為靜脈注射 LPS，這樣的 ALI 在分類上屬於間接性損傷(indirect injury)，與臨床病患大多是肺炎所致直接性(direct injury)ALI 大相徑庭，所以實驗結果亦無法反應臨床狀況。再者，大多使用純化物的文獻報告，均未探討原中藥藥物粗萃取物是否仍具有療效。基於上述理由，我們將實驗主軸設定在探討“LPS 直接誘發所致 ALI”，希望建立一個由高劑量 LPS 所誘發直接 ALI 大鼠模型，並使用活血化瘀藥-牡丹皮(*Moutan Cortex* Radicis, MCR)以及其主要的成分-丹皮酚(Paeonol)來驗證其是否具有治療效果，並探討其治療效果

與發炎反應以及凝血功能紊亂之間的關聯性。

1-4. 使用 LPS 經氣道直接誘發大鼠 ALI 動物模型的原因

目前已被廣為使用的 ALI 動物模式有 oleic acid injection[35, 36]、LPS injection[37-39]、Acid aspiration[40, 41]、hyperoxia[42]、bleomycin injection[43, 44]、saline lavage[45, 46]以及 cecal ligation[47, 48] 等。其中，較常被廣為使用，且可用於大型動物的有以下三類，分別是：肺表面張力素缺損 (LAV) 疾病動物模式；肺部注射 Oleic acid (OA) 疾病動物模式；以及肺部注射 LPS 疾病動物模式[39, 49-51]。LAV 的主要病理生理變化為肺微血管網及支氣管周邊水腫、淋巴管水腫合併第一型肺泡上皮細胞的死亡等，但這個模型的中性球浸潤並不明顯，且肺泡上皮及血管內皮細胞損傷的程度也不嚴重。因此，LAV 不能用來類比人類因肺炎所致的 ALI/ARDS，其病理表現與肺表面張力素缺失所引起的肺損傷較為相似；OA 注射模型的特色是可以看見典型 ALI/ARDS 的各個階段病理變化如急性期、增生期以及纖維期。然而，其病理生理原因與不飽和脂肪酸有關，與人類因肺炎所致肺泡內上皮細胞受損進而產生 ALI/ARDS 之臨床情況不盡相同。在這些模型當中，經氣管內注射 LPS 以誘發急性肺損的動物模型比較接近人類肺炎所致的 ALI/ARDS。且在誘發後的 24 小時內屬於急性期，是以中性球為主的發炎反應，會產生大量類似人類敗血性休克的發炎細胞

激素、氧化自由基以及細胞黏附因子。因此，我們決定採取高濃度的LPS(16 mg/kg)，直接將源自大腸桿菌的 LPS 以氣霧方式投到大鼠肺部來誘發 ALI/ARDS。然後進行投藥後時間序分析(time course analysis)，包括肺部病理解剖變化、肺泡液中細胞含量、肺泡液中蛋白濃度、肺組織骨髓過氧化脢(Myeloperoxidas; MPO)、肛溫變化等，以做為判定藥物療效最佳時間點之依據。

1-5. 使用活血化瘀藥-牡丹皮及其主要成分-丹皮酚之原因

牡丹皮(MCR)在過去中醫藥文獻當中記載，具有活血化瘀及清熱涼血的作用[52-60]。MCR 的現代藥理學研究顯示，其具有解熱陣痛、抗發炎以及抑制血液凝集的作用[61, 62]。Yoshikawa 等(2000 年)發現 MCR 具有清除自由基(free radicals)以及清除超氧陰離子(superoxide anion radicals)的作用[63]。近年來的研究也證實，MCR 可以有效的抑制氧化傷害進而對 DNA 具有保護作用[64, 65]。在細胞免疫調控方面，Kim 等(2007 年)的研究顯示，MCR 不僅對於嗜伊紅性血球的移行(eosinophil migration)具有抑制效果，也能抑制細胞趨化激素(chemokine)如：細胞間質激素(interleukin, IL)-8 以及中性球趨化蛋白(monocyte chemotactic protein, MCP)-1 的分泌[66]。Kim 等(2012 年)用 MCR 來治療關節炎的動物模型-type II collagen-induced arthritis (CIA)，結果發現 MCR 可以透過抑制 nuclear factor kappa B (NF-κB)以及 activator protein(AP)-1 的表現量，進而抑制

發炎反應細胞激素的釋放以及蝕骨細胞(osteoclast)的活化，達到抑制關節炎的效果[67]。基於傳統文獻以及現代藥理學的研究，MCR 的清熱涼血作用，可能對於 ALI 的肺部發炎反應具有治療效果；MCR 的活血化瘀作用，對於 ALI 病理機轉中日益受到重視的凝血功能紊亂及微小血栓形成等病理反應，可能具有治療潛力。綜上，我們認為 MCR 在改善以發炎反應以及凝血紊亂為主要病機的LPS誘發之大鼠ALI具有進一步研究的價值。由於 MCR 是固有藥材，本實驗採取口服餵食的方式，比較在 LPS 誘發 ALI 前及誘發 ALI 後給予口服餵食藥物，以評估 MCR 是否具有治療或者保護效果。

牡丹皮在化學上具有許多萃取物，主要有丹皮酚(paeonol)、芍藥苷(paeoniflorin)、丹皮酚苷(paeonoside)以及丹皮酚原苷(paeonolide)等多種化學成分[68-70]，其中，丹皮酚(paeonol)是MCR的主要成分。過去對於丹皮酚(paeonol)的文獻研究十分豐富，Hirai等(1983年)對丹皮酚進行凝血功能相關的研究，發現給與動物口服MCR每天3g，可以抑制血小板凝集以及thromboxane B2 (TXB2) 的形成[71]。細胞實驗也發現丹皮酚對Adenosine diphosphate (ADP) 以及collagen induced platelet aggregation具有抑制作用且呈現劑量效應[71, 72]。近年來關於丹皮酚的研究也有進展，由其是關於抗氧化及抗發炎反應相關的研究，如：Nizamutdinova等(2007年)研究顯示丹皮酚可以透過抑制p38、extracellular-signal-regulated

kinases (ERK) 以及NF-κB等分子訊號傳遞路徑，進而抑制細胞表面黏附因子(cell-surface adhesion molecules)的表現[73]；抑制發炎反應相關細胞激素如腫瘤壞死因子(tumor necrosis factor, TNF)-α[74]、Interleukin (IL)-1β的表現量[75]；透過抑制絲裂原活化蛋白基酶(mitogen-activated protein kinas, MAPK)的磷酸化進而抑制inducible NO synthase (iNOS)的表現量[76]，以降低發炎反應後氧化自由基的形成以及氧化傷害的程度[74-76]。綜上，我們認為丹皮酚對於LPS-induced ALI的發炎反應以及凝血紊亂，具有保護效用。本研究將以腹腔注射藥物的模式，採取以LPS誘發大鼠ALI後給藥，來模擬全身性給藥是否具有治療效果。

1-6. 體外實驗探討中性球角色的原因

在LPS-induced ALI，中性球(Neutrophil)由周邊血液被趨化至肺部扮演病理生理學上的主要角色[14, 15, 77, 78]。過去的研究顯示，給予LPS後會造成中性球的變形使其能夠穿過肺部微血循環、改變微血管及肺部上皮細胞的通透性，進而造成大量滲液及蛋白質滲漏至肺泡中[15, 79, 80]。這些來自周邊血液且被活化的中性球會趨使蛋白酶(protease)的活化、產生大量的氧化自由基，最後造成ALI[78, 80-83]。因此，我們對丹皮酚是否對中性球具有功能性調節作用如細胞凋亡作用(apoptosis)、吞噬能力(phagocytosis)以及移行能力(migration)進行體外研究。

本研究的目的為利用LPS-induced ALI動物模型，探討活血化瘀藥物-MCR對ALI是否具有治療或保護效用，進而探討其作用機轉；其次，探討注射丹皮酚對急性肺損傷是否具有治療效用。最後，我們將探討丹皮酚對中性球功能性的調控作用，期能更深入了解使用MCR或丹皮酚是否對急性肺損傷具有治療潛力。

第二章 文獻探討

2-1. 急性肺損傷/急性呼吸窘迫症(ALI/ARDS)在中醫藥之相關文獻

2-1-1. ALI/ARDS 之中醫病名

中醫典籍當中，無「急性肺損傷」和「急性呼吸窘迫症」相關之病名記載，但以辨證論治為主軸的中醫理論體系，卻可以找到類似「急性肺損傷/急性呼吸窘迫症」相關的症狀描述。依照定義，ALI/ARDS 是急性病症，病患最常見的症狀是喘促，伴隨有高熱、意識障礙等合併證，並且會快速進展至呼吸衰竭甚至休克，並表現出唇甲發黑、神昏譫語等。因此在對應到中醫相關病名時，許多學者將 ALI/ARDS 歸類於「暴喘」、「結胸」、「喘脫」等病症範圍[84-86]。李明富等(1980 年)提出，關於 ALI/ARDS 之中醫病名，應定義為「暴喘症」，主要的理由，係因因本證之診斷要排除原本心肺疾患所致之急性喘促，其誘發原因是創傷、溫病、癮疹等明確誘因所致，臨床表現是以呼吸頻數為主要表現的喘證[87, 88]。

2-1-2. ALI/ARDS 之病因病機及臟腑定位

關於 ALI/ARDS 在中醫病因病機及臟腑辨證定位等相關研究文獻，整理如下：

(1) ALI/ARDS 的臨床表現與「陽明腑實喘滿證」相似：中國大陸學者研

究指出：ALI/ARDS 的臨床表現與傷寒論所載之「陽明腑實喘滿證」相似。在中醫的臟象生理上，肺與大腸相表裡。ALI/ARDS 係屬急性病因所導致的上「喘」下「滿」證，最後交互影響，形成惡性循環的喘滿症，最後導致正氣脫竭而亡[89]。這樣的觀點，與敗血症病患在腸道衰竭後所產生的腸菌群移位所致之格蘭氏陰性菌的菌血症有關。耿耘等(2002 年)研究指出：「ARDS 的關鍵病機是熱、瘀、水(濕)、虛四個方面」。熱、瘀及濕屬於邪氣實，與 Systemic inflammatory response syndrome (SIRS)有關；正氣虛則與 Compensatory Anti-inflammatory Response syndrome (CARS)基本一致，最後正氣耗竭、邪實內閉、氣陰兩脫以致死亡[90]。

(2) 「虛實夾雜、本虛標實」是 ARDS/ALI 主要特色：李明富等(1980 年)認為 ARDS 是「本虛標實」及「虛實夾雜」的危急重症。主要涉及的虛證有「肺腎虧虛」以及「血虛」；實證的表現為「瘀血」、「水濕」或「熱毒」等壅滯肺氣，致使腎不納氣，發為暴喘[87, 88]。

(3) 「肺腸同病」是 ALI/ARDS 臟腑辨證定位：孟苗苗等(2011 年)針對在天津市各醫院所收治符合 ALI/ARDS 的病患共 86 人進行中醫臟腑證候判定調查。結果發現，ALI/ARDS 發病後證候表現涉及肺、心、腎及大腸等臟腑，具有多臟腑受累的臨床特點。涉及的臟腑以肺、心及大腸系證候頻次最多。再進一步分析肺腸證候之相關性，發現「痰熱壅肺」與「腸燥津虧」呈顯著正相關，驗證了「肺與大腸相表裡」的理論內容

[91]。謝玉寶等(2008 年)認為 ALI/ARDS：「外邪犯肺化熱傳入陽明，與腸中積滯相結而致熱結腸躁、氣機壅滯，上逆則喘、中阻則滿。熱迫血瘀、瘀熱互結，壅滯於肺，致肺通調水道功能失司，水液內停」[92]。

(4) ALI/ARDS 屬於溫病死證之「肺之化源速竭」：唐洪波等(2006 年)依照 ALI/ARDS 之產生原因多為感染症或者創傷所致、疾病進展速度十分迅速、主要症狀為喘促高熱等特性，將 ALI/ARDS 歸類於溫病之上焦及中焦病證，可以導致肺之化源速竭，屬於危急重症[93]。《溫病條辨・上・十一》:「太陰溫病，血從上溢，犀角地黃湯合銀翹散主之。其中焦病者，以中焦法治之」。根據原文，血從上溢，咳吐粉紅血水，是肺之化源速竭的第一死證，而上焦之太陰溫病或中焦之陽明溫病均可引起。肺之化源速竭的臨床表現，除了「咳吐粉紅血水」外，尚有《溫病條辨・上・八・自注》:「汗涌，鼻扇，脈散，皆化源欲竭之徵兆」也、以及《溫病條辨・上・二十六》:「汗多脈散大，喘喝欲脫」等。這些「鼻扇」、「喘喝欲脫」等症，就是 ARDS 呼吸衰竭的表現；「汗涌脈散」、「汗多脈散大」等症，就是敗血性休克的表現。因此，唐洪波等(2006 年)提出，「溫病中的毒損肺絡與 ARDS 的肺泡上皮細胞及肺微血管發炎性傷害，如出一轍」[93]。

綜上，我們將 ALI/ARDS 歸類於溫病學中的上焦太陰及中焦陽明溫病；在病因病機方面，為「虛實夾雜、本虛標實」，以「熱、瘀、濕、

虛」來概括其病因病機；在臟腑定位上，以太陰肺及陽明大腸為主要受犯之臟腑，表現為「痰熱壅肺」與「腸燥津虧」，甚至快速進展至「肺之化源速竭」的危急症候。

2-1-3. 對 ALI/ARDS 具有療效之中草藥及純化物研究

在中醫藥的範疇中，許多藥物及方劑，甚至中成藥，已在實驗動物模式當中證實具有保護大鼠 ALI 的效用，並發表在國際期刊。

(1) 槐花(Oxymatrine)：在以 oleic acid 誘發的 ALI 動物模型中，給予預防性腹腔注射槐花，可以減少大鼠肺泡內水腫及蛋白質滲出程度、降低肺損傷程度及肺水腫指數[28]。另外，以 LPS 誘發的 ALI 動物模型中，槐花亦有降低肺損傷的保護作用[94]。其機轉可能與槐花具有抑制 p38 MAPK 的磷酸化[28]、抑制 NF-kB 分子訊號傳遞[95]、減少 iNOS 合成[96]、增加 superoxidase dismutase(SOD)活性[94]、抑制 myeloperoxidase(MPO)活性[94]，進而降低中性球所致的發炎反應及氧化傷害有關。

(2) 蒲公英(Taraxacum officinale)：Liu 等(2010 年)給口服餵食蒲公英，然後再以 LPS 誘發大鼠 ALI，結果發現，蒲公英對 LPS-induced ALI 具有保護作用，且呈劑量關係。其機轉可能與抑制肺泡內細胞激素如 IL-6、TNF-α有關，進而降低肺水腫及肺損傷程度[97]。

(3) 北柴胡(Bupleurum chinense DC)：Xie 等(2012 年)在 LPS 誘發 ALI 後

兩小時給予餵食北柴胡，結果發現，北柴胡可以透過抑制肺泡液內的NO、MPO 以及 TNF-α的表現量，進而對肺部產生保護作用[98]。

(4) 小葉黑柴胡(Bupleurum smithii var. parvifolium)：Cheng 等(2012 年)以小葉黑柴胡在 LPS-induced ALI 後 30 分鐘給藥，結果發現，小葉黑柴胡可以透過液至肺部發炎反應以及抑制補體系統過度活化、減少補體 C3c 沉積於肺部，進而達到肺部的保護作用[99]。

(5) 藏紅花酸(Crocetin)：Crocetin 是從番紅花萃取出的有效成分，過去的研究顯示其除了具有抗氧化及抗發炎的作用外[100]，還能夠改善微循環[101]，使氧和狀態獲得改善[102]。Yang 等(2012 年)對 LPS-induced ALI 動物模型給予術前餵食紅花酸，結果發現，紅花酸除了可以抑制 SOD 以及肺部 MPO 活性，還有抑制肺組織 IL-6、macrophage chemoattractant protein-1 (MCP-1)以及 TNF-α的表現量已達到降低肺損傷的作用[103]。

(6) 厚朴酚(Magnolol)：Yunhe 等(2012 年)在 LPS 誘發 ALI 前 1 小時給予動物厚朴酚，結果發現，給予 Magnolnol 可以降低動物肺泡內細胞激素如 IL-6、TNF-α以及 IL-1β的表現量。其可能的機轉與抑制 Toll-like receptor-4 (TLR-4)所調控的 NF-κB 訊號路徑傳遞有關[104]。

(7) 橙皮苷(Hesperidin)：橙皮苷是從陳皮(Pericarpium Citri Reticulatae)所萃取出來的純化物。Yeh 等(2007 年)在誘發急性肺損傷前，使用橙皮苷 200 mg/kg 餵食小鼠，結果發現，橙皮苷(hesperidin)對急性肺損傷具有保

護作用，可以抑制肺泡液內的細胞激素如 TNF-α, IL-1β, IL-6, Keratinocyte Chemoattractant (KC), macrophage-inflammatory protein-2 (MIP-2), MCP-1, 以及 IL-12。此外，Hesperidin 可以透過抑制 NF-κB 的訊號傳遞以降低肺部的氧化傷害[32]。

2-1-4. 對 ALI/ARDS 具有療效之方劑研究

(1) 補中益氣湯(Hochu-ekki-to)：Tajima 等(2006 年)發現，將小鼠餵食補中益氣湯(Hochu-ekki-to)，劑量為 1 g/Kg/day 連續八周，可以對 LPS 所致 ALI 產生保護效用。餵食補中氣湯組之老鼠肺泡液內的中性球、吞噬細胞和蛋白滲出液均明顯下降，可能與透過抑制血中的細胞趨化激素-KC 有關[29]。

(2) 瀉白散(Xia-Bai-San)：瀉白散出自《小兒藥證直訣》:「治肺火皮膚蒸熱，灑淅寒熱，日晡尤甚，喘嗽氣急」，適用於肺有伏火鬱熱之喘咳證。Yeh 等(2006 年)發現使用瀉白散 1 mg/kg 術前餵食小鼠，對急性肺損傷具有保護作用。其機轉也與瀉白散可以抑制 TNF-α, IL-1β, IL-6, KC, MIP-2 以及 MCP-1 的表現量，另外也能增加抗氧化細胞激素 IL-10 的表現，以降低內毒素誘發後的氧化傷害[30]。另外，瀉白散對於 NF-κB 以及 intercellular adhesion molecule-1 (ICAM-1)也具有調控作用[105, 106]。

(3) 銀翹散(Gingyo-san)：銀翹散出自《溫病條辨・上焦篇・四》:「太陰風溫、溫熱、溫疫、冬溫，初起惡風寒者，桂枝湯主之；但熱不惡寒而

渴者，辛涼平劑銀翹散主之」;《溫病條辨・上焦篇・八》:「太陰溫病，惡風寒，服桂枝湯已，惡寒解，余病不解者，銀翹散主之。」具有辛涼解表、清熱解毒的作用。Yeh 等(2007 年)發現給予小鼠口服餵食銀翹散(Gingyo-san)，可以降低肺泡以及肺組織內細胞激素的表現量如 TNF-α、IL-1β、IL-6、KC、MCP-1、MIP-2 以及 iNOS，另外，也與抑制 NF-κB 和 AP-1 有關，進而達到 ALI 之保護作用[31]。

(4) 血必淨(Xuebijing)：係由中藥材如红花、赤芍藥、丹参、當歸及川芎等提取出，红花黃色素 A 為主要成分。藥物設計的概念是取其活血化瘀、疏通經络、潰散毒邪的作用。臨床實驗發現血必淨可以拮抗 LPS 並抑制內源性炎性介質如 TNF-α、IL-1 以及 IL-8 的大量釋放，進而抑制氧化傷害的產生並降低發炎反應[107, 108]。近年來，關於使用血必淨注射劑可以改善敗血症的研究日益豐富[108-110]。Sun 等(2010 年)發表關於使用血必淨注射至實驗用兔，可以經由抑制 IL-23 的表現量，對 LPS 注射引起之 ALI 具有保護作用[34]。Ma 等(2010 年)發現，血必淨注射液亦可以透過抑制肺部 TNF-α, IL-6, IL-8 的表現量而降低 ALI[111]。這個藥物甚至已經進入人體試驗的階段，Qi 等(2011 年) 用血必淨注射液來輔助嚴重肺炎病患的治療，發現使用血必淨組(40 個病患)的病患與對照組(40 個病患)相比，發熱程度以及發炎反應程度明顯改善，且治療組病患血中細胞激素如 TNF-α, IL-6, IL-8 等明顯降低[112]。歐等(2012 年) 使用血必淨注

射液輔助現代醫學治療 ALI 病患，發現合併血必淨治療組之病患血清中發炎反應細胞激素濃度如 TNF-α, IL-6, IL-10 等明顯降低，而且 hs-CRP 也明顯較未合併使用血必淨組低。病人在接受治療期後的 APACHE-II 分數顯著降低，且氧合指數明顯改善[113]。

2-2. ALI/ARDS 在現代醫學之相關文獻

急性肺損傷(acute lung injury, ALI)/急性呼吸窘迫症(acute respiratory distress syndrome, ARDS) 是加護病房內常見的急重症，臨床表現以急性缺氧性呼吸衰竭、胸部 X 光片呈現雙側性浸潤，且引起此病理生理變化的原因已排除心因性肺水腫。這個疾病肇始於嚴重的發炎反應，是造成急重症患者多器官衰竭甚至死亡的主要原因[4, 6]。即便在醫療先進國家，ALI 的年發生率大約有 190,000 個病案/年，造成的死亡人數為 74,500 人/年[1]。ALI 的住院病患死亡率大約為 38.5%，ARDS 則是更為嚴重的肺部發炎反應，其死亡率可以高達 41.1%[1]。造成罹患 ALI/ARDS 病患死亡的主要原因，通常不只是源於單純的呼吸衰竭，而是與敗血症(sepsis)所產生的瀰漫性溶血(Disseminated intravascular coagulation, DIC)與多重器官衰竭(Multiple organ dysfunction syndrome, MODS)有關[2-4]。這個疾病的歸納及描述，最先是由 Ashbaugh 等(1967 年)，根據 12 位病患的臨床表現、血氧狀況及 X 光片的變化而得到[5]，但直到 1994 年醫學界才對

這個疾病開始有了臨床定義及診斷標準[6]。經過近 20 年的發展與研究，對於這個疾病的發生原因、病理變化雖日益瞭解，然而，治療上的進展上卻十分有限。目前治療上，除了呼吸器的設定採取較小的潮氣容積進行保護性肺臟通氣策略(Lung-protective ventilator strategy) [7-9]、輸液及支持性的治療外[10-12]，並無明顯有療效的治療藥物。

2-2-1. ALI/ARDS 之診斷

ALI/ARDS 的歸納及描述，最先是由 Ashbaugh 等(1967 年)，根據 12 位病患的臨床表現、血氧狀況及 X 光片的變化而得到[5]。Murray 等(1988 年) 開始對這個疾病的嚴重度給予量化性描述，稱之為 Lung injury score (LIS)，係根據以下四個指標：X 光片是否呈現 consolidation、是否達到 hypoxemia、Respiratory compliance 以及使用吐氣末期陽壓 (positive end-expiratory pressure, PEEP)[114]。但直到 1994 年，由歐美聯席會議 (American-European Consensus Conference, AECC)[6]討論後才將 ALI/ARDS 定義如下：1)必須是急性發病；2)胸部 X 光片顯示為雙側肺浸潤；3)肺動脈契狀壓(pulmonary artery wedge pressure, PAWP)必須在 18mmHg 以下，或無左心房壓升高的臨床證據；4)動脈氧合障礙。PaO2/FiO2≦300mmHg 即為 ALI，PaO2/FiO2≦200mmHg 則為 ARDS[6]。由於 ALI/ARDS 自 1994 年採取上述定義以來，疾病嚴重程度無法由該定義給予量化，且定義當中的參數值並無法提供對死亡率風險的預測，

因此，歐洲急重症醫學會在 2011 年於德國柏林組成了一個專家小組來擬定 ARDS 的新定義，該定義於 2012 年 5 月發表於 JAMA 期刊上，成為 ARDS 最新的診斷標準與定義[115]。根據 Berlin definition，取消了原先 ALI 的定義，而將 ARDS 依照氧合缺失狀況分成 1)輕度 (PaO2/FiO2=201~300mmHg, PEEP≦5cmH2O)、2)中度 (PaO2/FiO2=101~200mmHg, PEEP≧5cmH2O)以及 3)重度(PaO2/FiO2≦100Hg, PEEP≧10cmH2O)三種級別。其死亡率依照輕、中、重的程度依次為 27%、32%以及 45%。疾病程度越重，呼吸器使用天數也隨之越長。由於新的定義對死亡率的預測效度遠高於 1994 年的舊定義，因此 Berlin definition 將成為醫學界診斷病患的新依據[115, 116]。

2-2-2. ALI/ARDS 之流行病學

過去關於 ALI/ARDS 的確切發生率的統計資料，一直存在著極大的差異性[4]，主要是因為 1) ALI/ARDS 直到 1994 年以後才開始有操作型定義、2) ALI/ARDS 是一個症候群，所以病患之間的疾病嚴重度具有極高的不均質性。在 1994 年以前，學界認為的年發生率大約在 1.5~8.3 人/10 萬人[117-119]。自從 1994 年 AECC 的診斷標準出爐後，根據操作型定義，ALI 的年發生率為 17.9 人/10 萬人、ARDS 年發生率為 13.5 人/10 萬人，遠高於過去的資料，顯示了 ALI/ARDS 的年發生率是被嚴重低估的[120]。

根據 Frutos-Vivar 等(2006 年)的研究，ALI 的年發生率應為 15.3~34 人/10 萬人、ARDS 的年發生率應為 13.5~28 人/10 萬人，死亡率約為 30-75%[121]。但根據 Rubenfeld 等(2005 年)研究，即便在美國這樣醫療先進國家，ALI 的年發生率大約有 78.9 人/10 萬人、ARDS 的年發生率大約為 58.7 人/10 萬人，這樣的估計全美每年約有 190,000 個新病案，造成的死亡人數為 74,500 人/年[1]。

ARDS 在重症加護病房內是一個不可被忽視的議題：根據在歐洲進行的大型前瞻性研究，住進加護病房的患者罹患 ARDS 的比率約為 7.1%；使用呼吸器的患者進展至 ARDS 的比率約為 16.1%[122]。

ARDS 是一個高死亡率的疾病：根據過去的文獻，ARDS 的住院死亡率約在 34~55%之間[122, 123]，若再細分，ALI 的死亡率約在 32~50%，ARDS 的死亡率約在 34~58%之間[124]。依照 2012 年 ARDS 最新的診斷分類，其死亡率依照輕、中、重的程度依次為 27%、32%以及 45%[115]。在 2012 年新的 ARDS 分類出爐後，對這個高致死率疾病的分類更為嚴謹，也較能預測疾病嚴重度與死亡率的關係。

雖然，台灣並無本土的 ALI/ARDS 流行病學資料，但這個高死亡率的疾病對於我們國人的健康而言，仍然不可輕視，所以有研究的價值。

2-2-3. ALI/ARDS 之致病原因及危險因子

導致成年人罹患 ARDS 的最主要原因是敗血症[4, 81, 82]，據統計，50% 的 ARDS 病患源於肺部的敗血症，而肺部以外的感染所致敗血症亦佔了 26%[125]，顯示了「肺炎所致敗血症」是 ARDS 最重要的致病因素及危險因子[3, 13, 126]。事實上，ARDS 的危險因子可以分成「直接性肺損傷」(direct lung injury)如：細菌性肺炎、吸入性肺炎、肺挫傷、溺水等；以及「間接性肺損傷」(indirect lung injury)如：肺外敗血症、燒燙傷、急性胰臟炎、輸血所致急性肺損傷等[3, 4, 6, 13, 81, 127]。

2-2-4. ALI/ARDS 的發病機制

ALI/ARDS 主要的病灶是肺泡上皮以及微血管內皮(alveolar-capillary membrane)。在肺泡受到直接或間接的刺激後，會導致發炎反應細胞激素大量的製造，趨使周邊血液的中性球移行並聚集至肺部微血管網內，而中性球在 recuritment 的過程中，又會不斷的釋出發炎反應物質，呈現出如瀑布效應的發炎反應 (inflammatory cascades)[3, 4, 19, 81]。整個 ARDS 的病理分期可以依時序之進展分為幾個階段：1)滲出期 (Exudative phase)：在細菌所釋放的內毒素攻擊肺泡後的數小時至前 7 天內，主要的表現是廣泛的肺泡以及肺間質水腫和出血、肺泡上皮細胞屏障破壞、造成大量蛋白質滲漏 (protein leakage)至肺泡內[3, 4, 128]。肺泡上

皮細胞是最主要的損傷部位，大量的第一型肺泡細胞 (type 1 alveolar epithelial cells)因受損而剝落，使得肺微血管內大量的蛋白質及水分滲入肺泡內，進而在肺泡壁上形成富含蛋白質的透明膜 (hyaline membrane)。肺泡內的巨噬細胞受到刺激後，會釋放出大量的發炎細胞激素如 IL-1、IL-8 以及 TNF-α，趨使來自周邊的中性球 (polymorphonuclear neutrophils; PMN) 黏附至肺血管壁，然後移行 (migration)穿過肺間質 (interstitium)進入肺泡內[17, 19, 129, 130]；2)增生期 (Proliferative phase)[3, 128]：在第 7-14 天後，會進入增生期，主要的病理生理變化就是受損的肺泡上皮細胞開始進行修復，特別是第二型的肺泡上皮細胞 (type II alveolar cells)延著基底膜增生，並開始分泌出表面張力素 (surfactant) 、肺泡內的水分開始被吸收、肺泡內由富含中性球 (Neutrophil)的滲出液轉而變成以淋巴球(lymphocyte)為主；3)纖維化期 (Fibrotic phase)[22-24, 131]：有些病患的急性肺損傷在增生期後肺泡內的水分會快速的吸收而沒留下後遺症，但另一部分的病患會進展至肺纖維化，主要的表現為肺泡內的間葉細胞(Mesenchymal cells)沿著新生的血管增生、纖維母細胞 (fibroblast)以及肌纖維母細胞 (myofibroblast)增生[132]、使得肺泡內大量沉積 type I 以及 type III 膠原 (collage)，通常代表不好的預後[133, 134]。

2-2-5. ALI/ARDS 與中性球所致發炎反應的關係

在 ALI/ARDS 的急性期，影響肺泡上皮細胞以及肺微血管內皮細胞損傷程度的主角，就是中性球 (Neutrophil)[14, 16]。根據人體試驗以及動物試驗顯示，當肺泡灌流液 (bronchoalveolar lavage, BAL)內的中性球濃度增加，也代表著 ARDS 的進一步惡化以及病患的死亡率上升，因此，中性球的活化程度以及移行至肺泡內的濃度，是 ALI/ARDS 惡化的指標[135-140]。中性球從周邊血液進入肺微血管網，然後移行至肺泡內的過程稱為「中性球召集」(Neutrophil recruitment)[14, 15, 77]。過度的中性球召集，會釋放出許多發炎反應細胞激素如 TNF-α、IL-1β、IL-6 等、蛋白質酵素活化如 MPO 以及 lysozyme、帶正電的多肽類 (cationic polypeptides)以及氧化自由基 (reactive oxygen species, ROS)，導致肺組織傷害以及過度激活發炎性免疫反應[82, 83, 141-145]。因此，如何能透過抑制中性球及其相關的發炎反應，就成為治療的目標[15, 78, 80]。

2-2-6. ALI/ARDS 與凝血功能紊亂的關係

近年來研究發現，ALI/ARDS 的發生與肺內凝血功能紊亂和纖維蛋白溶解作用異常有密切關係。主要的病理機轉為「組織因子活化」(Tissue factor activation)、「蛋白 C 活性下降」(protein C inactivation)以及「Plasminogen activators inhibitors-1 (PAI-1)產生增多」[146-148]。這些病理

變化，會消耗掉肺泡內的抗凝血作用，使得原本應該維持的「抗凝血」及「促進纖維蛋白溶解作用」失去平衡，而轉變成「促凝血」和「抗纖維蛋白溶解作用」[2, 25, 149-151]，最後造成肺微血管內出現血小板與纖維素組合而成的微小血栓、血管外纖維素沉積，形成瀰漫性血管內凝血(Disseminated intravascular coagulation; DIC)[25, 146, 152, 153]。在臨床研究方面，罹患 ARDS 的病患可以在肺泡液內發現高濃度的凝血相關因子的表現，如組織因子、factor VIIa (FVIIa)、TF-dependent factor X (FX)等，這些病患也有較高的死亡率[154-158]。在一個大型的多中心臨床研究顯示，罹患 ALI/ARDS 的病患如果有較高的 PAI-1 表現量，代表有較差的預後[159]。

綜上可知，調控「凝血功能紊亂與纖維蛋白溶解作用的平衡」，是未來治療 ALI/ARDS 的重要治療靶點，因此，中醫藥的活血化瘀相關理論及藥物方劑的運用是值得探討的方向。

2-2-7. ALI/ARDS 發炎反應與凝血功能紊亂之間的關係

綜合上述的文獻探討可知，ALI/ARDS 目前治療的兩大主軸是「降低發炎反應所產生的氧化傷害」以及「改善凝血功能紊亂與抗纖維蛋白溶解的失衡」。然而，發炎反應及後續凝血功能紊亂的產生有著密不可分的關連性，兩者並非各自為獨立事件，而有著因果關係及加乘效應。

在 ALI/ARDS 的急性期，大量的發炎反應前驅細胞激素(proinflammatory cytokines)，如 TNF-α、IL-1β、IL-6 等被釋放出來，除了會放大發炎反應而形成瀑布效應(inflammatory cascase)之外，還會驅動肺部凝血功能的紊亂(pulmonary coagulopathy)產生[2, 51, 160]。這些 proinflammatory cytokines 會藉由刺激 TF 的活化和增加 PAI-1 的釋放，來造成肺泡及肺微血管內瀰漫性血栓的形成[148, 153, 160]。首先，這些被活化的凝血酶(PAI-1)是強力的發炎反應促進劑，可以促進中性球黏附在血管內皮、促進 Selectin 的表現量、並活化血小板受體，加劇了肺部的發炎反應[26, 159, 161, 162]。其次，纖維素(fibrinogen)可以增加血管的通透性、活化內皮細胞，進而誘導中性球的黏附以及移行，也會加劇肺部的發炎反應[148, 163]。近年來，血小板在「召集白血球」(Neutrophil recruitment)的角色也日益清楚：Zarbock 等(2006 年)[164]研究顯示，血小板可以透過 P-selectin 與中性球產生交互作用，使中性球被活化、血小板在凝集的過程中釋放出大量的 thromboxane A2。這個 thromboxane A2 會活化血管內皮細胞，使其釋放出細胞黏附因子(Intercellular Adhesion Molecule -1, ICAM-1)，使得中性球上的β2-integrin 可以和 ICAM-1 穩定的結合[164, 165]。因此，起先的發炎產物刺激了凝血功能紊亂，造成凝血增強、大量的凝血產物增加，進一步又加重了內皮細胞損傷，使發炎反應放大，釋放出更多的發炎反應細胞激素，最後形成一個「發炎反應與凝血功能紊亂的交叉活化作用」。

綜上，一個同時可以抑制發炎反應，又可以改善凝血功能紊亂的藥物，就是治療 ALI/ARDS 的新契機。

2-3. ALI/ARDS 疾病動物模式文獻回顧

ALI/ARDS 的致病原因可以分類為直接原因以及間接原因兩大類，直接原因與肺有關，因此，其相應的動物模型也可以分為「肺內型」以及「肺外型」兩大類[166]。另外，也可以依照中性球是否為主要角色，分類成「Neutrophil-dependent」 以及「Neutrophil-independent」兩種[51]。至於使用呼吸器所產生的急性肺損傷(Ventilator-induced lung injury, VILI)[167, 168]，則不在本研究討論的範圍。茲介紹以下常用的動物模型，並分析其優缺點。

2-3-1. 肺表面張力素缺損 (Lavage, LAV)誘發 ALI/ARDS 疾病動物模式

這個模型的建立，主要是透過使用 37-39℃的等張性生理食鹽水，經過反覆的全肺灌流 (whole lung lavage)。將大約 10-30 ml/Kg (豬、兔等大型動物)或 1 ml/Kg (鼠等小型動物)的生理食鹽水灌入動物肺內 1 分鐘後，予以回收，間隔 1-10 分鐘後再灌洗一次，總共灌洗 5-8 次，或灌洗至 PaO2<100 mmHg (在使用 100%的氧氣供應下)[169-171]。病理機制：肺泡內有表面張力素，以作為克服表面張力、維持肺泡正常開闔的介面活性物質。當大量的生理食鹽水進行肺泡液灌流時，會造成肺泡內表面張

力素喪失，使得肺擴張不全、蛋白質漏出、肺透明膜形成，最後形成肺水腫[172-174]。在病理切片下，LAV 主要的變化就是肺血管網、支氣管周邊水腫、淋巴管水腫以及第一型肺泡上皮細胞的死亡等，但是中性球的浸潤以及肺泡上皮及血管內皮細胞損傷的程度並不嚴重。所以這個模型並不能類比人類因肺炎所致的 ALI/ARDS，其主要能夠類比的疾病為肺表面張力素缺失所引起的肺損傷[50]。

2-3-2. Oleic acid (OA) 誘發 ALI/ARDS 疾病動物模式

利用中央靜脈導管、股靜脈導管或者肺動脈導管，將油酸(Oleic acid, OA)以 0.06-10.15 ml/Kg 的劑量，混合生理食鹽水，緩慢地(約 20-30 分鐘)注射入右心房內，產生氧合障礙，使 PaO2/FiO2 比率降至 80-120 mmHg 的程度，以模擬脂肪酸產生肺栓塞的疾病模式[175-178]。病理機制：由於注射入的不飽和脂肪油酸會直接與肺微血管內皮細胞產生鍵結作用，造成血管內皮細胞受損、血管通透性改變，釋放出大量的發炎反應物質如 TNF-α以及 IL-8，造成中性球趨化並移行至肺泡內[179-181]。大量的水分以及蛋白質也會因微血管通透性改變而滲入肺泡，造成肺泡上皮細胞死亡、透明膜形成、表面張力素缺失等病變[182-184]。病理切片下，在 OA 注射後 6-12 小時就可以看到肺泡大量液體浸潤、微血管充血、肺部出血、肺組織局部壞死以及 fibrine 沉積在肺泡內的情況，除此之外，

大量的中性球以及巨噬細胞浸潤也會在 OA 注射後的數小時內被發現。但是一個星期後，OA 所致的肺部損傷主要是廣泛的肺纖維化反應進行，這時候可以看到肺泡內被纖維母細胞、巨噬細胞、淋巴球以及肥胖細胞佔據，另外就是第二型肺泡細胞的增生[185, 186]。OA 注射模型的好處是，典型的 ALI/ARDS 各個階段的病理變化如急性期、增生期以及纖維期，都可以在這個模型見到。然而，其導致 ALI/ARDS 的起始原因是不飽和脂肪酸對肺部微血管網的攻擊所產生的後續病變，與人類因肺炎所致肺泡內上皮細胞受損進而產生 ALI/ARDS 之臨床情況不盡相同，所以用這個動物模型來做為藥物的篩選要注意這一個侷限性。

2-3-3. LPS 誘發 ALI/ARDS 疾病動物模式

LPS 是革蘭氏陰性細菌細胞外膜主要的成分，可作為內毒素(endotoxin)，在生物體內引起嚴重的免疫反應。LPS 產生急性肺損傷的方式可分為兩種：1)靜脈注射法：將 LPS 溶於生理食鹽水後，以 2-4 ng/kg 的劑量注射至動物靜脈內，會產生類似敗血症的全身性發炎反應、瀰漫性血管內凝血、肺微血管內皮細胞受傷所致的發炎細胞激素大量釋放、中性球活化等[187-189]。2)氣管內誘發法：將 LPS 以 1-4 ng/kg 的劑量溶於生理食鹽水，接下來以霧化的方式經氣管內直接誘發 ALI/ARDS。這種方法在誘發後第 2-4 小時，實驗動物即會出現低血氧症、動脈二氧化碳

分壓增高、肺水腫以及以中性球為主要角色的急性肺損傷反應。實驗動物的肺泡沖洗液會出現大量的中性球、白蛋白滲出物以及大量的發炎反應細胞激素如 TNF-α、IL-1β、IL-6、G-CSF、IL-8、MCP-1、MIP-1 以及 ROS 等[49, 190-192]。LPS 經氣管內誘發 ALI/ARDS 在實務上比較接近人類肺炎所致的 ALI/ARDS，在誘發後的 24 小時內的急性期，是以中性球為主的發炎反應，會產生大量類似人類敗血性休克的發炎細胞激素、氧化自由基以及細胞黏附因子，因此，我們希望能建立這個形式的動物模型，以作為篩選驗證中醫藥理論基礎及有效藥物的實驗平台。

2-4. 牡丹皮與丹皮酚

2-4-1.傳統醫學有關牡丹皮的論述

牡丹皮為毛茛科植物-牡丹之干燥根皮。產于中國大陸的安徽、山東等地。在炮製法上，於秋季採挖其根部，除去細根及剝取根皮部分後予以曬乾，然後生用或炒用。牡丹皮之典籍論述摘錄如下：

(1)《神農本草經》:「牡丹味辛寒，主寒熱，中風瘈瘲，驚癇邪氣、除癥堅瘀血留舍腸胃，安五臟、療癰瘡，一名鹿韭，一名鼠姑，生山谷[193]。」列為中品。

(2)《本草綱目》:「滋陰降火，解斑毒，利咽喉，通小便血滯。後人乃專以黃蘗治相火，不知丹皮之功更勝也。赤花者利，白花者補，人亦罕

悟，宜分別之。[58]」

(3)《本草經疏》:「牡丹皮，其味苦而微辛，其氣寒而無毒，辛以散結聚，苦寒除血熱，入血分，涼血熱之要藥也。[57]」。

(4)《本草備要》記載牡丹皮:「辛甘微寒，入手足少陰厥陰經，瀉血中伏火，和血涼血而生血，破積血，通經脈，為吐衄必用之藥。治中風五勞，驚癇瘈瘲，治煩熱，療癰瘡，下胞胎，退無汗骨蒸。單瓣紅花者入藥，肉厚者佳，酒拌蒸用[194]。」

(5)《本草匯言》:「牡丹皮，同當歸、熟地則補血；同莪术、桃仁則破血；同生地、芩、連則涼血；同肉桂、炮姜則暖血；同川芎、白芍藥則調血；同牛膝、红花則活血；同枸杞、阿膠則生血；同香附、牛膝、歸、芎，又能調氣而和血。[195]」「牡丹皮，清心，養腎，和肝，利包絡，並治四經血分伏火。血中氣藥也。善治女人經脈不通，及產後惡血不止。又治衄血吐血，崩漏淋血，跌仆瘀血，凡一切血氣為病，統能治之。蓋其氣香，香可以調氣而行血；其味苦，苦可以下氣而止血；其性涼，涼可以和血而生血；其味又辛，辛可以推陳血，而致新血也。[195]」

(6)《本經疏證》:「牡丹皮入心，通血脈中壅滯與桂枝頗同，特桂枝氣溫，故所通者血脈中寒滯，牡丹皮氣寒，故所通者血脈中熱結。[52]」

據上可知，牡丹皮的性味是「氣香、味苦辛、性涼而寒」，為「血中之氣藥」，所以在「瀉降相火以涼血熱」、「調氣行血以化血瘀」的功

效是相當卓著的。歸結牡丹皮在傳統中醫臨床使用上的兩大作用：「清熱涼血」以及「活血化瘀」。

牡丹皮的清熱涼血作用，是因為味苦性涼的作用，主要是清相火以涼血分熱。方如：《溫病條辨》:「青蒿鱉甲湯，主治溫病後期，邪伏陰分證。青蒿 6 克，鱉甲 15 克，细生地 12 克，知母 6 克，丹皮 9 克。上藥以水五杯，煮取二杯，日再服。方中佐以牡丹皮辛苦性涼，瀉陰中之伏火，使火退而陰升」。又如《備急千金藥方》:「犀角地黃汤，主治熱入血分證，熱傷血絡證。水牛角 30 克，生地黃 24 克，赤芍 12 克，牡丹皮 9 克上藥四味，以水九升，煮取三升，分三服。方中丹皮苦辛微寒，入心肝腎，清熱涼血，活血散瘀，可收化斑之效。」

牡丹皮的活血化瘀作用，主要是氣香味辛可以散結，為血中之氣藥可以行血逐瘀。對於血滯經閉、痛經、跌打傷痛等血瘀滯痛均有治療效果。該品辛行苦瀉，有活血去瘀之功。治血滯經閉、痛經，可配桃仁、川芎、桂枝等藥用，如桂枝茯苓丸《金匱要略》；治跌打傷痛，可與红花、乳香、没藥等配伍，如牡丹皮散《證治準繩》。

由於牡丹皮同時具有「清熱涼血」以及「活血化瘀」兩大作用，因此，對於以發炎及凝血功能紊亂為以“發炎”以及“凝血功能紊亂”兩大病理生理反應為主軸的 ALI/ARDS，在學理上為十分具有治療潛力的藥物，因此本研究以牡丹皮來做為評估療效之藥物。

2-4-2. 牡丹皮現代藥理學之研究

牡丹皮又名丹皮、條丹皮、粉丹皮、吳牡丹皮以及木芍藥皮等，為毛茛科芍藥屬植物牡丹(*Paenoina Suffruticosa Andr*) 的根皮。現代藥理學研究顯示，牡丹皮中含以下主要成分，如丹皮酚(Paeonol) 、丹皮酚苷 (Paeonoside) 、芍藥苷 (Paeoniflorin) 、丹皮酚原苷丹皮酚新苷 (Apiopaeonoside) 、苯甲醯芍藥苷(Benzoylpaeoniflorin) 、氧化芍藥苷 (Oxypaeoniflorin) 、2 ,3-二羥基-4-甲氧基苯乙酮、2 ,5-二羥基-4-甲氧基苯乙酮、3-羥基-4-甲氧基苯乙酮、Paeonilide、揮發油及植物甾醇等[53, 70]。以下探討牡丹皮的藥理作用：

(1) 牡丹皮具有抗氧化

過去的文獻顯示，牡丹皮具有良好的抗氧化作用，特別是可以清除氧化自由基[63]。Rho 等(2005 年)的研究發現，牡丹皮具有清除自由基以及超氧陰離子的作用，進而抑制由 hemeoxygenase (HO)以及 cathecol-O-methyltransferase(COMT)過度表現所製造出來的大量氧化自由基及氧化傷害[64]。Okubo 等(2000 年)的研究也發現，牡丹皮對 DNA 的氧化傷害具有保護作用，可以減少 DNA 因氧化傷害產生的斷裂[65]。

(2) 牡丹皮具有抗發炎作用

Kim 等(2011 年)的使用大鼠關節炎動物模型(type II collagen-induced arthritis , CIA)來研究牡丹皮治療是否具有抗發炎作

用。結果發現，給予牡丹皮治療可以改善關節變形、降低 Th1 相關的發炎反應、降低matrix metalloproteinases (MMPs)以及發炎反應細胞激素(如 TNF-α、IL-1β、IL-6 等)表現量、抑制細胞趨化激素如 MIP-1 的釋放等。這個抗發炎的作用，可能是透過抑制 NF-κB 以及抑制 Activator Protein-1 (AP-1)的活化來達成[67]。

(3) 牡丹皮具有抑制噬伊紅性細胞作用

Kim 等(2007 年)以牡丹皮作用於 A549 人類上皮細胞的研究發現，牡丹皮可以抑制經 TNF-α、IL-4 以及 IL-1β刺激後上皮細胞分泌 Eotaxin 的表現，同時可以抑制噬伊紅性細胞移行至 A549 細胞，其作用機轉，可能與抑制 NF-κB 的活化有關[196]。

(4) 牡丹皮具有抑制神經性疼痛作用

Tatsumi 等(2004 年)發現，牡丹皮對於脊髓腔注射 prostaglandin F2α (PGF2α)所引起的神經性疼痛(Neuropathic pain)具有良好的抑制效果[61]。

2-4-3 牡丹皮主要成分丹皮酚

丹皮酚為從牡丹皮(*Moutan cortex* of *Paeonia suffruticosa* Andrews；MCR) 所抽取出來的重要有效成分，它也存在於芍藥(*Paeonia lactiflora* Pall (PL))與徐長卿(*Pycnostelma paniculatum* K.Schum)中[197]。丹皮酚被認為是一個具有抗發炎(anti-inflammatory)、抗氧化 (antioxidant)、抗腫瘤

(anti-tumor)、抗菌(anti-bacteria)與免疫調節(immune-regulation)的物[73, 198-200]。

2-4-4. 丹皮酚之化學結構及性質

丹皮酚的結構式如下圖(Figure 1-1)所示。丹皮酚分子式為$C_9H_{10}O_3$，學名為2'-羥基-4'-甲基苯乙酮(2'-hydroxy-4'-methoxyacetophenone)，分子量為166.18，呈白色或微黃色有光澤之結晶體，熔點為49 - 51°C，易溶於乙醇和甲醇，可溶於熱水，難溶於冷水[201]。

圖 2-1 丹皮酚的化學結構

2-4-5. 丹皮酚之藥物動力學

丹皮酚的藥物動力學如下：

(1)口服丹皮酚之藥物動力學：

Xie 等(2008 年)利用高效液相層析儀(High-performance liquid chromatography , HPLC)及二極矩陣偵測器(Diode Array Detector , DAD)

的方法來研究丹皮酚的代謝途徑。結果發現，大鼠在口服丹皮酚 20 分鐘後，可達血中最高濃度，同時丹皮酚也可被代謝成其它 4 種代謝產物，包括 resacetophenone-2-*O*-sulfate、2-hydroxy-4-methoxyacetophenone-5-*O*-sulfate、paeonol-2-*O*-sulfate 和 resacetophenone[202] 。丹皮酚經由口服餵食後，可經由肝臟中 cytochrome P450 1A2 進行去甲基[203]。李清俠等(2011 年)將丹皮酚用胃管給予小鼠一次性灌胃，來探討藥物動力學，結果發現，經灌胃給藥後 1 分鐘就可以在血中測到丹皮酚原型藥，5.3 分鐘後達到最高濃度，240 分鐘後在血中已測不到濃度。此外，丹皮酚主要分布於肝、其次是脾、小腸、腎及心肺等[204]。關於丹皮酚的排泄途徑，Gjertsen 等(1988 年)的研究顯示，丹皮酚主要是經由腎臟從尿液排出。口服餵食大鼠丹皮酚後，收集第 1-4 天的尿液，均可偵測到丹皮酚的代謝產物，其中濃度最高的包括丹皮酚原型、去甲基型(2, 4-dihydroxyacetophenone； resacetophenone)和羥基化型(2, 5-dihydroxy-4-methoxyacetophenone) [205]。

(2) 肌肉注射單皮酚之藥物動力學

Ma 等(2008 年)經肌肉注射濃度為 10 mg/kg 的濃度的丹皮酚到大鼠體內以探討藥物動力學，結果發現，丹皮酚達血漿最高濃的時間為 7.5 分鐘，其最高濃度為 0.71 mg/L (4.3 μM)，其平均排除半衰期(mean elimination half-life)約為 59.9 分鐘[201, 202]。

(3) 靜脈注射丹皮酚之藥物動力學

陳曉蘭等(2010 年)以 HPLC 的方法來探討經鼠尾靜脈注射 4mg/Kg 之丹皮酚至大鼠之藥物動力學，結果發現，C_{max}=(8.99±0.84) mg/L、Kel=(0.082±0.015)/min，$t_{1/2Kel}$=(8.73±1.54) min，大約 45 分鐘後血中濃度已經降至 t_{max} 的 1/10 以下，顯示丹皮酚在血中清除較快[206]。

2-4-6. 丹皮酚的現代醫學研究

(1) 丹皮酚具有抗發炎作用

Wu 等(2009 年)在細胞實驗中，以丹皮酚處理大鼠滑膜細胞(synoviocyte)，發現丹皮酚有降低 IL-1β 及 TNF-α 的效果[197]。Chae 等(2009 年)發現, 丹皮酚對於以 LPS 刺激巨噬細胞 RAW 264.7 所引發 nitric oxide synthase (iNOS)與 COX-2 大量表現，具有抑制效用[76]。Chou (2003 年)，使用丹皮酚事先或事後經腹腔注射到大鼠體內，結果發現，丹皮酚可以抑制鹿角菜膠(carrageenan)引起的 TNF-α、IL-1β、前列腺素 E_2 (prostaglandin E2 , PGE2)、iNOS、COX-2 等發炎物質的濃度，並可減少鹿角菜膠引起的疼痛[200]。在結腸炎模型中，丹皮酚的灌腸可減少 trinitrobenzene sulfonic acid (TNBS)誘發的小鼠結腸炎，同時也可以降低 MPO 活性與 iNOS 的產生；同一個團隊，在細胞實驗中發現，丹皮酚可抑制 TNF-α 及 interferon-γ (IFN-γ)所造成的 iNOS 蛋白質與 mRNA 表現，同時也可以抑制 NFκB 和 STAT1 的活化[207]。Hu 等(2010 年)在以食物中

加入 5%的酒精連續餵食小鼠 8 週所致的小鼠慢性酒精性肝炎模型中發現，給予丹皮酚可以減輕長期餵食酒精所造成血清中 aminotransferase 的上升，並且在肝臟病理切片中發現，丹皮酚可減輕酒精對肝細胞的破壞、脂肪肝(steatosis)和發炎細胞的浸潤、抑制肝細胞生脂基因(lipogenic genes)mRNA 的表現量，但同時丹皮酚卻不會抑制肝細胞 cytochrome P450 2E1 (CYP2E1)的蛋白質表現[208]。Huang 等(2008 年)，使用微陣列分析，發現 Panther 訊號包括細胞激素(cytokine、interleukin)及 toll-like 受體訊號，是與丹皮酚抑制經 LPS 誘發的巨噬細胞發炎反應最有相關的兩群調控基因[209]。

(2) 丹皮酚具有抗氧化作用

丹皮酚具有顯著的抗氧化作用[210, 211]。Okubo 等(2000 年)發現，丹皮酚可以減少強氧化劑 phenylhydroquinone (PHQ)造成的 DNA 斷裂程度、有效地清除產生的 superoxide 和 hydroxyl radical [65]。Hu 等(2010 年)發現，丹皮酚可以抑制酒精所造成的肝細胞脂質過氧化(lipid peroxidation)[208]。許多神經學相關的傷害模型，也證實了丹皮酚可以透過抗氧化作用、清除氧化自由機而達到保護神經的作用，如：Zhong 等(2009 年)發現，右旋半乳糖會刺激產生超氧化離子和氧源自由基(oxygen-derived free radicals)的產生，而使用丹皮酚，可降低右旋半乳糖(d-galactose)所造成的神經毒性與認知損傷(cognitive impairment)，同時

也增加 GSH 及 SOD 等自由清除劑的濃度[212]；Chen 等(2001 年)以及 Mi 等(2005 年)，在使用腦動脈阻塞或缺血-再灌流的動物模型進行相關的中風研究,也顯示了使用丹皮酚治療，具有減少腦梗塞面積及中風後神經功能損傷的保護作用[213, 214]。

(3) 丹皮酚具有抗凝血作用

Koo 等(2010 年)對牡丹皮之組成進行抗凝血功能的研究，結果發現牡丹皮所含的化學結構當中，對血小板凝集作用及對血液凝固作用具有抑制效果的主要化學物質為 Paeonol、Paeoniflorin、benzoylpaeoniflorin 等，顯示丹皮酚具有抗凝血作用[72]。細胞實驗也發現丹皮酚對 ADP 以及 collagen induced platelet aggregation 具有抑制作用且呈現劑量效應[71, 72]

(4) 丹皮酚具有神經保護作用

氧化傷害在神經細胞損傷中扮演重要的角色，丹皮酚具有良好的抗氧化作用，因此許多神經學研究團隊使用丹皮酚來進行研究，以探討其與神經保護作用的關係。Wu 等(2008 年)，利用缺糖缺氧(oxygen-glucose depreviation) 導致海馬神經元細胞損傷，產生大量釋放的 glutamate、鈣離子內流及 N-Methyl-D-aspartic acid (NMDA) 受體活化，來模擬大腦缺血傷害。結果發現，使用丹皮酚治療，會增加神經元細胞在缺氧缺糖環境下的存活率，同時減少鈣離子的內流、降低 NMDA 受體的結合能力，

顯示丹皮酚具有神經細胞保護作用[215]。Zhong 等(2009 年)利用 D-galactose 誘發的 ICR 小鼠衰老模型，測試丹皮酚對認知障礙小鼠記憶與學習的影響，結果發現，在 Morris 水迷宮試驗與被動迴避試驗(passive avoidance test)中，丹皮酚可有效的促進衰老小鼠的學習與記憶能力、減少 D-galactose 在海馬與額葉皮質所造成的的神經損傷、增加 acetylcholine (ACh)、SOD、Na^+- K^+-adenosine triphosphatase (Na^+-K^+-ATPase)的活性、降低 cholinesterase (AChe)的活性以及 malondialdehyde (MDA)的濃度[212]。Hsieh 等(2006 年)，使用丹皮酚治療大腦缺血-再灌流所致大鼠急性腦損傷模型，結果發現，在缺血前 20 分鐘先給予大鼠丹皮酚，可以有效的縮小腦梗塞的面積，同時降低了腦組織中 IL-1β 及超氧自由基的水平[75]。

(5) 丹皮酚具有抗過敏作用

Kim 等(2004 年)發現，丹皮酚可以減少肥大細胞釋放組織胺(histamine)、抑制肥大細胞釋放 TNF-α，同時在 B 細胞上抑制由 anti-CD40 抗體、重組的 IL-4、及重組的組織胺釋放因子(recombinant releasing factor)誘發產生的 immunoglobulin E (IgE)，進而抑制小鼠過敏性休克[216]。Lee 等(2008 年)，使用以去顆粒劑 48 / 80 誘發小鼠皮膚過敏反應模型，結果發現，牡丹皮萃取物中以丹皮酚最能減少小鼠皮膚的過敏反應、搔抓行為和肥大細胞去顆粒化，顯示丹皮酚對 IgE 相關的過敏反應有抑制作用

[217]。Du 等(2010 年)使用 ovalbumin-induced 氣喘的模型，來探討丹皮酚對於氣道的過敏反應是否具有保護效用，結果發現，給予小鼠經胃灌食丹皮酚 100 mg/天，可以降低肺泡灌洗液中的噬伊紅性細胞數、降低肺泡液細胞激素 IL-4 以及 IL-13 濃度，同時增加肺泡液 INF-γ濃度，並顯示丹皮酚可以降低血中 IgE 總量，以達到降低氣道過敏反應的效果[218]。

(6) 丹皮酚具有心血管保護作用

May 等(2006 年)，使用天竺鼠心室的心肌細胞加入不同濃度的丹皮酚，以探討丹皮酚的作用，結果發現，心肌細胞處於 160 μM 與 640 μM 的丹皮酚培養液中，會降低細胞膜上鈉離子通道相關快速動作電位，也會縮短動作電位的作用的時間，暗示了丹皮酚具有抗心律不整作用以及心肌保護作用[219]。丹皮酚具有抗動脈粥狀硬化的效用[220]。Nizamutdinova 等(2008 年)的研究顯示，血管內的上皮細胞發炎反應是動脈硬化形成的主因，而使用丹皮酚，對血管上皮發炎所引發的粥狀動脈硬化反應具有抑制作用，其機轉是透過抑制靜脈上皮細胞受 TNF-α 刺激所分泌的 intercellular adhesion molecule-1 (ICAM-1)，丹皮酚這樣的抑制效果，與抑制 NF-κB 路徑活化、以及抑制 p38、extracellular signal-regulated kinase (ERK)的磷酸化有關[73]。此外，研究顯示，丹皮酚也會藉著抑制 vascular cell adhesion molecule-1 (VCAM-1)來抑制 TNF-α 刺激主動脈中產生的單核球黏附[74]。Li 等(2009 年)，以高脂肪飲食連續餵食兔子 12 週後所誘

發動脈內粥狀硬化斑塊(atherosclerotic plaque)發生模型，給予口服餵食丹皮酚 6 週(75-150 mg / kg / day)後發現，經丹皮酚餵食的兔子，其動脈粥狀硬化斑塊明顯減少，同時，其血液中 TNF-α、IL-1β 和 C-reactive protein (CRP)濃度明顯降低，甚至連 NF-κB 的核轉移也同時被丹皮酚所抑制[221]。Nizamutdinova 等(2006 年)利用心臟冠狀動脈的缺血-再灌流模型造成心肌梗塞檢測丹皮酚的心血管保護作用，發現丹皮酚可以有效縮地小心臟經缺血-再灌流造成的梗塞面積，顯示丹皮酚確有良好的新血管保護作用[222]。

(7) 丹皮酚具有抗骨質疏鬆作用

在骨質疏鬆的病理機制中，破骨細胞的生成(osteoclastogenesis)是造成骨質溶解的主因，因而導致骨質疏鬆。Tsai 等(2008 年)使用 receptor activator of nuclear factor kappa B ligand (RANKL) 以及 M-CSF 來誘發骨髓 stromal 細胞分化為破骨細胞，然後給予丹皮酚治療，結果發現，丹皮酚具有顯著降低破骨細胞活化以及骨頭溶解的能力，同時，經 RANKL 誘發的巨噬細胞產生的 NF-κB 磷酸化、IκB 磷酸化，及 ERK 及 p38 的磷酸化，也會被丹皮酚抑制下來[223]。

(8) 丹皮酚具有抗焦慮作用

MAOA 和 MAOB 是腦中代謝單胺類神經傳導物質的酵素，MAOA 抑制劑是精神科常用來治療焦慮與憂鬱的藥物，而 MAOB 抑制劑可預

防與治療巴金森氏症[224]。Kong 等(2004 年)發現丹皮酚抑制大鼠大腦中 MAOA 與 MAOB 的活性，顯示丹皮酚具有抗焦慮的作用[225]。Mi 等(2005 年)給予小鼠口服餵食丹皮酚 17.5 mg/kg，結果發現，經丹皮酚餵食的小鼠，會增加進入高架迷宮(elevated plus maze)中開臂(open arms)的次數，同時給予餵食丹皮酚的小鼠，在 dark/light transition 試驗中也會增加待在亮室的時間，與該實驗所使用的陽性對照組 diazepam 具有同等效果。但給予餵食 diazepam 的小鼠，其行為表現較為安靜且有嗜睡的副作用，而給予餵食丹皮酚的小鼠卻無嗜睡的情況，顯示了丹皮酚具有等同於抗焦慮藥物的作用，但卻不會產生此類藥物的副作用[214]。

(9) 丹皮酚具有抗癌作用

丹皮酚可以抑制多種癌細胞的增生，包括大腸直腸癌、食道癌和肝癌等[199, 226, 227]。研究顯示，丹皮酚具有抑制血管新生與抗癌細胞轉移的能力，這可能與丹皮酚能抑制 Akt 磷酸化及減小 matrix metalloproteinase 活性有關[228]。Ye 等(2009 年)利用測量大腸直腸癌 HT-29 細胞的增生，來檢測丹皮酚的抗癌能力，以 3-(4,5-Dimethylthiazol-2-yl)-2,5-diphenyltetrazolium bromide (MTT)試驗及流式細胞技術(flow cytometry)的偵測結果發現，丹皮酚可以顯著抑制大腸癌細胞的增生[229]；使用丹皮酚在食道癌細胞，可以使癌細胞週期停在 S 期，並減少 bcl-2/bax 比例[227]；Yet 等(2009 年)發現，丹皮酚的抗癌作用與它在 0.094-1.504 mmole

/ L 的濃度可抑制細胞 COX-2 和蛋白質 p27 的表現有關[229]。另外，丹皮酚在 11.39 至 56.23 mg / L (0.069 至 0.33 mM)濃度範圍可抑制多種肝癌細胞 BEL-7404, SMMC-7721, and MHCC97 的增生[230]。除此之外，丹皮酚與化療藥物具有協同作用，Wan 等(2008 年)發現，添加丹皮酚可以會增加 cisplatin 對食道癌細胞的細胞毒殺效果，以達到更好的化學治療效果[231]。

綜上，由於丹皮酚具有良好的抗發炎、抗氧化以及抗凝血作用，因此選擇使用丹皮酚來作為進行 ALI/ARDS 療效評估的藥物。

第三章 材料與方法

3-1.實驗動物

本研究使用的動物為Spraque-Dawley (SD)品系、無感染性(pathogen-free)大鼠，體重約為250到300 g。在實驗進行前，本研究之動物實驗設計，皆經過台中榮民總醫院・研究部・動物實驗管理委員會之審查通過後，才開始進行。動物實驗皆依照台中榮民總醫院實驗動物管理委員會(Animal Stusy Protocol Review Board of Taichung Veterans Gerneal Hospital)的指導規則執行，以減少實驗動物之痛苦及不適。SD大鼠購買自「樂斯科生物科技股份有限公司」(BioLASCO Taiwan Co., Ltd)，飼養於台中榮民總醫院研究大樓之動物房，飼養環境為12小時光/暗周期，恆溫恆濕的環境，給與實驗鼠充足之飲水及飼料。

3-2. 實驗藥品及試劑

3-2-1. 實驗藥品

(1)牡丹皮：牡丹皮的來源是購買自科達製藥股份有限公司(KO DA Pharmaceutical CO., LTD, Taoyuan County 32459, Taiwan , R.O.C)，藥品為具有衛生署核可藥證字號(衛署藥製 040314)的牡丹皮濃縮科學中藥(MU DAN PI; KO DA; Product number: 420701903)。在製備的過程中，以生藥濃縮而成浸膏，最後 4.34 g 的牡丹皮生藥被濃縮成 0.67 g 的浸膏（生藥

與浸膏比例 4.34：0.67＝6.5：1），然後再添加入 0.33g 的澱粉為賦型劑，乾燥後製成牡丹皮濃縮顆粒。

(2)丹皮酚：丹皮酚之純化物結晶顆粒末由國立陽明大學傳統醫學研究所蔡東湖教授(陽明大學，台北，台灣)所提供，其製備過程如下：牡丹皮生藥購自台北中藥市場，經過國立中國醫藥研究所周正仁(Cheng-Jen Chou)研究員進行基源鑑定後，將牡丹皮進行萃取。萃取過程由蔡東湖教授提供，以 95%乙醇，在 50℃ 的條件下，體積比採 1:10，共進行 3 次萃取。所得到的乙醇萃取物再予以濃縮，然後以正己烷 4× 1.5 L)、乙酸乙酯(ethyl acetate, EtOAc, 4×1.5 L).進行分餾，最後在正己烷(n-Hexane)的那一層得到最大量的丹皮酚，然後以甲醇(methanol, MeOH)製備而形成細針狀的結晶體。經過質譜儀(NMR spectral properties)的鑑定後，證實所製備的結晶體微分子量 166.17 的丹皮酚，其結構為 2-hydroxy-4 methoxyacetophenone (Fig. 1). 1HNMR(CDCl3) d: 2.51 (3H, s, H-8), 3.80 (3H, s, 5-OCH3),6.37 (2H, m, H-4, 6), 7.57 (1H, br s, H-3), 12.71 (–OH); 13CNMR (CDCl3) d: 25.9 (q, C-8), 55.3 (q, 5-OCH3), 100.7 (d, C-6), 107.3 (d, C-4), 113.7 (s, C-2), 132.1 (d, C-3), 165.0 (s, C-1),165.9 (s, C-5), 202.4 (s, C-7)。

3-2-2. 實驗試劑

本實驗大部分的試劑以及進行分子生物檢測所需要的溶劑皆購自 Sigma Chemical (Deisenhofen, Germany)。誘發大鼠 ALI 所使用的內毒素 (Lipopolysaccharide, LPS; Escherichia coli 0055:B5, Sigma Chemical) 是購自 Sigma 公司(St. Louis, MO, USA). 發炎反應相關細胞激素 (Pro-inflammatory cytokines) 的來源如下：TNF-α (BMS622MST, BenderMedsytem)、IL-1β (BMS630, BenderMedsystem) 以及 IL-6 (BMS625MST, BenderMedsystem)是購自 Bender MedSystems (Vienna, Austria). IL-10 (14-8101-62, eBioscience)是購自 eBioscience Systems (San Diego, CA, USA). MIP-2 (#KRC1022)是購自 BioSource International, Inc (CA, USA). 凝血相關細胞激素：TATC (ET1020-1 Lot No. 1259916R1) 以及 PAI-1 (Catalog # RPAIKT-TOT)是購自 Molecular Innovations, Inc (Novi, MI, USA)。

3-3. 利用 HPLC 進行牡丹皮指標成分以及馬兜鈴酸含量之分析

3-3-1. 牡丹皮指標成分分析

目前用來鑑定牡丹皮的主要指標成分為丹皮酚(Paeonol)以及芍藥苷 (paeoniflorin)，將牡丹皮浸膏以 HPLC 系統(HPLC, interface D-7000, Pump L-7100, UV-Vis Detector L-7455, Autosampler L-7200, Hitachi Instruments

Service Co. Ltd., Ibaraki-ken, Japan) 來進行此兩種指標成分的比對，以做為鑑定牡丹皮的身分驗證(authenticator)以及品質保證(quality proof)的色譜指紋圖譜(chromatographic fingerprint)。所使用的層析管柱為: Mightysil RP-18 reversed-phase column (5 m, 250 mm x 4.6 mm) with 20 μL injection valve (Rheodyne)。

(1)指標成分丹皮酚(paeonol)的分析條件設定：丹皮酚的標準品由陽明大學蔡東湖教授所提供。移動相(the mobile phase)之起始條件為 38% acetonitrile (mixed with 62% of 0.03% H_3PO_4) 、流速 (flow rate) 為 1 ml/min、管柱溫度為 30℃以及偵測波長為 274 nm。詳細條件參考如下

Paeonol 之 HPLC 檢測：

高效液相層析條件：

A. 層析管柱：Mightysil RP-18，GP 250×4.6mm(5μm)

B. 移動相：

Time(min)	Acetonitrile (%)	0.03% H_3PO_4(%)
0	38	62
25	38	62

C. 流速：1.0ml/min

D. 檢測波長：UV274nm

(2)指標成分芍藥苷(paeoniflorin)的分析條件設定：芍藥苷的標準品購買自 China National Institutes for Food and Drug control。移動相(the mobile phase)之起始條件為 16% acetonitrile (mixed with 62% of 0.03% H_3PO_4)持續至 25 分鐘，流速為 1 ml/min，管柱溫度為 30℃，偵測波長(the detection wave-length)設定為 230 nm。管柱內 acetonitrile 的比重隨時間而調整為

30% (25~30 分)、50% (30~45 分)，最後 acetonitrile 的濃度為 16% (45~50 分)。詳細條件參考如下

Paeoniflorin 之 HPLC 檢測：

高效液相層析條件：

A. 層析管柱：Mightysil RP-18，GP 250×4.6mm(5μm)

B. 移動相：

Time(min)	Acetonitrile (%)	H_2O(%)
0	16	84
20	16	84
25	30	70
30	50	50
45	50	50
50	16	84

C. 流速：1.0ml/min

D. 檢測波長：UV230nm

3-3-2. 牡丹皮內馬兜鈴酸含量之分析

由於在投稿「Phytomedicine: International Journal of Phytotherapy and Phytopharmacology」的時候，期刊編審委員要求對本研究所使用的牡丹皮進行安全性分析，以確認牡丹皮內並不含馬兜鈴酸等會引起腎病變的有毒成分，因此進行以下分析：

馬兜鈴酸(aristolochic acid)的標準品購買自 Sigma 公司(SIGMA, USA)，其含有 40%的 aristolochic acid I (AA-I). 使用的鑑定系統是 HITACHI L-7000 liquid chromatographic system，包含了 pump (L-7100)、

column thermostat、a model 7725i injection value (sample loop 20 μL) 以及紫外光偵測器(UV detector, L-7455). 使用的層析管柱為 Mightysil RP-18 (GP 250 mm×4.6 mm, 5 μm)、管柱溫度為 30ºC、移動相(the mobile phase)條件為 acetonitrile (45%)以及 NaH_2PO_4 (55%, add 6.9 g of NaH_2PO_4 into 2 ml of 85% H_3PO_4 to a total volume of 1000 ml) 的混合液、流速設定為 1.0 mL/min、偵測波長為 400 nm。

3-4. LPS 誘發 ALI/ARDS 動物模型

本研究所採用的 ALI/ARDS 動物模型，係屬「LPS 直接經氣管內給藥」模式。簡言之，進行實驗前先檢視大鼠狀況，若大鼠呈現活動力或飲食量下降的情況，則不予以進入實驗。適合進行實驗的大鼠先與秤重以及測量肛溫(rectal temperature, RT)並記錄之。實驗動物使用的麻醉劑為氣體麻醉機，使用的麻醉藥物為 2% isoflurane (Halocarbon Laboratories Div Halocarbon Products Crop, River Edge, NJ)，與流速為 0.5 l/min 的氧氣混合。大鼠在被麻醉後，將其仰臥靜置於動物手術台。LPS (Escherichia coli 0055:B5, Sigma Chemical Co., St Louis, MO, USA)的劑量為 16mg/Kg 溶於 0.5 ml 的 Phosphate Buffer Saline (PBS)內，以 1cc 的空針管抽取，將針頭置換為霧化專用的 (Model IA-1B, Penn-Century, Inc., Wyndmoor, PA, USA)。使用小動物專用的喉鏡(Small Animal Laryngoscope, Model

LS-2)將大鼠喉頭挑開，在目視大鼠 vocal cord 的情況下，將 MicroSprayer® Aerosolizer 直接伸入氣管內予以投藥，投藥後需要將大鼠均勻搖動 30 秒，使投入的 LPS 能夠均勻地分部在兩側肺葉，然後再使大鼠俯臥，將舌頭稍微拉到旁邊，並保持大鼠氣道的通暢，上述誘發大鼠 ALI/ARDS 之實驗方法，係根據以往之文獻及本實驗室之前所發表的論文所述[51, 191, 192, 232]。

3-5. 支氣管肺泡沖洗液之細胞學檢測

大鼠在犧牲前先測量肛溫，然後置入密閉透明之壓克力盒內，給予高濃度的 CO_2 使其安樂死，帶大鼠死亡後，立即進行支氣管肺泡液沖洗術(Bronchoalveolar lavage, BAL)，取出肺泡灌洗液(BALF)以進行後續分析，實驗步驟簡述如下：將大鼠經頸部行正中切開術，游離出支氣管後，打開胸腔，連同心臟以及左右肺葉一同取出。以止血鉗夾住右主支氣管，然後自氣管內將 8 cc 的滅菌生理食鹽水注入左肺內，沖洗後再行回收，共 3 次，最後共注入約 24 ml 的生理食鹽水，回收約 20 ml 的肺泡灌流液(BALF)，經過 200 μm 的 mesh 過濾掉黏液後，再離心 (1500 x g, 4℃) 15 分鐘，分離細胞沉澱物以及上清液。將上清液分裝成 5 管，凍於 -80℃冰箱中，待之後進行細胞激素檢測；細胞沉澱物以 2 ml 的 PBS 進行 resuspension，以冷水及高張溶液(10X HBSS) 破壞掉紅血球後，再以

1 倍的 PBS 進行 wash，然後取得至少 2 x 10^5 來自 BALF 的細胞，使用 cytospin 將細胞固定於玻片上，然後進行劉氏染色(Liu`s stain)，以進行後續在顯微鏡下進行白血球種類之判斷及計數[232]。

3-6. 支氣管肺泡沖洗液之蛋白質濃度測定

使用 Bradford protein assay (Bio-Rad, Hercules, CA, USA)，將其他剩餘含細胞及蛋白質的肺泡液自 - 80℃冰箱中取出，使用 ELISA reader 測量 595 nm 吸光值，並依據 BSA 標準濃度及其吸光值繪製標準曲線圖，以標準曲線圖估計樣品之蛋白質濃度（μg/ml）[233-235]。

3-7. 肺組織病理切片之 ALI 判定及量化

大鼠在犧牲後，取出肺臟，將右肺取下，自氣管內灌入 10% paraformaldehyde 以進行固定，然後包埋於 paraffin 內，待之後進行病理切片。將包埋後的肺臟組織進行脫蠟及脫水後，切成 4 μm 公分厚的切片，固定後進行 H&E stain 染色。兩位研究人員分別對所有實驗組肺切片進行肺損傷程度判讀，在判讀時，大鼠之組別及編號均予以密封，且呈亂數擺片，以使判讀人員能夠在不知道組別的情況下進行客觀評估。肺損傷的判讀方式以及損傷程度判定評分標準，係依照 Kristof 等(1998 年)的方法進行修正[236]。簡言之，判讀人員在進行肺損傷程度評分時必須對評分標準有共識，每一隻實驗動物之肺切片皆有 3 個 lobes，以支氣

管為中心，上、中肺葉各選 3 個 fields，下肺葉選 4 個 fields，總共 10 個 fields 進行評分。評分項目分別為：1) alveolar and interstitial cellular infiltration (肺泡及間質發炎細胞浸潤程度)、2) alveolar protein exudation (肺泡內蛋白滲出程度)、以及 3) alveolar hemorrhage (肺泡內出血程度)等。每一項指標最嚴重的程度給予 3 分，完全沒有給予 0 分，佔 1/3 以下肺泡浸潤給予 1 分，有 1/2 以上肺泡浸潤給予 2 分。每一隻大鼠共有十個 lung fileds 需要給予評分，每一個獨立指標在加總 10 個 fileds 的分數後，予以紀錄為該項之總分。每一隻大鼠的肺損傷程度總分為 3 項指標分數之加總，紀錄為 totoal lung injury scores。如果兩位判斷人員之分數差距過大，將請病理科醫師進行最後判斷[232]。

3-8. 肺組織 MPO 活性之測定

在ALI/ARDS中，肺組織內MPO的表現量可以作為中性球浸潤的指標[16, 79]，進行方法如下[237]：取部分的右肺約1 g，在冰上使用1.5~4.0 N-ethymaleimide (Sigma)進行均質(homogenized) 約30秒，然後在4 ºC中進行離心12,000 g，共30分鐘。離心後將pellet以4 ml的potassium phosphate buffer (50 mM PH 6.0)和hexadecyl-trimethyl- ammonium bromide (HTAB)混合溶液進行resuspension。Buffer volume (ml)：Tissue weight (g) = 10：1。將resuspension的樣品在冰上進行超音波震盪60~90秒後，在4 ºC中進

行離心12,000 g，共30分鐘，取上清液。取10 μl 的上清液與o-dianisidine dihydrochloride (o-DA) solution (167 mg/ml; Sigma-Aldrich, USA) 進行incubation共30分鐘，最後以460 nm的波長進行吸光值的偵測，每30 sec讀一次吸光值，以進行酵素活性測定，測量時間0 - 3.5 min。o-DA solution的泡製方法為: 取10mg o-dianisidine dihydrochloride 溶於50 mM potassium phosphate buffer (KH_2PO_4, PH 6.0) 以及 12 μl 新鮮的H_2O_2 (1.5 M)。

3-9. 酵素免疫分析法(ELISA) 測定肺泡沖洗液之細胞激素

將大鼠肺泡灌流液取出後，進行發炎反應以及凝血相關細胞激素的測定。使用的抗體包括 TNF-α (BMS622MST, BenderMedsystem)、IL-1β (BMS630, BenderMedsystem)、MIP-2 (#KRC1022)、IL-6 (BMS625MST, BerderMedsystem)以及 IL-10 (14-8101-62, eBioscience)；TAT complex (TATc, ET1020-1 Lot No. 1259916R1)、PAI-1 (Catalog # RPAIKT-TOT, Molecular Innovations MI USA)。取 100 μL 的肺泡液與 ELISA 抗體 mix 均勻後，在 37℃ 中靜置 60 分鐘，然後將 well 內的溶液吸出，使用 wash solution 將每個 well wash 3 次。加入 Horseradish peroxidase (100 μL)與抗體結合，在 37℃ 中靜置 30 分鐘後，在每個 well 加入 100 μL 的 subtrate solution RMB(tetramethylbenzidine)，靜置於室溫下 15 分鐘。加入 stop

solution (100 μL, 1N solution of hydrochloric acid in water)，以 colorimetric determination (Microplate Reader BIO-RAD Laboratories CA, USA)設定在 450 nm 的吸光值下進行判讀。檢體所偵測到的吸光值，必須與 standard curve 進行比對，然後得到的數值單位為 pg/mL.

3-10. 西方點墨分析 iNOS 表現量

將取出來解凍的大鼠肺組織先以 lysis buffer (RIPA with protease inhibitor, with a ratio of lung tissue /lysis buffer equal to 100 mg /400 ml) 予以均質。將均質化的檢體 sonicated 並離心 30 分鐘 (12,000 x g, 4 ℃)，然後測量蛋白質濃度(Bradford protein assay, Bio-Rad, Hercules, CA) 。每次以 40 μg 蛋白質的樣品，以 7%十二烷基硫酸鈉聚丙烯醯胺膠體電泳 (sodium dodecyl sulfate-polyacrylamide gel electrophoresis ；SDS-PAGE) 分離蛋白，接著將蛋白質轉漬(transfer)到硝化纖維膜(nitrocellulose membranes, Amersham. USA)，硝化纖維膜以阻隔緩衝液(blocking buffer；20 mM Tris-HCl, pH 7.6, 140 mM NaCl, 0.1% Tween-20, 5% skim milk powder)來阻隔，然後以抗 polyclonal rabbit anti-mouse iNOS 抗體 (1:500 dilution, GTX213110-01, GeneTex, CA, USA)來結合 iNOS 蛋白質、抗 Actin 抗體來結合 Actin 蛋白質。結合的抗體以二次抗體 peroxidase-conjugated anti-rabbit antibody 及化學發光法 (chemiluminescence) ECL (Amersham, Buckinghamshire, UK)系統來使底

片顯像。

3-11. 肺部水腫程度分析

為了要評估大鼠肺部水腫程度，本研究另外進行了一組動物實驗，將大鼠全肺取出後至於固定大小及重量的錫箔紙上秤重，登記為濕重(Wet weight, W)。然後將肺組織送入 60℃的烘箱內靜置 48 小時後取出，在予以秤重，此重量為乾重 (Dry Weight, D)。將濕重 (W) 減去乾重(D)，所得到的重量即為 Lung Weight Gain (LWG)，可以反應大鼠肺水腫的程度。

3-12. 體外試驗之純化 Neutrophil

實驗動物為雄性成年健康大鼠，體重約 250~300 克，自鼠尾靜脈採血，收集於後含 EDTA 的試管中，以待進行中性球分離。分離中性球的方法為「Percoll gradient centrifugation method」，係依照 Delclaux 等(1997 年)所發表的方法進行[136]。首先，使用 Ficoll-Paque (1.077 g/ml)將細胞分離，然後在 18℃、300 x g 下進行離心 30 分鐘，將 plasma 移除後，將 Ficoll 以及 red blood cells (RBC) transferred 到含有 76% Percoll 的管子內。將細胞進行第二次離心(8℃、300 x g) 30 分鐘後，在 Hank Balanced Salt Solution (HBSS)以及 76% Percoll interface 之間的細胞即為 Neutrophils。將中性球收集並 transferred 到新的試管，以 1X PBS 進行、離心(300 x g, 5 min at 4 °C)、resuspended 於 6 ml 的 RPMI 1640 solution

(RPMI 1640/1%PS/10%FBS)，進行細胞計數，這時所得到的中性球純度>99%，以利接下來的實驗進行。

3-13. 細胞存活能力分析~trypan blue exclusion assay

根據 Wang 等(2010 年)以及 Tai 等(1993 年)之文獻，我們使用「Trypan blue exclusion test」的方法來計算存活的細胞數目[238, 239]。 簡言之，取出中性球(1×10^6) 將之與不同劑量的丹皮酚(0, 20, 50, and 200 μM) 進行 co-culture 六小時，然後將之離心 (100 x g, 5 分鐘)，去除上清液後，將 pellets resuspension 於 1 ml PBS 混合 0.4% trypan blue 的溶液中。將細胞與含 0.4% trypan blue 的混合液 incubation 於室溫下(20℃) 3 分鐘，然後取出細胞，在顯微鏡下進行細胞計數，存活細胞將不會被染上顏色(unstained)，而死亡的細胞將呈現 trypan blue 的顏色。染色過程不宜超過 5 分鐘，以免細胞因染劑而死亡，進而影響存活率之判讀。

3-14. 細胞凋亡分析~ PI/annexin V assay and flow cytometric analysis

我們參考 Van Engeland 等(1996 年)文獻，使用「PI/annexin V assay」來進行中性球經丹皮酚 co-culture 後之細胞凋亡(apoptosis) 作用分析[240]。簡言之，將未經活化的中性球與不同劑量的丹皮酚(0, 50, and 200 μM) 進行 co-culture 六小時，以 Annexin V-FITC Apoptosis Detection Kit (Pharmingen, San Diego, CA, USA) 進行染色後，使用流式細胞儀(flow

cytometric)來分析細胞表面與 annexin V 的結合程度，以反應細胞凋亡狀況。 將與丹皮酚 co-cutlure 的中性球以 PBS wash 後，再以 100 L of annexin V binding buffer (Pharmingen, San Diego, CA, USA)將細胞 resuspension，再加入 5 μL 含有 FITC-conjugated annexin V (Pharmingen) 以及 5 g/mL propidium iodide (Sigma)的混合液加入。將細胞與混合液混合均勻後，於室溫下進行 incubation 15 分鐘，然後以 400 μL binding buffer 進行 dilution，上機使用流式細胞儀進行分析。Apoptotic cells 將會被標記上 annexin V (AV)。Apoptotic cells 的比率，係以(AV+/PI- plus AV+/PI+ cells)作為計算。

3-15. 中性球細胞吞噬能力分析

中性球($1x10^6$cells)在與不同劑量的丹皮酚(0, 50, and 200 μM) 進行 co-culture 後，再添加入 fluorescent-labeled (yellow-green) latex beads (10^7 beads/mL; 2.0 μM, 2.5% solids, Sigma Missouri USA) 於 37℃的溫度下進行 6 小時的 incubation。根據 Wu 等(2009 年)的方法，使用流式細胞儀，以 fluorescence intensity (mean ± SEM)來表示中性球吞噬 fluorescent-labeled beads 的比率，這個數值就是「phagocytosis index」[(191)]。

3-16. 中性球細胞移行能力分析

中性球受到趨化作用所產生的移行能力(Neutrophil chemotaxis)，係根據

Kawa 等(1997 年)文獻所使用的方法進行[241]，簡言之，使用 transwell chamber (Costar, Cambridge, MA)，在 well 底下加入 6.5 mm diameter polycarbonate filters (3 μM pore size)。 將中性球、600 μl RPMI 1640 、0.5μM fMLP 以及不同劑量的丹皮酚(0, 50, and 200 μM)進行 incubation 後，將中性球 (5×10^5 neutrophils /200 μl /well) seededing 入上層的 transwell chamber，每個 well 內所含的 600 μl RPMI1640 以及 0.5 μM fMLP 作為趨化劑 (chemoattractant). 將上層與下層的 well 合而為一後，於 5% CO_2 的保溫箱(37°C)中 incubated 6 小時，然後再將下層的細胞離心，並以 trypan blue exclusion method 計算其數量。 下層細胞與總細胞數的比值，即為中性球移行能力 (neutrophil migration ability)。

3-17. 統計方法

本研究所有的統計數字表示方式均以 mean ± SEM，所有的動物實驗之各組樣本數均在 N=6 以上，iNOS 的樣本數為 N=4，細胞實驗的結果為至少進行 3 重複後的結果。統計軟體係使用 Prism 3.02 software (GraphicPad Software Inc. CA, USA)，使用 one-way ANOVA 進行多組織間的比較 (post hoc Tukey test). 本研究所有結果，在 $p < 0.05$ 方具有統計學上的顯著差距。

第四章 結果

4-1. LPS 誘發 ALI/ARDS 大鼠之 Time course 研究

4-1-1. 實驗設計與流程設計

為了決定治療介入後最佳的觀察時間點，我們進行了以 LPS 誘發大鼠 ALI 之時序性病理生理變化相關實驗。依照時序，分成未經誘發組(0 hr)、誘發後 8 小時(8 hr)、誘發後 16 小時(16 hr)、誘發後 24 小時(24 hr)以及誘發後 48 小時(48 hr)等共 5 組，每組 N=6。實驗流程如圖 4-1 所示。

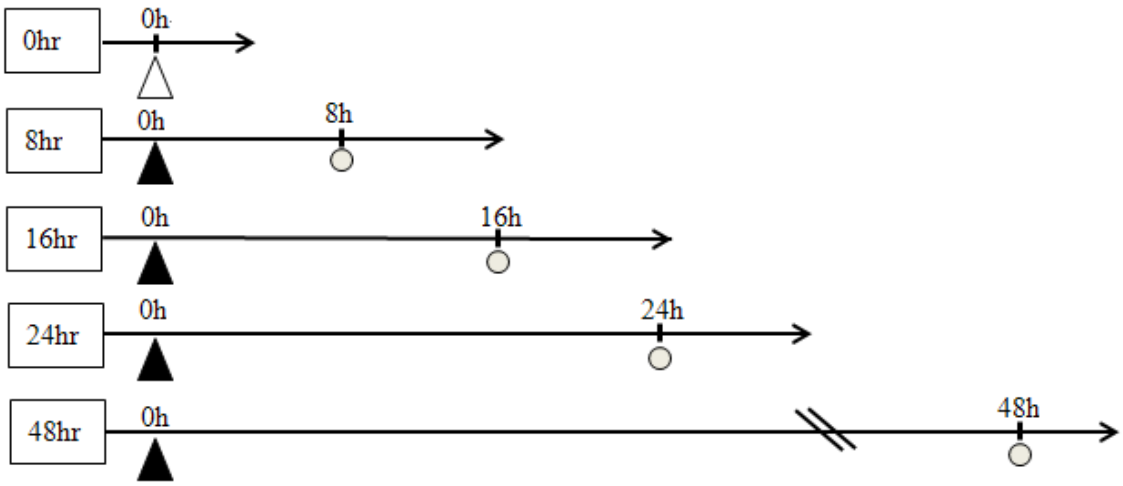

圖 4-1. 以 LPS 誘發 ALI 之時序性研究

0 hr 組：未經 LPS 誘發即予以犧牲；8 hr 組：在 LPS 誘發後 8 小時予以犧牲；16 hr 組：在 LPS 誘發後 16 小時予以犧牲；24 hr 組：在 LPS 誘發後 24 小時予以犧牲；48 hr 組：在 LPS 誘發後 48 小時予以犧牲。符號▲：代表予以 LPS 經氣管內投藥；符號△：代表未施行 LPS 經氣管內投藥；符號◯：代表將大鼠犧牲的時間點。

4-1-2. 大鼠肛溫變化

如圖 4-2 所示，大鼠在經 LPS 誘發後，依時序呈現體溫逐漸下降，至第 16 小時達到最低點，然後逐步回升，至第 48 小時後又會回到接近術前的溫度。各組肛溫依序如下：0 hr：37.1 ± 0.2℃、8 hr：35.8 ± 0.5℃、16 hr：34.7 ± 0.3℃、24 hr：35.8 ± 0.4℃、48 hr：36.4 ± 0.3℃。這種情形，與人類在嚴重感染所致敗血症，所呈現的體溫低下症狀相似。

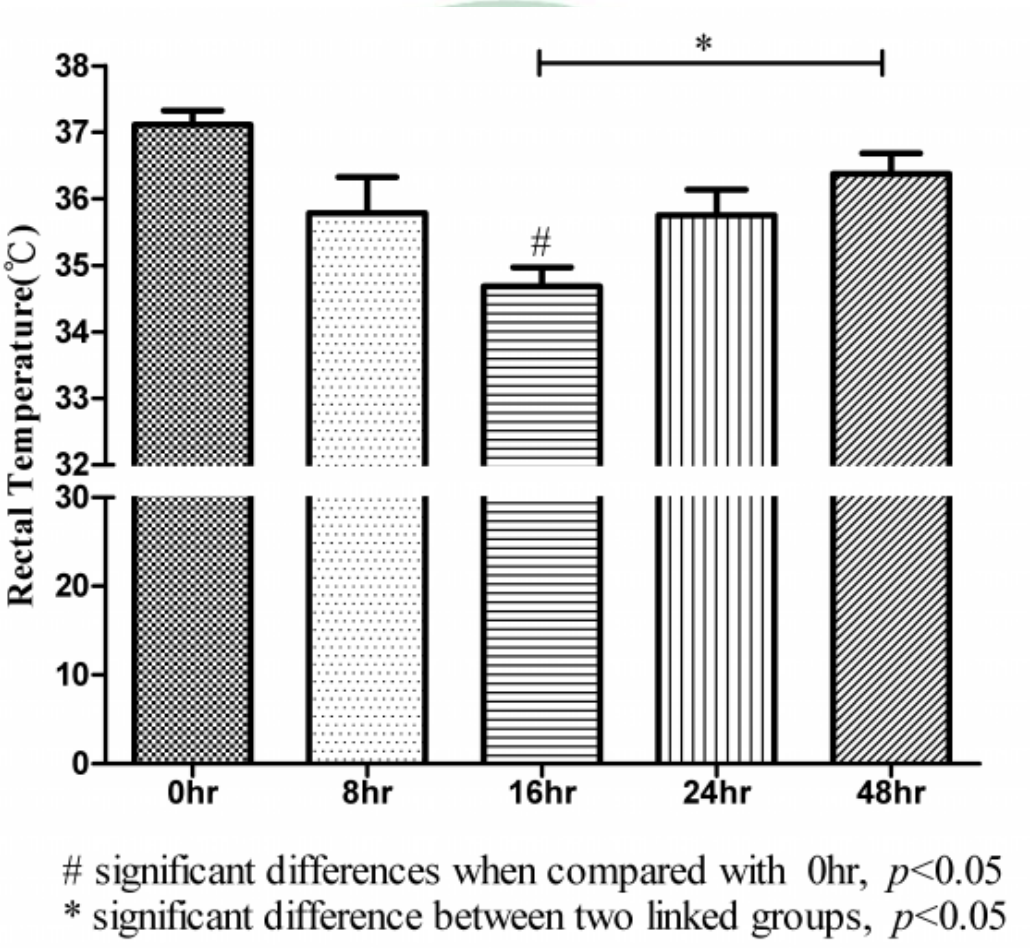

圖 4-2. 大鼠在經 LPS 誘發 ALI 後之時序性肛溫變化。

0 hr 組：未經 LPS 誘發即予以犧牲；8 hr 組：在 LPS 誘發後 8 小時予以犧牲；16 hr 組：在 LPS 誘發後 16 小時予以犧牲；24 hr 組：在 LPS 誘

發後 24 小時予以犧牲；48 hr 組：在 LPS 誘發後 48 小時予以犧牲。各組 N=6。#代表與 0hr 相比，呈現統計顯著差異，$p < 0.05$。*代表 8 hr、16 hr、24 hr 以及 48 hr 各組之間互相比較，呈現統計顯著差異，$p<0.05$。

4-1-3. 大鼠病理切片之肺損傷程度變化

以 LPS 誘發大鼠 ALI 之時序性肺損傷程度變化如表 4-1 以及圖 4-3 以及圖 4-4 所示。 肺損傷程度之總分係由 3 個分數加總而得，依次為肺泡內細胞浸潤程度(cellularity)、肺泡內蛋白質滲出程度(protein exudation)以及肺泡內出血程度(hemorrhage)。

在肺損傷總分方面：與 0 hr 相比，各組之肺損傷程度、肺泡內細胞浸潤程度均呈現顯著上升。隨時序之進展，24 hr 後肺損傷程度逐漸下降，至 48 hr 時肺損傷程度總分已降至 28.6 ± 1.8，顯示本實驗結果與過去文獻所報導之 24 小時內為急性期有較高之肺損傷程度相符合。

在肺泡內細胞浸潤程度方面：以第 16 小時為最高，但 8 hr、16 hr 以及 24hr 三組之間無顯著統計差異。至 48 hr 持續下降，且與 16 hr 相比，呈現顯著統計差異。

在肺泡內蛋白質滲出程度方面：以第 8 小時為最高，但 8 hr、16 hr 以及 24 hr 三組之間無顯著統計差異。至 48 hr 持續下降，且與 8 hr 相比，呈現顯著統計差異。

在肺泡內出血程度方面：以第 16 小時為最高，但 8 hr 與 16 hr 兩組之間無顯著統計差異。至 24 hr 及 48 hr 持續下降，且與 8 hr、16 hr 相比，均呈現顯著統計差異。

表 4-1. 大鼠在經 LPS 誘發 ALI 之各組肺損傷程度比較表

	Cellularity	Protein exudation	Hemorrhage	Scores
0hr	2.3± 0.6	4.5±0.5	5.0±1.2	11.8±1.4
8hr	18.8±1.9 $^{\#}$	13.6±1.3 $^{\#\delta}$	12.1±0.6 $^{\#\gamma\delta}$	44.5±2.4 $^{\#\gamma\delta}$
16hr	20.9±1.0 $^{\#\delta}$	12.4±0.9 $^{\#}$	13.4±1.0 $^{\#\gamma\delta}$	46.7±1.3 $^{\#\gamma\delta}$
24hr	18.9±1.5 $^{\#}$	10.5±1.7 $^{\#}$	7.5±1.2 $^{\alpha\beta}$	36.9±2.1 $^{\#\alpha\beta\delta}$
48hr	15.8±0.5 $^{\#\beta}$	8.1±1.0$^{\alpha}$	4.7±1.0 $^{\alpha\beta}$	28.6±1.8 $^{\#\alpha\beta\gamma}$

Data are presented as mean ± SEM. #: $p < 0.05$, compared with 0hr, α: $p < 0.05$, compared with 8 hr; β: $p < 0.05$, compared with 16 hr; γ: $p < 0.05$, compared with 24 hr; δ: $p < 0.05$, compared with 48 hr. N=6

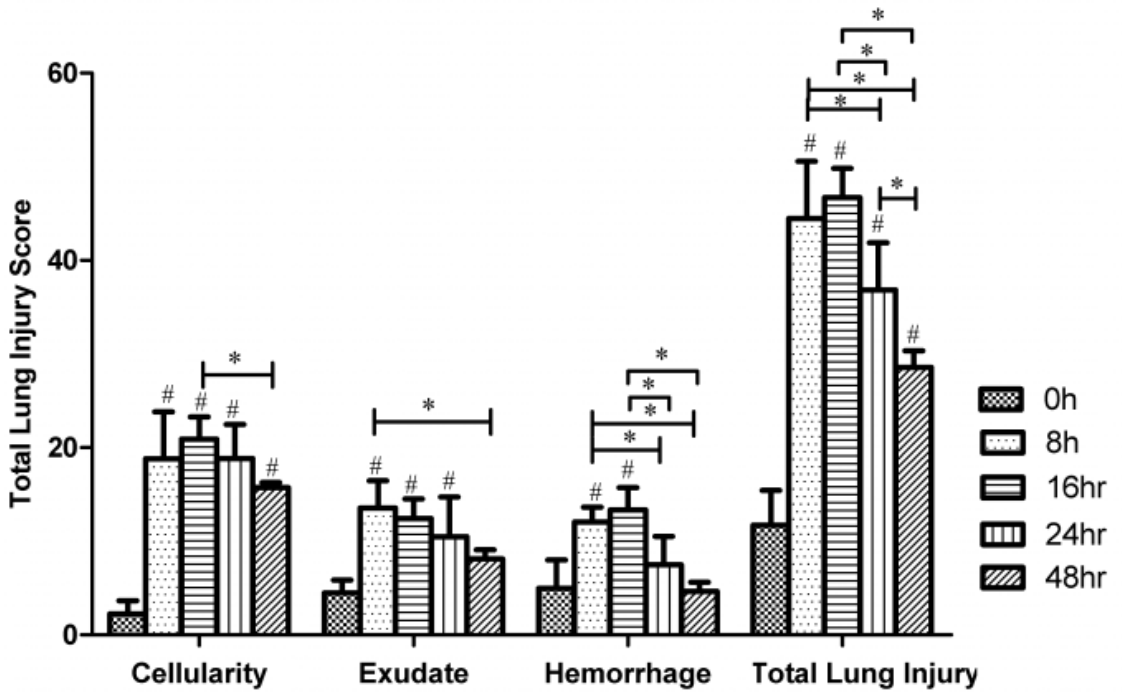

圖 4-3. 大鼠在經 LPS 誘發 ALI 後病理切片之肺損傷程度變化

肺損傷程度之總分係由 3 個分數加總而得，依次為肺泡內細胞浸潤程度(cellularity)、肺泡內蛋白質滲出程度(protein exudation)以及肺泡內出血程度(hemorrhage)。#：代表與 0 hr 相比具有統計學顯著差異, $p < 0.05$；*：代表標示之兩組相比較，呈現統計顯著差異，$p < 0.05$。

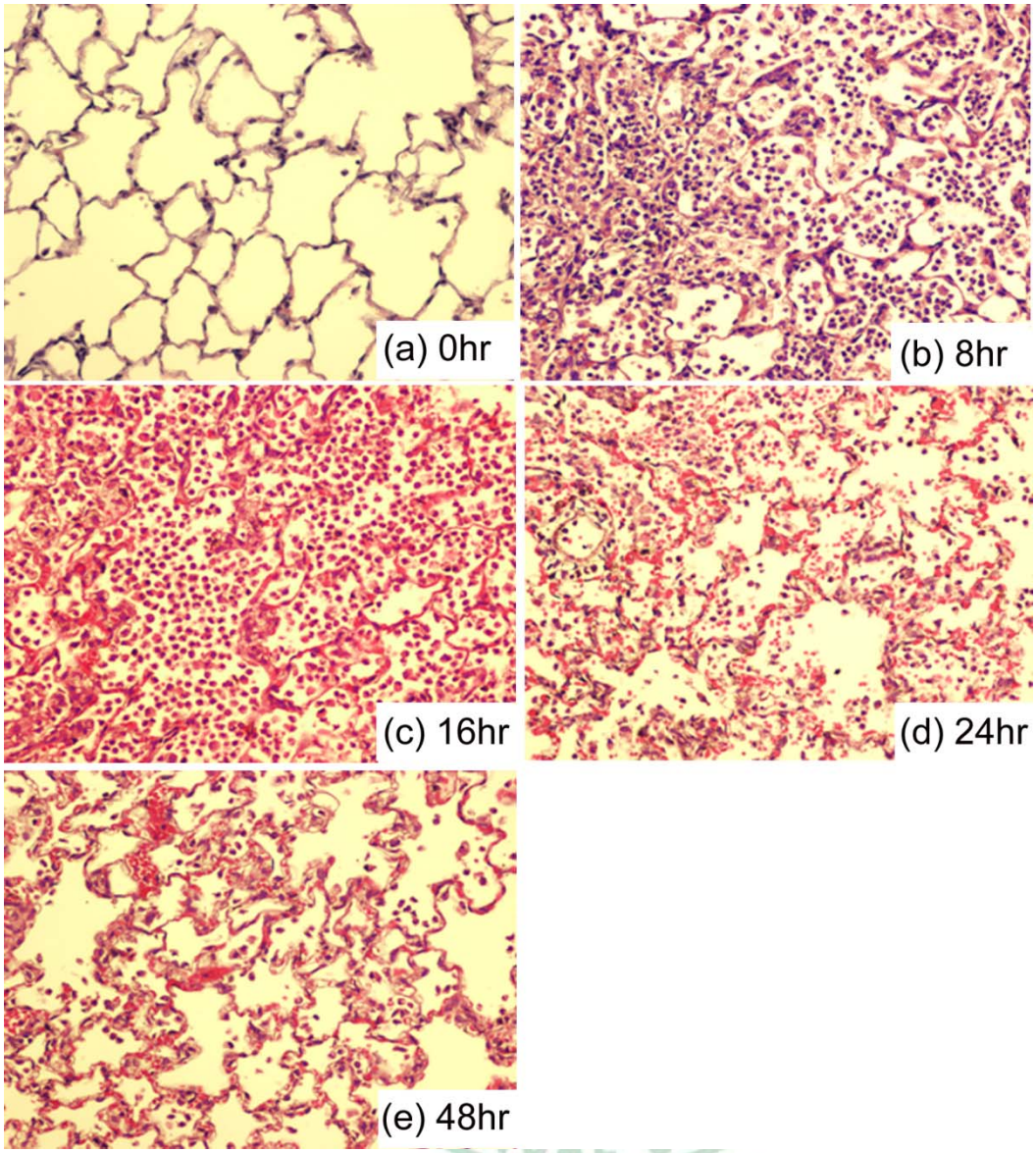

圖 4-4. 大鼠在經 LPS 誘發 ALI 後之時序性肺病理切片

本圖之放大倍數為 200 倍之病理切片。依時序性依次為(a) 0 hr、(b) 8 hr、(c) 16 hr、(d) 24 hr 以及(e) 48 hr。大鼠在犧牲後取其右肺進行病理切片，以 H&E stain 染色後進行肺損傷程度之判定。圖(a) 0 hr 時肺泡內幾乎無中性球、紅血球或蛋白質滲出液存在。肺泡內沉積細胞越多，反應出越嚴重的肺損傷程度。

4-1-4. 大鼠肺泡沖洗液細胞計數之變化

以 LPS 誘發大鼠急性肺損傷之時序性肺泡細胞計數變化如圖 4-5 所示。肺泡液之細胞總數(total cell counts)如圖 4-5 (a)所示，以第 16 小時為最高，但 8 hr、16 hr 以及 24 hr 三組之間無顯著統計差異。至 48 hr 持續下降，且與 8 hr、16 hr 及 24 hr 相比，均呈現顯著統計差異。肺泡液之中性球(neutrophil counts)如圖 4-5 (b)所示，以第 16 小時為最高，但 8 hr、16 hr 以及 24 hr 三組之間無顯著統計差異。至 48 hr 持續下降，且與 8 hr、16 hr 及 24 hr 相比，均呈現顯著統計差異。

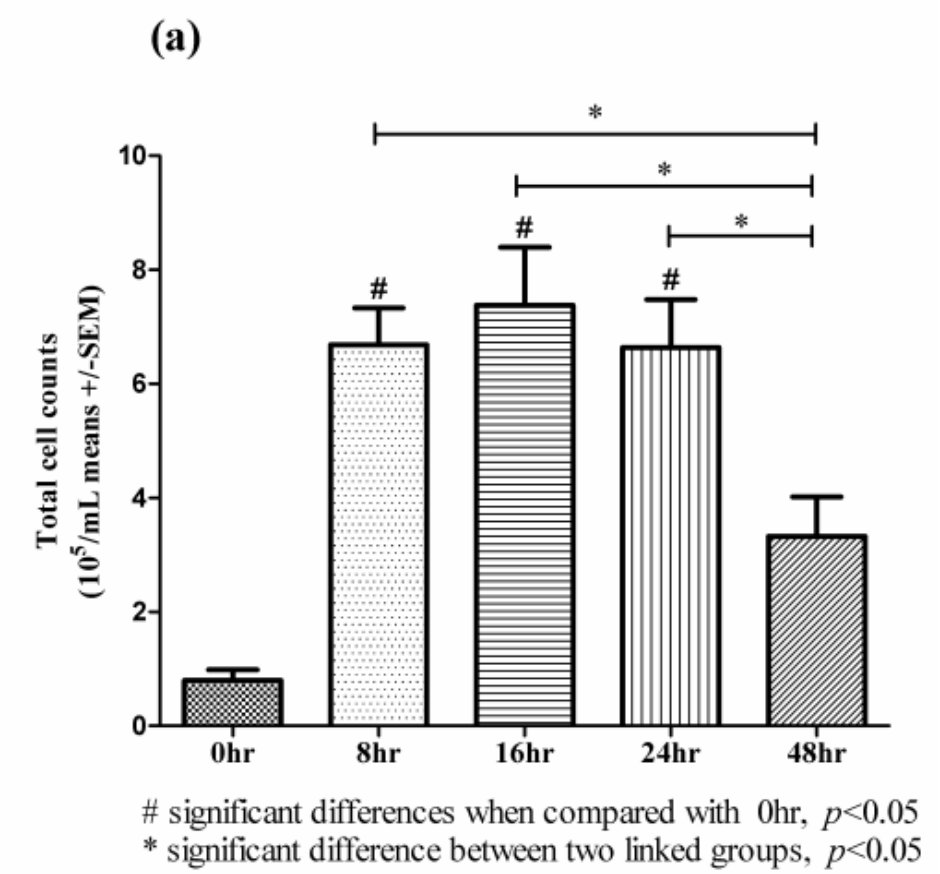

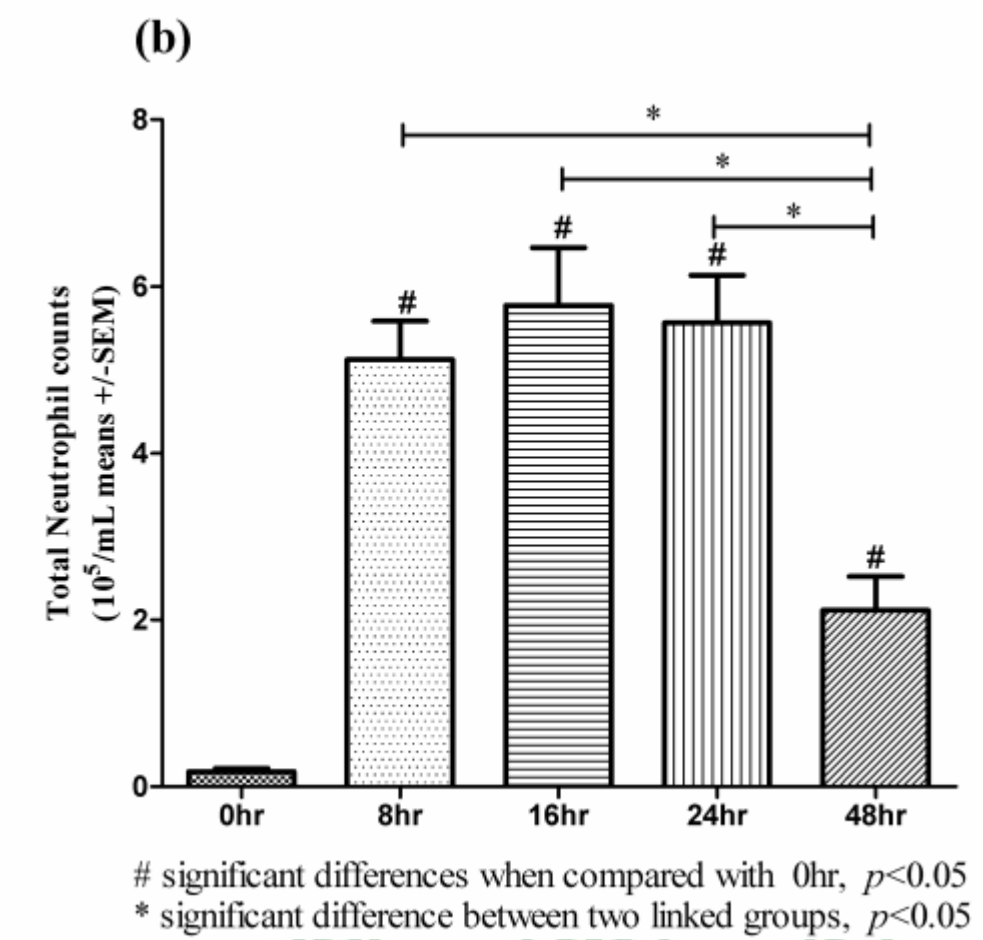

圖 4-5. LPS 誘發 ALI 後大鼠肺泡液細胞計數之變化

(a)肺泡內各組細胞總數變化(total cell counts)。(b)肺泡內各組中性球(neutrophil counts)變化。#：代表與 0 hr 相比具有統計學顯著差異, $p < 0.05$；*：代表標示之兩組間比較，呈現統計顯著差異，$p < 0.05$。

4-1-5. 大鼠肺泡沖洗液蛋白濃度之變化

以 LPS 誘發大鼠急性肺損傷之時序性肺泡沖洗液蛋白濃度變化如圖 4-6 所示。肺泡液之蛋白濃度(protein concentration mg/ml)，以第 8 小時為最高，但 8 hr、16 hr 以及 24 hr 三組之間無顯著統計差異。至 48 hr 持續下降，且與 8 hr、16 hr 及 24 hr 相比，均呈現顯著統計差異。

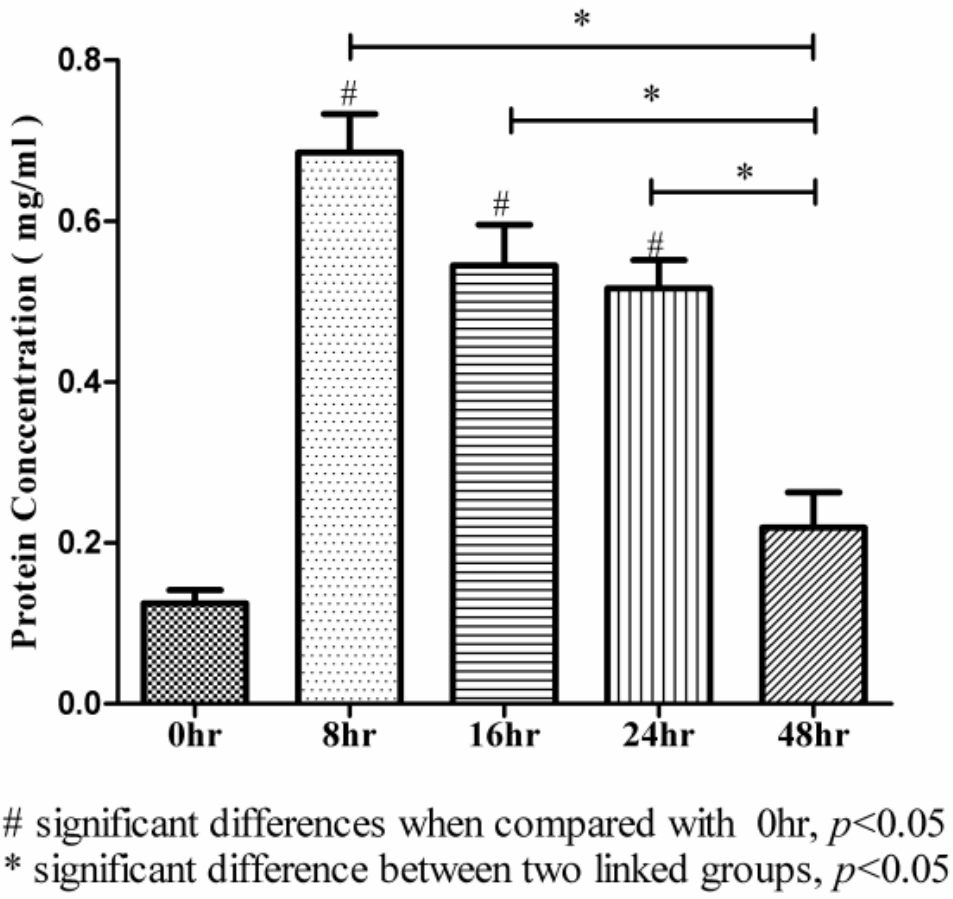

significant differences when compared with 0hr, $p<0.05$
* significant difference between two linked groups, $p<0.05$

圖 4-6. LPS 誘發 ALI 後大鼠肺泡液蛋白濃度之變化

#：代表與 0 hr 相比具有統計學顯著差異, $p < 0.05$；*：代表標示之兩組間比較，呈現統計顯著差異，$p < 0.05$。

4-1-6. 大鼠肺泡沖洗液發炎相關細胞激素之變化

以 LPS 誘發大鼠急性肺損傷之時序性肺泡沖洗液發炎相關細胞激素之變化如圖 4-7 所示。(a) TNF-α之表現量以第 8 小時為最高，然後至第 16 hr 以後就顯著降低。第 8 小時之 TNF-α表現量與 16 hr、24 hr 以及 48 hr 相比，均呈現顯著統計之差異。(b) IL-1β之表現量自第 8 小時後開始顯著上升，以第 16 小時為最高，但 8 hr、16 hr 以及 24 hr 三組之間無顯著統計差異。至 48 hr 持續下降，且與 8 hr 及 16 hr 相比，均呈現顯著統計差異。(c) IL-6 之表現量自第 8 小時後開始顯著上升，在第 16 小時仍然維持在較高的表現量，8 hr 以及 16 hr 之間無顯著統計差異。至第 24 hr 以後開始顯著下降，至第 48 小時的表現量降至最低。8 hr 與 24 hr 及 48 hr 組相比，均呈現顯著統計差異。16 hr 與 24 hr 及 48 hr 組相比，亦呈現顯著統計差異。

(a)

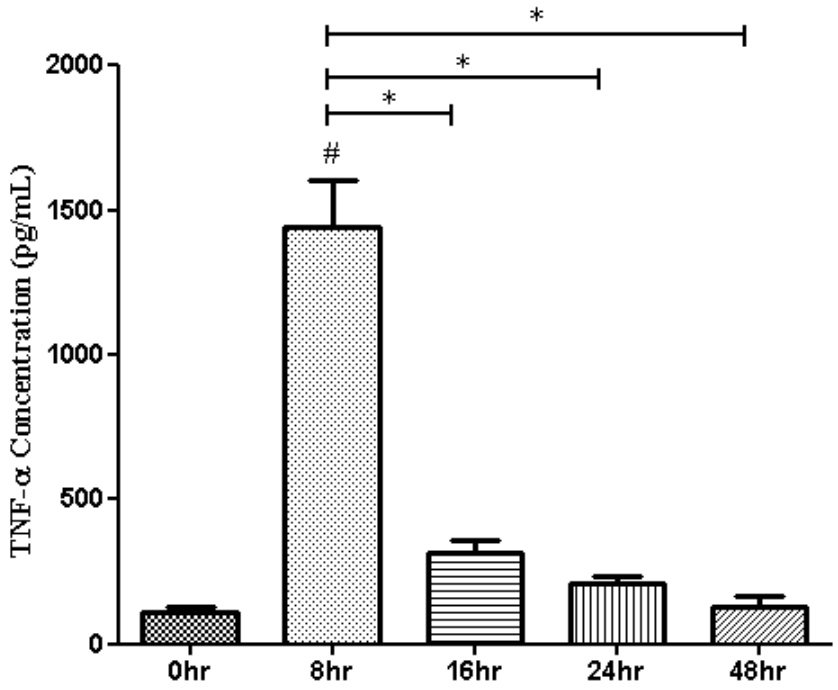

significant differences when compared with 0hr, $p<0.05$
* significant difference between two linked groups, $p<0.05$

(b)

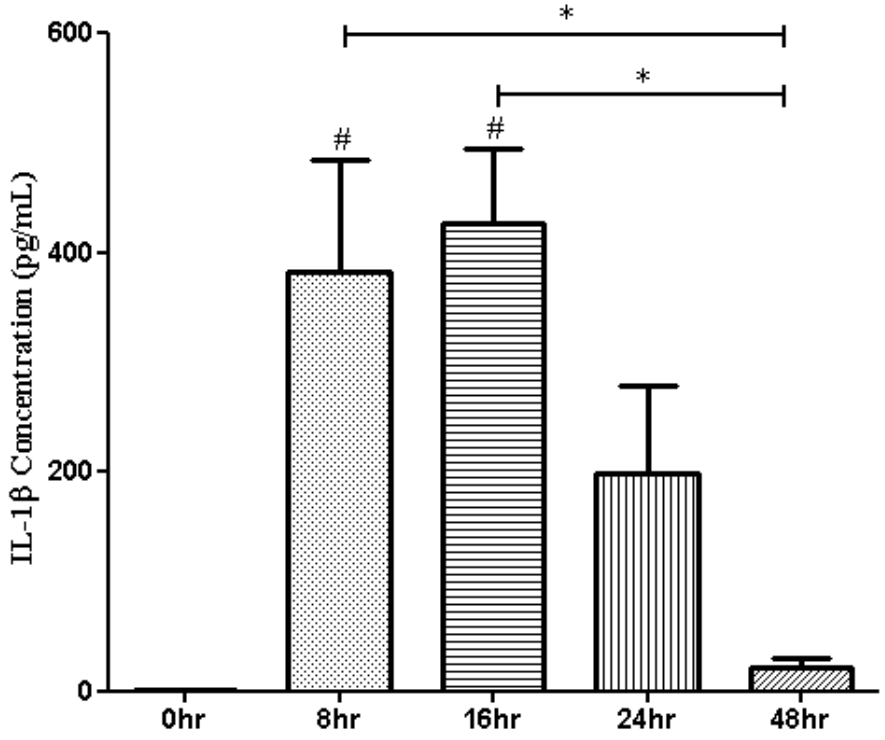

significant differences when compared with 0hr, $p<0.05$
* significant difference between two linked groups, $p<0.05$

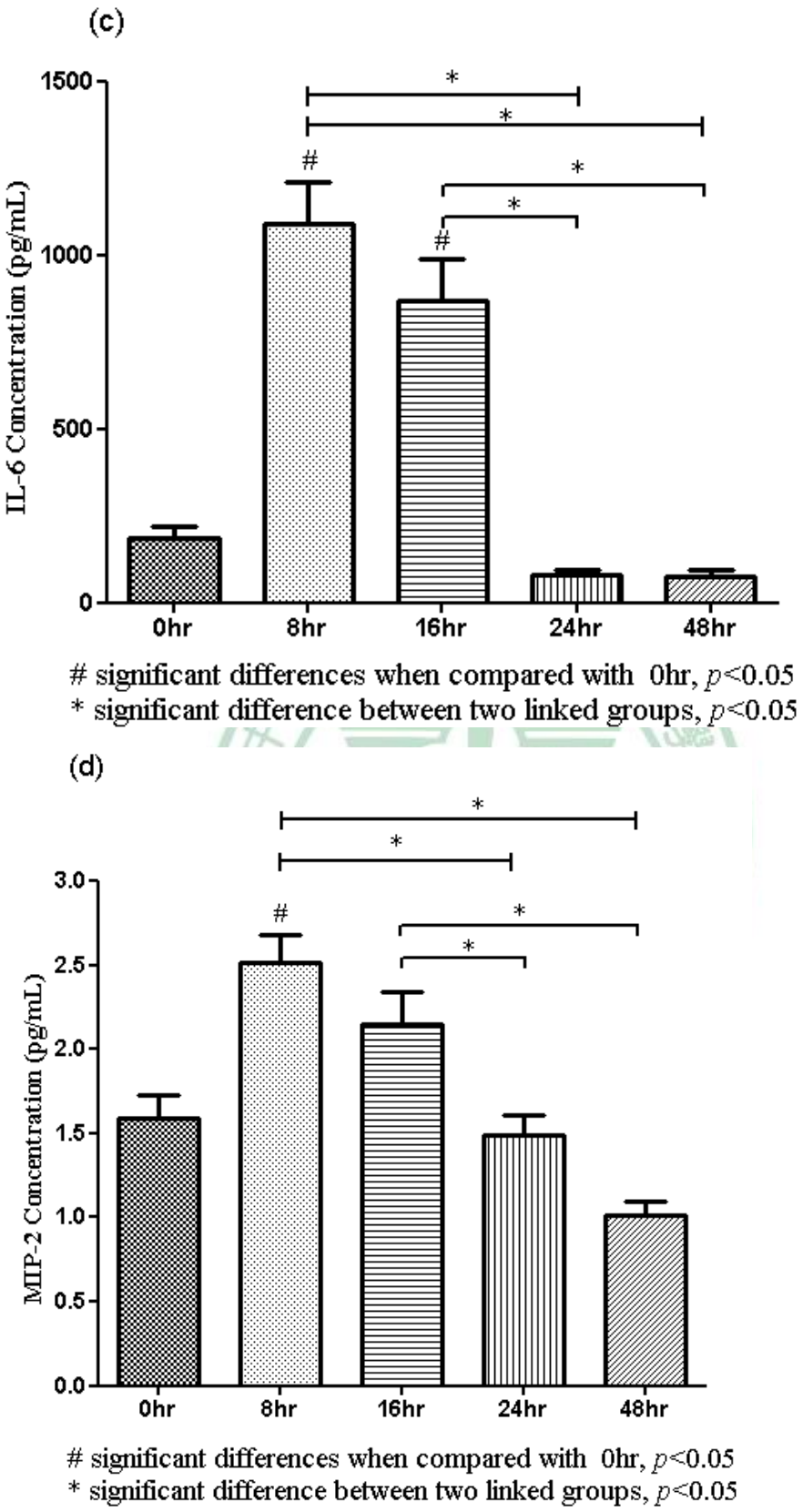

圖 4-7. LPS 誘發 ALI 後大鼠肺泡液發炎相關細胞激素之變化

(a)肺泡液 TNF-α表現量。(b)肺泡液 IL-1β表現量。(c) 肺泡液 IL-6 表現

量。(d) 肺泡液 MIP-2 表現量。#：代表與 0 hr 相比 $p < 0.05$；*代表標示之兩組間比較，呈現統計顯著差異，$p < 0.05$

4-1-7. 大鼠肺泡沖洗液凝血相關細胞激素之變化

以 LPS 誘發大鼠急性肺損傷之時序性肺泡沖洗液凝血相關細胞激素之變化如圖 4-8 所示。(a) 各組在 TATC 之表現量無顯著統計學差異；(b) 肺泡液內之 PAI-1 表現量自第 8 小時後開始顯著上升，以第 16 小時為最高，但 8 hr 以及 16 hr 兩組之間無顯著統計差異。自 24 小時至 48 hr 持續下降，且與 8 hr 及 16 hr 相比，均呈現顯著統計差異。

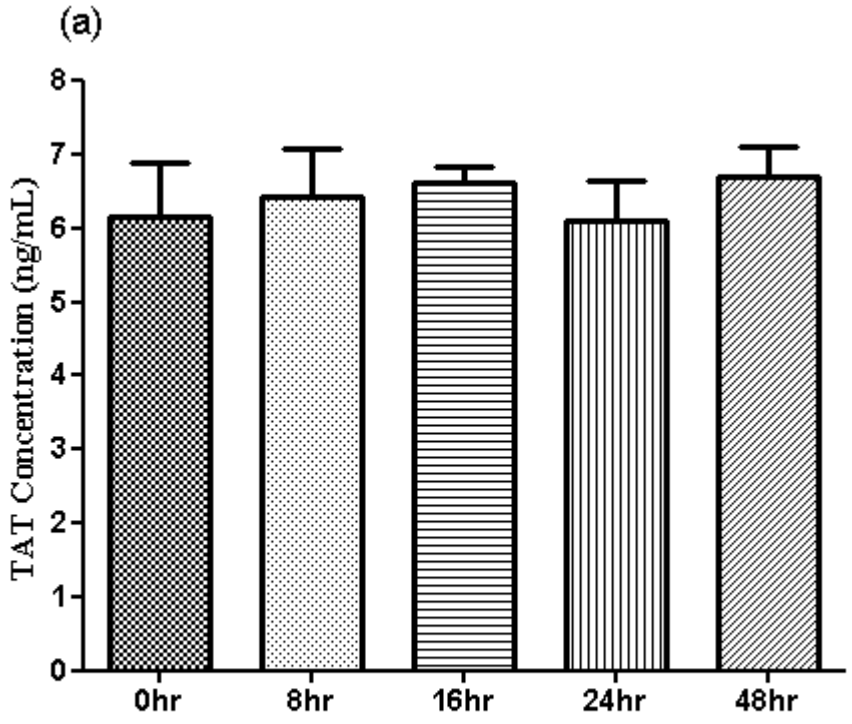

significant differences when compared with 0hr, $p<0.05$
* significant difference between two linked groups, $p<0.05$

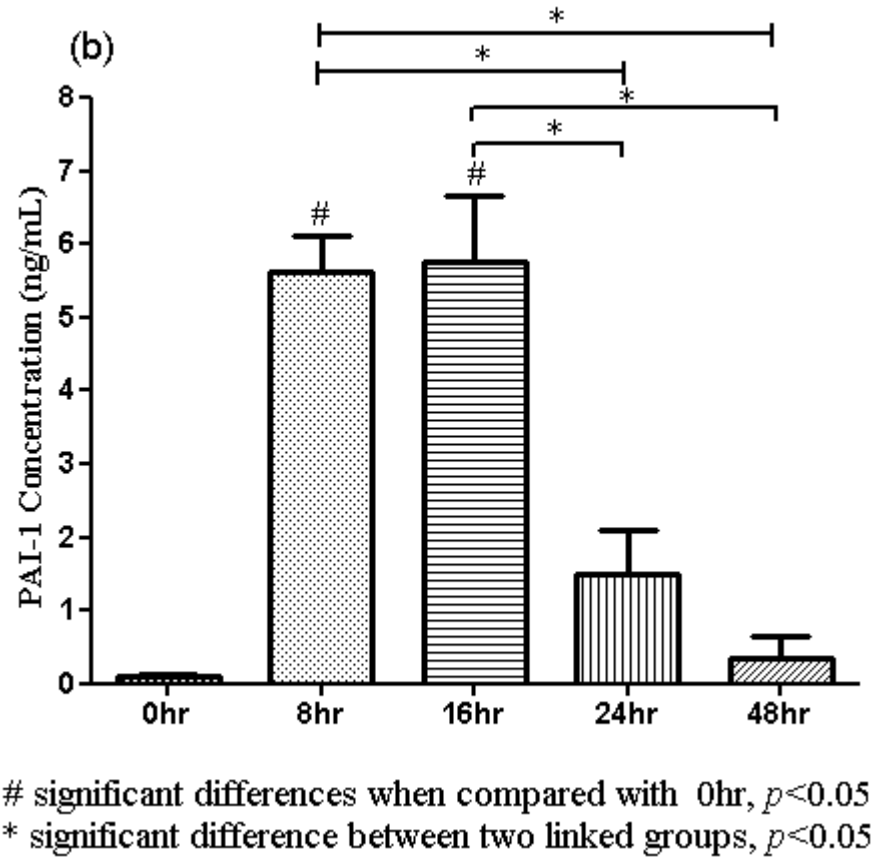

圖 4-8. LPS 誘發 ALI 後大鼠肺泡液凝血相關細胞激素之變化

(a) 肺泡液 TATC 表現量。(b) 肺泡液 PAI-1 表現量。#：代表與 0 hr 相比具有統計學顯著差異, $p < 0.05$；*代表標示之兩組間比較，呈現統計顯著差異，$p < 0.05$。

4-1-8. 大鼠肺組織 MPO 表現量之變化

以 LPS 誘發大鼠急性肺損傷之時序性肺組織 MPO 表現量變化如圖 4-9 所示。肺組織的 MPO 表現量：經誘發後各時間點與 0 小時組相比，均達統計學顯著意義，顯示本實驗模型穩定。MPO 表現量以第 8 小時為最高。與第 8 小時相比，第 24 小時與第 48 小時顯著下降。第 8 小時與

第 16 小時相比，則無統計學差異。與第 16 小時相比，第 48 小時顯著下降，但第 24 小時與第 16 小時相比，則未達統計顯著差異。顯示，給予 LPS 經氣管內誘發後，肺部會產生以中性球為主之急性發炎反應，其 MPO 在第 8 小時達到最高點，然後依時序進展而遞減。

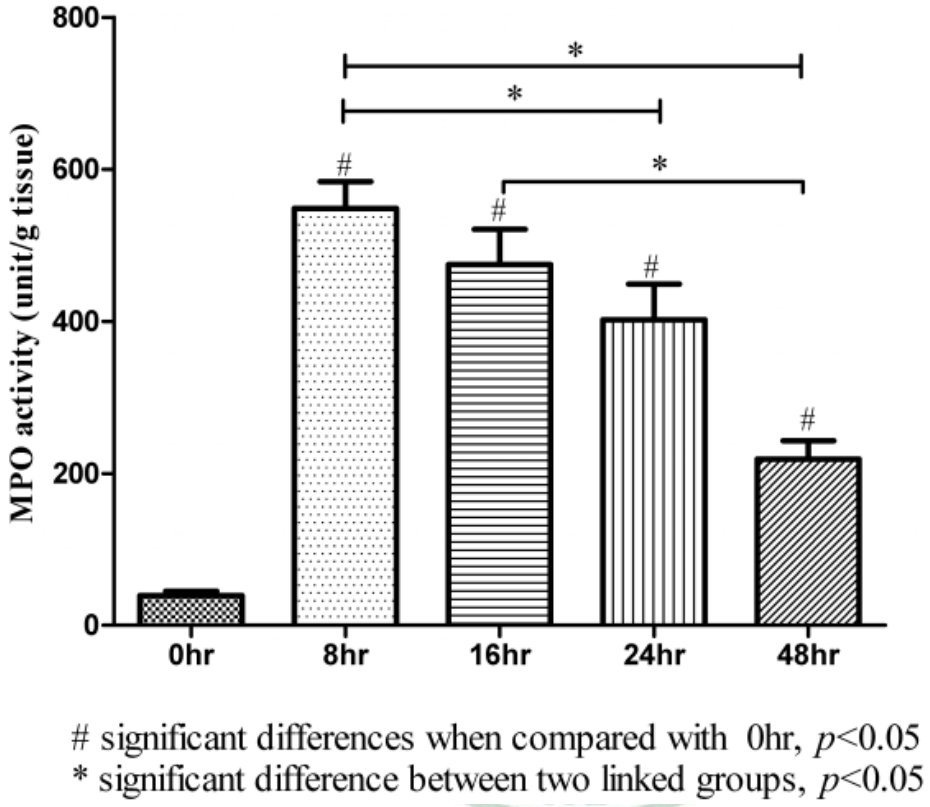

圖 4-9. LPS 誘發 ALI 後大鼠肺組織 MPO 表現量之變化

#：代表與 0 hr 相比具有統計學顯著差異, $p < 0.05$；*代表標示之兩組相比較，呈現統計顯著差異，$p < 0.05$。

4-2. 牡丹皮對 LPS 誘發 ALI/ARDS 大鼠之肺部保護作用及機轉探討

4-2-1. 實驗設計與流程設計

牡丹皮具有清熱涼血、活血化瘀的作用，對於急性肺損傷之發炎反應以及凝血功能紊亂是否具有保護效用或者治療效用，是本實驗所欲探討的問題。在決定治療介入後最佳的觀察時間點後，我們以 LPS-induced ALI 為動物模型，分別在誘發前以及誘發後給予大鼠餵食連續三個劑量口服之牡丹皮，以評估其是否具有治療潛力。大鼠誘發與否、給藥之時間，分成(A) PBS 組；(B) LPS 組；(C) Pre-treatment 組 (MCR-LPS)；(D) Post-treatment 組 (LPS-MCR)。各組於第 16 小時後予以犧牲，並進行後續評估。每組 N=6，實驗流程如圖 4-10 所示。

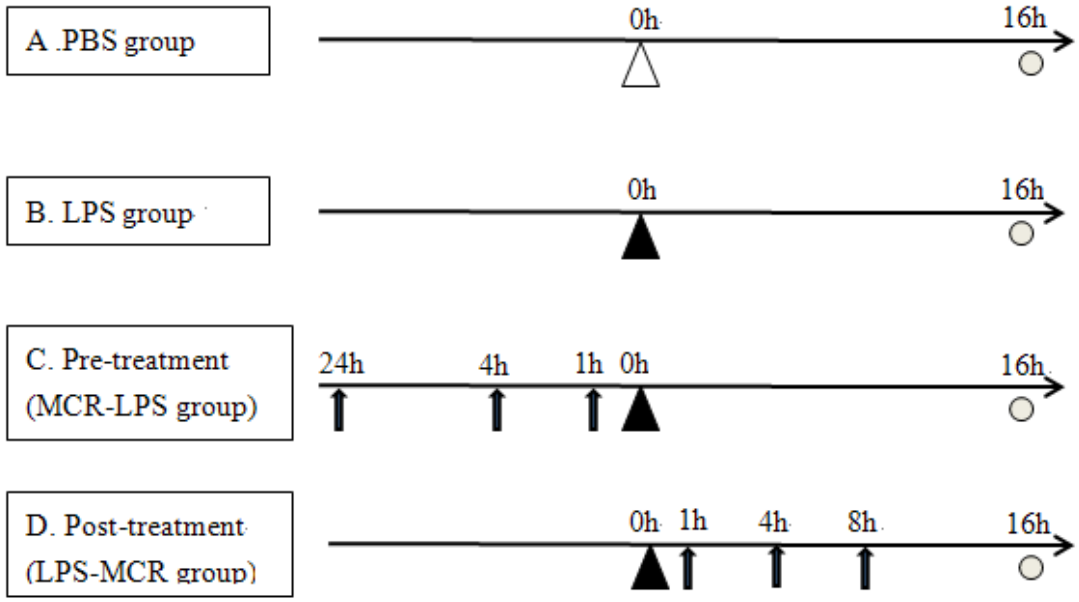

圖 4-10. 牡丹皮治療 LPS 誘發 ALI 效用評估實驗設計

(A) PBS 組：給予氣管內注射 PBS，在第 16 小時後予以犧牲；(B) LPS

組：經氣管給予 LPS 誘發 ALI，在第 16 小時後予以犧牲；C) Pre-treatment 組 (MCR-LPS 組)：在以 LPS 誘發 ALI 前 24 小時，開始給予口服餵食牡丹皮 2 g/Kg 共 3 次，在誘發 ALI 後第 16 小時予以犧牲；(D) Post-treatment 組 (LPS-MCR 組)：在以 LPS 誘發大鼠 ALI 後 1 小時開始，給予口服餵食牡丹皮 2 g/Kg 共 3 次，然後在誘發肺損傷後第 16 小時予以犧牲；符號▲：代表予以 LPS 經氣管內投藥；符號△：代表未施行 LPS 經氣管內投藥；符號○：代表將大鼠犧牲的時間點。

4-2-2. 牡丹皮之 HPLC 指標成分鑑定及不含馬兜鈴酸之確定

牡丹皮中最主要的指標成分為 Paeonol 以及 Paeoniflorin。本實驗以這兩個純化物作為牡丹皮濃縮中藥之比對 (圖 4-11)。使用 Paeonol 作為 standard，在 retention time 為 14.68 分鐘時有一個 peak 值出現 (圖 4-11a)，而本實驗所使用之濃縮牡丹皮中藥粉，與標準品(paeonol) 相比，同樣在 retention time 為 14.68 分鐘時也有一個 peak 值(#)出現 (圖 4-11b)，代表含有指標成分 paeonol。圖 4-11c 為使用 Paeoniflorin 作為 standard，在 retention time 為 8.46 分鐘時有一個 peak 值(**)出現，而本實驗所使用之濃縮牡丹皮中藥粉，與標準品 (paeoniflorin) 相比，同樣在 retention time 為 8.46 分鐘時也有一個 peak 值出現，代表含有指標成分 Paeoniflorin (圖 4-12d)。在投稿的時候，期刊編審委員要求證實本實驗所用之 MCR 中藥

不含馬兜鈴酸，遂進行 HPLC 比對。圖 4-12e 為使用馬兜鈴酸之指標成分 Aristolochic Acid-1(AA-1)作為 standard，在 retention time 為 15.89 分鐘時有一個 peak 值出現，而本實驗所使用之濃縮 MCR 中藥粉，與 AA-1 標準品相比，同樣在 retention time 為 15.89 分鐘時並未出現 peak 值 (圖 4-12f)，代表本實驗所使用的濃縮 MCR 中藥不含有 AA-1。

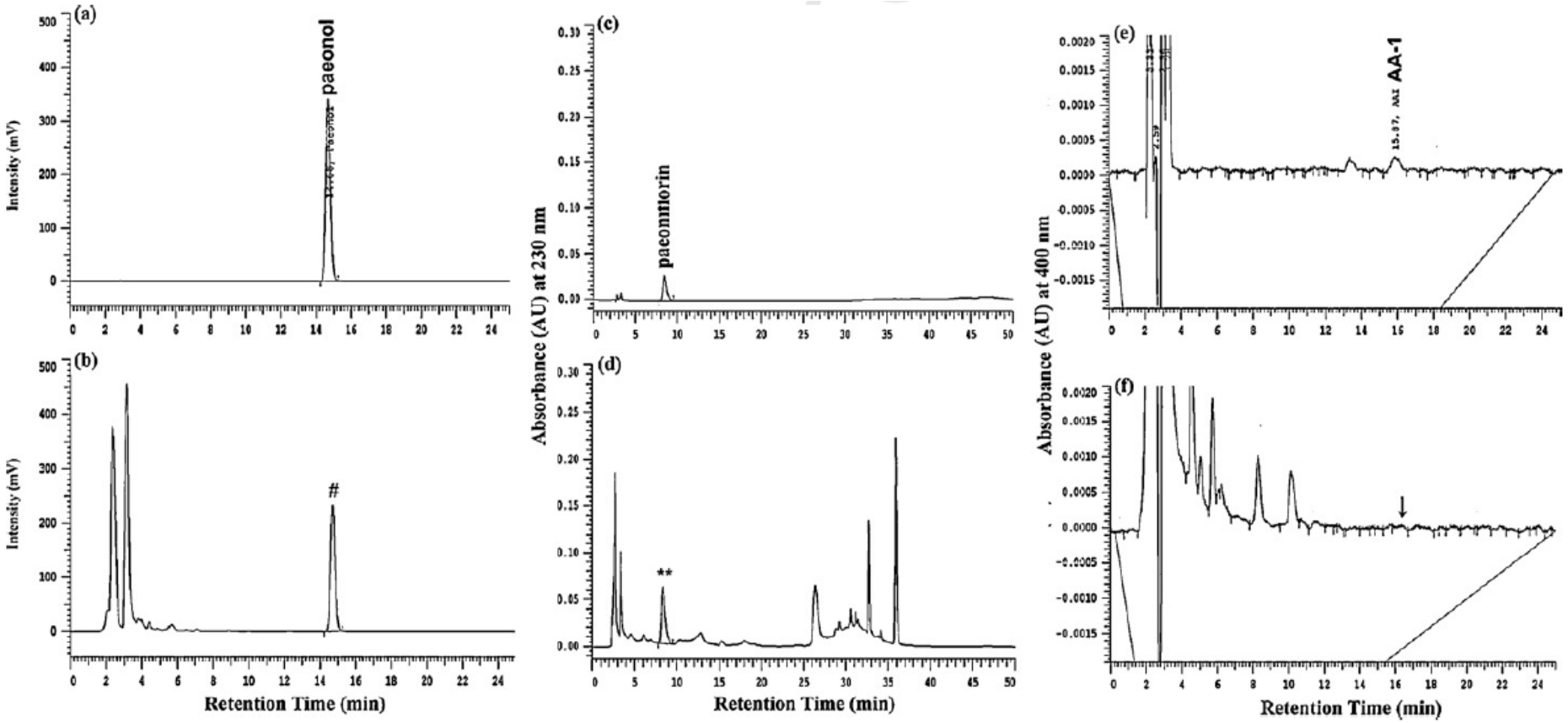

圖4-11. 牡丹皮濃縮藥之HPLC指標成分分析。

(a)使用 Paeonol 作為標準品，於 retention time 為 14.68 分鐘之 HPLC 分析；(b)濃縮牡丹皮中藥粉於 retention time 為 14.68 分鐘之 HPLC 分析；(c)使用 Paeoniflorin 為標準品，於 retention time 為 8.46 分鐘之 HPLC 分析；(d)濃縮牡丹

皮中藥粉於 retention time 為 8.46 分鐘之 HPLC 分析；(e)為使用馬兜鈴酸之指標成分 Aristolochic Acid-1(AA-1)為標準品於 retention time 為 15.89 分鐘之 HPLC 分析;(f) 濃縮牡丹皮中藥粉於 retention time 為 15.89 分鐘之 HPLC 分析。

4-2-3. 大鼠肛溫變化

圖 4-12 為各組在第 0 小時以及第 16 小時之大鼠肛溫變化圖。與 0 小時相比，LPS 組呈顯著體溫下降、PBS 組呈現體溫上升，這個現象與 Time course 實驗結果相似，亦即經過 LPS 16 mg/Kg 誘發後，大鼠會在犧牲前呈現低體溫的現象；而 PBS 為經氣道給與 PBS，大鼠在第 16 小時之肛溫略高。至於給予 MCR 組，不論術前給藥組(MCR-LPS)或者術後給藥組(LPS-MCR)，第 16 小時與第 0 小時之肛溫差異不大，均未達顯著統計差距，顯示給予 MCR 組可能具有直接體溫調節作用，或者經由降低肺損傷程度而減少發炎反應之嚴重度而減少低體溫的發生。

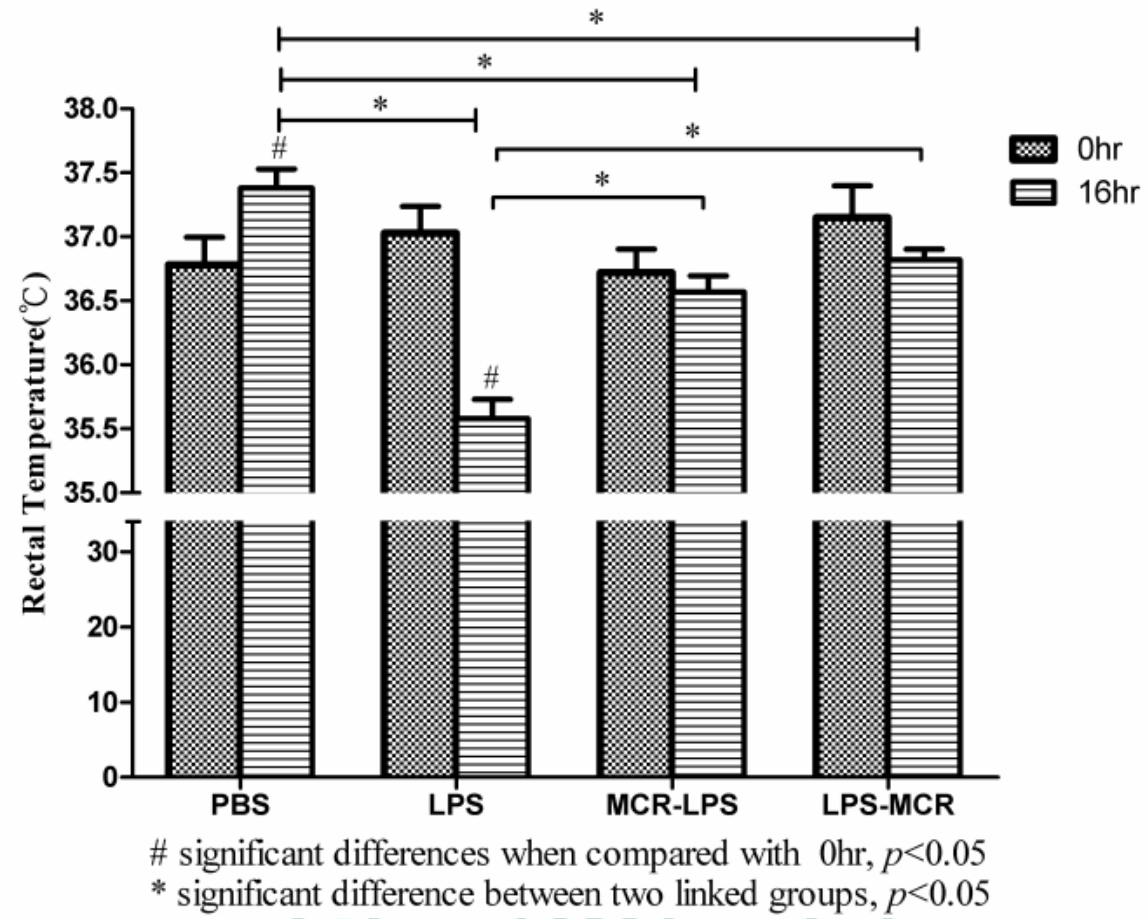

圖 4-12. 牡丹皮治療 LPS 誘發 ALI 之各組肛溫變化圖

PBS 組：經氣道給予 0.5 cc 之 PBS，在第 16 小時後予以犧牲；LPS 組：經氣道給予 LPS (16 mg/Kg)，在誘發後第 16 小時後予以犧牲；MCR-LPS 組：在術前 24 小時開始給予 3 次口服 MCR (2 g/Kg)，然後經氣道給予 LPS (16 mg/Kg)，在誘發後第 16 小時後予以犧牲；LPS-MCR 組：經氣道給予 LPS (16 mg/Kg)，在誘發後 1 小時開始，給予口服餵食 MCR 2 g/Kg 共 3 次，然後在誘發肺損傷後第 16 小時予以犧牲；各組 N=6。#代表與 0 hr 相比，呈現統計顯著差異，$p < 0.05$。*代表標示之兩組相比較，呈現統計顯著差異，$p < 0.05$。

4-2-4. 大鼠病理切片之肺損傷程度變化

本實驗以 LPS 誘發 ALI 之動物模型，來評估 MCR 治療效用，其各組之肺損傷程度變化如表 4-2 以及圖 4-13 以及圖 4-14 所示。肺損傷程度之總分係由 3 個分數加總而得，依次為肺泡內細胞浸潤程度(cellularity)、肺泡內蛋白質滲出程度(protein exudation)以及肺泡內出血程度(hemorrhage)。

在肺損傷總分方面：肺損傷嚴重程度依次為:LPS (48.1±2.2) > LPS-MCR (44.8 ± 1.4) > MCR-LPS (32.2 ± 1.3) > PBS (11.1 ± 1.7)。各組與 PBS 相比，皆有統計顯著差異。給予牡丹皮術前治療組與 LPS 相比 (MCR-LPS & LPS)，肺損傷程度顯著降低；術後治療組與 LPS 組相比 (LPS-MCR & LPS)，肺損傷程度略為下降，但無統計學顯著差異。術前治療組與術後治療組相比 (MCR-LPS & LPS-MCR)，術前給藥組之肺損傷程度較低，達統計學顯著差異。綜上顯示，MCR 術前治療組能降低肺損傷程度。

在肺泡內細胞浸潤程度方面：以 LPS 組為最高(20.2 ± 1.1)，其次為 LPS-MCR 組(15.3 ± 0.8)，然後才是 MCR-LPS 組(12.3 ± 0.9)。其中，MCR-LPS 組較 LPS 組及 LPS-MCR 組為低，達顯著統計差異；LPS 與 LPS-MCR 兩組相比，無顯著統計學差異。顯示牡丹皮術前治療組(MCR-LPS)能降低肺組織內之白血球浸潤。

在肺泡內蛋白質滲出程度方面：以 LPS 組為最高(13.0 ± 0.9)，其次為 LPS-MCR 組(11.1 ± 0.7)，然後才是 MCR-LPS 組(7.9 ± 0.7)。其中，MCR-LPS 組較 LPS 組及 LPS-MCR 組為低，達顯著統計差異；LPS 與 LPS-MCR 兩組相比，無顯著統計學差異。顯示牡丹皮術前治療組(MCR-LPS)能降低肺組織內之蛋白質滲出程度。

在肺泡內出血程度方面：以 LPS-MCR 組為最高(18.4 ± 0.8)，其次為 LPS 組(14.9 ± 0.6)，然後才是 MCR-LPS 組(12.0 ± 0.4)。其中，MCR-LPS 及 LPS 組均較 LPS-MCR 組為低，達顯著統計差異；LPS 與 MCR-LPS 兩組相比，無顯著統計學差異。顯示在誘發大鼠肺損傷後再給予口服 MCR，會加重大鼠肺泡內出血的程度。

表 4-2. 牡丹皮治療 LPS 誘發 ALI 之各組肺損傷程度比較表

	Cellularity	Protein exudation	Hemorrhage	Total Scores
PBS	1.6±0.8	4.5±0.5	5.0±1.2	11.1±1.7
LPS	20.2±1.1$^{\#}$	13.0±0.9$^{\#}$	14.9±0.6$^{\#}$	48.1±2.2$^{\#}$
MCR-LPS	12.3±0.9$^{\#,*}$	7.9±0.7$^{\#,*}$	12.0±0.4$^{\#}$	32.2±1.3$^{\#,*}$
LPS-MCR	15.3±0.8$^{\#,*}$	11.1±0.7$^{\#,\$}$	18.4±0.8$^{\#,*,\$}$	44.8±1.4$^{\#,\$}$

Data are presented as mean ± SEM, *n*=6. **PBS:** PBS group with PBS challenge; **LPS**: LPS group with lipopolysaccharide (LPS) challenge; **MCR-LPS**: MCR-LPS group; oral treatment with *Moutan Cortex Radicis* (MCR) before LPS challenge. **LPS-MCR**: LPS-MCR group; treatment with MCR after LPS challenge. $^{\#}p$ <.05 compared with PBS; $^{*}p$ < .05 compared with LPS; $^{\$}p$ < .05 compared with MCR-LPS

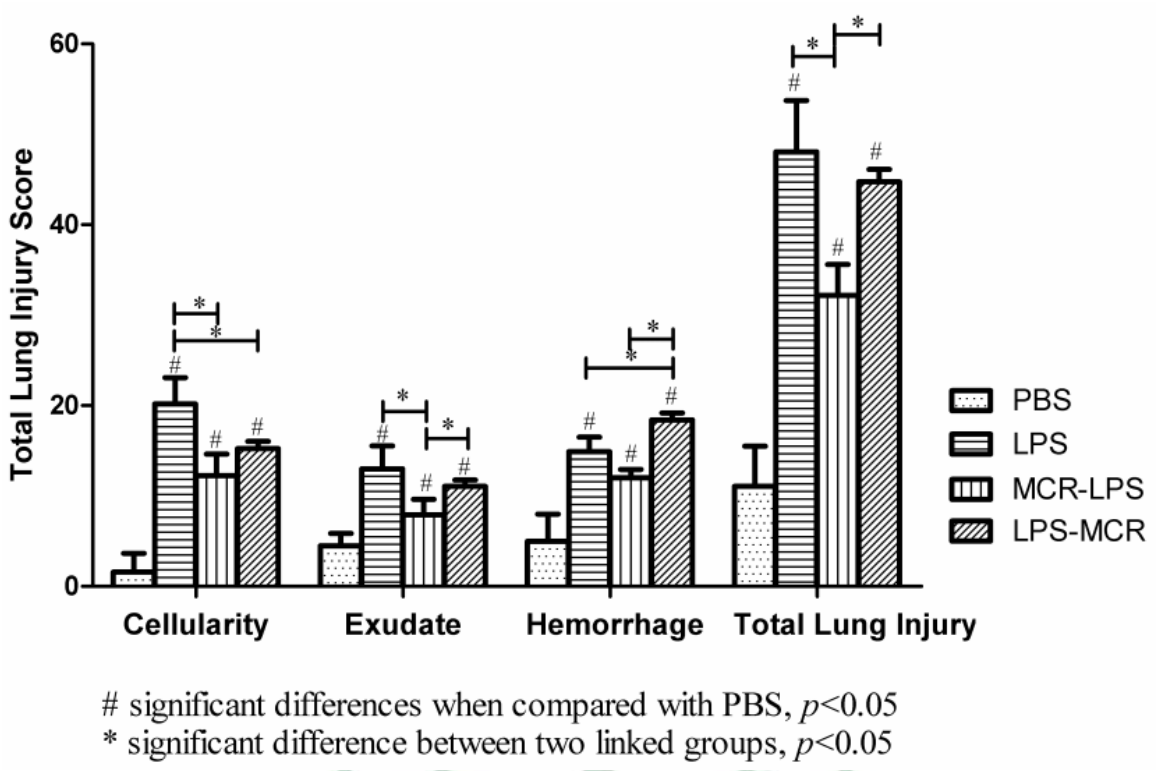

圖 4-13. 牡丹皮治療 LPS 誘發 ALI 之大鼠肺損傷程度

肺損傷程度之總分係由 3 個分數加總而得，依次為肺泡內細胞浸潤程度(cellularity)、肺泡內蛋白質滲出程度(protein exudation)以及肺泡內出血程度(hemorrhage)。#：代表與 PBS 組相比具有統計學顯著差異, $p < 0.05$；*：代表標記之兩組相比，具有統計學顯著差異 $p < 0.05$。

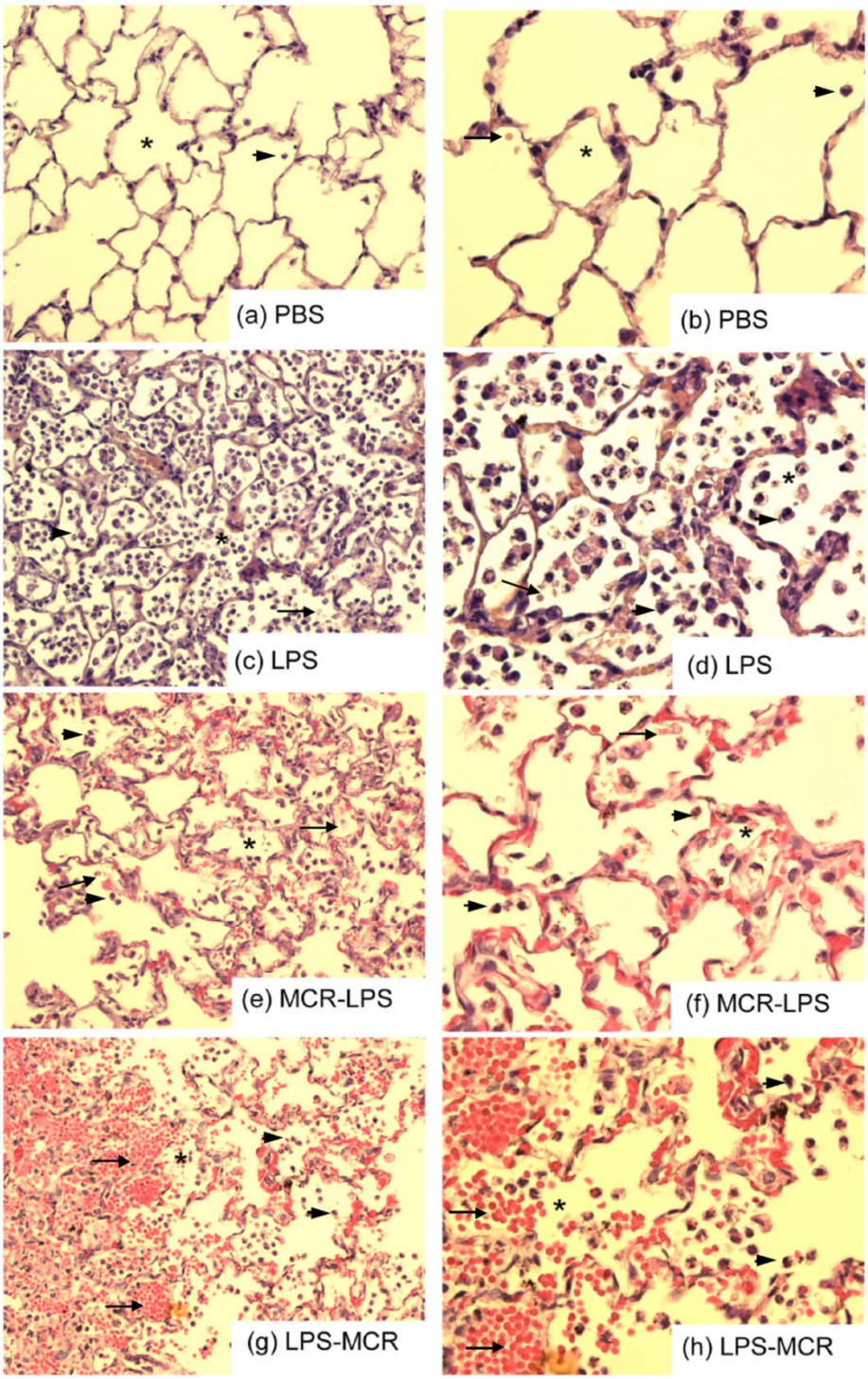

圖 4-14. 牡丹皮治療 LPS 誘發 ALI 之大鼠肺病理切片

本圖之(a)(c)(e)(g)放大倍數為 200 倍之病理切片；(b)(d)(f)(h) 放大倍數為 400 倍之病理切片。(a)(b)為 PBS 組；(c)(d)為 LPS 組；(e)(f)為 MCR-LPS

組；(g)(h)為 LPS-MCR 組。大鼠在犧牲後取其右肺進行病理切片，以 H & E stain 染色後進行肺損傷程度之判定。圖(a) 0 hr 之肺泡內幾乎無中性球、紅血球或蛋白質滲出液存在。肺泡內沉積細胞越多，反應出越嚴重的肺損傷程度。*代表肺泡；▸代表單核球及中性球浸潤；→代表肺泡內的蛋白質及紅血球滲出。

4-2-5. 大鼠肺泡沖洗液細胞計數之變化

以 LPS 誘發大鼠急性肺損傷之動物模型來評估牡丹皮治療效用之大鼠肺泡沖洗液細胞計數變化如圖 4-15 所示。肺泡液之細胞總數(total cell counts)如圖 4-15 (a) 所示，以 LPS 組為最高，與 PBS 組相比，肺泡液細胞數顯著上升達統計學意義，顯示本實驗模型穩定。與 LPS 組相比，給予牡丹皮術前治療組(MCR-LPS)以及術後治療組(LPS-MCR)均能降低肺泡液細胞數，達顯著統計學差異。術前給藥組(MCR-LPS)與術後給藥組(LPS-MCR)相比，MCR-LPS 降低肺泡液細胞數的效果更為明顯，達顯著統計差異。

肺泡液之中性球(neutrophil counts)如圖 4-15 (b) 所示。與 PBS 組相比，LPS 組有顯著上升，代表誘發後肺泡液之細胞浸潤增多以中性球為主。與 LPS 組相比，MCR-LPS 組以及 LPS-MCR 組大鼠之肺泡液中性球皆呈統計學顯著之下降。MCR-LPS 組肺泡液中性球數目與 LPS-MCR

組相比為低，達統計學顯著差異。

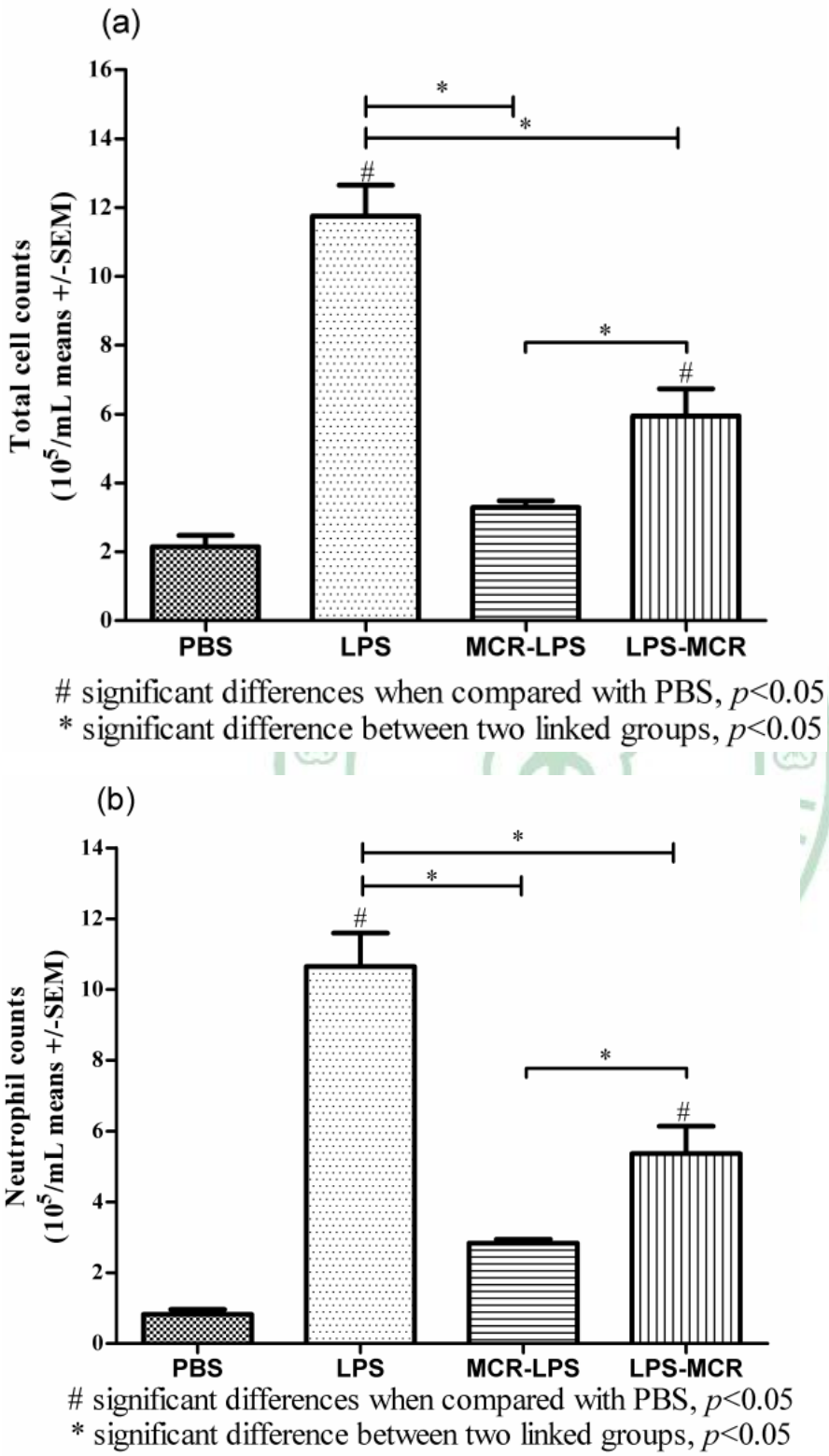

圖 4-15. 牡丹皮治療 LPS 誘發 ALI 之大鼠肺泡液細胞計數

(a)肺泡內各組細胞總數變化(total cell counts)。(b)肺泡內各組中性球

(neutrophil counts)變化。#：代表與 PBS 相比具有統計學顯著差異, $p < 0.05$；*：代表標示之兩組相比較，呈現統計顯著差異，$p < 0.05$。

4-2-6. 大鼠肺泡沖洗液蛋白濃度之變化

以 LPS 誘發大鼠 ALI 之動物模型來評估 MCR 治療效用之大鼠肺泡沖洗液蛋白濃度變化如圖 4-16 所示。肺泡液之蛋白濃度(protein concentration mg/ml)，LPS 組為最高，與 PBS 組相比，達統計學顯著意義，顯示本實驗模型穩定。與 LPS 組相比，給予牡丹皮術前治療組(MCR-LPS)能降低肺泡液蛋白濃度，達顯著統計學差異。術後治療組(LPS-MCR)與 LPS 組相比，雖然有下降之趨勢，但未達統計學顯著差異。MCR-LPS 組較 LPS-MCR 組之肺泡液蛋白濃度為低，但未達統計學顯著差異。顯示，術前給藥組對肺泡液蛋白質滲出情況之改善較術後給藥組優。

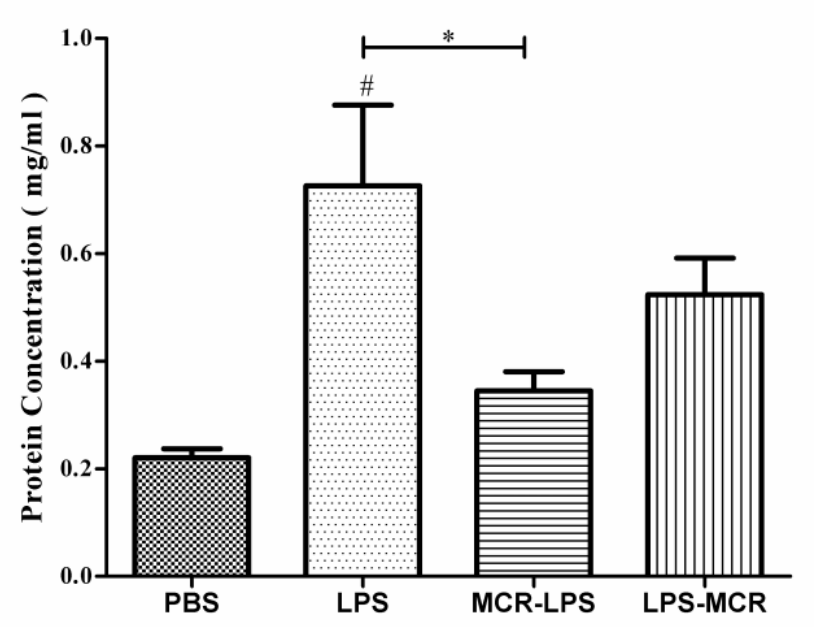

significant differences when compared with PBS, $p<0.05$
* significant difference between two linked groups, $p<0.05$

圖 4-16. 牡丹皮治療 LPS 誘發 ALI 之大鼠肺泡液蛋白濃度

#：代表與 PBS 相比具有統計學顯著差異, $p < 0.05$；*：代表標示之兩組相比較，呈現統計顯著差異，$p < 0.05$。

4-2-7. 大鼠肺泡沖洗液發炎相關細胞激素之變化

以以 LPS 誘發大鼠急性肺損傷之動物模型來評估 MCR 治療效用之大鼠肺泡沖洗液發炎相關細胞激素之變化如圖 4-17 所示。(a) TNF-α 之表現量各組之間無顯著統計差異；(b) IL-1β 之表現量：與 PBS 組相比，LPS 組顯著上升，達統計學顯著差異。與 LPS 相比，MCR-LPS 呈現顯著統計學下降，但 LPS-MCR 雖然有下降趨勢，但未達統計學顯著差異；(c) MIP-2 之表現量：與 PBS 組相比，LPS 組顯著上升，達統計學顯著差異。與 LPS 相比，MCR-LPS 呈現顯著統計學下降，但 LPS-MCR 雖然有下

降趨勢，但未達統計學顯著差異。MCR-LPS 組與 LPS-MCR 組有顯著下降趨勢，達統計顯著差異；(d) IL-6 之表現量：與 PBS 組相比，LPS 組顯著上升，達統計學顯著差異。與 LPS 相比，MCR-LPS 組以及 LPS-MCR 組均為下降，達統計學顯著差異；(e) IL-10 之表現量：與 PBS 組相比，LPS 組顯著上升，達統計學顯著差異。與 LPS 相比， MCR-LPS 呈現顯著統計學下降，但 LPS-MCR 雖然有下降趨勢，但未達統計學顯著差異。

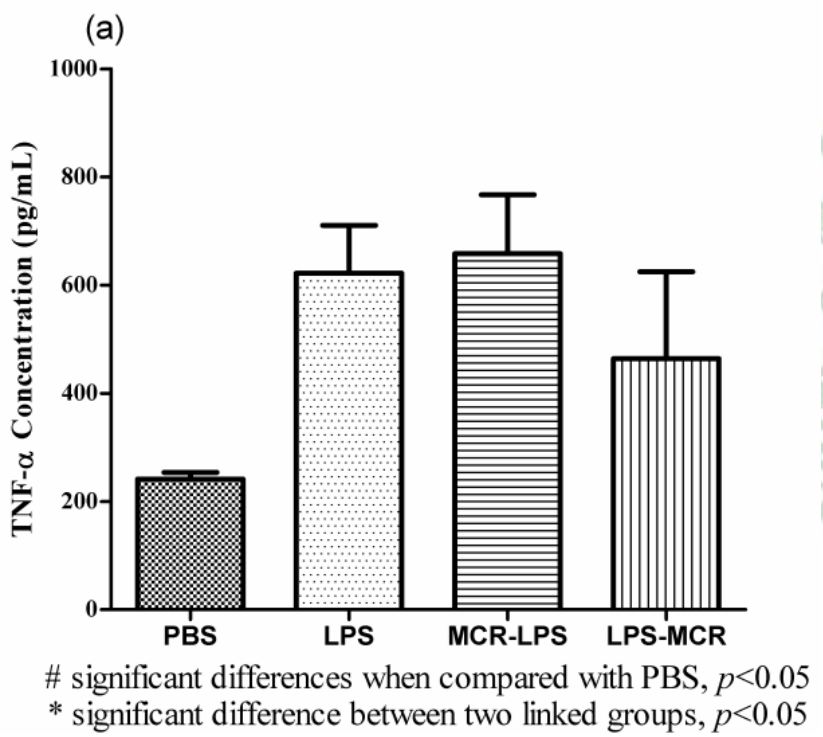

(b)

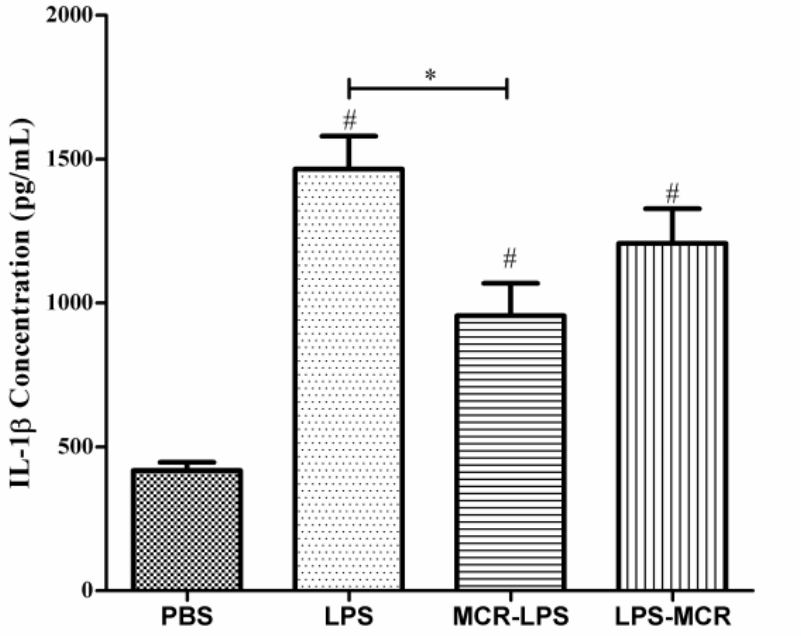

significant differences when compared with PBS, $p<0.05$
* significant difference between two linked groups, $p<0.05$

(c)

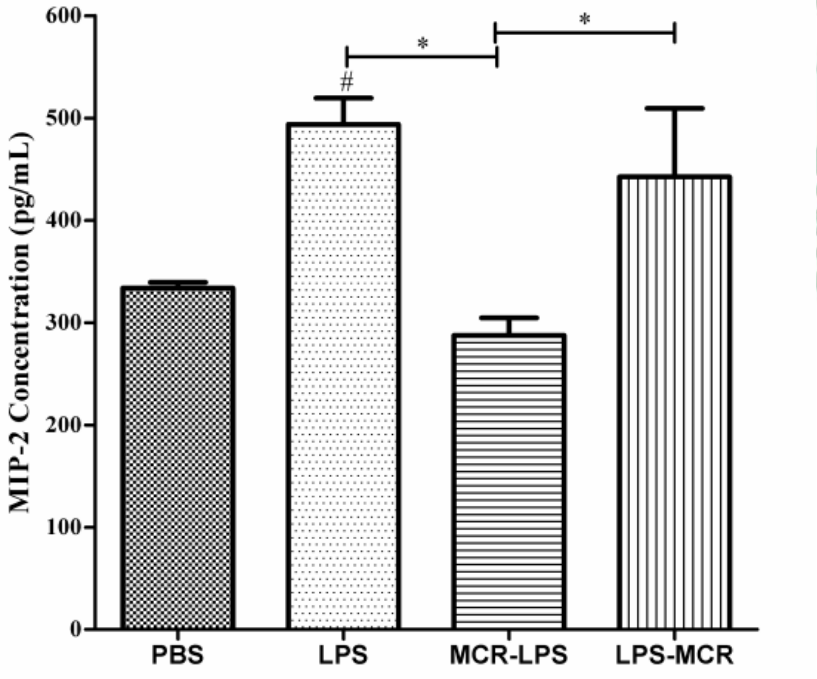

significant differences when compared with PBS, $p<0.05$
* significant difference between two linked groups, $p<0.05$

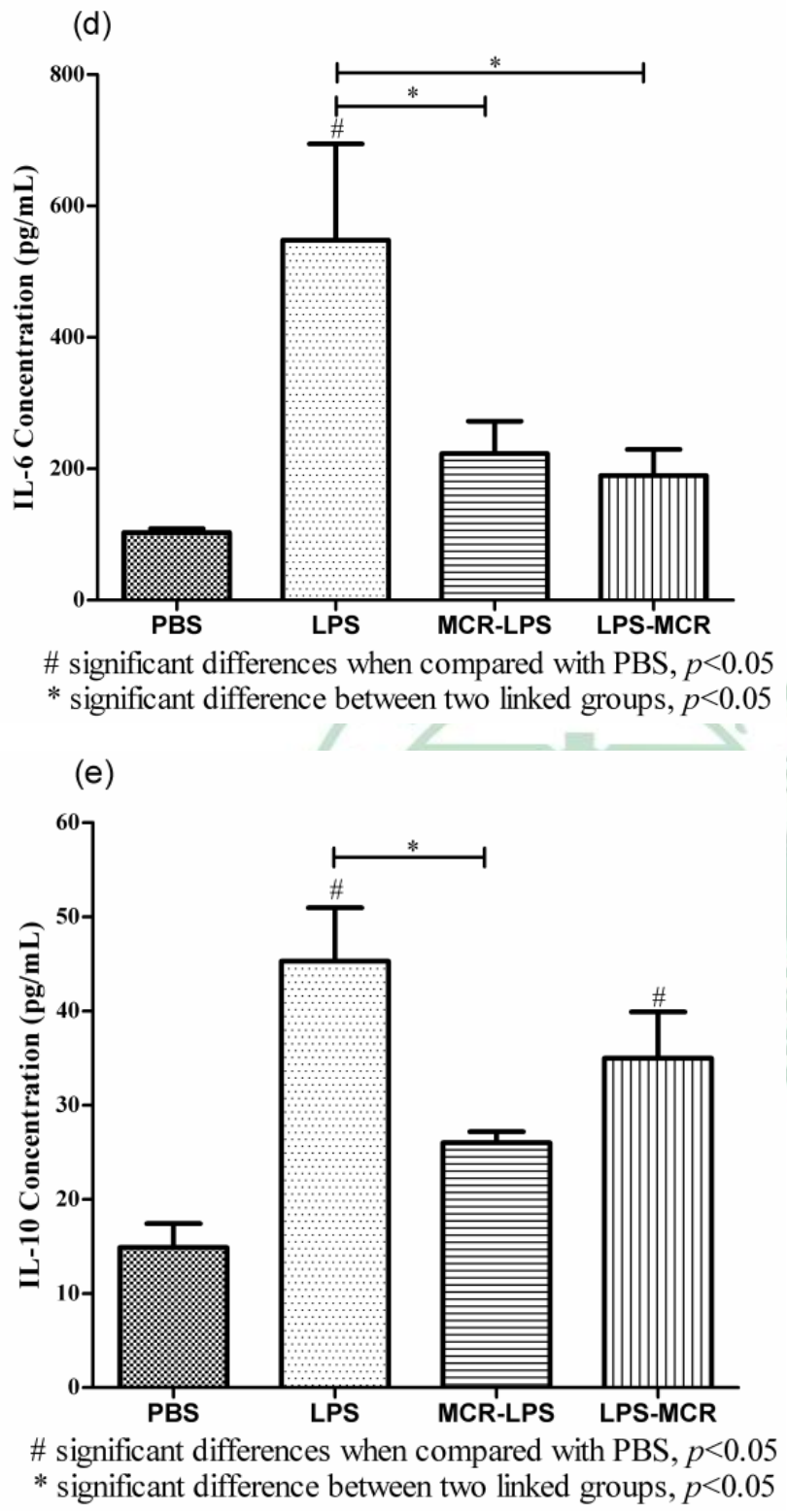

圖 4-17. 牡丹皮治療 LPS 誘發 ALI 之大鼠肺泡液中發炎相關細胞激素之變化

(a) 肺泡液 TNF-α表現量；(b) 肺泡液 IL-1β表現量；(c) 肺泡液 IL-6 表

現量；(d) 肺泡液 MIP-2 表現量；(e) 肺泡液 IL-10 表現量。#：代表與 PBS 相比 $p < 0.05$；*代表標示之兩組相比較，呈現統計顯著差異，$p < 0.05$

4-2-8. 大鼠肺泡沖洗液凝血相關細胞激素之變化

以 LPS 誘發大鼠 ALI 之動物模型來評估牡丹皮治療效用之大鼠肺泡沖洗液凝血相關細胞激素之變化如圖 4-18 所示。(a)各組在 TATC 之表現量無顯著統計學差異；(b)肺泡液內之 PAI-1 表現量：與 PBS 相比，LPS 組上升達統計學顯著差異。其他各組之間均未達統計顯著差異。

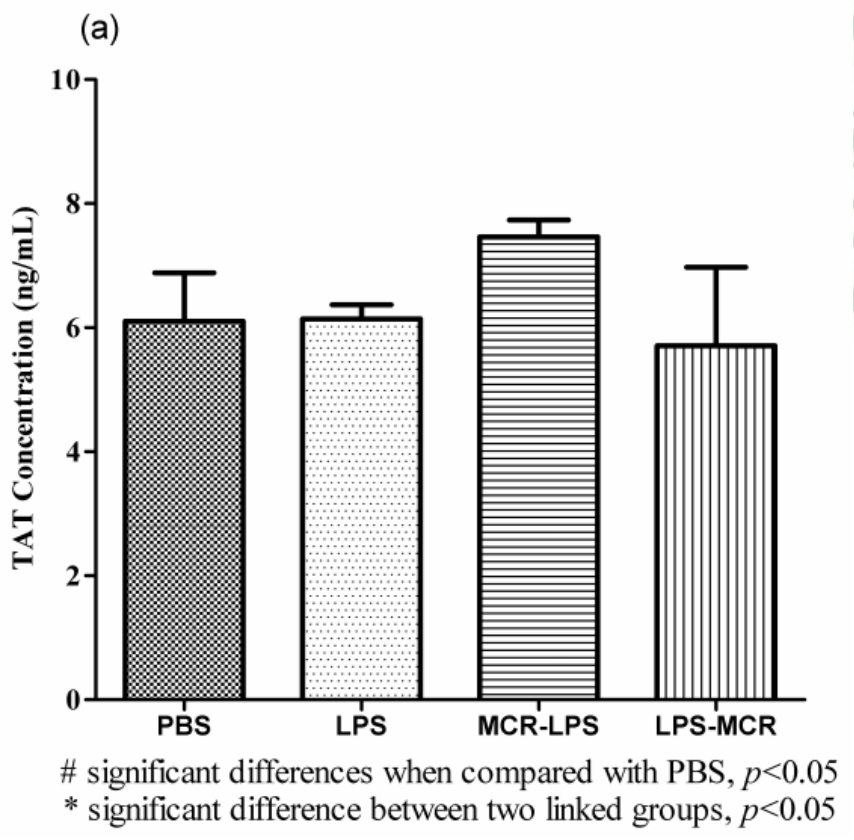

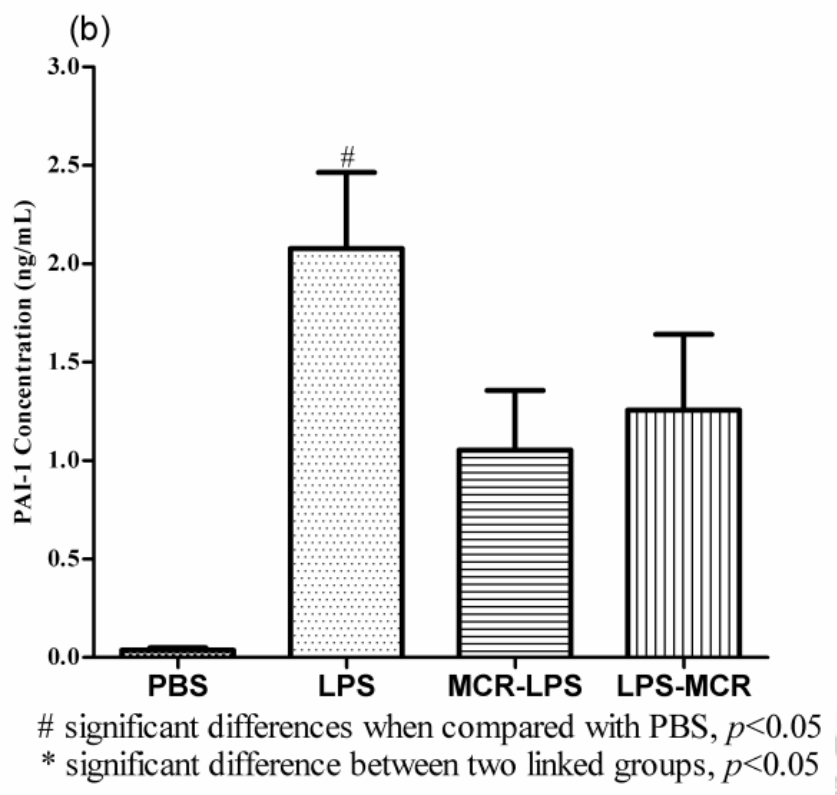

圖 4-18. 牡丹皮治療 LPS 誘發 ALI 之大鼠肺泡液中凝血相關細胞激素之變化

(a)肺泡液 TATC 表現量；(b)肺泡液 PAI-1 表現量。#：代表與 PBS 相比具有統計學顯著差異, $p < 0.05$；*代表標示之兩組相比較，呈現統計顯著差異，$p < 0.05$。

4-2-9. 大鼠肺組織 MPO 表現量之變化

以 LPS 誘發大鼠 ALI 之動物模型來評估 MCR 治療效用之大鼠肺組織 MPO 表現量之變化如圖 4-19 所示。肺組織的 MPO 表現量：與 PBS 組相比，LPS 組達統計學顯著意義，顯示本實驗模型穩定。與 LPS 組相比，MCR-LPS 組以及 LPS-MCR 組之 MPO 表現量均為下降，達統計學

顯著差異。MCR-LPS 與 LPS-MCR 組相比，未達統計學顯著差異。顯示，給予 MCR 口服，不論是術前或術後給藥，均有抑制大鼠肺部 MPO 表現量的效果。

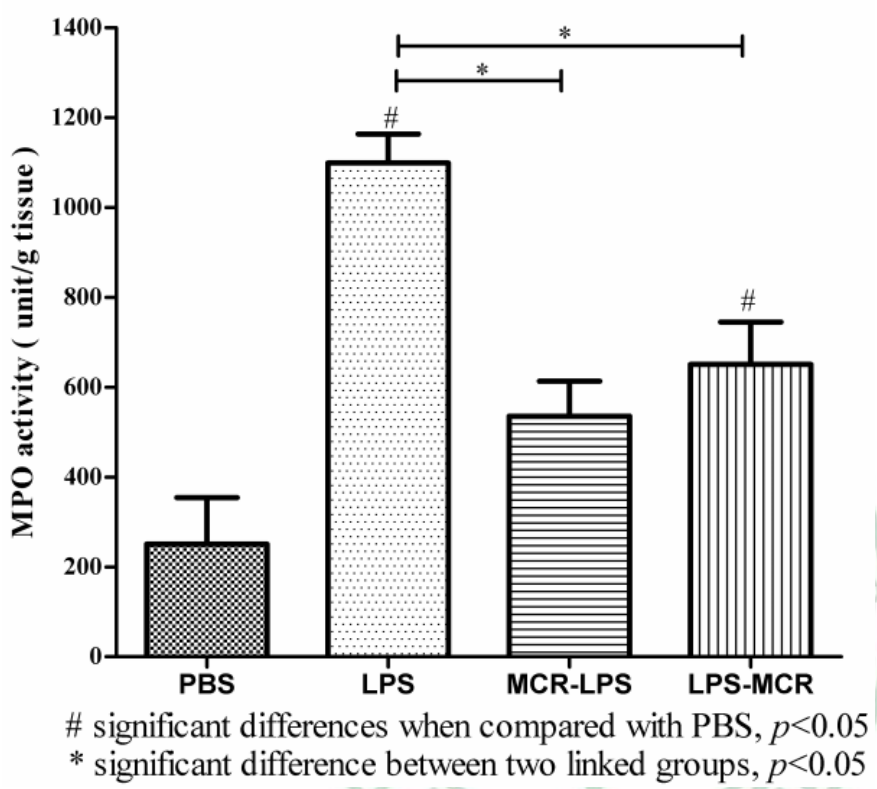

圖 4-19. 牡丹皮治療 LPS 誘發 ALI 之大鼠肺部 MPO 表現量

#：代表與 0 hr 相比具有統計學顯著差異, $p < 0.05$；*代表標示之兩組相比較，呈現統計顯著差異，$p < 0.05$。

4-3. 丹皮酚對 LPS 誘發 ALI/ARDS 大鼠之肺部保護作用及機轉探討

4-3-1. 實驗設計與流程示意

MCR 具有清熱涼血、活血化瘀的作用，上述實驗結果顯示：術前給予大鼠口服 MCR，能對 ALI 之發炎反應產生保護作用。然而，臨床上細菌感染肺部後所產生的 ALI 通常是無法預防性投藥，而且發生後，病人很快地就會進展至器官衰竭，所以注射劑型的藥物在發生後給予，比較接近實際情形。丹皮酚是 MCR 中最重要的純化物，本實驗欲探討在誘發大鼠 ALI 後，給予注射丹皮酚，是否能改善大鼠 ALI 程度，且在治療上是否具有劑量效用。我們以 LPS 誘發 ALI 為動物模型，在誘發後 10 分鐘內給予大鼠腹腔注射丹皮酚(25 mg/Kg 以及 50 mg/kg)，以評估其是否具有治療潛力。大鼠誘發與否、給藥之劑量，分成(A) PBS-DMSO 組(經氣管內給予 PBS，腹腔注射 DMSO)；(B) PBS-Paeonol 組(經氣管內給予 PBS，腹腔注射溶於 DMSO 的 paeonol 25 mg/Kg)；(C) LPS-DMSO 組 (經氣管內給予 LPS16 mg/Kg，腹腔注射 DMSO)；(D) LPS-paeonol-25 組(經氣管內給予 LPS，腹腔注射溶於 DMSO 的 paeonol 25 mg/Kg)；(E) LPS-paeonol-50 組(經氣管內給予 LPS，腹腔注射溶於 DMSO 的 paeonol 50 mg/Kg)。各組於第 16 小時後予以犧牲，並進行後續評估。每組 N=6。實驗流程如圖 4-20 所示。

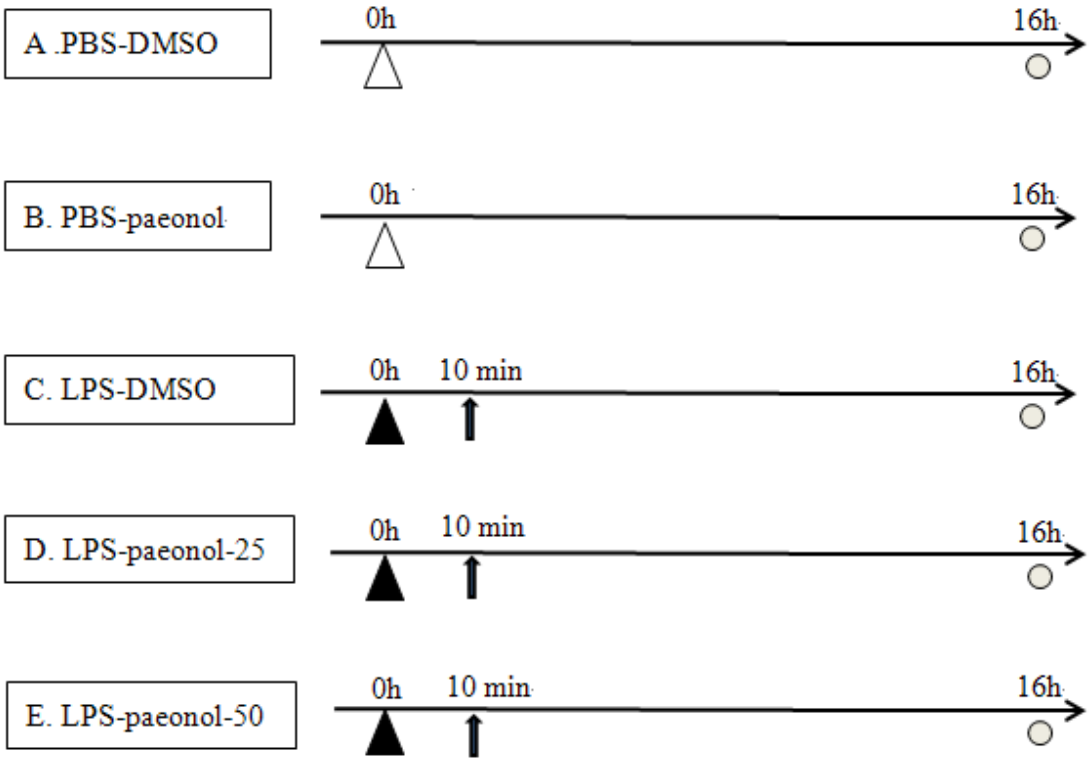

圖 4-20. 丹皮酚治療 LPS 誘發 ALI 效用評估實驗設計

(A)PBS-DMSO (i.t PBS，i.p DMSO)

(B)PBS-Paeonol (i.t PBS，i.p paeonol 25 mg/Kg)

(C)LPS-DMSO (i.t LPS16 mg/Kg，i.p DMSO)

(D)LPS-paeonol-25 組(i.t LPS，i.p paeonol 25 mg/Kg)

(E)LPS-paeonol-50 組(i.t LPS，i.p paeonol 50 mg/Kg)

i.t ：代表經氣管內注射；i.p：代表從腹腔內注射給藥；符號▲：代表予以 LPS 經氣管內投藥；符號△：代表未施行 LPS 經氣管內投藥；符號◯：代表將大鼠犧牲的時間點。

4-3-2. 大鼠肛溫變化

圖 4-21 為各組在第 0 小時以及第 16 小時之大鼠肛溫變化圖。與 0 小時相比，LPS 組與呈顯著體溫下降、PBS 呈現體溫上升，這個現象與 Time course 實驗結果相符合，亦即經過 LPS16 mg/Kg 誘發後，大鼠會在犧牲前呈現低體溫的現象；而 PBS 為經氣道給與 PBS，大鼠在第 16 小時之肛溫略高。至於給予丹皮酚 i.p 治療組(LPS-paeonol-25 以及 LPS-paeonol-50)，第 16 小時與第 0 小時之肛溫差異不大，均未達顯著統計差距，顯示給予丹皮酚可能具有直接體溫調節作用，或者經由降低肺損傷、降低發炎反應之嚴重度而減少低體溫的發生。

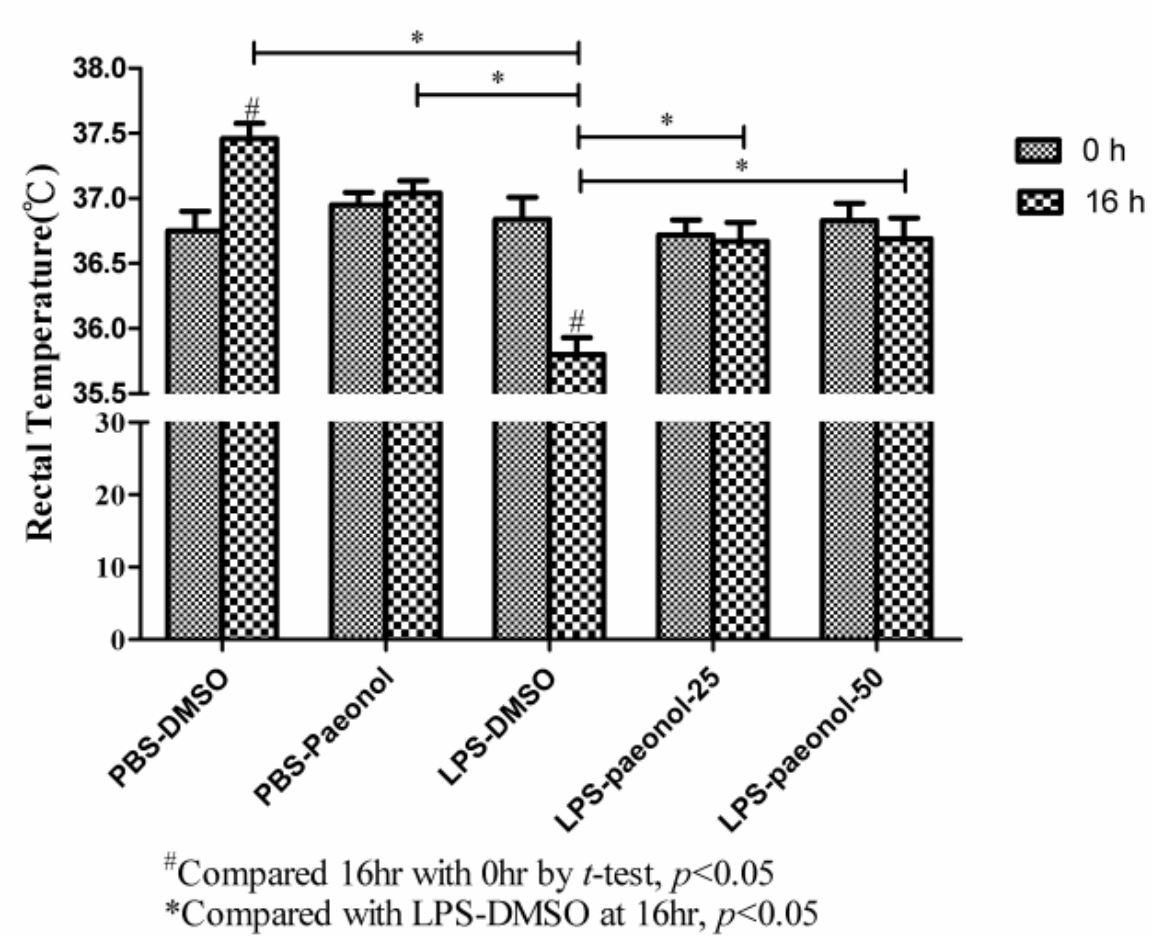

#Compared 16hr with 0hr by *t*-test, $p<0.05$
*Compared with LPS-DMSO at 16hr, $p<0.05$

圖 4-21. 丹皮酚治療 LPS 誘發 ALI 之各組肛溫變化圖

#代表各組之第 16 小時與第 0 小時相比，呈現統計顯著差異，$p < 0.05$。

*代表標示之兩組相比較，呈現統計顯著差異，$p < 0.05$。

4-3-3. 大鼠病理切片之肺損傷程度變化

本實驗以 LPS 誘發急性大鼠肺損傷之動物模型，來評估丹皮酚治療效用，其各組之肺損傷程度變化如表 4-3 以及圖 4-22 以及圖 4-23 所示。肺損傷程度之總分係由 3 個分數加總而得，依次為肺泡內細胞浸潤程度(cellularity)、肺泡內蛋白質滲出程度(protein exudation)以及肺泡內出血程度(hemorrhage)。

在肺損傷總分方面：肺損傷嚴重程度依次為: LPS-DMSO (45.4 ± 1.0) > LPS-paeonol-25 (26.8 ± 2.4) > LPS-paeonol-50 (23.7 ± 2.9) > PBS-DMSO (19.0 ± 2.5) > PBS-paeonol (14.9 ± 1.2)。PBS-paeonol 與 PBS-DMSO 相比，無統計學差異，且注射丹皮酚反而使損傷總分有下降的趨勢，顯示了丹皮酚注射本身並不會造成未誘發大鼠之肺損傷。LPS-DMSO 與 PBS-DMSO 相比，達統計學顯著差異，顯示本實驗誘發模型穩定。給予丹皮酚治療組(LPS-paeonol-25 以及 LPS-paeonol-50)與 LPS-DMSO 相比，均能顯著降低肺損傷程度，且有劑量效應。使用丹皮酚 50 mg/kg 為最佳治療劑量。

在肺泡內細胞浸潤程度方面：以 LPS-DMSO 組為最高(18.0 ± 0.7)，其次為 LPS-MCR 組(15.3 ± 0.8)，然後才是 LPS-paeonol-25 組(10.8 ± 0.9)以及

LPS-paeonol-50 組(9.1 ± 1.2)，治療組與 LPS-DMSO 相比，皆達統計學顯著差異。顯示丹皮酚注射組能降低肺組織內之白血球浸潤。

在肺泡內蛋白質滲出程度方面：以 LPS-DMSO 組為最高(10.9 ± 0.8)，然後才是 LPS-paeonol-25 組(4.5 ± 0.8)以及 LPS-paeonol-50 組(4.1 ± 0.4)，治療組與 LPS-DMSO 相比，皆達統計學顯著差異。顯示丹皮酚注射組能降低肺組織內之蛋白質滲出程度。

在肺泡內出血程度方面：以 LPS-DMSO 組為最高 (16.4 ± 1.0)，然後才是 LPS-paeonol-25 組(11.5 ± 1.5)以及 LPS-paeonol-50 組(10.5 ± 1.5)，LPS-paeonol-50 組與 LPS-DMSO 相比，達統計學顯著差異。顯示注射丹皮酚 50 mg/kg 能降低肺泡內出血的程度。

表 4-3. 丹皮酚治療 LPS 誘發 ALI 之各組肺損傷程度比較表

	Cellularity	Protein exudation	Hemorrhage	Scores
PBS-DMSO	7.2± 1.0	3.8±0.6	8.1±1.8	19.0±2.5
PBS-paeonol	4.5±0.2	2.7±0.6	7.8±0.7	14.9±1.2
LPS-DMSO	18.0±0.7	10.9±0.8	16.4±1.0	45.4±1.0
LPS-paeonol-25	10.8±0.9$^{\#}$	4.5±0.8$^{\#}$	11.5±1.5	26.8±2.4$^{\#}$
LPS-paeonol-50	9.1±1.2$^{\#}$	4.1±0.4$^{\#}$	10.5±1.5$^{\#}$	23.7±2.9$^{\#}$

Data are presented as mean ± SEM, *n*=6. **PBS-DMSO:** PBS group，i.t challenge with PBS and i.p 1ml DMSO; **PBS-paeonol**: PBS-paeonol group，i.t challenge with PBS and i.p with paeonol 25 mg/kg dissolved in 1 ml of DMSO; **LPS-DMSO**: LPS-DMSO group，i.t challenge with LPS and i.p with 1 ml DMSO；**LPS-paeonol-25**: LPS-paeonol-25 mg/kg group，i.t challenge with LPS and i.p with paeonol 25 mg/kg dissolved in 1ml of DMSO；**LPS-paeonol-50**: LPS-paeonol-50 mg/kg group，i.t challenge with LPS and i.p with paeonol 50 mg/kg dissolved in 1ml of DMSO；$^{\#}p < 0.05$ compared with LPS-DMSO

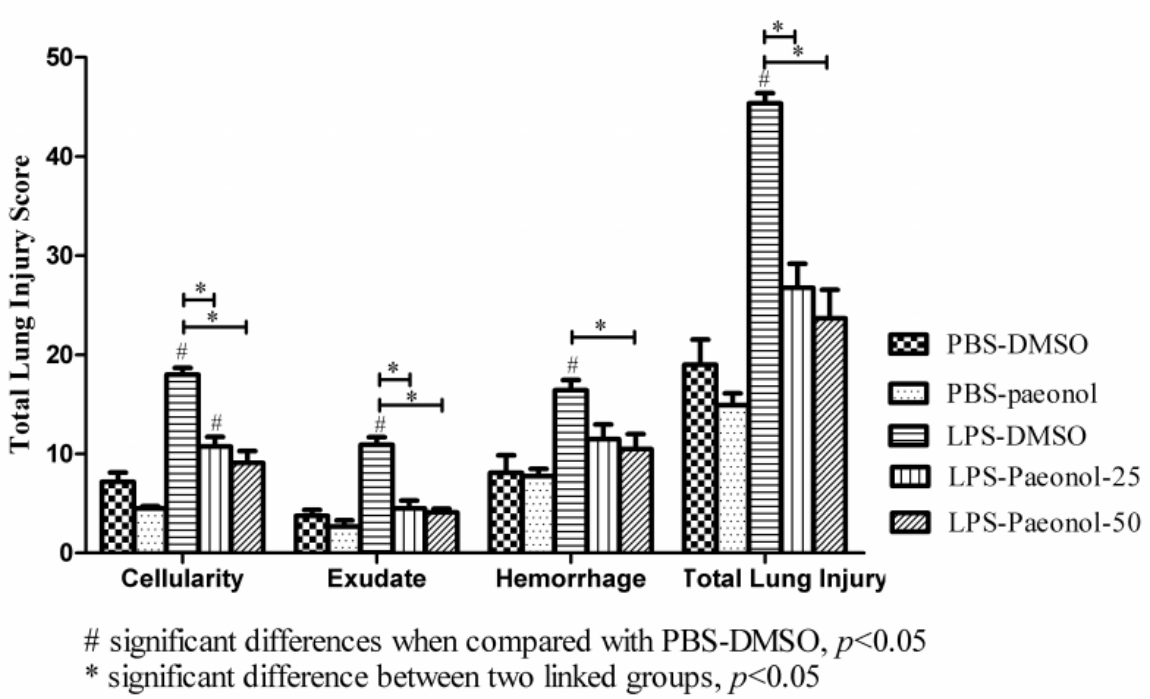

圖 4-22. 丹皮酚治療 LPS 誘發 ALI 之大鼠肺損傷程度

肺損傷程度之總分係由 3 個分數加總而得，依次為肺泡內細胞浸潤程度(cellularity)、肺泡內蛋白質滲出程度(protein exudation)以及肺泡內出血程度(hemorrhage)。#：代表與 PBS 組相比具有統計學顯著差異, $p < 0.05$；*：代表標記之兩組相比，具有統計學顯著差異 $p < 0.05$。

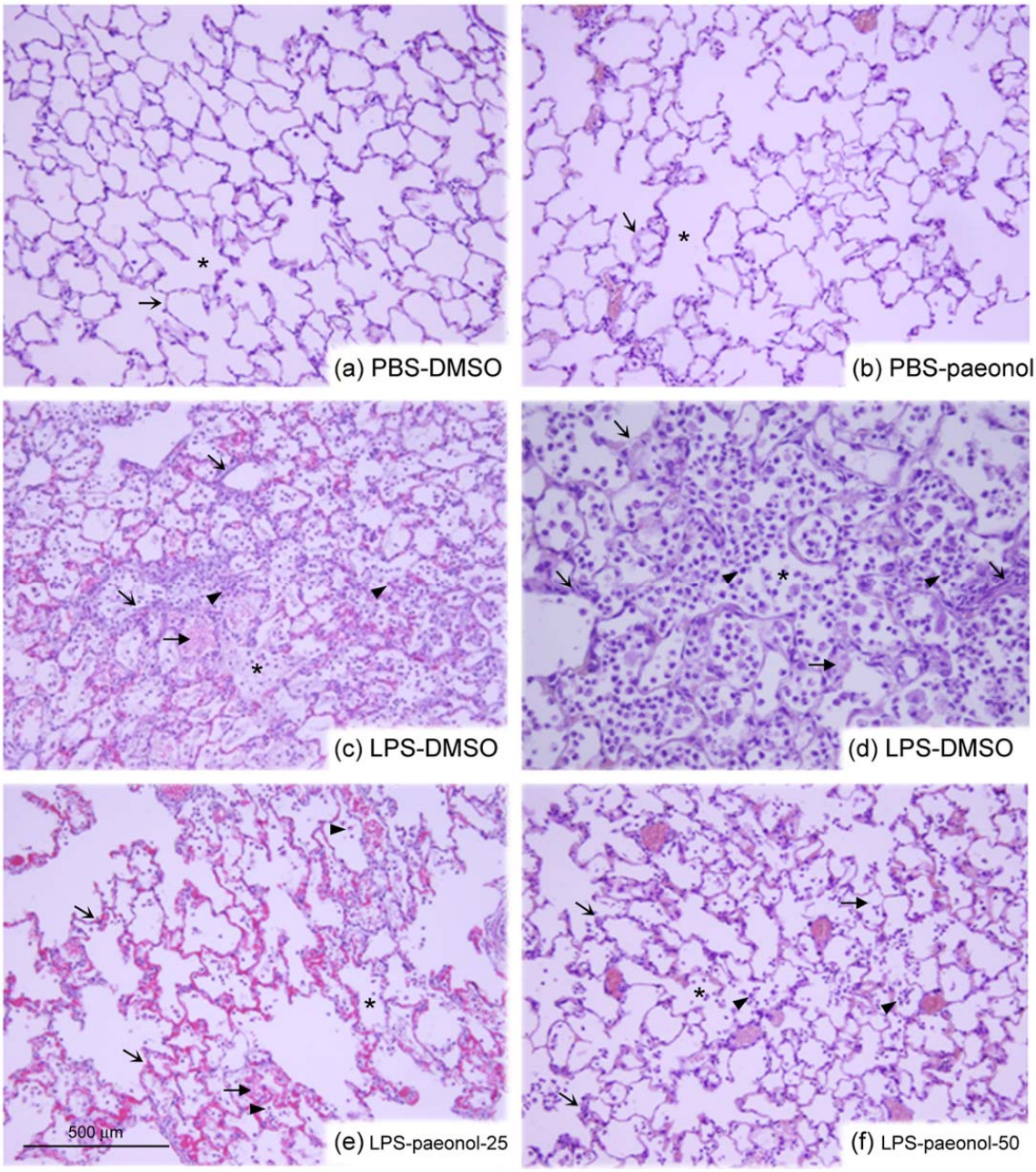

圖 4-23. 丹皮酚治療 LPS 誘發 ALI 之大鼠肺病理切片

本圖之(a) (b) (c) (e) (f) 放大倍數為 200 倍之病理切片; 本圖之 (d) 放大倍數為 400 倍之病理切片。(a) 為 PBS-DMSO 組；(b) 為 PBS-paeonol 組；(c) 為 LPS-DMSO 組；(d) LPS-DSMO 組，放大至 400 倍；(e) 為 LPS-paeonol-25 組；(f) 為 LPS-paoenol-50 組。大鼠在犧牲後取其右肺進行病理切片，以 H&E stain 染色後進行肺損傷程度之判定。圖 (a) (b) 係以 PBS 經氣管內灌

注，可發現其肺泡內幾乎無中性球、紅血球或蛋白質滲出液存在。圖(c)(d)係以 LPS 經氣道內誘發急性大鼠肺損傷，可見其肺泡內之細胞浸潤、蛋白質滲出以及紅血球滲漏明顯，反應出較為嚴重的肺損傷程度。圖(e)(f)係以 LPS 經氣道內誘發急性大鼠肺損傷後，給予腹腔內注射丹皮酚作為治療。與(c)(d)相比，可見其肺泡內之細胞浸潤、蛋白質滲出以及紅血球滲漏情形較為改善，反應出肺損傷程度經治療後的降低。*代表肺泡；▸代表單核球及中性球浸潤；→代表肺泡內的蛋白質及紅血球滲出。

4-3-4. 大鼠肺部濕重之變化

肺部水腫程度與急性肺損傷之嚴重度呈現正相關。為了要評估給予丹皮酚 50mg/kg 注射治療後是否會改善大鼠肺組織水腫程度，進行了這個實驗。將各組大鼠犧牲後取出肺臟，分離出左右兩頁，至於固定重量之錫箔紙上秤重，所得到的重量為濕重(Wet Lung weight，WLW)，將錫箔紙與雙肺質於 60℃之烘箱置放 48 小時後取出，此時所秤之重量為乾重(Dry lung weight, DLW)。將濕重減去乾重(WLW-DLW)，所得的重量就是大鼠肺部的淨濕重(Lung wet gain, LWG)(圖 4-24)。如圖所示，經過 LPS 誘發之 LPS-DMSO 組以及 LPS-paeonol-50 組與 PBS-DMSO 組相比，淨濕重(LWG)皆呈統計顯著上升。PBS-paeonol 組與 PBS-DMSO 組相比，並無統計學差異，顯示丹皮酚之注射並不會造成健康大鼠之肺水腫。LPS-paeonol-5 組與

LPS-DMSO 組相比，呈統計學顯著之下降，顯示丹皮酚治療可以改善 LPS 所致肺損傷之肺水腫。

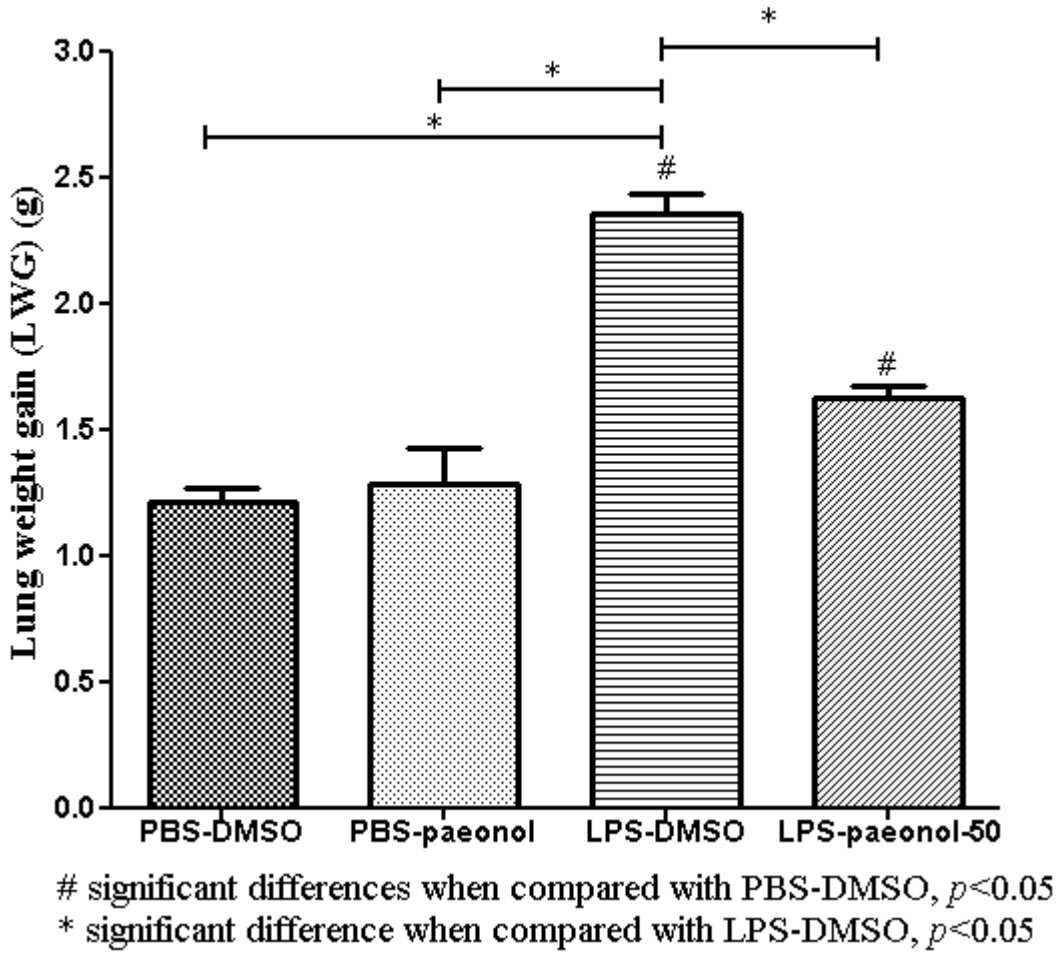

圖 4-24. 丹皮酚治療 LPS 誘發 ALI 之大鼠肺部濕重變化

#：代表與 PBS-DMSO 相比具有統計學顯著差異, $p < 0.05$；*：代表標示之兩組相比較(與 LPS-DMSO 相比)，呈現統計顯著差異，$p < 0.05$。

4-3-5. 大鼠肺泡沖洗液細胞計數之變化

以 LPS 誘發大鼠 ALI 之動物模型來評估丹皮酚治療效用之大鼠肺泡沖洗液細胞計數變化如圖 4-3-5 所示。圖 4-25 (a)所示，PBS-paeonol 與

PBS-DMSO 相比，無統計學差異，且注射 paeonol 反而使肺泡液內的細胞總數有下降的趨勢，顯示了丹皮酚注射本身並不會造成未誘發大鼠之肺發炎。LPS-DMSO 與 PBS-DMSO 相比，達統計學顯著差異，顯示本實驗誘發模型穩定。給予丹皮酚治療組(LPS-paeonol-25 以及 LPS-paeonol-50)與 LPS-DMSO 相比，均能顯著降低肺泡液內的細胞總數，且有劑量效應。肺泡液之中性球(neutrophil counts)如圖 4-25 (b)所示。與 PBS-DMSO 組相比，LPS-DMSO 組有顯著上升，代表誘發後肺泡液之細胞浸潤增多以中性球為主。給予丹皮酚治療組(LPS-paeonol-25 以及 LPS-paeonol-50)與 LPS-DMSO 相比，均能顯著降低肺泡液內的中性球數，且有劑量效應。因此，使用丹皮酚 50 mg/kg 為最佳治療劑量。

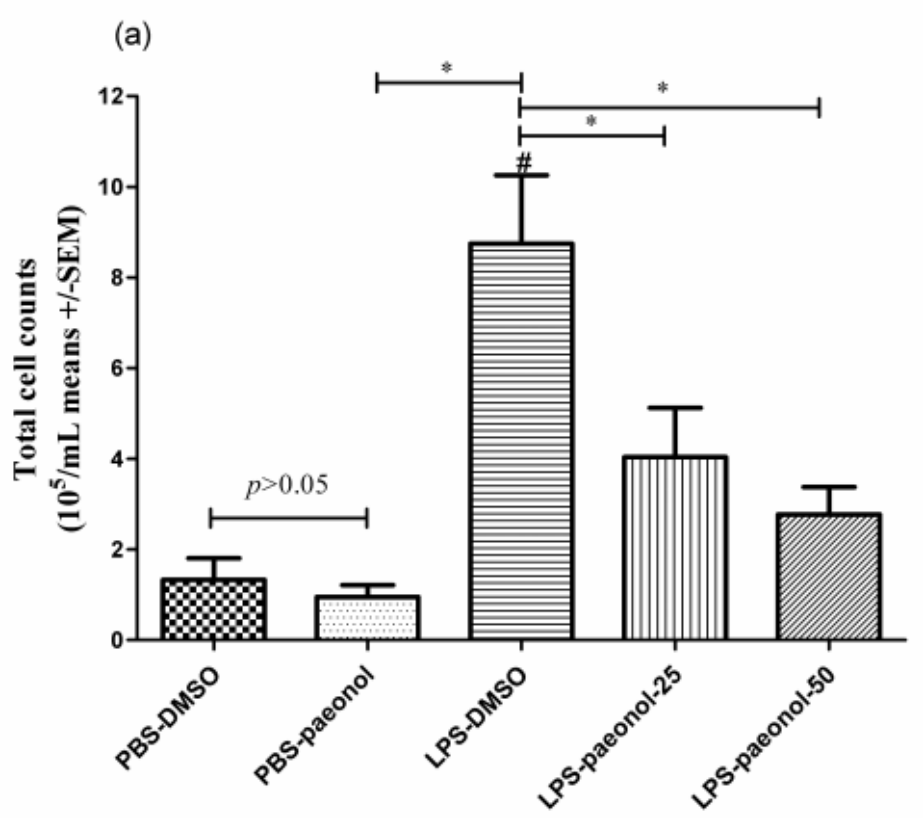

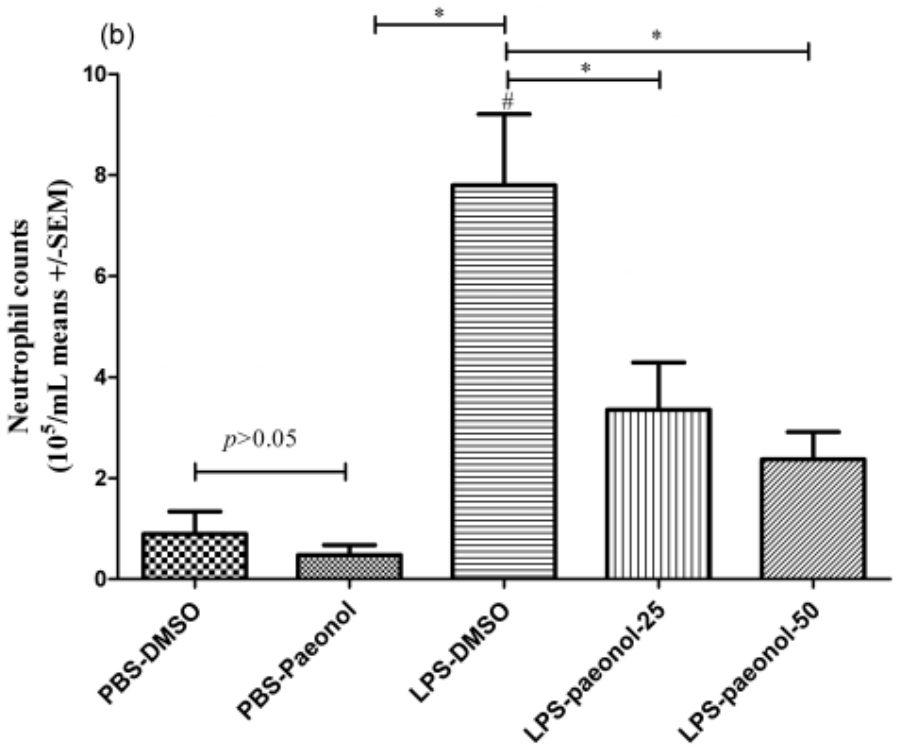

圖 4-25. 丹皮酚治療 LPS 誘發 ALI 之大鼠肺泡液細胞計數

(a)肺泡內各組細胞總數變化(total cell counts)。(b)肺泡內各組中性球(neutrophil counts)變化。#：代表與 PBS 相比具有統計學顯著差異, $p < 0.05$；*：代表標示之兩組相比較，呈現統計顯著差異，$p < 0.05$。

4-3-6. 大鼠肺泡沖洗液蛋白濃度之變化

以 LPS 誘發大鼠 ALI 之動物模型來評估丹皮酚治療效用之大鼠肺泡沖洗液蛋白濃度變化如圖 4-26 所示。圖 4-26 所示，PBS-paeonol 與 PBS-DMSO 相比，無統計學差異，顯示了丹皮酚注射本身並不會加重大鼠之肺泡蛋白質滲漏。LPS-DMSO 與 PBS-DMSO 相比，達統計學顯著差異，顯示本實驗誘發模型穩定。給予丹皮酚治療組(LPS-paeonol-25 以及 LPS-paeonol-50)與

LPS-DMSO 相比，均能顯著降低肺泡液內的蛋白濃度，且有劑量效應。因此，使用丹皮酚 50 mg/kg 為最佳治療劑量。

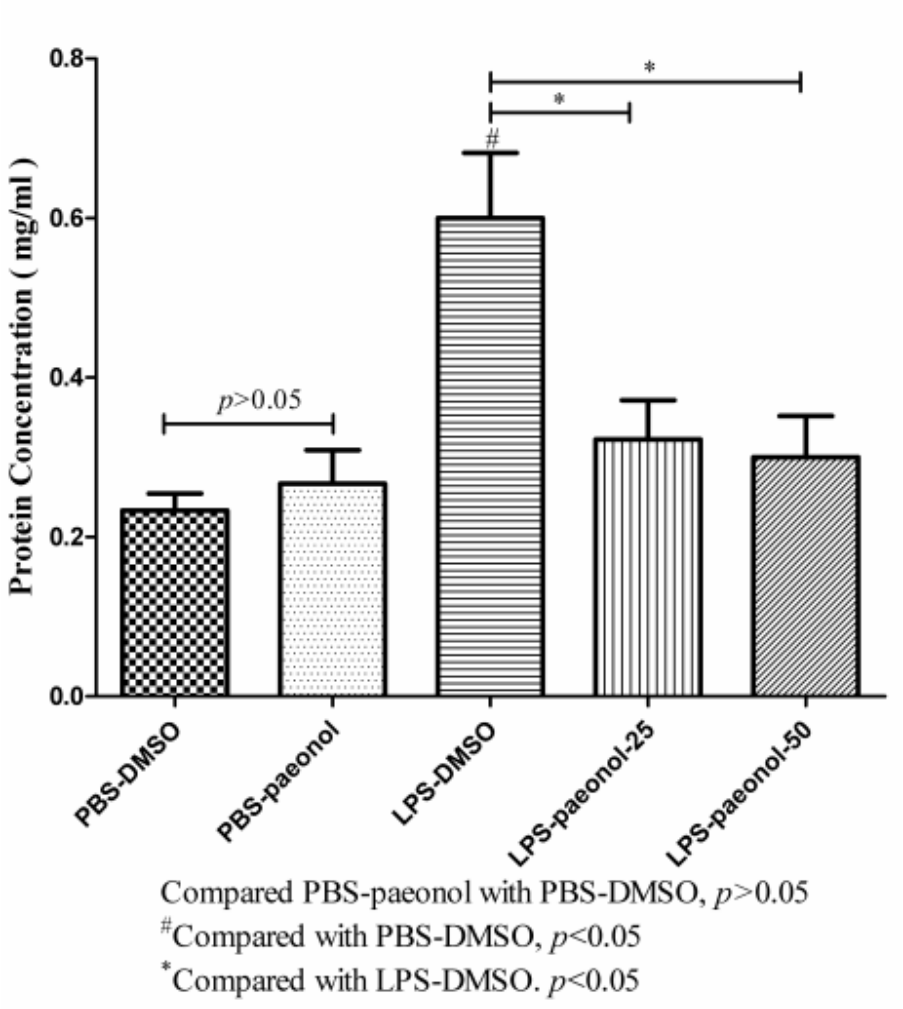

圖 4-26. 丹皮酚治療 LPS 誘發 ALI 之大鼠肺泡液蛋白濃度

#：代表與 PBS 相比具有統計學顯著差異, $p < 0.05$；*：代表標示之兩組相比較，呈現統計顯著差異，$p < 0.05$。

4-3-7. 大鼠肺泡沖洗液發炎相關細胞激素之變化

以以 LPS 誘發大鼠 ALI 之動物模型來評估丹皮酚治療效用之大鼠肺泡沖洗

液發炎相關細胞激素之變化如圖 4-27 所示。(a)TNF-α之表現量：與 PBS-DMSO 組相比， LPS-DMSO 組顯著上升，達統計學顯著差異。與 LPS-DMSO 組相比，LPS-paeonol-50 組的 TNF-α下降達顯著統計學差異。LPS-paeonol-25 組有下降之趨勢，但與 LPS-DMSO 組相比，未達統計顯著差異；(b) IL-1β 之表現量：與 PBS-DMSO 組相比，LPS-DMSO 組顯著上升，達統計學顯著差異。與 LPS-DMSO 組相比，LPS-paeonol-25 及 LPS-paeonol-50 組的 IL-1β 下降達顯著統計學差異；(c) IL-6 之表現量：與 PBS-DMSO 組相比， LPS-DMSO 組顯著上升，達統計學顯著差異。與 LPS-DMSO 組相比，LPS-paeonol-25 及 LPS-paeonol-50 組的 IL-6 下降達顯著統計學差異；(e) IL-10 之表現量：與 PBS-DMSO 組相比， LPS-DMSO 組顯著上升，達統計學顯著差異。與 LPS-DMSO 組相比，LPS-paeonol-25 及 LPS-paeonol-50 組的 IL-10 下降達顯著統計學差異。

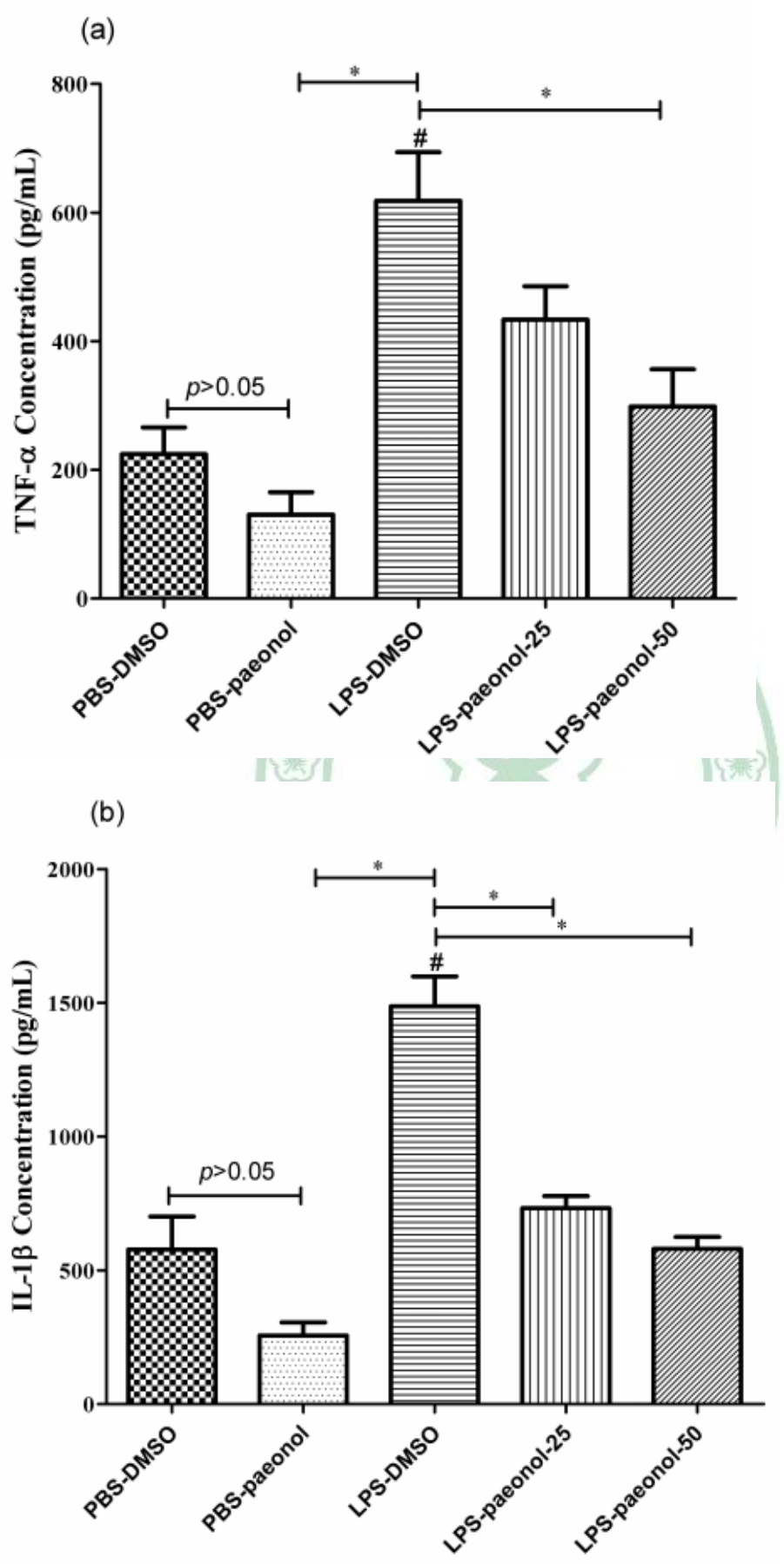
(a)
TNF-α Concentration (pg/mL)
800
600
400
200
0
*
*
#
p>0.05
PBS-DMSO
PBS-paeonol
LPS-DMSO
LPS-paeonol-25
LPS-paeonol-50
(b)
IL-1β Concentration (pg/mL)
2000
1500
1000
500
0
*
*
*
#
p>0.05
PBS-DMSO
PBS-paeonol
LPS-DMSO
LPS-paeonol-25
LPS-paeonol-50

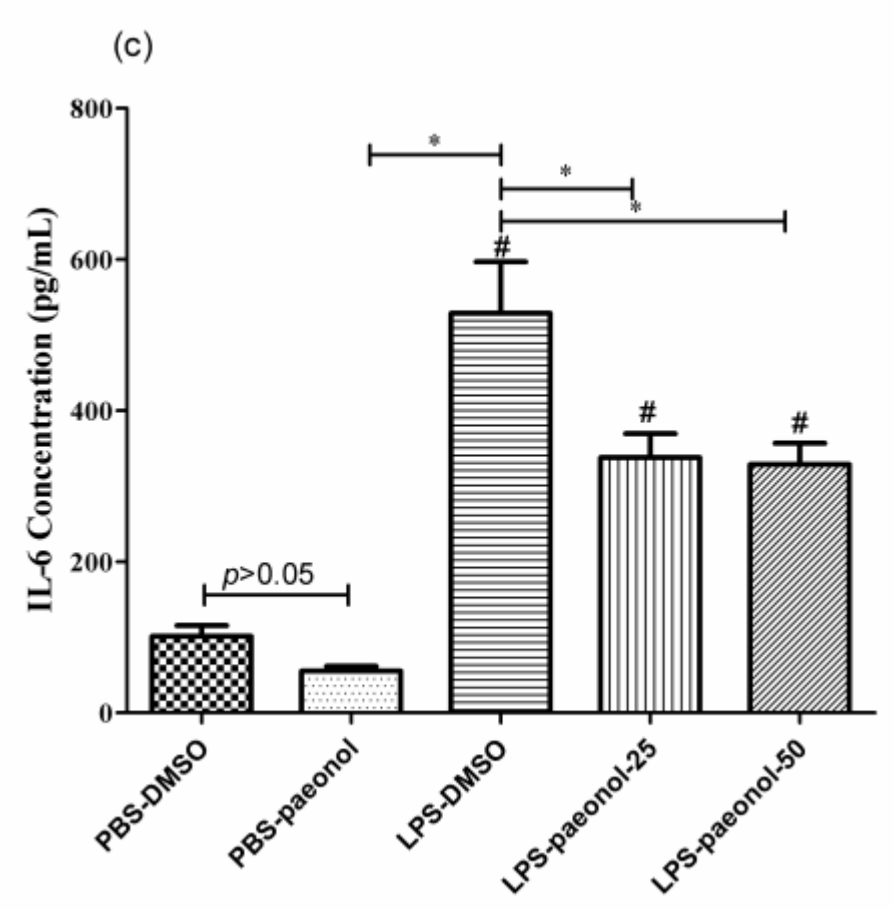

圖 4-27. 丹皮酚治療 LPS 誘發 ALI 之大鼠肺泡液中發炎相關細胞激素之變化

(a) 肺泡液 TNF-α 表現量。(b) 肺泡液 IL-1β表現量。(c) 肺泡液 IL-6 表現量。(d) 肺泡液 IL-10 表現量。#：代表與 PBS-DMSO 相比 $p < 0.05$；*：代表標示之兩組相比較(與 LPS-DMSO 組相比)，呈現統計顯著差異，$p < 0.05$

4-3-8. 大鼠肺泡沖洗液凝血相關細胞激素之變化

以 LPS 誘發大鼠急性肺損傷之動物模型來評估丹皮酚治療效用之大鼠肺泡沖洗液凝血相關細胞激素之變化如圖 4-28 所示。(a) 各組在 TATC 之表現量無顯著統計學差異；(b) 肺泡液內之 PAI-1 表現量：與 PBS-DMSO

組相比，LPS-DMSO 組顯著上升，達統計學顯著差異。與 LPS-DMSO 組相比，LPS-paeonol-25 及 LPS-paeonol-50 組的 PAI-1 下降達顯著統計學差異。

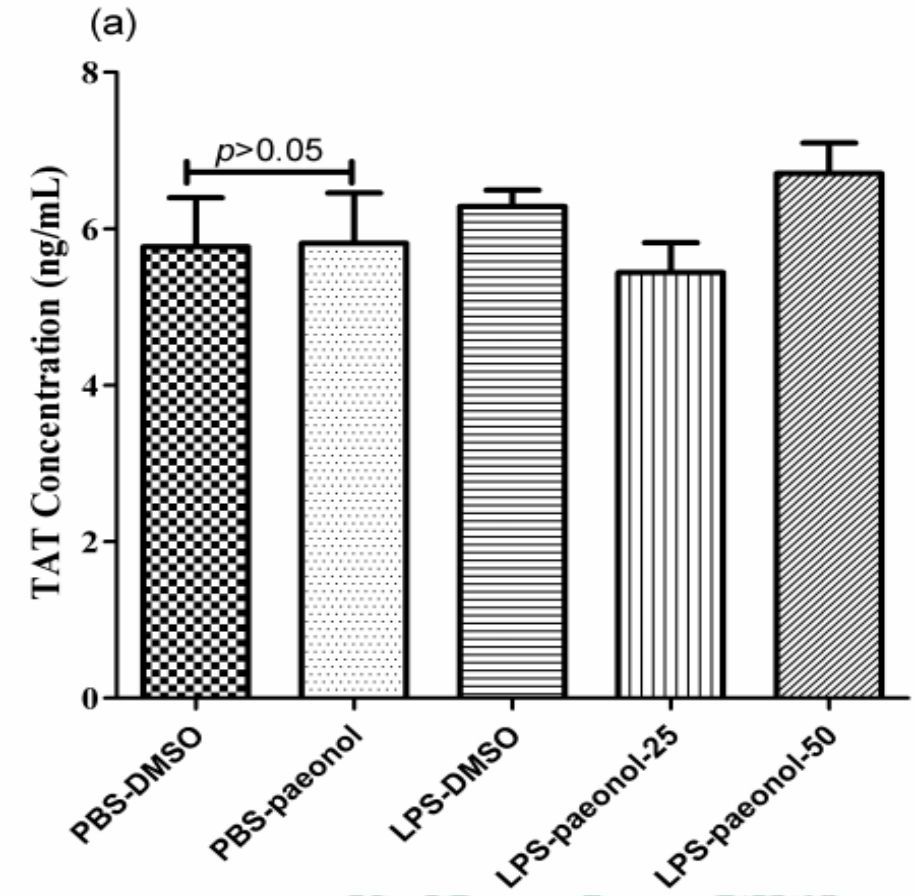

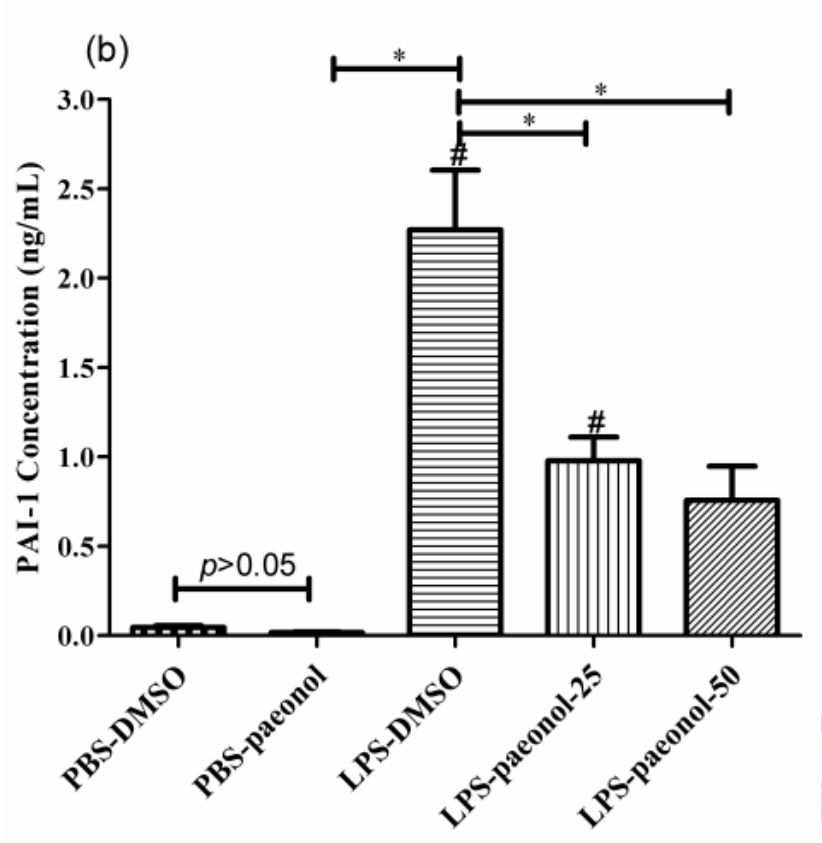

圖 4-28. 丹皮酚治療 LPS 誘發 ALI 之大鼠肺泡液中凝血相關細胞激素之變化

(a) 肺泡液 TATC 表現量；(b) 肺泡液 PAI-1 表現量；#：代表與 PBS-DMSO 相比 $p < 0.05$；*代表標示之兩組相比較(與 LPS-DMSO 組相比)，呈現統計顯著差異，$p < 0.05$。

4-3-9. 大鼠肺組織 MPO 表現量之變化

以 LPS 誘發大鼠急性肺損傷之動物模型來評估丹皮酚治療效用之大鼠肺組織 MPO 表現量之變化如圖 4-29 所示。肺組織之 MPO 表現量：PBS-paeonol 與 PBS-DMSO 相比，無統計學差異，顯示了丹皮酚注射本身

並不會加重大鼠之肺組織發炎反應。LPS-DMSO 與 PBS-DMSO 相比，達統計學顯著差異，顯示本實驗誘發模型穩定。給予丹皮酚治療組(LPS-paeonol-25 以及 LPS-paeonol-50)與 LPS-DMSO 相比，均能顯著降低肺組織的 MPO 表現量，且有劑量效應。因此，使用丹皮酚 50 mg/kg 為最佳治療劑量。

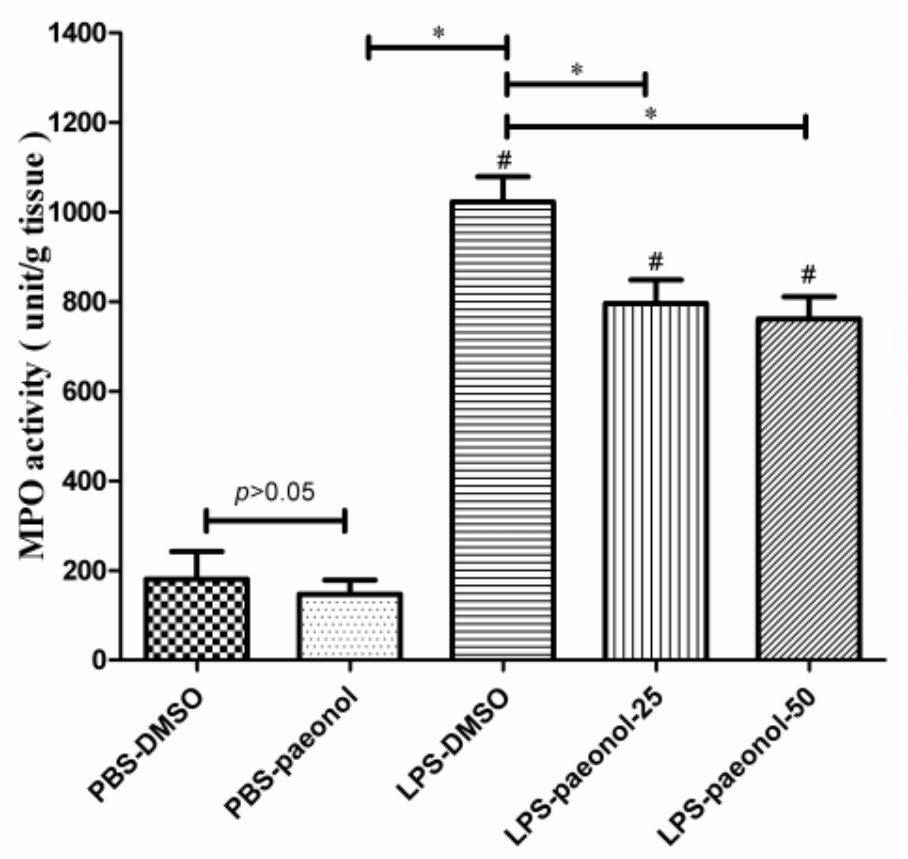

圖 4-29. 丹皮酚治療 LPS 誘發 ALI 之大鼠肺部 MPO 表現量

#：代表與 PBS-DMSO 相比 $p < 0.05$；*：代表標示之兩組相比較(與 LPS-DMSO 組相比)，呈現統計顯著差異，$p < 0.05$。

4-3-10. 大鼠肺組織 iNOS 表現量之變化

以 LPS 誘發大鼠急性肺損傷之動物模型來評估牡丹皮治療效用之大鼠肺組織 iNOS 表現量之變化如圖 4-30 所示。肺組織之 iNOS 表現量：PBS-paeonol 與 PBS-DMSO 相比，無統計學差異，顯示了丹皮酚注射本身並不會使肺組織增加 iNOS 的表現量。LPS-DMSO 與 PBS-DMSO 相比，達統計學顯著差異，顯示本實驗誘發模型穩定。給予丹皮酚治療組(LPS-paeonol-50)與 LPS-DMSO 相比，能顯著降低肺組織的 iNOS 表現量。

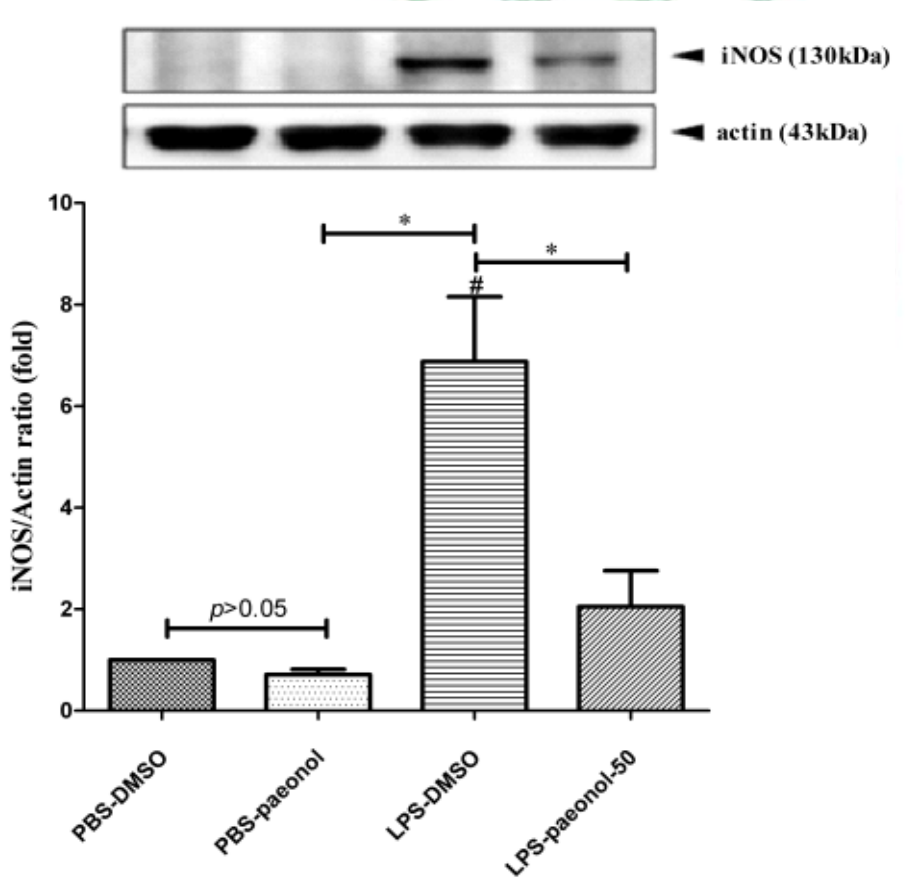

圖 4-30. 丹皮酚治療 LPS 誘發 ALI 之大鼠肺部 iNOS 表現量

#：代表與 PBS-DMSO 相比 $p < 0.05$；*：代表標示之兩組相比較(與 LPS-DMSO 組相比)，呈現統計顯著差異，$p < 0.05$。

4-4. 丹皮酚對中性球之調控作用

4-4-1. 實驗假說示意

過去的研究顯示，丹皮酚具有抑制細胞表面黏附因子[73]、抑制發炎反應細胞激素如 TNF-α and IL-1β[74, 75]，以及抑制氧化自由基表現量的功效[75, 76]。在動物實驗上，我們使用經腹腔內注射丹皮酚，可以有效的抑制肺泡內中性球浸潤以及 MIP-2、MPO 表現量，而肺泡內的中性球大多數又是從肺微血管網移行至肺泡內，因此，我們想要探討丹皮酚是直接在血管內抑制中性球的表現，包括促進中性球的細胞凋亡、抑制中性球的 migration 以及調控中性球的吞噬能力等，如圖 4-31。本實驗將大鼠周邊血液分離出中性球，以丹皮酚來進行體外試驗，以評估丹皮酚對中性球之功能性調控。

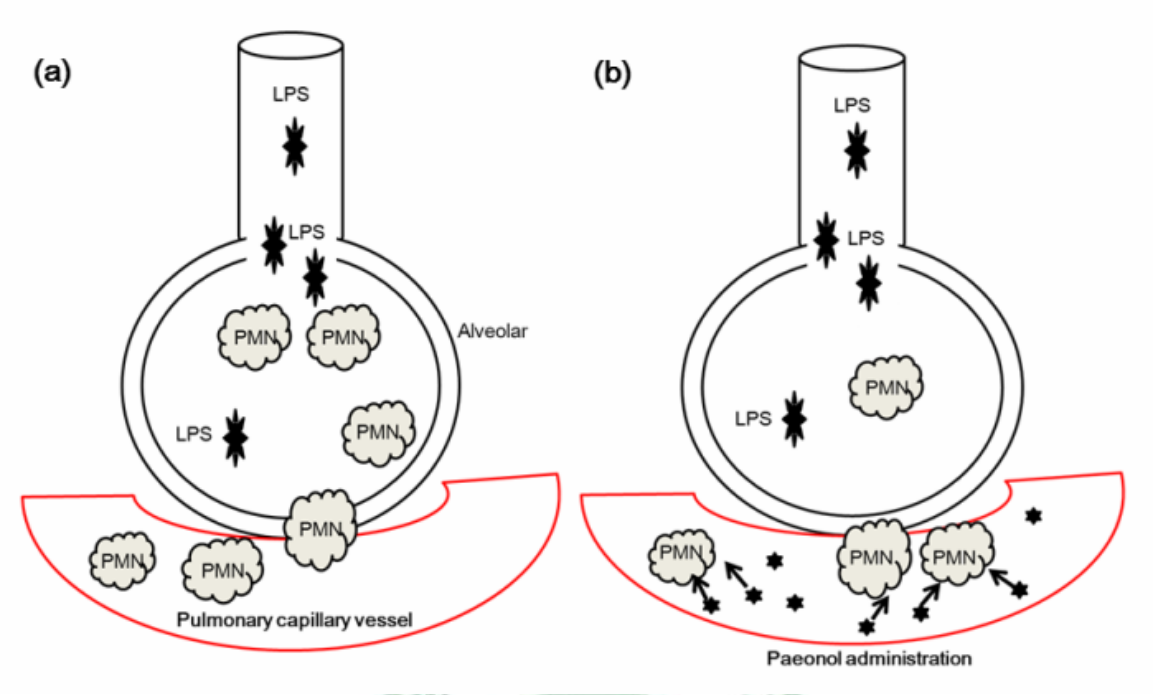

圖 4-31. 丹皮酚體外試驗實驗設計示意

(a) LPS 經氣管內灌注入大鼠肺泡，釋放出發炎反應細胞激素、趨化激素，使得中性球自肺部微血管網移行至肺泡內。(b) 給予丹皮酚腹腔注射後，肺微血管之丹皮酚可能對中性球之調控作用，包括促進細胞凋亡、抑制中性球移行以及抑制中性球吞噬作用等。

4-4-2. 丹皮酚對中性球之細胞存活影響

如圖 4-32 所示，使用 trypan blue exclusion assay 來評估中性球在不同劑量丹皮酚作用下的存活率。在丹皮酚濃度為 50 μM 以下，中性球的存活率幾乎不受影響，各組間無統計差異。但丹皮酚濃度到 200 μM 時，中性球的存活率顯著下降，與各組相比，達統計學顯著差異。根據過去的文獻顯示，丹皮酚在進行細胞實驗的是當劑量為 20-50 μM，這段濃度範圍內，丹皮酚對於中性球亦無濃度毒殺作用。

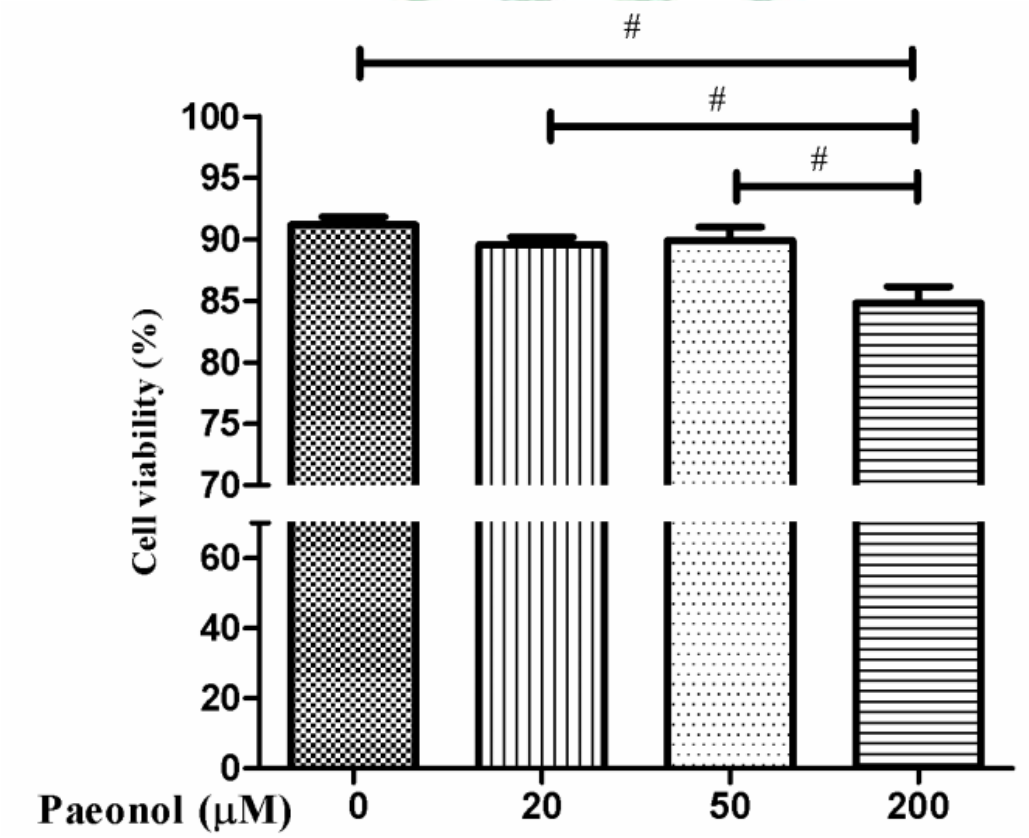

圖 4-32. 丹皮酚對中性球之細胞存活影響

#：代表標示之兩組相比較，呈現統計顯著差異，$p < 0.05$。

4-4-3. 丹皮酚對中性球之細胞凋亡影響

如圖 4-33 所示，使用 Propidium iodide/annexin V assay 以及流式細胞儀來分析丹皮酚是否對於中性球具有促細胞凋亡的作用。將各濃度之數據進行比較，顯示丹皮酚濃度在 50 μM 以下時，各組之間無顯著統計差異；然而，丹皮酚濃度在 200 μM 時，與其他各組相比，明顯有促進中性球細胞凋亡的作用。

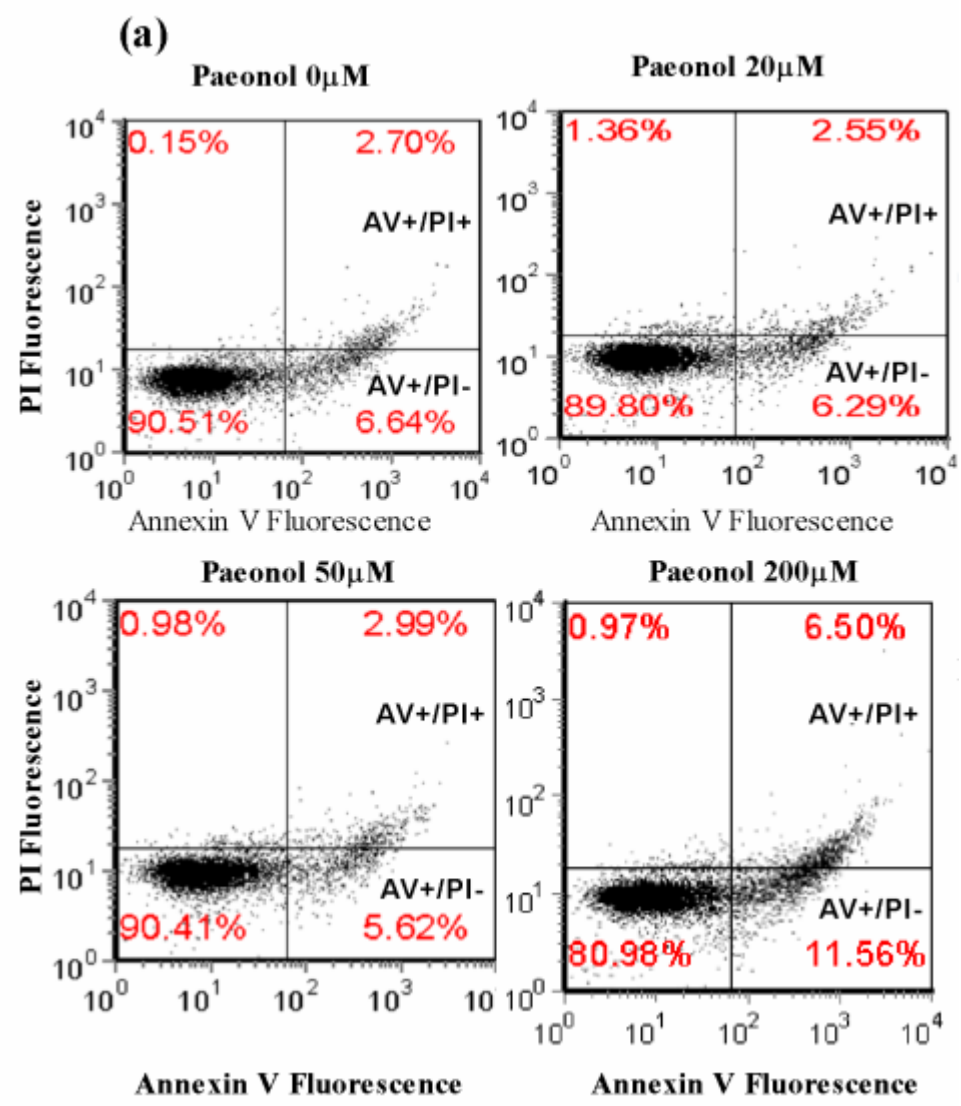

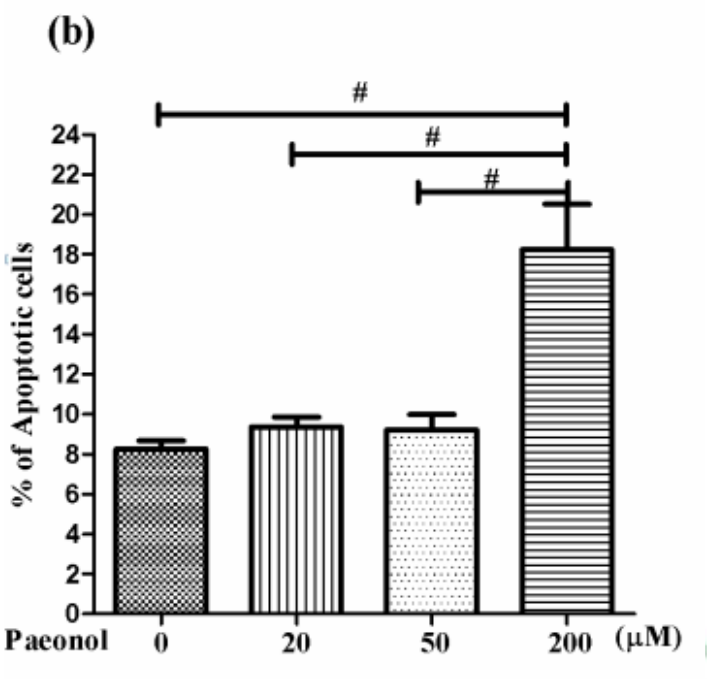

圖 4-33. 丹皮酚對中性球之細胞凋亡影響

#：代表標示之兩組相比較，呈現統計顯著差異，$p < 0.05$。

(a) 使用流式細胞儀來分析中性球在經過與丹皮酚共置 6 小時候，丹皮酚是否對中性球具有促進細胞凋亡的作用。早期凋亡細胞 (Early apoptotic cells) 為右下角之細胞群 (AV+/PI-)，代表細胞膜仍然維持完整；圖(a)之各組右上角細胞群(AV+/PI+)，代表晚期凋亡細胞(late apoptotic cells)或者早期壞死細胞(early necrotic cells)；計算出(AV+/PI- plus AV+/PI+)細胞占所有細胞的比率，此數值即為"細胞凋亡比率"。(b) 將各濃度之數據進行比較，顯示丹皮酚濃度在 50 μM 以下時，各組之間無顯著統計差異；然而，丹皮酚濃度在 200 μM 時，與其他各組相比，明顯有促進中性球細胞凋亡的作用。

4-4-4. 丹皮酚對中性球之吞噬能力影響

如圖 4-4-4 所示，使用螢光磁珠給予中性球吞噬並使用流式細胞儀分析其吞噬比率，來代表中性球吞噬能力的實驗結果如下圖。丹皮酚濃度在 50 μM 時，與濃度為 0 μM 相比，具有統計學顯著差異；然而，丹皮酚濃度在 200 μM 時，與其他各組相比，明顯有抑制中性球吞噬能力的作用。

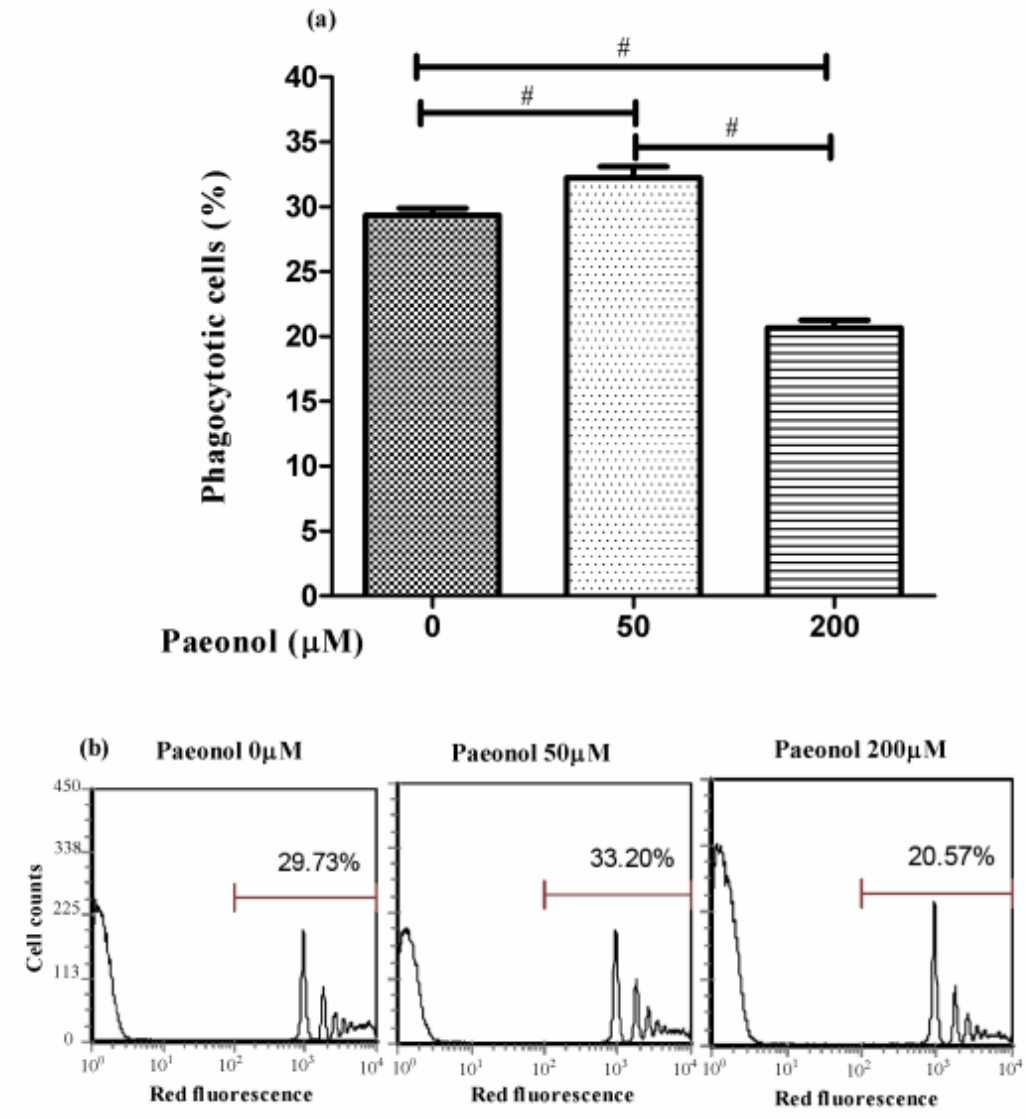

圖 4-34. 丹皮酚對中性球之吞噬能力影響

#：代表標示之兩組相比較，呈現統計顯著差異，$p < 0.05$。(a) 丹皮酚 50 μM

與 0 μM 以及 200 μM 相比，能促進中性球的吞噬能力，達統計學顯著差異；丹皮酚 200 μM 與 0 μM 以及 50 μM 相比，能抑制中性球的吞噬能力，達統計學顯著差異；(b) 使用具螢光標示能力的磁珠給予中性球進行吞噬作用，並用流式細胞儀來分析其吞噬比率，可以代表中性球之吞噬能力。

4-4-5. 丹皮酚對中性球之移行能力影響

如圖 4-35 所示，使用「transwell chamber (Costar, Cambridge, MA)」，其具有 3 μM 的孔洞，來進行中性球移行能力的分析。結果顯示，丹皮酚濃度 50 μM 以及 200μM 與 0μM 相比，具有顯著抑制中性球移行能力的作用 $p < 0.05$ (圖 4-35).

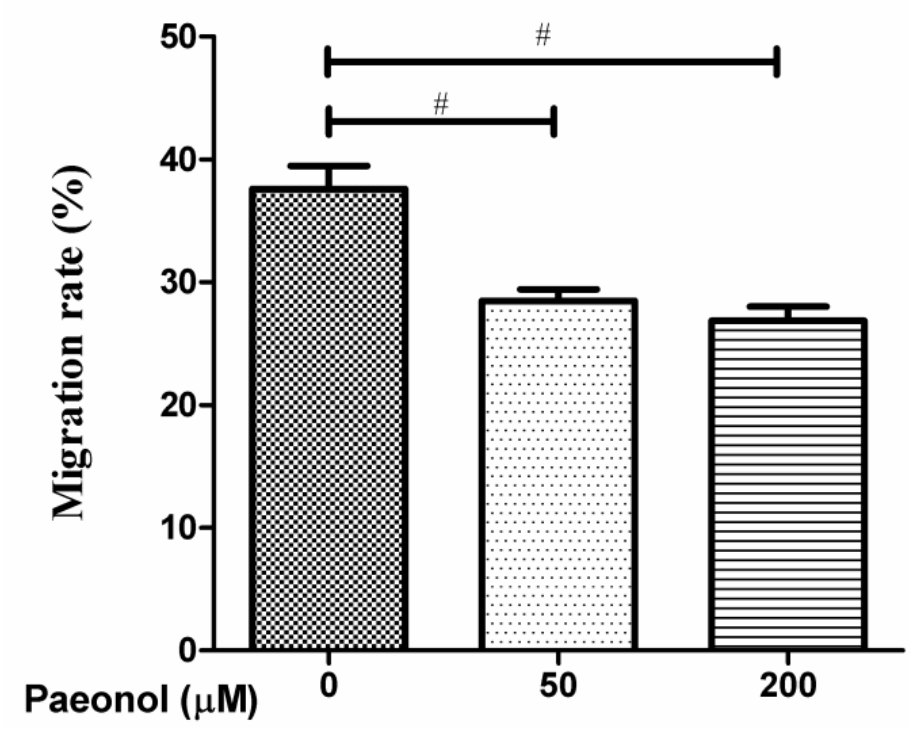

圖 4-35. 丹皮酚對中性球之移行能力影響

#：代表標示之兩組相比較，呈現統計顯著差異，$p < 0.05$。

第五章 討論

本研究包含四大部分，首先是實驗動物模型的建立，以模擬人類在肺炎所致ALI之病理生理反應。我們進行動物模型時序性的研究，包括肺泡液細胞計數、細胞激素的分析及肺部病理組織切片肺損傷程度的判定等，以作為選擇LPS誘發肺損傷後第16小時為治療效果觀測時間點之依據；其次，以本動物模型來進行傳統中藥~MCR之療效評估。我們發現在術前給予MCR口服餵食實驗大鼠，對於急性肺損傷具有保護作用，其作用為可能與抑制肺部發炎反應細胞激素如IL-6、IL-1β以及MIP-2的表現量有關。不論是術前給藥或者術後給藥組，MCR均有調節體溫、抑制MPO表現量的作用。第三：MCR的主要有效化學物質為丹皮酚，過去的文獻顯示其具有良好的抗發炎作用。雖然術前口服MCR具有保護作用，然而，口服劑型對於處於肺炎所致呼吸窘迫症的臨床病患，並非理想給藥模式，主要是因為發生呼吸窘迫之病患多合併有嚴重敗血症所致消化不良，使口服吸收效果更差。此外，急性呼吸窘迫症的發生並無法事前被預測而給予預防性投藥，加上口服中藥的個體代謝差異率無法被精確掌控，更無法預測其血中有效濃度。因此，基於上述理由，我們使用丹皮酚注射至LPS誘發急性肺損傷之大鼠，來評估其是否具有治療效用。結果發現，給予丹皮酚在誘發肺損傷後注射，具有顯著療效，其機轉可能與抑制肺部發炎反應，如抑制TNF-α、IL-1β、IL-6以及MPO和iNOS的表現量，同時，丹皮酚注射也可以抑制大鼠

肺泡內PAI-1的表現量，以降低凝血功能紊亂。這個實驗顯示，丹皮酚具有抗發炎以及抗凝血的作用。作為活血化瘀藥-牡MCR的主要指標純化物，我們可以推測，MCR的活血化瘀功效，可能與丹皮酚有關。第四個部分，由於注射丹皮酚的療效遠勝於口服MCR，且肺泡內的中性球在丹皮酚注射組顯著下降，所以我們推測丹皮酚可以直接調控血液中的中性球功能。我們將大鼠中性球自血液分離出來，使用不同濃度的丹皮酚與之作用，進行相關中性球功能的體外實驗。結果顯示，丹皮酚具有顯著抑制中性球移行能力的作用，同時促進中性球的吞噬能力。本研究為選擇一目前現代醫學治療上有瓶頸之臨床疾病，經由實驗動物模型的建立，來進行篩選及驗證潛在具有治療效果之中草藥，並探討其可能之作用機轉。本研究在後續更可以深入探討同類中草藥之可能治療靶點，以做為臨床使用的理論依據，以及新藥開發臨床試驗的起始點。以下就實驗的細部進行討論。

在疾病動物模式的討論：過去有許多動物模式被開發及應用來模擬內毒素所致急性肺損傷[38, 50, 51]，其中，以LPS誘發所致的ALI/ARDS與應臨床因肺炎所致肺損傷的病理生理較為接近。這個模型的特色，在於用LPS直接氣管內給藥後，可以產生Neutrophil-dependent ALI/ARDS，使周邊血液的中性球受到發炎反應細胞激素或者趨化激素的作用，經由adhesion以及migration而聚集至肺泡內，可反映出臨床ALI/ARDS在急性期以中性球浸潤為主的病理反應[4, 14, 15]。至於LPS的誘發，本研究使用的16 mg/kg較過去文

獻為高，所致的肺部損傷程度亦較嚴重，在病理切片上可以看出肺泡內大量的發炎細胞、蛋白質滲出液以及紅血球浸潤，這樣的嚴重肺損傷，更能作為藥物有效與否之驗證。在時間點的選擇上，過去文獻以誘發後24小時作為分類，在24小時內的觀察點為急性期，超過24小時以後的觀察點定義為慢性期。本研究進行了LPS誘發急性肺損傷後的時序性研究，我們選擇了0、8、16、24以及48小時為觀察時間點，在肺泡液的分析方面，進行了血球計數、蛋白質濃度、細胞激素表現量等；在肺組織分析方面，進行了組織病理切片以及MPO的分析；在生理指標分析方面，進行了大鼠肛溫的監測。結果顯示，本實驗可以穩定的誘發建置LPS所致急性肺損傷大鼠模型，與文獻所述之肺部表現一致：大量的中性球浸潤、肺泡上皮細胞損傷、肺間質浸潤以及大量的蛋白滲漏至肺泡內[4, 13, 16, 130]。在時間點的選擇上，誘發後第8小時的細胞激素表現量達到最高，但肺損傷程度則以第16小時較為嚴重，但與第8小時相比，並無顯著統計差異。所以，在誘發後第8-16小時皆為適合觀測的時間點，而本實驗的時間點選擇上以之前同實驗室所選擇的第16小時為觀測時間點。

抑制LPS-induced ALI相關發炎反應討論：以LPS誘發之急性肺損傷模型中，發炎前趨細胞激素的大量表現，如TNF-α、IL-1β以及IL-6等扮演了促進發炎反應以及形成inflammatory cascas的核心角色[2, 51]。這些細胞激素，如TNF-α、IL-1β、IL-6、IL-8以及IL-10等是由於肺泡內的巨噬細胞受

到刺激後所分泌的產物，目的是能吸引以及趨化更多的中性球至肺泡內，以對抗內毒素的攻擊[4, 137, 141, 242, 243]。除上述之細胞激素外，MIP-2(CXCL-2)被認為是趨化中性球至肺泡內最重要細胞激素[14, 142]；MPO的表現量則可以做為肺組織內中性球濃度的標誌[16, 79]；而iNO的表現量增加，會使肺組織內的NO上升，進而產生更多的peroxynitrite[243-246]，因而產生氧化傷害[236, 243, 246, 247]。在以牡丹皮進行的研究方面：術前給予牡丹皮可以抑制肺泡液內發炎反應細胞激素IL-1β以及IL-6的濃度、抑制細胞趨化激素MIP-2的濃度、降低肺泡液內中性球數目以及蛋白質滲出的濃度。然而，術後給藥組(LPS-MCR)，除了可以降低肺泡內IL-6的表現量外，與其餘之細胞激素表現量的下降程度與LPS組相比均未有顯著統計差異。此外，給予大鼠餵食MCR後，肺組織中的MPO的表現量也呈現顯著下降。因此，我們可以推論，口服牡丹皮在LPS誘發前給藥，可以透過抗發炎反應，來降低大鼠肺部之急性肺損傷；術後給藥組由於抑制發炎反應的效果未若術前組顯著，所以無法顯著的抑制中性球趨化所致的肺損傷。在以丹皮酚注射禁行的研究方面：給予丹皮酚經腹腔內注射可以抑制肺泡液內發炎反應細胞激素TNF-α、IL-1β以及IL-6的濃度、降低肺泡液內中性球數目及蛋白質滲出的濃度，同時，也使肺組織中的MPO的表現量呈現顯著下降。因此，我們可以推論，在LPS誘發後給予注射丹皮酚，可以透過抑制發炎反應，來降低大鼠肺部之急性肺損傷。綜上，本研究結果顯示，給予術前口服MCR以及術後注射丹

皮酚，皆能抑制肺泡液發炎細胞激素的表現量。注射丹皮酚，雖然是術後給藥，但其抑制的效果更顯著於術前口服牡丹皮濃縮藥物。推論其中的差距，可能與口服藥物尚需要生物體代謝才能進入血中，以及丹皮酚是MCR中重要的抑制發炎反應的化學結構有關。過去的文獻曾經報導丹皮酚在細胞實驗中，可以透過抑制MAPK訊號傳遞路徑，使得RAW 264.7 macrophage-like cells在經LPS刺激後所產生的iNOS下降[76]，然而，關於丹皮酚是否在動物實驗具有調控iNOS表現量的研究，特別是LPS-induced ALI model，並未有相關的報導。本研究結果同時也證實了丹皮酚在動物實驗中，對於iNOS的表現量也具有顯著的抑制效果[232]。

抑制LPS-induced ALI相關凝血功能紊亂討論：急性肺損傷的另外一個重要的病理變化為：「肺泡內fibrin以及platelet plugs沉積，造成肺泡及肺微血管的栓塞」，當肺泡內的fibrin過度沉積後，也會使中性球以及fibroblasts更進一步的被活化與趨化，使得肺損傷加重[4]。這個由發炎反應以及凝血功能紊亂所錯縱而成的病理變化，就是產生肺部氣體交換受限、肺泡內大量滲液堆積以及形成肺微血管障礙及血栓所致多器官衰竭甚至致死的主因[18]。事實上，凝血功能紊亂的產生，與發炎反應細胞激素的過度表現有關，如TNF-α、IL-1β以及IL-6等，這些細胞激素的過度表現，不但會刺激Tissue factor (TF)的活化，同時也會透過釋放出PAI-1而抑制內生性纖維溶解作用，最後的結果就是大量的血栓形成[2, 25, 146, 152, 153]。在MCR口服給藥的動

物實驗中，我們發現，各組之肺泡液TATC表現量均無顯著之差異。然而，在PAI-1的表現量上，雖然誘發前口服給藥以及誘發後口服給藥均可使PAI-1表現量下降，但均未達顯著統計學差異。然而，在以丹皮酚腹腔內注射的實驗中發現，丹皮酚的注射治療，雖然對於大鼠肺泡液內TATC表現量影響不大，但是對於PAI-1的表現量卻有顯著的抑制作用，且呈現劑量效應。因此，可以推論，MCR中的丹皮酚具有透過抑制PAI-1的表現量來對抗「抑制纖維溶解作用」，這與傳統中醫藥典及所記載的「活血化瘀」作用，有一定程度的呼應。至於這樣的作用是直接透過抑制PAI-1的表現量，還是因為抑制了IL-6的表現量使得PAI-1的表現也被間接抑制而產生作用，仍然需要進一步的研究。其他中醫藥典籍所記載之活血化瘀類藥物，是否都同樣具有抑制PAI-1的作用，也還需要進一步研究。

在丹皮酚調控中性球功能相關之研究方面：過去的文獻顯示，中性球是人體肺部遭受感染後，首先由周邊血液被趨化及召集至肺組織內的周邊血液細胞[248, 249]。中性球的主要生理功能，就是對於入侵人體的細菌或黴菌具有吞噬調理作用[248, 250, 251]。經由吞噬調理作用的進行，外來的病原體會被吞入phagosome內，然後被大量的氧化自由基、NO以及對抗細菌的蛋白或peptide攻擊，以進行人體免疫反擊[250-252]。在丹皮酚的動物實驗可以發現，給予丹皮酚後，大鼠肺組織MPO表現量以及iNOS表現量顯著下降。在細胞實驗發現，丹皮酚在50 μM可以促進中性球的吞噬作用，但是在高劑量

200 μM時反而會抑制中性球之吞噬作用。這樣的結果是否與高劑量的丹皮酚對中性球反而有毒殺作用有關，可繼續深入研究。其次，中性球由周邊血液趨化至肺部，主要參與的細胞激素有TNF-α、IL-1β、IL-6、IL-8、IL-10以及CXCL-5等，大多源自肺泡內的巨噬細胞所分泌[74, 142, 242, 243, 253]。過去的研究顯示，丹皮酚可以抑制經TNF-α刺激而表現的細胞黏附因子VCAM-1以及ICAM-1來降低血管內皮的發炎反應[73]。我們的動物實驗顯示，經由丹皮酚注射，肺組織內ICAM-1表現量在免疫染色上呈現顯著差異。細胞實驗也顯示，將中性球給予丹皮酚後，其移行能力在丹皮酚濃度為50 μM以及200 μM皆呈顯著下降。至於這個現象是否透過間接抑制細胞激素如IL-6、IL-8或者直接抑制ICAM-1或者VCAM-1而達成，可進行後續深入的研究探討。

第六章 結論

本論文選擇在現代醫學迄今在治療仍為棘手的疾病—ALI/ARDS，建立較為嚴重的疾病動物模式，經過文獻探討後，從其主要的兩大病理生理機轉「發炎與凝血功能紊亂」作為切入點，對照中醫理論之溫病學說，選擇活血化瘀相關藥物，以驗證傳統活血化瘀之理論體系及活血化瘀藥物之效用評估。在藥物方面，選擇同時具有「清熱涼血」以及「活血去瘀」作用的牡丹皮，做為評估藥物。經動物實驗模型驗證後，發現在術前給藥具有保護作用，且對於發炎反應有明顯的調控作用以及對肺局部環境內的凝血功能紊亂可能具有調控作用。然後再驗證牡丹皮之主要純化物丹皮酚是否為作用之主要角色。經動物實驗驗證後，證實丹皮酚透過抑制發炎反應以及抗凝血功能紊亂，降低LPS所致大鼠肺損傷。由於中性球相關之發炎反應，是本實驗模式之主要病理生理基礎，因此，我們進行了丹皮酚對中性球功能性調控之相關研究，並推論其可能與抑制中性球之移行能力有關。這樣的研究模式，係從臨床問題開始，回過頭來建立疾病動物模式，然後在現代醫學以及中醫藥理論體系架構下，驗證潛在具有療效藥物及其可能之機轉，提供了中西醫在現代醫學結合的模式，研究的成果也分別發表在Evidence-Based Complementary and Alternative Medicine (eCAM)以及Phytomedicine等國際期刊。展望今後，除了對牡丹皮以及丹皮酚之作用機轉進行更深入的研究探討外，我們也希望在此動物模型上，進行更多的活

血化瘀藥物或者活血化瘀複方的治療效用評估，除了對溫病學說的內容以及活血化瘀的意涵進行理論現代化的闡釋外，更希望研究成果能進入藥物開發及臨床應用的階段，達到實質上中西醫結合的目的。

參考文獻

1. Rubenfeld GD, Caldwell E, Peabody E, Weaver J, Martin DP, Neff M, Stern EJ, Hudson LD. Incidence and outcomes of acute lung injury. *N Engl J Med*. 2005;353:1685-1693
2. Schultz MJ, Haitsma JJ, Zhang H, Slutsky AS. Pulmonary coagulopathy as a new target in therapeutic studies of acute lung injury or pneumonia--a review. *Crit Care Med*. 2006;34:871-877
3. Tsushima K, King LS, Aggarwal NR, De Gorordo A, D'Alessio FR, Kubo K. Acute lung injury review. *Intern Med*. 2009;48:621-630
4. Ware LB, Matthay MA. The acute respiratory distress syndrome. *N Engl J Med*. 2000;342:1334-1349
5. Ashbaugh DG, Bigelow DB, Petty TL, Levine BE. Acute respiratory distress in adults. *Lancet*. 1967;2:319-323
6. Bernard GR, Artigas A, Brigham KL, Carlet J, Falke K, Hudson L, Lamy M, Legall JR, Morris A, Spragg R. The american-european consensus conference on ards. Definitions, mechanisms, relevant outcomes, and clinical trial coordination. *Am J Respir Crit Care Med*. 1994;149:818-824
7. Ventilation with lower tidal volumes as compared with traditional tidal volumes for acute lung injury and the acute respiratory distress syndrome. The acute respiratory distress syndrome network. *N Engl J Med*. 2000;342:1301-1308
8. Stewart TE, Meade MO, Cook DJ, Granton JT, Hodder RV, Lapinsky SE, Mazer CD, McLean RF, Rogovein TS, Schouten BD, Todd TR, Slutsky AS. Evaluation of a ventilation strategy to prevent barotrauma in patients at high risk for acute respiratory distress syndrome. Pressure- and volume-limited ventilation strategy group. *N Engl J Med*. 1998;338:355-361
9. Brochard L, Roudot-Thoraval F, Roupie E, Delclaux C, Chastre J, Fernandez-Mondejar E, Clementi E, Mancebo J, Factor P, Matamis D, Ranieri M, Blanch L, Rodi G, Mentec H, Dreyfuss D, Ferrer M, Brun-Buisson C, Tobin M, Lemaire F. Tidal volume reduction for prevention of ventilator-induced lung injury in acute respiratory distress syndrome. The multicenter trail group on tidal volume reduction in ards. *Am J Respir Crit Care Med*. 1998;158:1831-1838
10. Roch A, Guervilly C, Papazian L. Fluid management in acute lung injury and ards. *Ann Intensive Care*. 2011;1:16
11. Wiedemann HP, Wheeler AP, Bernard GR, Thompson BT, Hayden D, deBoisblanc B, Connors AF, Jr., Hite RD, Harabin AL. Comparison of two fluid-management strategies in acute lung injury. *N Engl J Med*. 2006;354:2564-2575
12. Mitchell JP, Schuller D, Calandrino FS, Schuster DP. Improved outcome based on

fluid management in critically ill patients requiring pulmonary artery catheterization. *Am Rev Respir Dis*. 1992;145:990-998

13. Dreyfuss D, Ricard JD. Acute lung injury and bacterial infection. *Clin Chest Med*. 2005;26:105-112
14. Grommes J, Soehnlein O. Contribution of neutrophils to acute lung injury. *Mol Med*. 2011;17:293-307
15. Balamayooran G, Batra S, Fessler MB, Happel KI, Jeyaseelan S. Mechanisms of neutrophil accumulation in the lungs against bacteria. *Am J Respir Cell Mol Biol*. 2010;43:5-16
16. Abraham E. Neutrophils and acute lung injury. *Crit Care Med*. 2003;31:S195-199
17. Abraham E, Carmody A, Shenkar R, Arcaroli J. Neutrophils as early immunologic effectors in hemorrhage- or endotoxemia-induced acute lung injury. *Am J Physiol Lung Cell Mol Physiol*. 2000;279:L1137-1145
18. Sapru A, Wiemels JL, Witte JS, Ware LB, Matthay MA. Acute lung injury and the coagulation pathway: Potential role of gene polymorphisms in the protein c and fibrinolytic pathways. *Intensive Care Med*. 2006;32:1293-1303
19. Lee WL, Downey GP. Neutrophil activation and acute lung injury. *Curr Opin Crit Care*. 2001;7:1-7
20. Meduri GU, Belenchia JM, Estes RJ, Wunderink RG, el Torky M, Leeper KV, Jr. Fibroproliferative phase of ards. Clinical findings and effects of corticosteroids. *Chest*. 1991;100:943-952
21. Gunther A, Mosavi P, Heinemann S, Ruppert C, Muth H, Markart P, Grimminger F, Walmrath D, Temmesfeld-Wollbruck B, Seeger W. Alveolar fibrin formation caused by enhanced procoagulant and depressed fibrinolytic capacities in severe pneumonia. Comparison with the acute respiratory distress syndrome. *Am J Respir Crit Care Med*. 2000;161:454-462
22. Fukuda Y, Ishizaki M, Masuda Y, Kimura G, Kawanami O, Masugi Y. The role of intraalveolar fibrosis in the process of pulmonary structural remodeling in patients with diffuse alveolar damage. *Am J Pathol*. 1987;126:171-182
23. Martin C, Papazian L, Payan MJ, Saux P, Gouin F. Pulmonary fibrosis correlates with outcome in adult respiratory distress syndrome. A study in mechanically ventilated patients. *Chest*. 1995;107:196-200
24. Bellingan GJ. The pulmonary physician in critical care * 6: The pathogenesis of ali/ards. *Thorax*. 2002;57:540-546
25. Bastarache JA, Ware LB, Bernard GR. The role of the coagulation cascade in the continuum of sepsis and acute lung injury and acute respiratory distress syndrome. *Semin Respir Crit Care Med*. 2006;27:365-376
26. Sebag SC, Bastarache JA, Ware LB. Therapeutic modulation of coagulation and

fibrinolysis in acute lung injury and the acute respiratory distress syndrome. *Curr Pharm Biotechnol*. 2011;12:1481-1496

27. Hofstra JJ, Haitsma JJ, Juffermans NP, Levi M, Schultz MJ. The role of bronchoalveolar hemostasis in the pathogenesis of acute lung injury. *Semin Thromb Hemost*. 2008;34:475-484
28. Xu GL, Yao L, Rao SY, Gong ZN, Zhang SQ, Yu SQ. Attenuation of acute lung injury in mice by oxymatrine is associated with inhibition of phosphorylated p38 mitogen-activated protein kinase. *J Ethnopharmacol*. 2005;98:177-183
29. Tajima S, Bando M, Yamasawa H, Ohno S, Moriyama H, Takada T, Suzuki E, Gejyo F, Sugiyama Y. Preventive effect of hochu-ekki-to on lipopolysaccharide-induced acute lung injury in balb/c mice. *Lung*. 2006;184:318-323
30. Yeh CC, Lin CC, Wang SD, Chen YS, Su BH, Kao ST. Protective and anti-inflammatory effect of a traditional chinese medicine, xia-bai-san, by modulating lung local cytokine in a murine model of acute lung injury. *Int Immunopharmacol*. 2006;6:1506-1514
31. Yeh CC, Lin CC, Wang SD, Hung CM, Yeh MH, Liu CJ, Kao ST. Protective and immunomodulatory effect of gingyo-san in a murine model of acute lung inflammation. *J Ethnopharmacol*. 2007;111:418-426
32. Yeh CC, Kao SJ, Lin CC, Wang SD, Liu CJ, Kao ST. The immunomodulation of endotoxin-induced acute lung injury by hesperidin in vivo and in vitro. *Life Sci*. 2007;80:1821-1831
33. Luo Y, Zhang B, Xu DQ, Liu Y, Dong MQ, Zhao PT, Li ZC. Protective effect of bicyclol on lipopolysaccharide-induced acute lung injury in mice. *Pulm Pharmacol Ther*. 2011;24:240-246
34. Sun J, Xue Q, Guo L, Cui L, Wang J. Xuebijing protects against lipopolysaccharide-induced lung injury in rabbits. *Exp Lung Res*. 2010;36:211-218
35. Schuster DP. Ards: Clinical lessons from the oleic acid model of acute lung injury. *Am J Respir Crit Care Med*. 1994;149:245-260
36. Martynowicz MA, Minor TA, Walters BJ, Hubmayr RD. Regional expansion of oleic acid-injured lungs. *Am J Respir Crit Care Med*. 1999;160:250-258
37. Wiener-Kronish JP, Albertine KH, Matthay MA. Differential responses of the endothelial and epithelial barriers of the lung in sheep to escherichia coli endotoxin. *J Clin Invest*. 1991;88:864-875
38. van Helden HP, Kuijpers WC, Steenvoorden D, Go C, Bruijnzeel PL, van Eijk M, Haagsman HP. Intratracheal aerosolization of endotoxin (lps) in the rat: A comprehensive animal model to study adult (acute) respiratory distress syndrome. *Exp Lung Res*. 1997;23:297-316
39. Chen H, Bai C, Wang X. The value of the lipopolysaccharide-induced acute lung

injury model in respiratory medicine. *Expert Rev Respir Med*. 2010;4:773-783
40. Folkesson HG, Matthay MA, Hebert CA, Broaddus VC. Acid aspiration-induced lung injury in rabbits is mediated by interleukin-8-dependent mechanisms. *J Clin Invest*. 1995;96:107-116
41. Modelska K, Pittet JF, Folkesson HG, Courtney Broaddus V, Matthay MA. Acid-induced lung injury. Protective effect of anti-interleukin-8 pretreatment on alveolar epithelial barrier function in rabbits. *Am J Respir Crit Care Med*. 1999;160:1450-1456
42. Frank L, Bucher JR, Roberts RJ. Oxygen toxicity in neonatal and adult animals of various species. *J Appl Physiol*. 1978;45:699-704
43. Moore BB, Hogaboam CM. Murine models of pulmonary fibrosis. *Am J Physiol Lung Cell Mol Physiol*. 2008;294:L152-160
44. Gharaee-Kermani M, Ullenbruch M, Phan SH. Animal models of pulmonary fibrosis. *Methods Mol Med*. 2005;117:251-259
45. Dos Santos CC, Slutsky AS. Invited review: Mechanisms of ventilator-induced lung injury: A perspective. *J Appl Physiol*. 2000;89:1645-1655
46. Lachmann B, Robertson B, Vogel J. In vivo lung lavage as an experimental model of the respiratory distress syndrome. *Acta Anaesthesiol Scand*. 1980;24:231-236
47. Hubbard WJ, Choudhry M, Schwacha MG, Kerby JD, Rue LW, 3rd, Bland KI, Chaudry IH. Cecal ligation and puncture. *Shock*. 2005;24 Suppl 1:52-57
48. Villar J, Ribeiro SP, Mullen JB, Kuliszewski M, Post M, Slutsky AS. Induction of the heat shock response reduces mortality rate and organ damage in a sepsis-induced acute lung injury model. *Crit Care Med*. 1994;22:914-921
49. Bastarache JA, Blackwell TS. Development of animal models for the acute respiratory distress syndrome. *Dis Model Mech*. 2009;2:218-223
50. Wang HM, Bodenstein M, Markstaller K. Overview of the pathology of three widely used animal models of acute lung injury. *Eur Surg Res*. 2008;40:305-316
51. Matute-Bello G, Frevert CW, Martin TR. Animal models of acute lung injury. *Am J Physiol Lung Cell Mol Physiol*. 2008;295:L379-399
52. 鄒澍. 本經疏證. 台北: 志遠書局; 1997:pp. 190-193.
53. 雷載權. 中藥學. 上海: 上海科學技術出版社; 1995:pp. 91-92.
54. 焦樹德. 中藥用法十講. 台北: 知音出版社; 1984:pp. 188-189.
55. 杜文燮. 藥鑒. 北京: 中國中醫藥出版社; 1993:pp. 65.
56. 戴新民. 中藥臨床應用. 台北: 啓業書局; 1981:pp. 72-73.
57. 林乾良、王貴淼. 經方中藥研究集成. 北京: 中醫古籍出版社; 1986:pp. 406-408.
58. 周岩. 本草思辨錄. 北京: 人民衛生出版社; 1982:pp. 48-49.
59. 李中梓. 雷公炮製藥性賦. 台南: 綜合出版社; 2001:pp. 52.
60. 仲昴庭. 本草崇原集說. 北京: 人民衛生出版社; 1997:pp. 84.

61. Tatsumi S, Mabuchi T, Abe T, Xu L, Minami T, Ito S. Analgesic effect of extracts of chinese medicinal herbs moutan cortex and coicis semen on neuropathic pain in mice. *Neurosci Lett*. 2004;370:130-134
62. Lin HC, Ding HY, Ko FN, Teng CM, Wu YC. Aggregation inhibitory activity of minor acetophenones from paeonia species. *Planta Med*. 1999;65:595-599
63. Yoshikawa M, Ohta T, Kawaguchi A, Matsuda H. Bioactive constituents of chinese natural medicines. V. Radical scavenging effect of moutan cortex. (1): Absolute stereostructures of two monoterpenes, paeonisuffrone and paeonisuffral. *Chem Pharm Bull (Tokyo)*. 2000;48:1327-1331
64. Rho S, Chung HS, Kang M, Lee E, Cho C, Kim H, Park S, Kim HY, Hong M, Shin M, Bae H. Inhibition of production of reactive oxygen species and gene expression profile by treatment of ethanol extract of moutan cortex radicis in oxidative stressed pc12 cells. *Biol Pharm Bull*. 2005;28:661-666
65. Okubo T, Nagai F, Seto T, Satoh K, Ushiyama K, Kano I. The inhibition of phenylhydroquinone-induced oxidative DNA cleavage by constituents of moutan cortex and paeoniae radix. *Biol Pharm Bull*. 2000;23:199-203
66. Oh GS, Pae HO, Choi BM, Jeong S, Oh H, Oh CS, Rho YD, Kim DH, Shin MK, Chung HT. Inhibitory effects of the root cortex of paeonia suffruticosa on interleukin-8 and macrophage chemoattractant protein-1 secretions in u937 cells. *J Ethnopharmacol*. 2003;84:85-89
67. Kim HS, Kim AR, Lee JM, Kim SN, Choi JH, Kim do K, Kim JH, Kim B, Her E, Yang YM, Kim YM, Choi WS. A mixture of trachelospermi caulis and moutan cortex radicis extracts suppresses collagen-induced arthritis in mice by inhibiting nf-kappab and ap-1. *J Pharm Pharmacol*. 2012;64:420-429
68. Xu SJ, Yang L, Zeng X, Zhang M, Wang ZT. Characterization of compounds in the chinese herbal drug mu-dan-pi by liquid chromatography coupled to electrospray ionization mass spectrometry. *Rapid Commun Mass Spectrom*. 2006;20:3275-3288
69. 姜春華. 活血化瘀研究新編. 上海醫科大學出版社; 1990:pp. 430.
70. 陳可冀. 活血化瘀藥化學藥理與臨床. 濟南: 山東科學技術出版社; 1995:pp.54-60.
71. Hirai A, Terano T, Hamazaki T, Sajiki J, Saito H, Tahara K, Tamura Y, Kumagai A. Studies on the mechanism of antiaggregatory effect of moutan cortex. *Thromb Res*. 1983;31:29-40
72. Koo YK, Kim JM, Koo JY, Kang SS, Bae K, Kim YS, Chung JH, Yun-Choi HS. Platelet anti-aggregatory and blood anti-coagulant effects of compounds isolated from paeonia lactiflora and paeonia suffruticosa. *Pharmazie*. 2010;65:624-628
73. Nizamutdinova IT, Oh HM, Min YN, Park SH, Lee MJ, Kim JS, Yean MH, Kang SS, Kim YS, Chang KC, Kim HJ. Paeonol suppresses intercellular adhesion molecule-1

expression in tumor necrosis factor-alpha-stimulated human umbilical vein endothelial cells by blocking p38, erk and nuclear factor-kappab signaling pathways. *Int Immunopharmacol*. 2007;7:343-350

74. Pan LL, Dai M. Paeonol from paeonia suffruticosa prevents tnf-alpha-induced monocytic cell adhesion to rat aortic endothelial cells by suppression of vcam-1 expression. *Phytomedicine*. 2009;16:1027-1032
75. Hsieh CL, Cheng CY, Tsai TH, Lin IH, Liu CH, Chiang SY, Lin JG, Lao CJ, Tang NY. Paeonol reduced cerebral infarction involving the superoxide anion and microglia activation in ischemia-reperfusion injured rats. *J Ethnopharmacol*. 2006;106:208-215
76. Chae HS, Kang OH, Lee YS, Choi JG, Oh YC, Jang HJ, Kim MS, Kim JH, Jeong SI, Kwon DY. Inhibition of lps-induced inos, cox-2 and inflammatory mediator expression by paeonol through the mapks inactivation in raw 264.7 cells. *Am J Chin Med*. 2009;37:181-194
77. Reutershan J, Ley K. Bench-to-bedside review: Acute respiratory distress syndrome - how neutrophils migrate into the lung. *Crit Care*. 2004;8:453-461
78. Bhatia M, Zemans RL, Jeyaseelan S. Role of chemokines in the pathogenesis of acute lung injury. *Am J Respir Cell Mol Biol*. 2012;46:566-572
79. Zemans RL, Colgan SP, Downey GP. Transepithelial migration of neutrophils: Mechanisms and implications for acute lung injury. *Am J Respir Cell Mol Biol*. 2009;40:519-535
80. Zhou XH, Dai QC, Huang XL. Neutrophils in acute lung injury. *Front Biosci*. 2012;17:2278-2283
81. Saguil A, Fargo M. Acute respiratory distress syndrome: Diagnosis and management. *Am Fam Physician*. 2012;85:352-358
82. Bhargava M, Wendt CH. Biomarkers in acute lung injury. *Transl Res*. 2012;159:205-217
83. Barletta KE, Ley K, Mehrad B. Regulation of neutrophil function by adenosine. *Arterioscler Thromb Vasc Biol*. 2012;32:856-864
84. 林嬿釗, 韓云, 李芳. 中西醫結合治療重症肺炎合併急性呼吸窘迫綜合症臨床分析. *中國中醫急症*. 2006;15:113-115
85. 陳天琪, 葛正行. 淺談中醫對急性肺損傷的認識. *貴陽中醫學院學報*. 2006;28:7-8
86. 耿耘, 魏星. 急性呼吸窘迫綜合症的中醫發病機理探討. *江西中醫藥*. 2002;33:11-12
87. 李明富, 楊明鈞, 李堂圃. 中醫對呼吸窘迫綜合症的認識. *成都中醫學院學報*. 1980;3:3-6
88. 盧軍鋒, 顧勤, 劉寧. 中醫藥在急性呼吸窘迫綜合症診療中的應用. *吉林中醫藥*. 2008;28:243-245

89. 王今達, 高天元, 崔乃杰. 祖國醫學"肺與大腸相表裡"學說的臨床意義及其本質的探討. *中西醫結合雜誌*. 1982;2:77-81
90. 耿耘, 魏星. 急性肺損傷、急性呼吸窘迫綜合證的中醫發病機理探討. *江西中醫藥*. 2002;33:11-12
91. 孟苗苗, 傅敏, 鄭莉, 劉恩順, 孫增濤. Ali/ards 臟腑證候分布及肺腸相關特徵的初步調查. *天津中醫藥大學學報*. 2011;30:215-217
92. 謝玉寶, 梁子敬, 黃偉青. 急性肺損傷的中醫藥治療進展. *實用臨床醫藥雜誌*. 2008;12:113-115
93. 唐洪波, 陳寶國, 董俊玲. 從肺之化源速竭探討 ards 辨治. *江西中醫藥*. 2006;11:16
94. Yuan X, Wang Y, Du D, Hu Z, Xu M, Liu Z. The effects of the combination of sodium ferulate and oxymatrine on lipopolysaccharide-induced acute lung injury in mice. *Inflammation*. 2012;35:1161-1168
95. Xu M, Yang L, Hong LZ, Zhao XY, Zhang HL. Direct protection of neurons and astrocytes by matrine via inhibition of the nf-kappab signaling pathway contributes to neuroprotection against focal cerebral ischemia. *Brain Res*. 2012;1454:48-64
96. Liu L, Lu W, Ma Z, Li Z. Oxymatrine attenuates bleomycin-induced pulmonary fibrosis in mice via the inhibition of inducible nitric oxide synthase expression and the tgf-beta/smad signaling pathway. *Int J Mol Med*. 2012;29:815-822
97. Liu L, Xiong H, Ping J, Ju Y, Zhang X. Taraxacum officinale protects against lipopolysaccharide-induced acute lung injury in mice. *J Ethnopharmacol*. 2010;130:392-397
98. Xie JY, Di HY, Li H, Cheng XQ, Zhang YY, Chen DF. Bupleurum chinense dc polysaccharides attenuates lipopolysaccharide-induced acute lung injury in mice. *Phytomedicine*. 2012;19:130-137
99. Cheng XQ SL, Li H, Di H, Zhang YY, Chen DF. Beneficial effect of the polysaccharides from bupleurum smithii var. Parvifolium on "two-hit" acute lung injury in rats. *Inflammation*. 2012
100. Tseng TH, Chu CY, Huang JM, Shiow SJ, Wang CJ. Crocetin protects against oxidative damage in rat primary hepatocytes. *Cancer Lett*. 1995;97:61-67
101. Wang Y, Yan J, Xi L, Qian Z, Wang Z, Yang L. Protective effect of crocetin on hemorrhagic shock-induced acute renal failure in rats. *Shock*. 2012;38:63-67
102. Yan J, Qian Z, Sheng L, Zhao B, Yang L, Ji H, Han X, Zhang R. Effect of crocetin on blood pressure restoration and synthesis of inflammatory mediators in heart after hemorrhagic shock in anesthetized rats. *Shock*. 2010;33:83-87
103. Yang R, Yang L, Shen X, Cheng W, Zhao B, Ali KH, Qian Z, Ji H. Suppression of nf-kappab pathway by crocetin contributes to attenuation of lipopolysaccharide-induced acute lung injury in mice. *Eur J Pharmacol*.

2012;674:391-396
104. Yunhe F BL, Xiaosheng F, Fengyang L, Dejie L, Zhicheng L, Depeng L, Yongguo C, Xichen Z, Naisheng Z, Zhengtao Y. The effect of magnolol on the toll-like receptor 4/nuclear factor kappa b signaling pathway in lipopolysaccharide-induced acute lung injury in mice. *Eur J Pharmacol*. 2012
105. Burns JJ, Zhao L, Taylor EW, Spelman K. The influence of traditional herbal formulas on cytokine activity. *Toxicology*. 2010;278:140-159
106. Lee KH, Yeh MH, Kao ST, Hung CM, Chen BC, Liu CJ, Yeh CC. Xia-bai-san inhibits lipopolysaccharide-induced activation of intercellular adhesion molecule-1 and nuclear factor-kappa b in human lung cells. *J Ethnopharmacol*. 2009;124:530-538
107. 吳彩軍, 李春盛. 中藥注射液血必淨對感染性休克犬促凝物質的影響. *中華急診醫學雜誌*. 2009;18:140-143
108. Zhang SW, Sun CD, Wen Y, Yin CH. [effect of treatment with xuebijing injection on serum inflammatory mediators and th1/2 of spleen in rats with sepsis]. *Zhongguo Wei Zhong Bing Ji Jiu Yi Xue*. 2006;18:673-676
109. Li YP, Qiao YJ, Wu ZX, Qian FF, Yao YM, Yu Y, Wu Y. [effects of xuebijing injection on protein c and tumor necrosis factor-alpha mrna in rats with sepsis]. *Zhongguo Wei Zhong Bing Ji Jiu Yi Xue*. 2007;19:488-491
110. Zhu XQ, Wang L, Liu QQ, Yao YM. [protective effects of xuebijing injection on kidney in rats with sepsis]. *Zhongguo Wei Zhong Bing Ji Jiu Yi Xue*. 2006;18:680-683
111. 馬小美, 劉虹, 高青芳. 血必淨對內毒素致急性肺損傷大鼠炎症反應的影響. *中國藥物與臨床*. 2010;10:526-528
112. Qi F, Liang ZX, She DY, Yan GT, Chen LA. A clinical study on the effects and mechanism of xuebijing injection in severe pneumonia patients. *J Tradit Chin Med*. 2011;31:46-49
113. 歐陽潭, 歐陽玉萍, 魏全金. 中藥血必淨注射液對急性肺損傷病人呼吸功能和早期炎性反應的影響. *中醫臨床研究*. 2012;4:6-8
114. Murray JF, Matthay MA, Luce JM, Flick MR. An expanded definition of the adult respiratory distress syndrome. *Am Rev Respir Dis*. 1988;138:720-723
115. Ranieri V, Rubenfeld G, Thompson B, Ferguson N, Caldwell E, Fan E, Camporota L, Slutsky A. Acute respiratory distress syndrome. The berlin definition. *JAMA*. 2012;307:2526-2533
116. Angus D. The acute respiratory distress syndrome. What's in a name? *JAMA*. 2012;307:2542-2544
117. Thomsen GE, Morris AH. Incidence of the adult respiratory distress syndrome in the state of utah. *Am J Respir Crit Care Med*. 1995;152:965-971
118. Villar J, Slutsky AS. The incidence of the adult respiratory distress syndrome. *Am Rev Respir Dis*. 1989;140:814-816

119. Webster NR, Cohen AT, Nunn JF. Adult respiratory distress syndrome--how many cases in the uk? *Anaesthesia*. 1988;43:923-926
120. Luhr OR, Antonsen K, Karlsson M, Aardal S, Thorsteinsson A, Frostell CG, Bonde J. Incidence and mortality after acute respiratory failure and acute respiratory distress syndrome in sweden, denmark, and iceland. The arf study group. *Am J Respir Crit Care Med*. 1999;159:1849-1861
121. Frutos-Vivar F, Ferguson ND, Esteban A. Epidemiology of acute lung injury and acute respiratory distress syndrome. *Semin Respir Crit Care Med*. 2006;27:327-336
122. Brun-Buisson C, Minelli C, Bertolini G, Brazzi L, Pimentel J, Lewandowski K, Bion J, Romand JA, Villar J, Thorsteinsson A, Damas P, Armaganidis A, Lemaire F. Epidemiology and outcome of acute lung injury in european intensive care units. Results from the alive study. *Intensive Care Med*. 2004;30:51-61
123. Bersten AD, Edibam C, Hunt T, Moran J. Incidence and mortality of acute lung injury and the acute respiratory distress syndrome in three australian states. *Am J Respir Crit Care Med*. 2002;165:443-448
124. Rubenfeld GD, Herridge MS. Epidemiology and outcomes of acute lung injury. *Chest*. 2007;131:554-562
125. Acute lung injury and the acute respiratory distress syndrome in ireland: A prospective audit of epidemiology and management. *Crit Care*. 2008;12:R30
126. Levy MM, Fink MP, Marshall JC, Abraham E, Angus D, Cook D, Cohen J, Opal SM, Vincent JL, Ramsay G. 2001 sccm/esicm/accp/ats/sis international sepsis definitions conference. *Crit Care Med*. 2003;31:1250-1256
127. Shaz BH, Stowell SR, Hillyer CD. Transfusion-related acute lung injury: From bedside to bench and back. *Blood*. 2011;117:1463-1471
128. Matthay MA, Zemans RL. The acute respiratory distress syndrome: Pathogenesis and treatment. *Annu Rev Pathol*. 2011;6:147-163
129. Kinoshita M, Ono S, Mochizuki H. Neutrophils mediate acute lung injury in rabbits: Role of neutrophil elastase. *Eur Surg Res*. 2000;32:337-346
130. Chignard M, Balloy V. Neutrophil recruitment and increased permeability during acute lung injury induced by lipopolysaccharide. *Am J Physiol Lung Cell Mol Physiol*. 2000;279:L1083-1090
131. Quesnel C, Nardelli L, Piednoir P, Lecon V, Marchal-Somme J, Lasocki S, Bouadma L, Philip I, Soler P, Crestani B, Dehoux M. Alveolar fibroblasts in acute lung injury: Biological behaviour and clinical relevance. *Eur Respir J*. 2010;35:1312-1321
132. Bitterman PB. Pathogenesis of fibrosis in acute lung injury. *Am J Med*. 1992;92:39S-43S
133. Idell S. Coagulation, fibrinolysis, and fibrin deposition in acute lung injury. *Crit Care Med*. 2003;31:S213-220

134. Tomashefski JF, Jr. Pulmonary pathology of acute respiratory distress syndrome. *Clin Chest Med*. 2000;21:435-466
135. Sheridan BC, McIntyre RC, Jr., Moore EE, Meldrum DR, Agrafojo J, Fullerton DA. Neutrophils mediate pulmonary vasomotor dysfunction in endotoxin-induced acute lung injury. *J Trauma*. 1997;42:391-396; discussion 396-397
136. Delclaux C, Rezaiguia-Delclaux S, Delacourt C, Brun-Buisson C, Lafuma C, Harf A. Alveolar neutrophils in endotoxin-induced and bacteria-induced acute lung injury in rats. *Am J Physiol*. 1997;273:L104-112
137. Steinberg KP, Milberg JA, Martin TR, Maunder RJ, Cockrill BA, Hudson LD. Evolution of bronchoalveolar cell populations in the adult respiratory distress syndrome. *Am J Respir Crit Care Med*. 1994;150:113-122
138. Parsons PE, Fowler AA, Hyers TM, Henson PM. Chemotactic activity in bronchoalveolar lavage fluid from patients with adult respiratory distress syndrome. *Am Rev Respir Dis*. 1985;132:490-493
139. Matthay MA, Eschenbacher WL, Goetzl EJ. Elevated concentrations of leukotriene d4 in pulmonary edema fluid of patients with the adult respiratory distress syndrome. *J Clin Immunol*. 1984;4:479-483
140. Matthay MA. Conference summary: Acute lung injury. *Chest*. 1999;116:119S-126S
141. Shinbori T, Walczak H, Krammer PH. Activated t killer cells induce apoptosis in lung epithelial cells and the release of pro-inflammatory cytokine tnf-alpha. *Eur J Immunol*. 2004;34:1762-1770
142. Olson TS, Ley K. Chemokines and chemokine receptors in leukocyte trafficking. *Am J Physiol Regul Integr Comp Physiol*. 2002;283:R7-28
143. Matthay MA, Geiser T, Matalon S, Ischiropoulos H. Oxidant-mediated lung injury in the acute respiratory distress syndrome. *Crit Care Med*. 1999;27:2028-2030
144. Chabot F, Mitchell JA, Gutteridge JM, Evans TW. Reactive oxygen species in acute lung injury. *Eur Respir J*. 1998;11:745-757
145. Schutte H, Lohmeyer J, Rosseau S, Ziegler S, Siebert C, Kielisch H, Pralle H, Grimminger F, Morr H, Seeger W. Bronchoalveolar and systemic cytokine profiles in patients with ards, severe pneumonia and cardiogenic pulmonary oedema. *Eur Respir J*. 1996;9:1858-1867
146. Ware LB, Bastarache JA, Wang L. Coagulation and fibrinolysis in human acute lung injury--new therapeutic targets? *Keio J Med*. 2005;54:142-149
147. Gando S, Kameue T, Matsuda N, Hayakawa M, Morimoto Y, Ishitani T, Kemmotsu O. Imbalances between the levels of tissue factor and tissue factor pathway inhibitor in ards patients. *Thromb Res*. 2003;109:119-124
148. Welty-Wolf KE, Carraway MS, Ortel TL, Piantadosi CA. Coagulation and inflammation in acute lung injury. *Thromb Haemost*. 2002;88:17-25

149. Bastarache JA, Wang L, Wang Z, Albertine KH, Matthay MA, Ware LB. Intra-alveolar tissue factor pathway inhibitor is not sufficient to block tissue factor procoagulant activity. *Am J Physiol Lung Cell Mol Physiol*. 2008;294:L874-881
150. MacLaren R, Stringer KA. Emerging role of anticoagulants and fibrinolytics in the treatment of acute respiratory distress syndrome. *Pharmacotherapy*. 2007;27:860-873
151. Ware LB, Camerer E, Welty-Wolf K, Schultz MJ, Matthay MA. Bench to bedside: Targeting coagulation and fibrinolysis in acute lung injury. *Am J Physiol Lung Cell Mol Physiol*. 2006;291:L307-311
152. Wygrecka M, Jablonska E, Guenther A, Preissner KT, Markart P. Current view on alveolar coagulation and fibrinolysis in acute inflammatory and chronic interstitial lung diseases. *Thromb Haemost*. 2008;99:494-501
153. Abraham E. Coagulation abnormalities in acute lung injury and sepsis. *Am J Respir Cell Mol Biol*. 2000;22:401-404
154. Rijneveld AW, Weijer S, Bresser P, Florquin S, Vlasuk GP, Rote WE, Spek CA, Reitsma PH, van der Zee JS, Levi M, van der Poll T. Local activation of the tissue factor-factor viia pathway in patients with pneumonia and the effect of inhibition of this pathway in murine pneumococcal pneumonia. *Crit Care Med*. 2006;34:1725-1730
155. Schultz MJ, Millo J, Levi M, Hack CE, Weverling GJ, Garrard CS, van der Poll T. Local activation of coagulation and inhibition of fibrinolysis in the lung during ventilator associated pneumonia. *Thorax*. 2004;59:130-135
156. Fuchs-Buder T, de Moerloose P, Ricou B, Reber G, Vifian C, Nicod L, Romand JA, Suter PM. Time course of procoagulant activity and d dimer in bronchoalveolar fluid of patients at risk for or with acute respiratory distress syndrome. *Am J Respir Crit Care Med*. 1996;153:163-167
157. Idell S, James KK, Coalson JJ. Fibrinolytic activity in bronchoalveolar lavage of baboons with diffuse alveolar damage: Trends in two forms of lung injury. *Crit Care Med*. 1992;20:1431-1440
158. Idell S, Koenig KB, Fair DS, Martin TR, McLarty J, Maunder RJ. Serial abnormalities of fibrin turnover in evolving adult respiratory distress syndrome. *Am J Physiol*. 1991;261:L240-248
159. Ware LB, Matthay MA, Parsons PE, Thompson BT, Januzzi JL, Eisner MD. Pathogenetic and prognostic significance of altered coagulation and fibrinolysis in acute lung injury/acute respiratory distress syndrome. *Crit Care Med*. 2007;35:1821-1828
160. Levi M, Ten Cate H. Disseminated intravascular coagulation. *N Engl J Med*. 1999;341:586-592
161. Liu KD, Glidden DV, Eisner MD, Parsons PE, Ware LB, Wheeler A, Korpak A,

Thompson BT, Chertow GM, Matthay MA. Predictive and pathogenetic value of plasma biomarkers for acute kidney injury in patients with acute lung injury. *Crit Care Med*. 2007;35:2755-2761

162. Ware LB. Prognostic determinants of acute respiratory distress syndrome in adults: Impact on clinical trial design. *Crit Care Med*. 2005;33:S217-222
163. Welty-Wolf KE, Carraway MS, Idell S, Ortel TL, Ezban M, Piantadosi CA. Tissue factor in experimental acute lung injury. *Semin Hematol*. 2001;38:35-38
164. Zarbock A, Singbartl K, Ley K. Complete reversal of acid-induced acute lung injury by blocking of platelet-neutrophil aggregation. *J Clin Invest*. 2006;116:3211-3219
165. Kuebler WM. Selectins revisited: The emerging role of platelets in inflammatory lung disease. *J Clin Invest*. 2006;116:3106-3108
166. 李竹英, 王雪慧, 劉建秋. 急性肺損傷動物模型研究進展. *中國中醫急症*. 2011;20:1817-1818
167. Planck A, Eklund A, Grunewald J. Markers of activity in clinically recovered human leukocyte antigen-dr17-positive sarcoidosis patients. *Eur Respir J*. 2003;21:52-57
168. Chu EK, Whitehead T, Slutsky AS. Effects of cyclic opening and closing at low- and high-volume ventilation on bronchoalveolar lavage cytokines. *Crit Care Med*. 2004;32:168-174
169. Bellardine Black CL, Hoffman AM, Tsai LW, Ingenito EP, Suki B, Kaczka DW, Simon BA, Lutchen KR. Relationship between dynamic respiratory mechanics and disease heterogeneity in sheep lavage injury. *Crit Care Med*. 2007;35:870-878
170. Zick G, Frerichs I, Schadler D, Schmitz G, Pulletz S, Cavus E, Wachtler F, Scholz J, Weiler N. Oxygenation effect of interventional lung assist in a lavage model of acute lung injury: A prospective experimental study. *Crit Care*. 2006;10:R56
171. Lethvall S, Lindgren S, Lundin S, Stenqvist O. Tracheal double-lumen ventilation attenuates hypercapnia and respiratory acidosis in lung injured pigs. *Intensive Care Med*. 2004;30:686-692
172. Schermuly RT, Gunther A, Weissmann N, Ghofrani HA, Seeger W, Grimminger F, Walmrath D. Differential impact of ultrasonically nebulized versus tracheal-instilled surfactant on ventilation-perfusion (va/q) mismatch in a model of acute lung injury. *Am J Respir Crit Care Med*. 2000;161:152-159
173. Holm BA, Matalon S. Role of pulmonary surfactant in the development and treatment of adult respiratory distress syndrome. *Anesth Analg*. 1989;69:805-818
174. Kuckelt W, Dauberschmidt R, Bender V, Hieronymi U, Mrochen H, Winsel K, Meyer M. Experimental investigations in adult respiratory distress syndrome (ards). Repeated pulmonary lavage in lewe-mini-pigs. I. Pulmonary mechanics, gas exchange, and pulmonary hemodynamics. *Exp Pathol*. 1981;20:88-104
175. Claesson J, Lehtipalo S, Bergstrand U, Arnerlov C, Winso O. Negative mesenteric

effects of lung recruitment maneuvers in oleic acid lung injury are transient and short lasting. *Crit Care Med*. 2007;35:230-238

176. Roch A, Michelet P, Lambert D, Delliaux S, Saby C, Perrin G, Ghez O, Bregeon F, Thomas P, Carpentier JP, Papazian L, Auffray JP. Accuracy of the double indicator method for measurement of extravascular lung water depends on the type of acute lung injury. *Crit Care Med*. 2004;32:811-817
177. Gust R, McCarthy TJ, Kozlowski J, Stephenson AH, Schuster DP. Response to inhaled nitric oxide in acute lung injury depends on distribution of pulmonary blood flow prior to its administration. *Am J Respir Crit Care Med*. 1999;159:563-570
178. Neumann P, Berglund JE, Mondejar EF, Magnusson A, Hedenstierna G. Effect of different pressure levels on the dynamics of lung collapse and recruitment in oleic-acid-induced lung injury. *Am J Respir Crit Care Med*. 1998;158:1636-1643
179. Ito K, Mizutani A, Kira S, Mori M, Iwasaka H, Noguchi T. Effect of ulinastatin, a human urinary trypsin inhibitor, on the oleic acid-induced acute lung injury in rats via the inhibition of activated leukocytes. *Injury*. 2005;36:387-394
180. Eiermann GJ, Dickey BF, Thrall RS. Polymorphonuclear leukocyte participation in acute oleic-acid-induced lung injury. *Am Rev Respir Dis*. 1983;128:845-850
181. Moriuchi H, Zaha M, Fukumoto T, Yuizono T. Activation of polymorphonuclear leukocytes in oleic acid-induced lung injury. *Intensive Care Med*. 1998;24:709-715
182. Vadasz I, Morty RE, Kohstall MG, Olschewski A, Grimminger F, Seeger W, Ghofrani HA. Oleic acid inhibits alveolar fluid reabsorption: A role in acute respiratory distress syndrome? *Am J Respir Crit Care Med*. 2005;171:469-479
183. Cousineau D, Rose CP, Goresky CA. Plasma expansion effect on cardiac capillary and adrenergic exchange in intact dogs. *J Appl Physiol*. 1986;60:147-153
184. Hofman WF, Ehrhart IC. Permeability edema in dog lung depleted of blood components. *J Appl Physiol*. 1984;57:147-153
185. Derks CM, Jacobovitz-Derks D. Embolic pneumopathy induced by oleic acid. A systematic morphologic study. *Am J Pathol*. 1977;87:143-158
186. Miyazawa T, Nakagawa H, Hiramoto M, Arita K, Hiramoto T, Nishida O. Ultrastructural study on the alveolar-capillary injury with pulmonary edema induced by oleic acid in dogs. *Hiroshima J Med Sci*. 1981;30:183-190
187. Brigham KL, Meyrick B. Endotoxin and lung injury. *Am Rev Respir Dis*. 1986;133:913-927
188. Welbourn CR, Young Y. Endotoxin, septic shock and acute lung injury: Neutrophils, macrophages and inflammatory mediators. *Br J Surg*. 1992;79:998-1003
189. Bannerman DD, Goldblum SE. Mechanisms of bacterial lipopolysaccharide-induced endothelial apoptosis. *Am J Physiol Lung Cell Mol Physiol*. 2003;284:L899-914
190. O'Grady NP, Preas HL, Pugin J, Fiuza C, Tropea M, Reda D, Banks SM, Suffredini

AF. Local inflammatory responses following bronchial endotoxin instillation in humans. *Am J Respir Crit Care Med*. 2001;163:1591-1598

191. Wu CL, Lin LY, Yeh HM, Chan MC, Yang CH, Hsueh CM. Delay of lps-induced acute lung injury resolution by soluble immune complexes is neutrophil dependent. *Shock*. 2009;32:276-285
192. Wu CL, Lin LY, Yang JS, Chan MC, Hsueh CM. Attenuation of lipopolysaccharide-induced acute lung injury by treatment with il-10. *Respirology*. 2009;14:511-521
193. 孫星衍、孫馮翼. 神農本草經. 台北: 文光圖書公司; 1982:pp.162.
194. 汪昂. 增補本草備要. 台北: 文光圖書公司; 1986.
195. 倪朱謨. 本草匯言. 上海: 上海科学技術出版社; 2005.
196. Kim J, Lee H, Lee Y, Oh BG, Cho C, Kim Y, Shin M, Hong M, Jung SK, Bae H. Inhibition effects of moutan cortex radicis on secretion of eotaxin in a549 human epithelial cells and eosinophil migration. *J Ethnopharmacol*. 2007;114:186-193
197. Wu M, Gu Z. Screening of bioactive compounds from moutan cortex and their anti-inflammatory activities in rat synoviocytes. *Evid Based Complement Alternat Med*. 2009;6:57-63
198. Riley CM, Ren TC. Simple method for the determination of paeonol in human and rabbit plasma by high-performance liquid chromatography using solid-phase extraction and ultraviolet detection. *J Chromatogr*. 1989;489:432-437
199. Li N, Fan LL, Sun GP, Wan XA, Wang ZG, Wu Q, Wang H. Paeonol inhibits tumor growth in gastric cancer in vitro and in vivo. *World J Gastroenterol*. 2010;16:4483-4490
200. Chou TC. Anti-inflammatory and analgesic effects of paeonol in carrageenan-evoked thermal hyperalgesia. *Br J Pharmacol*. 2003;139:1146-1152
201. Ma LY, Xu XD, Zhang Q, Miao JH, Tang BL. Paeonol pharmacokinetics in the rat following i.M. Administration. *Eur J Drug Metab Pharmacokinet*. 2008;33:133-136
202. Xie Y, Zhou H, Wong YF, Xu HX, Jiang ZH, Liu L. Study on the pharmacokinetics and metabolism of paeonol in rats treated with pure paeonol and an herbal preparation containing paeonol by using hplc-dad-ms method. *J Pharm Biomed Anal*. 2008;46:748-756
203. Liu HX, Hu Y, Liu Y, He YQ, Li W, Yang L. Cyp1a2 is the major isoform responsible for paeonol o-demethylation in human liver microsomes. *Xenobiotica*. 2009;39:672-679
204. 李清俠, 趙春陽, 莫家鈺, 劉曉華, 富志軍, 馮鋒. 丹皮酚對小鼠體內藥動學及組織分布情況的研究. *海峽藥學*. 2011;23:45-47
205. Gjertsen FB, Solheim E, Scheline RR. Metabolism of aromatic plant ketones in rats: Acetovanillone and paeonol. *Xenobiotica*. 1988;18:225-234

206. 陳曉蘭, 陸洋, 杜守穎, 姚宗玲, 王珊, 李鵬躍. Hplc 測定丹皮中丹皮酚在大鼠體內血藥濃度及藥動學研究. *中國中藥雜誌*. 2010;35:2826-2828
207. Ishiguro K, Ando T, Maeda O, Hasegawa M, Kadomatsu K, Ohmiya N, Niwa Y, Xavier R, Goto H. Paeonol attenuates tnbs-induced colitis by inhibiting nf-kappab and stat1 transactivation. *Toxicol Appl Pharmacol*. 2006;217:35-42
208. Hu S, Shen G, Zhao W, Wang F, Jiang X, Huang D. Paeonol, the main active principles of paeonia moutan, ameliorates alcoholic steatohepatitis in mice. *J Ethnopharmacol*. 2010;128:100-106
209. Huang H, Chang EJ, Lee Y, Kim JS, Kang SS, Kim HH. A genome-wide microarray analysis reveals anti-inflammatory target genes of paeonol in macrophages. *Inflamm Res*. 2008;57:189-198
210. Zhang HY, Ge N, Zhang ZY. Theoretical elucidation of activity differences of five phenolic antioxidants. *Zhongguo Yao Li Xue Bao*. 1999;20:363-366
211. Li Q, Engelhardt JF. Interleukin-1beta induction of nfkappab is partially regulated by h2o2-mediated activation of nfkappab-inducing kinase. *J Biol Chem*. 2006;281:1495-1505
212. Zhong SZ, Ge QH, Qu R, Li Q, Ma SP. Paeonol attenuates neurotoxicity and ameliorates cognitive impairment induced by d-galactose in icr mice. *J Neurol Sci*. 2009;277:58-64
213. Chen J, Sanberg PR, Li Y, Wang L, Lu M, Willing AE, Sanchez-Ramos J, Chopp M. Intravenous administration of human umbilical cord blood reduces behavioral deficits after stroke in rats. *Stroke*. 2001;32:2682-2688
214. Mi XJ, Chen SW, Wang WJ, Wang R, Zhang YJ, Li WJ, Li YL. Anxiolytic-like effect of paeonol in mice. *Pharmacol Biochem Behav*. 2005;81:683-687
215. Wu JB, Song NN, Wei XB, Guan HS, Zhang XM. Protective effects of paeonol on cultured rat hippocampal neurons against oxygen-glucose deprivation-induced injury. *J Neurol Sci*. 2008;264:50-55
216. Kim SH, Kim SA, Park MK, Park YD, Na HJ, Kim HM, Shin MK, Ahn KS. Paeonol inhibits anaphylactic reaction by regulating histamine and tnf-alpha. *Int Immunopharmacol*. 2004;4:279-287
217. Lee B, Shin YW, Bae EA, Han SJ, Kim JS, Kang SS, Kim DH. Antiallergic effect of the root of paeonia lactiflora and its constituents paeoniflorin and paeonol. *Arch Pharm Res*. 2008;31:445-450
218. Du Q, Feng GZ, Shen L, Cui J, Cai JK. Paeonol attenuates airway inflammation and hyperresponsiveness in a murine model of ovalbumin-induced asthma. *Can J Physiol Pharmacol*. 2010;88:1010-1016
219. Ma YL, Bates S, Gurney AM. The effects of paeonol on the electrophysiological properties of cardiac ventricular myocytes. *Eur J Pharmacol*. 2006;545:87-92

220. Siu D. A new way of targeting to treat coronary artery disease. *J Cardiovasc Med (Hagerstown)*. 2010;11:1-6
221. Li H, Dai M, Jia W. Paeonol attenuates high-fat-diet-induced atherosclerosis in rabbits by anti-inflammatory activity. *Planta Med*. 2009;75:7-11
222. Nizamutdinova IT, Jin YC, Kim JS, Yean MH, Kang SS, Kim YS, Lee JH, Seo HG, Kim HJ, Chang KC. Paeonol and paeoniflorin, the main active principles of paeonia albiflora, protect the heart from myocardial ischemia/reperfusion injury in rats. *Planta Med*. 2008;74:14-18
223. Tsai HY, Lin HY, Fong YC, Wu JB, Chen YF, Tsuzuki M, Tang CH. Paeonol inhibits rankl-induced osteoclastogenesis by inhibiting erk, p38 and nf-kappab pathway. *Eur J Pharmacol*. 2008;588:124-133
224. Kanazawa I. Short review on monoamine oxidase and its inhibitors. *Eur Neurol*. 1994;34 Suppl 3:36-39
225. Kong LD, Cheng CH, Tan RX. Inhibition of mao a and b by some plant-derived alkaloids, phenols and anthraquinones. *J Ethnopharmacol*. 2004;91:351-355
226. Xing G, Zhang Z, Liu J, Hu H, Sugiura N. Antitumor effect of extracts from moutan cortex on dld-1 human colon cancer cells in vitro. *Mol Med Report*. 2010;3:57-61
227. Sun GP, Wan X, Xu SP, Wang H, Liu SH, Wang ZG. Antiproliferation and apoptosis induction of paeonol in human esophageal cancer cell lines. *Dis Esophagus*. 2008;21:723-729
228. Kim SA, Lee HJ, Ahn KS, Lee EO, Choi SH, Jung SJ, Kim JY, Baek N, Kim SH. Paeonol exerts anti-angiogenic and anti-metastatic activities through downmodulation of akt activation and inactivation of matrix metalloproteinases. *Biol Pharm Bull*. 2009;32:1142-1147
229. Ye JM, Deng T, Zhang JB. Influence of paeonol on expression of cox-2 and p27 in ht-29 cells. *World J Gastroenterol*. 2009;15:4410-4414
230. Chunhu Z, Suiyu H, Meiqun C, Guilin X, Yunhui L. Antiproliferative and apoptotic effects of paeonol on human hepatocellular carcinoma cells. *Anticancer Drugs*. 2008;19:401-409
231. Wan XA, Sun GP, Wang H, Xu SP, Wang ZG, Liu SH. Synergistic effect of paeonol and cisplatin on oesophageal cancer cell lines. *Dig Liver Dis*. 2008;40:531-539
232. Fu PK, Wu CL, Tsai TH, Hsieh CL. Anti-inflammatory and anticoagulative effects of paeonol on lps-induced acute lung injury in rats. *Evidence-Based Complementary and Alternative Medicine*. 2012;2012
233. Bradford MM. A rapid and sensitive method for the quantitation of microgram quantities of protein utilizing the principle of protein-dye binding. *Anal Biochem*. 1976;72:248-254
234. Zor T, Selinger Z. Linearization of the bradford protein assay increases its sensitivity:

Theoretical and experimental studies. *Anal Biochem*. 1996;236:302-308
235. Noble JE, Bailey MJ. Quantitation of protein. *Methods Enzymol*. 2009;463:73-95
236. Kristof AS, Goldberg P, Laubach V, Hussain SN. Role of inducible nitric oxide synthase in endotoxin-induced acute lung injury. *Am J Respir Crit Care Med*. 1998;158:1883-1889
237. Odell EW, Segal AW. The bactericidal effects of the respiratory burst and the myeloperoxidase system isolated in neutrophil cytoplasts. *Biochim Biophys Acta*. 1988;971:266-274
238. Wang P, Henning SM, Heber D. Limitations of mtt and mts-based assays for measurement of antiproliferative activity of green tea polyphenols. *PLoS One*. 2010;5:e10202
239. Tai H, Kobayashi T, Hara K. Changes in complement and immunoglobulin g receptor expression on neutrophils associated with porphyromonas gingivalis-induced inhibition of phagocytosis. *Infect Immun*. 1993;61:3533-3535
240. van Engeland M, Ramaekers FC, Schutte B, Reutelingsperger CP. A novel assay to measure loss of plasma membrane asymmetry during apoptosis of adherent cells in culture. *Cytometry*. 1996;24:131-139
241. Kawa S, Kimura S, Hakomori S, Igarashi Y. Inhibition of chemotactic motility and trans-endothelial migration of human neutrophils by sphingosine 1-phosphate. *FEBS Lett*. 1997;420:196-200
242. Williams EA, Quinlan GJ, Anning PB, Goldstraw P, Evans TW. Lung injury following pulmonary resection in the isolated, blood-perfused rat lung. *Eur Respir J*. 1999;14:745-750
243. Kobayashi A, Hashimoto S, Kooguchi K, Kitamura Y, Onodera H, Urata Y, Ashihara T. Expression of inducible nitric oxide synthase and inflammatory cytokines in alveolar macrophages of ards following sepsis. *Chest*. 1998;113:1632-1639
244. Su CF, Yang FL, Chen HI. Inhibition of inducible nitric oxide synthase attenuates acute endotoxin-induced lung injury in rats. *Clin Exp Pharmacol Physiol*. 2007;34:339-346
245. Razavi HM, Wang le F, Weicker S, Rohan M, Law C, McCormack DG, Mehta S. Pulmonary neutrophil infiltration in murine sepsis: Role of inducible nitric oxide synthase. *Am J Respir Crit Care Med*. 2004;170:227-233
246. Razavi HM, Werhun R, Scott JA, Weicker S, Wang le F, McCormack DG, Mehta S. Effects of inhaled nitric oxide in a mouse model of sepsis-induced acute lung injury. *Crit Care Med*. 2002;30:868-873
247. Enkhbaatar P, Murakami K, Shimoda K, Mizutani A, Traber L, Phillips GB, Parkinson JF, Cox R, Hawkins H, Herndon D, Traber D. The inducible nitric oxide synthase inhibitor bbs-2 prevents acute lung injury in sheep after burn and smoke

inhalation injury. *Am J Respir Crit Care Med*. 2003;167:1021-1026
248. Mayer-Scholl A, Averhoff P, Zychlinsky A. How do neutrophils and pathogens interact? *Curr Opin Microbiol*. 2004;7:62-66
249. Hampton MB, Kettle AJ, Winterbourn CC. Inside the neutrophil phagosome: Oxidants, myeloperoxidase, and bacterial killing. *Blood*. 1998;92:3007-3017
250. Borregaard N. Neutrophils, from marrow to microbes. *Immunity*. 2010;33:657-670
251. Lee WL, Harrison RE, Grinstein S. Phagocytosis by neutrophils. *Microbes Infect*. 2003;5:1299-1306
252. Shen YC, Chiou WF, Chou YC, Chen CF. Mechanisms in mediating the anti-inflammatory effects of baicalin and baicalein in human leukocytes. *Eur J Pharmacol*. 2003;465:171-181
253. Strieter RM, Kunkel SL. Acute lung injury: The role of cytokines in the elicitation of neutrophils. *J Investig Med*. 1994;42:640-651

Anti-inflammatory and Anticoagulative Effects of *Moutan Cortex* Radices and Paeonol on LPS-induced Acute Lung Injury in Rats

Name: Pin-Kuei Fu

Major Advisor: Ching-Liang Hsieh

Institute: School of Chinese Medicine, China Medical University, Taichung, Taiwan

Abstract

Moutan Cortex Radicis (MCR) is a Chinese herbal medicine that was widely used over a long period as an analgesic, antipyretic, and anti-inflammatory agent in China. Paeonol is a major active component of *Moutan Cortex Radicis*. Lipopolysaccharide (LPS)-induced acute lung injury (ALI) in rat models is considered similar to adult respiratory distress syndrome (ARDS) in humans. Therefore, the present study investigates the effect of MCR and Paeonol on ALI. The ALI model was developed through the intra-tracheal (IT) administration of LPS (16 mg/kg) to Sprague-Dawley (SD) rats, which formed the LPS group. MCR was orally administered before and after LPS was introduced into rats (MCR-LPS group and LPS-MCR group, respectively). In the MCR-LPS group, rats received MCR 2 g/kg/times 3 times before LPS challenge; the LPS-MCR group received MCR 2 g/kg/times 3 times after LPS challenge. The results of this experiment indicate that the number of total cells

and neutrophils and the concentration of protein exudation in bronchoalveolar lavage fluid (BALF) significantly decreased in the MCR-LPS group. Cytokine levels, including IL-1b, MIP-2, IL-6, and IL-10, in BALF were also significantly inhibited at 16 h after LPS administration in the MCR-LPS group. Myeloperoxidase (MPO) activity in lung tissue was reduced in the MCR-LPS and LPS-MCR groups at 16 h after LPS administration. Furthermore, leukocyte infiltration and protein exudation in the alveolar space were less severe in the MCR-LPS group than in the LPS group. Therefore, the findings of this study suggest that the administration of MCR prior to LPS improves ALI, possibly mediating ALI through antiinflammation.

The intraperitoneal administration of paeonol successfully reduced histopathological scores and attenuated myeloperoxidase-reactive cells as an index of polymorphonuclear neutrophils infiltration and also reduces inducible nitric oxide synthase expression in the lung tissue, at 16 h after LPS administration. In addition, paeonol reduced proinflammatory cytokines in bronchoalveolar lavage fluid, including TNF-α, IL-1β, IL-6, and PAI-1. These results indicated that paeonol successfully attenuates inflammatory and coagulation reactions to protect against ALI

Key words: *Moutan Cortex* Radicis; paeonol; Lipopolysaccharide; Acute lung injury; Anti-inflammation; Anti-coagulation

Phytomedicine 19 (2012) 1206–1215

Contents lists available at SciVerse ScienceDirect

Phytomedicine

journal homepage: www.elsevier.de/phymed

Moutan cortex radicis improves lipopolysaccharide-induced acute lung injury in rats through anti-inflammation

Pin-Kuei Fu[a,b], Chi-Yu Yang[c], Tung-Hu Tsai[d], Ching-Liang Hsieh[e,f,*]

[a] *Division of Critical Care & Respiratory Therapy, Department of Internal Medicine, Taichung Veterans General Hospital, Taichung 40407, Taiwan*
[b] *Graduate Institute of Chinese Medical Science, College of Chinese Medicine, China Medical University, Taichung 40402, Taiwan*
[c] *Division of Animal Medicine, Animal Technology Institute Taiwan, Miaoli 35053, Taiwan*
[d] *Institute of Traditional Medicine, School of Medicine, National Yang-Ming University, Taipei 11221, Taiwan*
[e] *Department of Chinese Medicine, China Medical University Hospital, Taichung 40402, Taiwan*
[f] *Graduate Institute of Integrated Medicine, College of Chinese Medicine, China Medical University, 91 Hsueh-Shih Road, Taichung 40402, Taiwan, ROC*

ARTICLE INFO

Keywords:
Moutan cortex radicis (MCR)
Lipopolysaccharide (LPS)
Acute lung injury (ALI)
Anti-inflammation

ABSTRACT

Moutan cortex radicis (MCR) is a Chinese herbal medicine that was widely used over a long period as an analgesic, antipyretic, and anti-inflammatory agent in China. Lipopolysaccharide (LPS)-induced acute lung injury (ALI) in rat models is considered similar to adult respiratory distress syndrome (ARDS) in humans. Therefore, the present study investigates the effect of MCR on ALI. The ALI model was developed through the intra-tracheal (IT) administration of LPS (16 mg/kg) to Sprague-Dawley (SD) rats, which formed the LPS group. MCR was orally administered before and after LPS was introduced into rats (MCR-LPS group and LPS-MCR group, respectively). In the MCR-LPS group, rats received MCR 2 g/kg/times 3 times before LPS challenge; the LPS-MCR group received MCR 2 g/kg/times 3 times after LPS challenge. The results of this experiment indicate that the number of total cells and neutrophils and the concentration of protein exudation in bronchoalveolar lavage fluid (BALF) significantly decreased in the MCR-LPS group. Cytokine levels, including levels of interleukin (IL)-1β, macrophage-inflammatory peptide (MIP)-2, IL-6, and IL-10, in BALF were also significantly inhibited at 16 h after LPS administration in the MCR-LPS group. Myeloperoxidase (MPO) activity in lung tissue was reduced in the MCR-LPS and LPS-MCR groups at 16 h after LPS administration. Furthermore, leukocyte infiltration and protein exudation in the alveolar space were less severe in the MCR-LPS group than in the LPS group. Therefore, the findings of this study suggest that the administration of MCR prior to LPS improves ALI, possibly mediating ALI through anti-inflammation.

Introduction

Acute lung injury (ALI) and acute respiratory distress syndrome (ARDS) are responsible for significant morbidity and mortality in critically ill patients (Ware and Matthay 2000). Inflammatory cascades developed in the lungs are the major manifestations of ALI and ARDS. These inflammatory responses can be summarized as polymorphonuclear neutrophil (PMN) accumulation (Abraham et al. 2000; Chignard and Balloy 2000; Kinoshita et al. 2000; Abraham 2003), disruption of epithelial integrity, interstitial edema, and protein exudation leakage into the alveolar space (Ware and Matthay 2000; Dreyfuss and Ricard 2005; Sapru et al. 2006). Several animal models, including models with *in vivo* intra-tracheal (IT) administration of lipopolysaccharide (LPS), have been developed to study the pathophysiologic mechanism of ARDS. These models possess high clinical relevance (van Helden et al. 1997; Matute-Bello et al. 2008; Wang et al. 2008) and have been successfully implemented in our previous studies (Wu et al. 2009a,b; Fu et al. 2012). LPS-induced ALI is considered a neutrophil-dependent ALI that contributes to local recruitment and activation of neutrophils (Sheridan et al. 1997; Abraham et al. 2000; Kinoshita et al. 2000; Abraham 2003); the release of pro-inflammatory cytokines (Schutte et al. 1996; Matthay et al. 1999; Bauer et al. 2000; Shinbori et al. 2004), such as tumor necrosis factor (TNF)-α, Interleukine (IL)-1β, and IL-6; and the formation of reactive oxygen and nitrogen species (Schutte et al. 1996; Matthay et al. 1999; Williams et al. 1999; Nys et al. 2002). Neutrophil recruitment in the lungs is regarded as a histological hallmark in the progression of ALI (Reutershan and Ley 2004; Balamayooran et al. 2010; Grommes and Soehnlein 2011). In rat models with ALI and ARDS, macrophage-inflammatory peptide-2 (MIP-2, also called CXCL2) plays a crucial role in neutrophil accumulation in the lungs (Gupta et al. 1996; Olson and Ley 2002;

* Corresponding author at: Graduate Institute of Integrated Medicine, College of Chinese Medicine, China Medical University, 91 Hsueh-Shih Road, Taichung 40402, Taiwan, ROC. Tel.: +886 4 22053366x3500; fax: +886 4 22037690.
E-mail address: clhsieh@mail.cmuh.org.tw (C.-L. Hsieh).

0944-7113/$ – see front matter.
http://dx.doi.org/10.1016/j.phymed.2012.07.013

Abraham 2003; Reutershan and Ley 2004). Whereas MIP-2 (CXCL2) has been suggested as the most important chemoattractant for neutrophil recruitment, TNF-α and IL-1β have been determined to increase the expression of cell adhesion molecules. Activated and recruited neutrophils contribute to increases in protease activity (e.g., myeloperoxidase (MPO) and lysozyme activity) and promote the formation of various oxygen metabolites, finally leading to diffused alveolar matrix damage (Zemans et al. 2009).

Recently, increasing evidence has been presented concerning the connection between coagulation and inflammation in ALI and ARDS (Sapru et al. 2006; Schultz et al. 2006; Slofstra et al. 2006; Ware et al. 2006). High levels of pro-inflammatory cytokines, such as TNF-α, IL-1β, and IL-6, are released during ALI and ARDS, leading to an inflammatory cascade and simultaneously triggering pulmonary coagulopathy (Ware et al. 2005; Sapru et al. 2006; Schultz et al. 2006; Wygrecka et al. 2008). The coagulation cascade is possibly activated because the inflammatory cascade stimulates tissue factor (TF) expression, attenuates fibrinolysis by stimulating the release of plasminogen activator inhibitors (PAI), and finally causes fibrin deposition in the airspaces and lung microvasculature (Levi and Ten Cate 1999; Abraham 2000; Ware et al. 2005; Bastarache et al. 2006; Wygrecka et al. 2008). Although pulmonary coagulopathy is now accepted as a new target in the treatment of ALI and ARDS (Schultz et al. 2006; Ware et al. 2006), no effective medicines currently approved by the Food and Drug Administration (FDA) are available to treat these severe diseases.

Moutan cortex radicis (MCR), the root cortex of *Paeonia suffruticosa Andrews*, is widely applied as an analgesic, antipyretic, and anti-inflammatory agent in traditional Chinese medicine (TCM; Lin et al. 1999; Tatsumi et al. 2004). In TCM, MCR has been shown to alleviate sickness in humans by eliminating heat, promoting blood flow, and removing blood stasis. Previous studies have demonstrated that MCR has a scavenging effect on free radicals and superoxide anion radicals (Yoshikawa et al. 2000), inhibits the production of ROS and oxidative stress by over-expression of heme oxygenase (HO) and cathechol-*O*-methyltransferase (COMT) (Rho et al. 2005), and restrains oxidative DNA cleavage (Okubo et al. 2000). MCR is also reported to inhibit eosinophil migration (Kim et al. 2007) and the secretion of IL-8 and monocyte chemotactic protein (MCP)-1 (Oh et al. 2003). The major chemical components of MCR include paeonol, paeonoside, paeonolide, and paeoniflorin (Rho et al. 2005). Paeonol, a major phenolic component of MCR, is reported to improve blood circulation by inhibiting both platelet aggregation and blood coagulation (Hirai et al. 1983; Koo et al. 2010), and to inhibit the expression of cell surface adhesion molecules (Nizamutdinova et al. 2007), pro-inflammatory cytokines such as TNF-α and IL-1β (Hsieh et al. 2006; Pan and Dai 2009), and reactive oxygen species production (Hsieh et al. 2006; Chae et al. 2009). In addition, recent research performed by the authors of this study has demonstrated that paeonol attenuates LPS-induced ALI through anti-inflammatory and anti-coagulative effects (Fu et al. 2012). However, the paeonol component of MCR employed in our previous study was dissolved in DMSO solution and administered through intra-peritoneal injection. Consequently, this study investigates MCR's effects and mechanisms when a subtle granular extract formula of MCR widely used in Taiwanese clinical settings to treat ALI is employed as well as the effects of MCR administration before and after LPS challenge.

Materials and methods

Reagents

Almost all reagents and media used in this study were purchased from Sigma Chemical (Deisenhofen, Germany), except for specific cytokines. Lipopolysaccharide (LPS; *Escherichia coli* 0055:B5, Sigma Chemical) was purchased from Sigma Chemical (St. Louis, MO, USA). Pro-inflammatory cytokines, such as TNF-α (BMS622MST, BenderMedsytem), IL-1β (BMS630, BenderMedsystem), and IL-6 (BMS625MST, BenderMedsystem), were purchased from Bender MedSystems (Vienna, Austria). IL-10 (14-8101-62, eBioscience) was purchased from eBioscience Systems (San Diego, CA, USA). MIP-2 (#KRC1022) was purchased from BioSource International, Inc (CA, USA). TATC (ET1020-1 Lot No. 1259916R1) and PAI-1 (Catalog # RPAIKT-TOT) were purchased from Molecular Innovations, Inc (Novi, MI, USA).

Preparation of MCR

Subtle granular MCR extract (MU DAN PI; KO DA; Product number: 420701903) was obtained from Koda Pharmaceuticas Ltd (Taoyuan, Taiwan). During preparation, 4.34 g of crude MCR was made into 0.67 g of plaster, and the ratio of crude MCR to plaster MCR was 6.5:1. Finally, the plaster was added to 0.33 g of starch to become subtle granular MCR extract.

High performance liquid chromatography (HPLC) system

Paeonol and paeoniflorin, the major chemical components of MCR, served as the authenticator and quality proof of this drug were used for the chromatographic fingerprint analysis. The plaster was identified using a HPLC system (interface D-7000, Pump L-7100, UV-Vis Detector L-7455, Autosampler L-7200, Hitachi Instruments Service Co. Ltd., Ibaraki-ken, Japan). Separation was carried out on a Mightysil RP-18 reversed-phase column (5 μm, 250 mm × 4.6 mm). For paeonol analysis (paeonol as a standard from the laboratory room of Professor Tsai, National Yang-Ming University, Taipei, Taiwan), the mobile phase was set at 38% acetonitrile (mixed with 62% of 0.03% H_3PO_4) with the flow rate 1 ml/min, the column temperature was 30 °C and the detection wavelength was set at 274 nm. For paeoniflorin analysis (paeoniflorin as a standard from China National Institutes for Food and Drug control), the mobile phase was started with 16% acetonitrile (mixed with 62% of 0.03% H_3PO_4) for 25 min with the flow rate 1 ml/min, the column temperature was 30 °C and the detection wavelength was set at 230 nm. The percentage of acetonitrile was increased to 30% at 25 min, 50% at 30–45 min and finally to 16% at 50 min. A 20 μl injection valve (Rheodyne) was used in all analyses.

The aristolochic acid of MCR was authenticated by using the aristolochic acid (SIGMA, USA) which contains 40% of aristolochic acid I (AA-I) as a standard. All analyses were performed on a HITACHI L-7000 liquid chromatographic system which consisted of a pump (L-7100), a column thermostat, a model 7725i injection value (sample loop 20 μl) and a UV detector (L-7455). The analysis was carried out on a Mightysil RP-18 (GP 250 mm × 4.6 mm, 5 μm) column at 30 °C. The mobile phase was a mixture of acetonitrile (45%) and NaH_2PO_4 buffer (55%, add 6.9 g of NaH_2PO_4 into 2 ml of 85% H_3PO_4 to a total volume of 1000 ml) with isocratic elution at a flow rate of 1.0 ml/min. The column eluate was monitored at 400 nm. The injection volume was 10 μl.

HPLC fingerprint analysis of paeonol, paeoniflorin and aristolochic acid from subtle granular MCR extract was marker in Fig. 2a–f. Therefore, there has components of paeonol and paeoniflorin in the subtle granular MCR extract, but no aristolochic acid component was detected. Each gram of the extract contained 0.67 g of MCR and an 8.68 mg dose of paeonol, and 15.79 mg dose of paeoniflorin.

Effects of MCR on LPS-induced ALI

Animals and experimental design

During the animal study, pathogen-free Sprague-Dawley (SD) rats, weighing approximately 250–300 g were obtained from

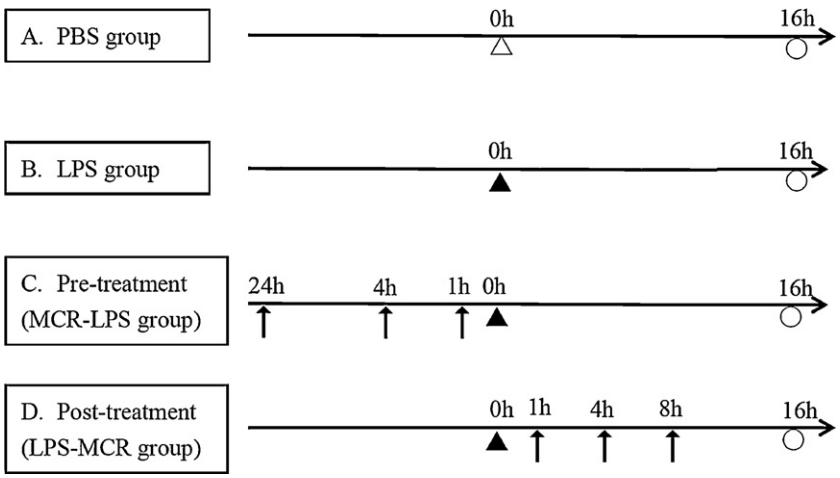

Fig. 1. Experimental designs for the *in vivo* study. Sprague-Dawley (SD) rats were randomly assigned to 4 groups ($n = 6$ for each group). (A) The PBS group: rats received 0.5 ml of PBS (phosphate buffer saline) through intra-tracheal administration (△) at 0 h and were sacrificed (○) at 16 h; (B) the LPS group: rats received lipopolysaccharide (LPS; 16 mg/kg) through intra-tracheal administration (▲) at 0 h and were sacrificed at 16 h; (C) the MCR-LPS group: rats received oral treatment with *Moutan cortex radicis* (MCR; 2 g/kg, 3 times) (↑) prior to LPS challenge; (D) the LPS-MCR group: rats received MCR (2 g/kg; 3 times) after LPS challenge.

BioLASCO Taiwan Co., Ltd (Taipei, Taiwan). The rats were housed in climate-controlled quarters with a 12-h light and dark cycle and free access to food and water. Animal experiments were conducted according to principles presented in the *Guide for the Care and Use of Laboratory Animals*, and were approved by the Animal Study Protocol Review Board of Taichung Veterans General Hospital. The rats were randomly divided into 4 groups, and each group consisted of at least 6 rats. Some animals were challenged with IT administration of 16 mg/kg LPS dissolved in 0.5 ml PBS ($n = 6$), whereas others were treated with 3 consecutive doses of orally administered MCR (2 g/kg) before ($n = 6$) and after ($n = 6$) LPS challenge. The control group received intra-tracheal instillation of PBS only (0.5 ml PBS; $n = 6$). The pre-LPS treatment group was treated with MCR (2 g/kg, dissolved in 2 ml of distilled water). Groupings and experimental designs are shown in Fig. 1. Prior to the experiment, body weight and rectal temperature (RT) were record; the animals were then anesthetized using inhaled 2% isoflurane (Halocarbon Laboratories Div Halocarbon Products Crop, River Edge, NJ) in 0.5 l/min O_2. Following anesthesia, an IT spray was administered by inserting a MicroSprayer® Aerosolizer (Model IA-1B, Penn-Century, Inc., Wyndmoor, PA, USA) into the trachea under visual guidance. The micro-sprayer was then removed and the animals were placed in a vertical position and rotated for 30 s to let the spray distribute evenly throughout the lungs as described in a previous study (Fu et al. 2012). Sixteen hours after inoculation, RT was measured again and rats were then sacrificed using CO_2 asphyxiation.

Cell counts and total protein assay in bronchoalveolar lavage (BAL)

Sixteen hours after LPS administration, animals were anesthetized through the inhalation of 2% isoflurane in 0.5 l/min O_2, and the thoracic cages of the rats were carefully opened after they

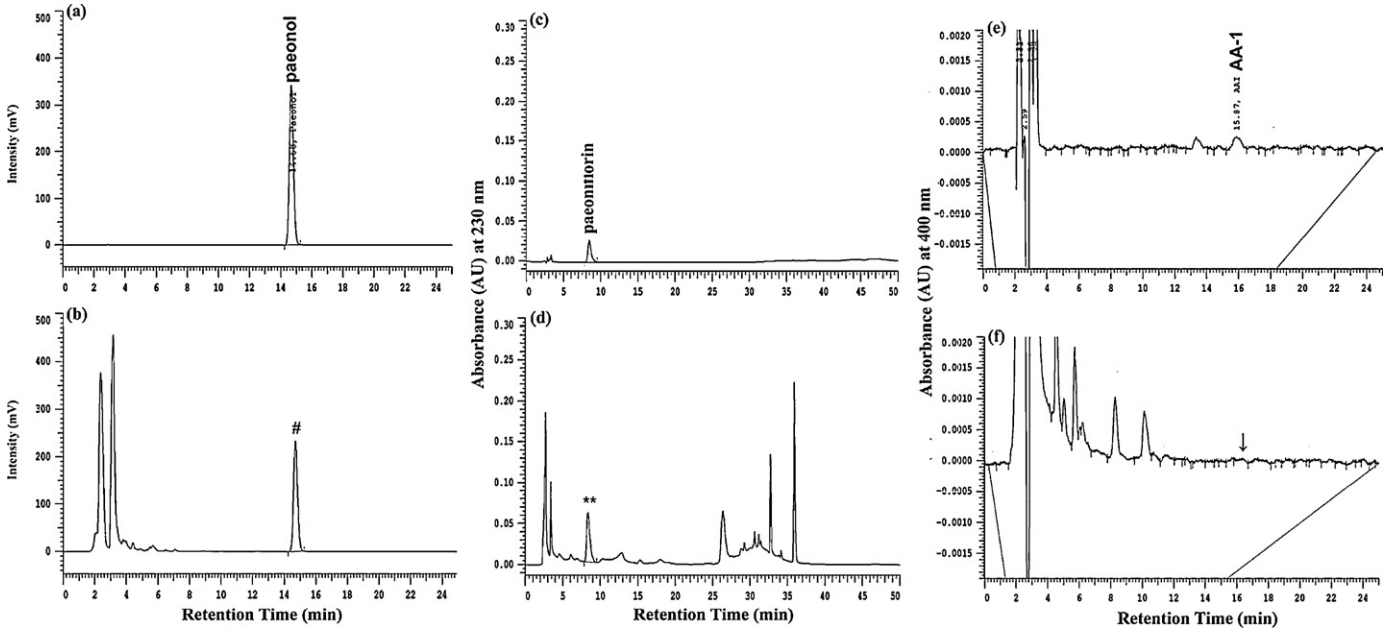

Fig. 2. HPLC fingerprint analysis of subtle granular MCR extract. Contents of chemical markers of subtle granular MCR extract were detected as follows: both retention time of paeonol were 14.68 min in the standard (a) and in the subtle granular MCR extract (b; #); both retention time of paeoniflorin were 8.46 min in the standard (c) and in the subtle granular MCR extract (d; **); The retention time aristolochic acid I was 15.89 min in the standard (e), but no peak was identified in the subtle granular MCR extract (f; ↓).

were sacrificed. The right main bronchus was subsequently ligated and a catheter was inserted from the trachea into the left lung. Eight milliliters of warm saline (37 °C) was run through the catheter 3 times. Resulting bronchoalveolar lavage fluids (BALF) were then passed through mesh (200 μm) to remove mucus, and centrifugation (1500 × *g*) at 4 °C for 15 min followed. The resulting pellets were re-suspended in 2 ml PBS. Erythrocytes were lysed using cold water and a hypertonic recovery solution (10× HBSS). The erythrocyte-free cell suspension was then washed once using 1× PBS and was employed for total cell count. Finally, 2×10^5 BALF-derived cells were evenly distributed onto a cytospin slide and then stained with Liu's stain for 2 min to perform further cell counting under a microscope (Wu et al. 2009a). The resulting supernatants were stored at −70 °C until the analysis stage. The total protein concentrations in BALF were measured using a bicinchoninic acid (BCA) assay according to company protocol (Bradford protein assay, Bio-Rad, Hercules, CA, USA).

The determination of cytokine levels in BALF

Cytokine levels in BALF, such as those for TNF-α (BMS622MST, BenderMedsystem), IL-1β (BMS630, BenderMedsystem), IL-6 (BMS625MST, BenderMedsystem), MIP-2 (#KRC1022), and IL-10 (14-8101-62, eBioscience), were measured using commercially available ELISA kits and in accordance with manufacturer protocol (Assay Designs, Inc., MI, USA). BALF supernatants were added to pre-coated monoclonal antibody microelisa wells and were measured using a micro-plate reader (Microplate Reader BIO-RAD Laboratories, CA, USA) at 450 nm for 15 min. Concentrations of BALF cytokines were measured by comparing the absorbance of standards, and expressed as picograms per milliliter (pg/ml).

Thrombin–anti-thrombin complexes (TATC) were used as a measure of coagulation through the tissue factor pathway; a high TATC level reflects the activation of the coagulation system (Weijer et al. 2004; Slofstra et al. 2006). TATC levels in BALF were measured using the TATC enzyme-linked immunosorbent assay Micrognost kit and by following suggestions from the manufacturer's instructions (AssayMax human thrombin–anti-thrombin TAT complex ELISA kit, ET1020-1 Lot No. 1259916R1). The levels of plasminogen activator inhibitor (PAI-1) antigen in BALF were measured by applying a Rat PAI-1 total antigen assay ELISA kit (Catalog # RPAIKT-TOT, Molecular Innovations, MI, USA) according to the manufacturer's instructions.

Measurement of MPO activity in lung tissue

The level of MPO in lung tissue, a marker of neutrophil infiltration (Abraham 2003; Zemans et al. 2009), was also measured. Right lung tissues (1 g) were homogenized in approximately 1.5–4.0 N-ethylmaleimide (Sigma) for 30 s on ice and were then centrifuged at 1.2×10^4 g for 30 min at 4 °C. The resulting pellet was re-suspended in 4 ml of potassium phosphate buffer (50 mM, pH 6.0) with 0.5% hexadecyltrimethylammonium bromide (HTAB). The sample was sonicated for approximately 30–90 s on ice. It was then incubated at 60 °C for 2 h to deactivate tissue MPO inhibitors, and was then centrifuged at 1.2×10^4 g for 10 min. The supernatant fluids containing MPO were incubated in a 50 mM potassium phosphate buffer (KH_2PO_4, PH 6.0) containing H_2O_2 (1.5 M) and o-dianisidine dihydrochloride (167 mg/ml; Sigma–Aldrich, USA) as substrate for 30 min. Enzymatic activity was determined spectrophotometrically using a 96-well plate reader to measure the change in absorbance at 460 nm.

Assessment of histopathological changes

The right lungs of the rats were fixed with 10% paraformaldehyde through trachea infusion and embedded with paraffin. Hematoxylin and eosin (H&E) staining was conducted using 4-μm tissue slides. Lung injury assessment was conducted following the modified scoring system described by Kristof et al. (1998). In brief, two experienced pulmonologists randomly selected 10 fields of lung sections from 3 lobes of right lung tissue for each rat, and used a microscope at 200× magnification to read and score the damaged levels in these sections according to the presence and extent of interstitial cellular infiltration, alveolar protein exudation, and tissue hemorrhage as previously performed in a series of studies written by the authors of the present work (Wu et al. 2009a,b; Fu et al. 2012). The sum of each category from 10 different microscopic fields was recorded as the final damaged score for a rat. The total lung injury score for each rat was determined as the sum of 3 individual scores for alveolar cellularity, protein exudation, and tissue hemorrhage. If the interpretations of the two physicians differed significantly, the slides were checked by a pathologist.

Statistical analysis

All data were expressed as mean ± SEM using *in vivo* data from at least 6 rats. Statistical analysis of the data was conducted using Prism 3.02 software (GraphicPad Software Inc., CA, USA), and one-way ANOVA was applied for multiple comparisons (post hoc Tukey test). Results of $p < .05$ were considered statistically significant.

Results

Effects of MCR on RT in LPS-induced ALI rats

The RT in the LPS group at 16 h after LPS administration was lower than that at the baseline (0 h) ($p < .05$; Fig. 3), whereas the RT at 16 h in the MCR-LPS and LPS-MCR groups was similar to RT at the baseline (both $p > .05$; Fig. 3). The RT at 16 h after LPS administration in the PBS group was higher than that at the baseline ($p < .05$; Fig. 3).

Effects of MCR on BALF leukocyte accumulation and protein exudation in LPS-induced ALI rats

The total leukocyte counts in BALF were higher in the LPS group than in the PBS group at 16 h after LPS administration ($p < .05$; Fig. 4a), and total BALF leukocyte counts were lower in the MCR-LPS and LPS-MCR groups than in the LPS group at 16 h (both $p < .05$; Fig. 4a). The total leukocyte counts for BALF were lower in the MCR-LPS group than in the LPS-MCR group ($p < .01$; Fig. 4a).

The total PMN counts in BALF were higher in the LPS group than in the PBS group at 16 h after LPS administration ($p < .05$; Fig. 4b),

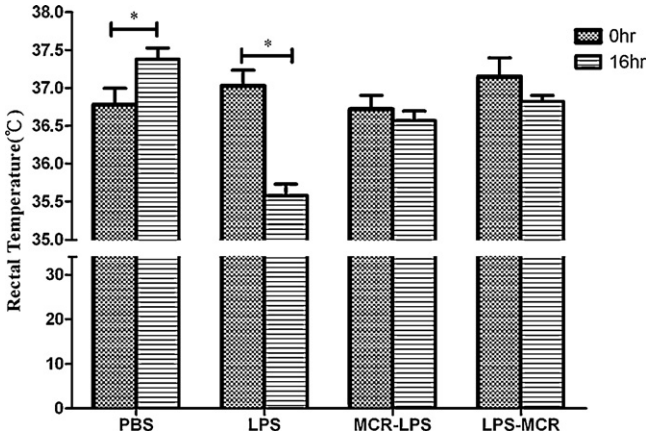

Fig. 3. Effect of *Moutan cortex radicis* (MCR) on rectal temperature (RT) changes in lipopolysaccharide (LPS)-induced acute lung injury (ALI) in rats. The RT in the PBS group was higher at 16 h than at 0 h, whereas the RT in the LPS group was lower at 16 h after LPS administration than at 0 h. PBS, PBS group; LPS, LPS group; MCR-LPS, MCR-LPS group; LPS-MCR, LPS-MCR group; *$p < .05$.

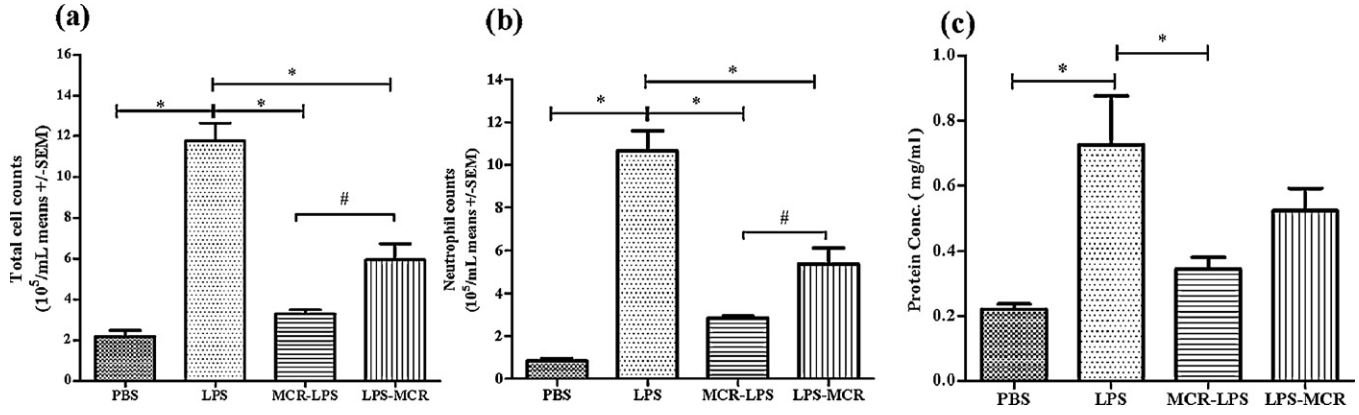

Fig. 4. Effects of *Moutan cortex radicis* (MCR) on cell analysis and protein exudation level in bronchoalveloar fluid (BALF) for lipopolysaccharide (LPS)-induced acute lung injury (ALI) in rats. Cells counts and protein exudation levels for BALF were measured at 16 h after LPS administration. The total leukocyte counts in BALF were higher in the LPS group than in the PBS, MCR-LPS, and LPS-MCR groups (a); the total leukocyte counts in BALF were lower in the MCR-LPS group than in the LPS-MCR group (a); total PMN counts in BALF were higher in the LPS group than in the PBS, MCR-LPS, and LPS-MCR groups (b); total PMN counts in BALF were lower in the MCR-LPS group than in the LPS-MCR group (b); the protein concentration in BALF was higher in the LPS group than in the PBS and MCR-LPS groups (c); LPS, LPS group; MCR-LPS, MCR-LPS group; LPS-MCR, LPS-MCR group; $^*p < .05$ compared with LPS; $^{\#}p < .05$ compared with MCR-LPS.

and total counts were lower in the MCR-LPS and LPS-MCR groups than in the LPS group at 16 h (both $p < .05$; Fig. 4b). Total PMN counts for BALF were lower in the MCR-LPS group than in the LPS-MCR group ($p < .01$; Fig. 4b).

The protein concentration for BALF was higher in the LPS group than in the PBS and MCR-LPS groups at 16 h after LPS administration (both $p < .05$; Fig. 4c). BALF protein concentration in the LPS-MCR group was similar to that in the LPS group ($p > .05$; Fig. 4c) and also similar to that in the MCR-LPS group ($p > .05$; Fig. 4c).

Effect of MCR on BALF cytokine levels in LPS-induced ALI rats

The TNF-α level for BALF at 16 h after LPS administration in the LPS group was similar to that found in the PBS, MCR-LPS, and LPS-MCR groups (all $p > .05$; Fig. 5a). The BALF TNF-α level was not significantly different between the PBS and MCR-LPS groups, between the PBS and LPS-MCR groups, or between the MCR-LPS and LPS-MCR groups at 16 h after LPS administration (all $p > .05$; Fig. 5a).

The IL-1β level in BALF was higher in the LPS group than in the PBS and MCR-LPS groups at 16 h after LPS administration (both $p < .05$; Fig. 5b), and this level was not significantly different between the PBS and MCR-LPS groups, between the PBS and LPS-MCR groups, or between the MCR-LPS and LPS-MCR groups at 16 h (all $p > .05$; Fig. 5b).

The MIP-2 level for BALF was higher in the LPS group than in the PBS and MCR-LPS groups at 16 h after LPS administration (both $p < .05$; Fig. 5c), and this level was lower in the MCR-LPS group than in the LPS-MCR group at 16 h ($p < .05$; Fig. 5c). The MIP-2 level was not significantly different between the PBS and MCR-LPS groups or between the PBS and LPS-MCR groups (both $p > .05$; Fig. 5c).

The IL-6 level for BALF was higher in the LPS group than in the PBS, MCR-LPS, and LPS-MCR groups at 16 h after LPS administration (all $p < .05$; Fig. 5d). Furthermore, the level was not significantly different between the PBS and MCR-LPS groups, between the PBS and LPS-MCR groups, or between the MCR-LPS and LPS-MCR groups at 16 h (all $p > .05$; Fig. 5d).

The IL-10 level for BALF was higher in the LPS group than in the PBS and MCR-LPS groups at 16 h after LPS administration (both $p < .05$; Fig. 5e). This level was not significantly different between the PBS and MCR-LPS groups, between the PBS and LPS-MCR groups, or between the MCR-LPS and LPS-MCR groups at 16 h (all $p > .05$; Fig. 5e).

Effect of MCR on BALF TATC and PAI-1 levels in LPS-induced ALI rats

The BALF TATC level at 16 h after LPS administration in the LPS group was similar to that discovered in the PBS, MCR-LPS, and LPS-MCR groups (all $p > .05$; Fig. 6a). Furthermore, this level was not significantly different between the PBS and MCR-LPS groups, between the PBS and LPS-MCR groups, or between the MCR-LPS and LPS-MCR groups at 16 h after LPS administration (all $p > .05$; Fig. 6a).

The BALF PAI-1 level was higher in the LPS group than in the PBS group at 16 h after LPS administration ($p < .05$; Fig. 6b). This level was not significantly different between the PBS and MCR-LPS groups, between the PBS and LPS-MCR groups, or between the MCR-LPS and LPS-MCR groups at 16 h (all $p > .05$; Fig. 6b).

Effect of MRC on MPO activity in lung tissue for LPS-induced ALI rats

MPO activity in lung tissue was greater in the LPS group than in the PBS, MCR-LPS, and LPS-MCR groups at 16 h after LPS administration (all $p < .05$; Fig. 7), and MPO was not significantly different between the PBS and MCR-LPS groups, between the PBS and LPS-MCR groups, or between the MCR-LPS and LPS-MCR groups at 16 h (all $p > .05$; Fig. 7).

Effects of MCR on histopathological changes in the lungs of LPS-induced ALI rats

Histopathological changes in lung tissue were observed 16 h after LPS administration. In the PBS group, fluid and protein accumulation and the infiltration of inflammatory cells and red blood cells was not prominent in the alveolar space (Fig. 8a and b). By contrast, the alveolar space for rats in the LPS group demonstrated fluid and protein accumulation, large amounts of inflammatory cells, and red blood cell infiltration (Fig. 8c and d). When MCR was administered orally before LPS challenge (MCR-LPS group), inflammatory cell infiltration and alveolar wall thickening were markedly attenuated and alveolar edema was reduced (Fig. 8e and f). However, when MCR was administered orally after LPS challenge (LPS-MCR group), marked alveolar hemorrhage and moderate alveolar edema were induced, despite some attenuation in leukocyte infiltration (Fig. 8g and h). A semi-quantitative analysis of the histopathological scores for rat lungs is shown in Table 1.

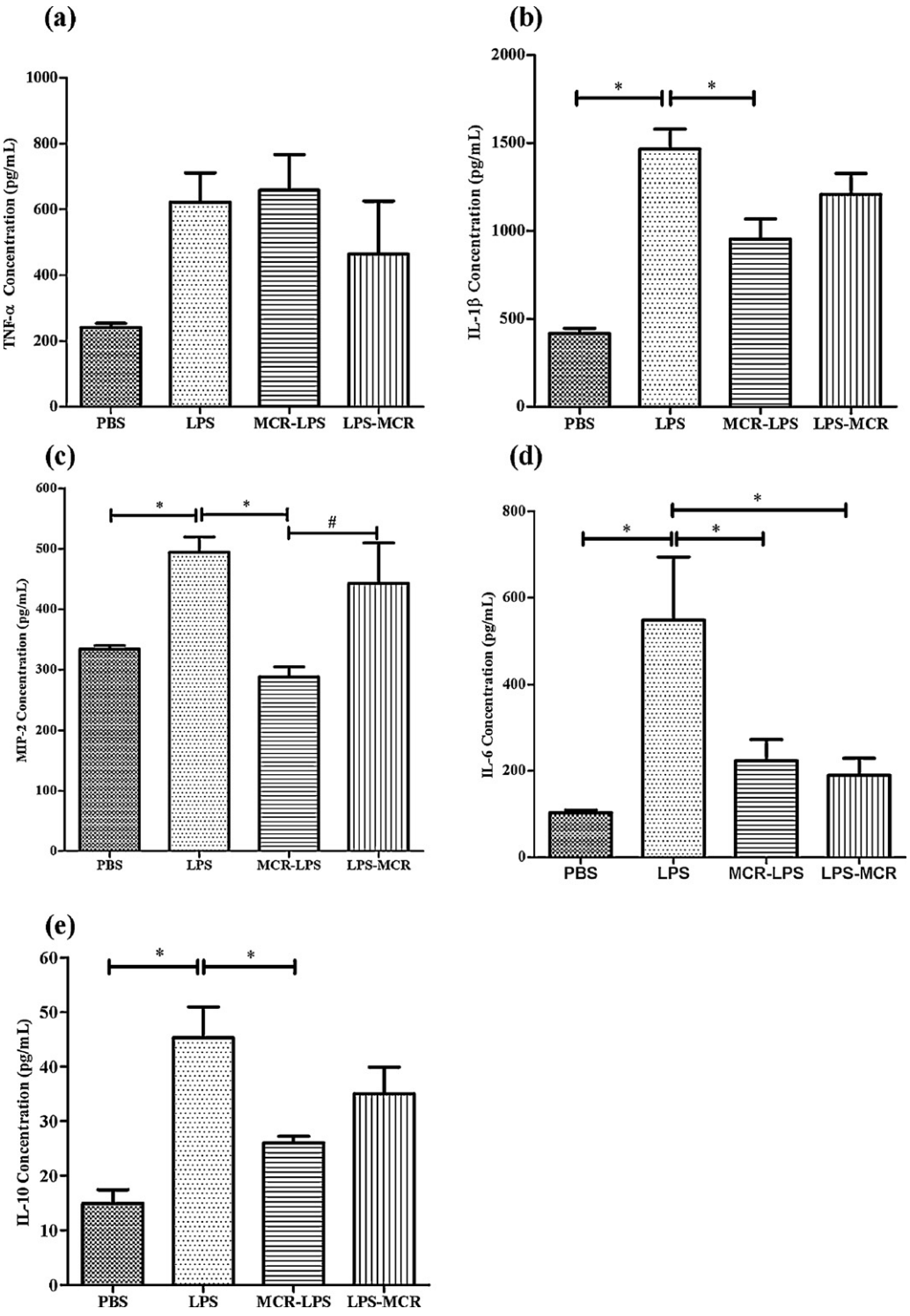

Fig. 5. Effects of *Moutan cortex radicis* (MCR) on cytokine levels in bronchoalveloar fluid (BALF) for lipopolysaccharide (LPS)-induced acute lung injury (ALI) in rats. Cytokine levels in BALF were measured at 16 h after LPS administration. The TNF-α level in BALF for the LPS group was similar to that for the PBS, MCR-LPS, and LPS-MCR groups (a); the IL-1β level in BALF was higher in the LPS group than in the PBS and MCR-LPS groups (b); the MIP-2 level in BALF was higher in the LPS group than in the PBS and MCR-LPS groups (c); the MIP-2 level in BALF was lower in the MCR-LPS group than in the LPS-MCR group (c); the IL-6 level in BALF was higher in the LPS group than in the PBS, MCR-LPS, and LPS-MCR groups (d); the IL-10 level in BALF was higher in the LPS group than in the PBS and MCR-LPS groups (e); LPS, LPS group; MCR-LPS, MCR-LPS group; LPS-MCR, LPS-MCR group; $^{*}p < .05$ compared with LPS; $^{\#}p < .05$ compared with MCR-LPS.

Discussion

The results of the present study indicate that treatment with MCR before LPS challenge can reduce histopathological damage scores in LPS-induced ALI rat models, whereas similar results cannot be obtained with MCR treatment after LPS challenge. Pre-treatment with MCR down-regulated the level of the pro-inflammatory cytokines IL-1β and IL-6 as well as the chemokine MIP-2, and also reduced the infiltration of activated PMN and protein-rich exudation in BALF (i.e., the alveolar space). In addition,

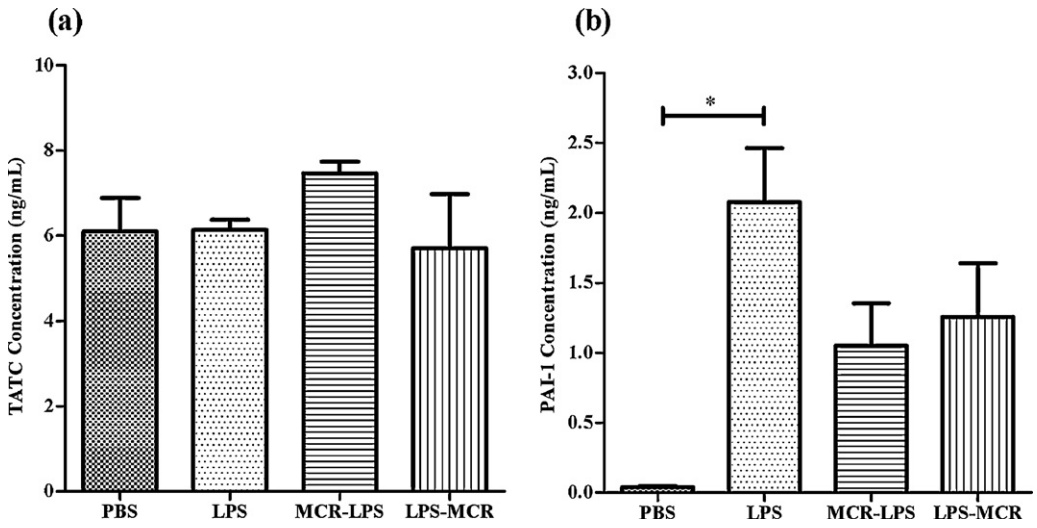

Fig. 6. Effects of *Moutan cortex radicis* (MCR) on thrombin–anti-thrombin complexes (TATC) level and plasminogen activator inhibitor (PAI-1) level in bronchoalveloar fluid (BALF) for lipopolysaccharide (LPS)-induced acute lung injury (ALI) in rats. TATC and PAI-1 levels were measured at 16 h after LPS administration. The TATC level in BALF for the LPS group was similar to that for the PBS, MCR-LPS, and LPS-MCR groups (a); the PAI-1 level of BALF was higher in the LPS group than in the PBS group (b); LPS, LPS group; MCR-LPS, MCR-LPS group; LPS-MCR, LPS-MCR group; $^{*}p < .05$ compared with LPS.

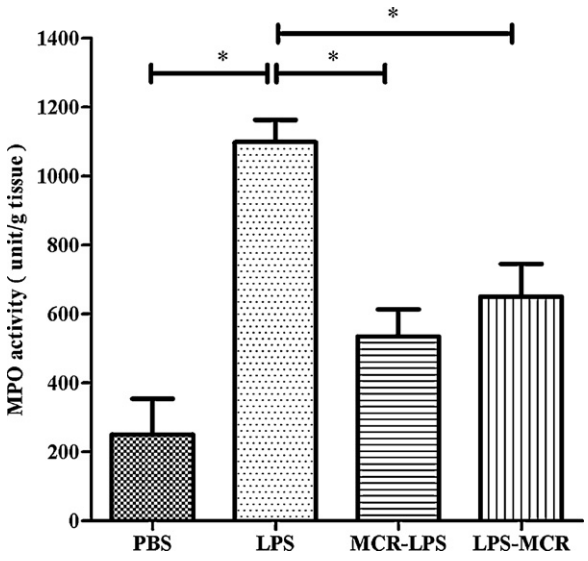

Fig. 7. Effects of *Moutan cortex radicis* (MCR) on myeloperoxidase (MPO) activity in the lung tissues for lipopolysaccharide (LPS)-induced acute lung injury (ALI) in rats. MPO activity was greater in the LPS group than in the PBS, MCR-LPS, and LPS-MCR groups. LPS, LPS group; MCR-LPS, MCR-LPS group; LPS-MCR, LPS-MCR group; $^{*}p < .05$ compared with LPS.

MPO activity decreased in lung tissue because of MCR treatment. Therefore, we suggest that MCR reduces lung tissue damage in LPS-induced ALI rat models. This effect of MCR is closely related to its anti-inflammatory effects. The results of the present study were also somewhat similar to our previous findings that paeonol (a component of MCR) can inhibit the migration of neutrophils from capillaries into lung tissue, and that it enhances the phagocytotic ability of neutrophils in alveolar space (these results are as of yet unpublished).

Several animal models have been developed to mimic the pathophysiology of ALI after LPS exposure (van Helden et al. 1997; Matute-Bello et al. 2008; Wang et al. 2008). In the present study, we produced a consistent and reproducible rat model to investigate the protective and therapeutic effects of MCR on ALI by delivering LPS directly into the airways of rats in our laboratory (Wu et al. 2009a,b; Fu et al. 2012). Similar to findings from our previous studies, an IT challenge with a high dose of LPS (16 mg/kg) induced hypothermia at 16 h after LPS administration (Fu et al. 2012). The results of the *in vivo* study indicate that MCR treatment (both pre-LPS and post-LPS treatment) reduce the drop in RT that typically follows LPS challenge. Hypothermia may be an early indicator of sepsis; thus, MCR may play a critical role in preventing sepsis development. The finding that MCR regulates RT after LPS challenge is similar to results presented in our recently published study, which evaluated the effect of paeonol on LPS-induced ALI in rats (Fu et al. 2012).

Numerous studies have provided circumstantial evidence that neutrophil recruitment in lungs is a histological hallmark of ALI

Table 1
The effect of MCR on histopathological scores in lipopolysaccharide-induced acute lung injury in rats.

	Cellularity	Protein exudation	Hemorrhage	Total scores
PBS	1.6 ± 0.8	4.5 ± 0.5	5.0 ± 1.2	11.1 ± 1.7
LPS	20.2 ± 1.1$^{\#}$	13.0 ± 0.9$^{\#}$	14.9 ± 0.6$^{\#}$	48.1 ± 2.2$^{\#}$
MCR-LPS	12.3 ± 0.9$^{\#,*}$	7.9 ± 0.7$^{\#,*}$	12.0 ± 0.4$^{\#}$	32.2 ± 1.3$^{\#,*}$
LPS-MCR	15.3 ± 0.8$^{\#,*}$	11.1 ± 0.7$^{\#,\$}$	18.4 ± 0.8$^{\#,*,\$}$	44.8 ± 1.4$^{\#,\$}$

PBS, PBS group with PBS challenge; LPS, LPS group with lipopolysaccharide (LPS) challenge; MCR-LPS, MCR-LPS group; oral treatment with *Moutan cortex radicis* (MCR) before LPS challenge. LPS-MCR, LPS-MCR group; treatment with MCR after LPS challenge.
Data are presented as mean ± SEM, $n = 6$.
$^{\#}$ $p < .05$ compared with PBS.
* $p < .05$ compared with LPS.
$^{\$}$ $p < .05$ compared with MCR-LPS.

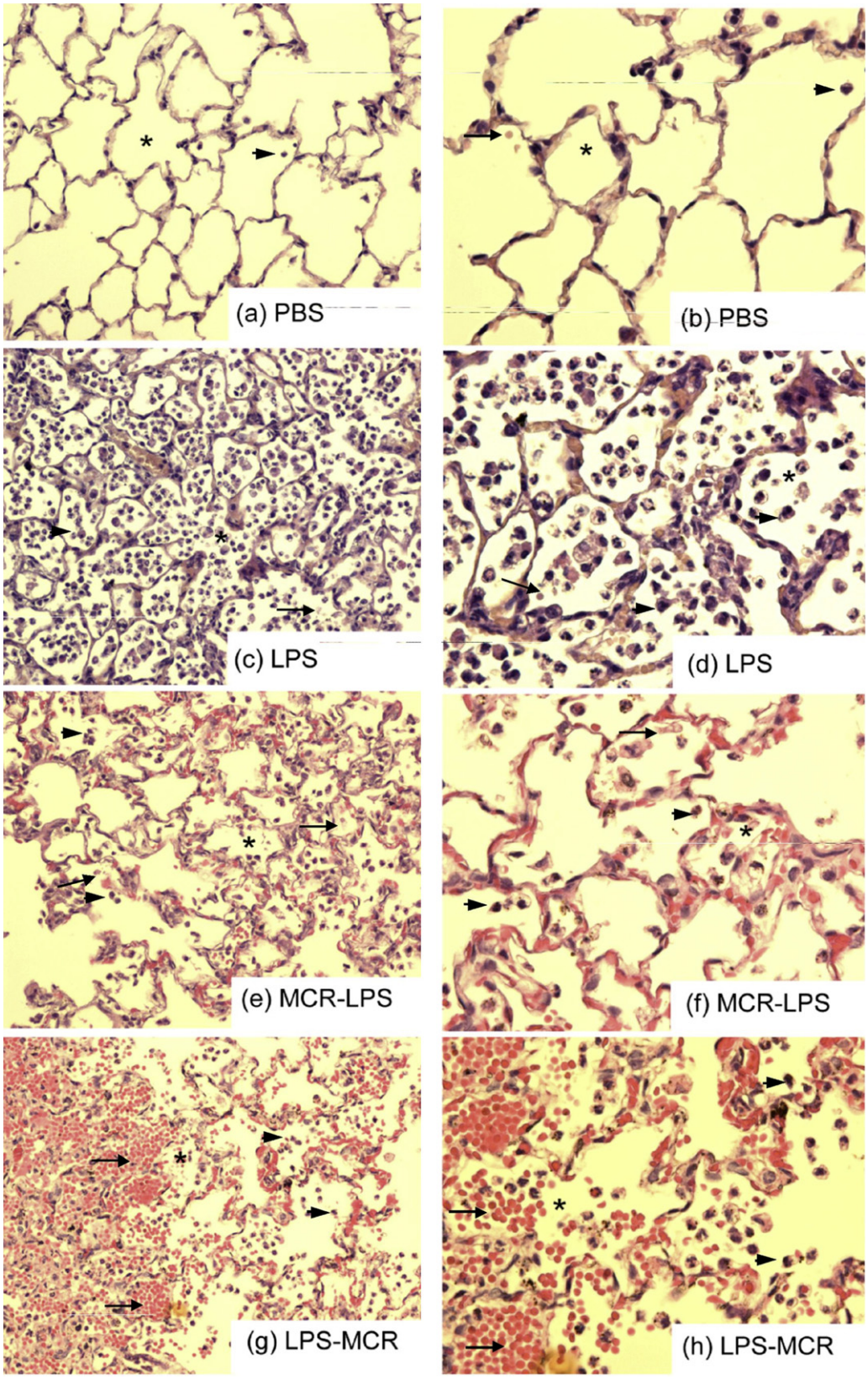

Fig. 8. Effects of *Moutan cortex radicis* (MCR) on histopathological changes for lipopolysaccharide (LPS)-induced acute lung injury (ALI) in rats. Histopathological damage in lung tissue developed 16 h after LPS (16 mg/kg) administration (at 200× (c), at 400× (d)). The alveolar spaces (*) were filled with a mixed mononuclear and neutrophilic infiltrate (►), red blood cells (→), and protein exudation. Cellular debris and proteinaceous material were present in the air spaces in the lung tissue of the LPS group (at 200× (c), at 400× (d)). No prominent neutrophil infiltration, red blood cells, or protein exudates were seen in the PBS group (at 200× (a), at 400× (b)). The infiltration of neutrophils and protein exudation was reduced in the MCR-LPS group (at 200× (e), at 400× (f)). In the LPS-MCR group (at 200× (g), at 400× (h)), a significant number of alveolar red blood cells, comparable to those seen in the LPS group, appeared. LPS, LPS group; MCR-LPS, MCR-LPS group; LPS-MCR, LPS-MCR group.

(Balamayooran et al. 2010; Grommes and Soehnlein 2011). The early effects of ALI in humans on pulmonary histopathological changes are characterized by marked accumulation of neutrophils, disruption of epithelial integrity, interstitial edema, and leakage of a large amount of protein into alveolar spaces (Abraham et al. 2000; Chignard and Balloy 2000; Kinoshita et al. 2000; Ware and Matthay 2000). Administration of LPS through an intra-alveolar route serves as a model of typical neutrophil-dependent ALI, and induces adhesion and migration of neutrophils from pulmonary capillaries into the alveolar space. In the present study, we demonstrated that treatment with MCR (both pre-LPS and post-LPS treatment) significantly attenuated total cell and neutrophil counts in BALF. A comparison of the MCR-LPS group to the LPS-MCR group demonstrates that pre-treatment with MCR suppresses neutrophil infiltration into and protein-rich fluid flooding of the airspace more significantly than post-treatment (Fig. 3).

High levels of pro-inflammatory cytokines, such as TNF-α, IL-1β, and IL-6, perform a central role in the initiation and propagation of the inflammatory cascade in LPS-induced ALI (Schultz et al. 2006; Matute-Bello et al. 2008). Cytokines, such as TNF-α, IL-1β, IL-6, IL-8, and IL-10, that are secreted by alveolar macrophages stimulate more chemotaxis and attract more neutrophils to injured lungs (Strieter and Kunkel 1994; Kobayashi et al. 1998; Williams et al. 1999; Ware and Matthay 2000; Shinbori et al. 2004). It has also been suggested that MIP-2 (CXCL2) is the most essential chemoattractant for neutrophil recruitment in the LPS-induced model (Olson and Ley 2002; Grommes and Soehnlein 2011). Fig. 4 shows that the expression of IL-1β, MIP-2, IL-6, and IL-10 in BALF was significantly lower in the MCR-LPS group than in the LPS group at 16 h after LPS challenge. These reductions may have contributed to the decreased neutrophil count in BALF in the LPS-induced ALI model treated with MCR before LPS challenge. However, in a comparison of the post-LPS treatment group (LPS-MCR) and the LPS group, cytokine levels (except those for IL-6) in BALF in the LPS-MCR group were not significantly lower than those in the LPS group. In addition, MIP-2 expression in the MCR-LPS group was significantly lower than that in the LPS-MCR group. These differences in cytokine expression in BALF may have contributed to the varying effects of pre-treatment and post-treatment with MCR.

Another major pathologic feature of ALI is the deposition of fibrin and platelet plugs, which induces the occlusion of microvasculature in the alveolar space (Ware and Matthay 2000). When excessive fibrin is deposited in airways, neutrophils and fibroblasts may be further activated. This scenario compromises gas exchange and pulmonary endothelial integrity, decreases alveolar fluid clearance, and finally leads to pulmonary microcirculation damage and death (Sapru et al. 2006). Pulmonary coagulopathy is now accepted as a target in therapeutic studies of acute lung injury or pneumonia (Schultz et al. 2006; Ware et al. 2006; Wygrecka et al. 2008). Available data suggest that high levels of pro-inflammatory cytokines, such as TNF, IL-1β, and IL-6, may activate coagulation cascade by stimulating TF expression. High levels of these cytokines may also attenuate fibrinolysis by stimulating the release of PAI (Abraham 2000; Ware et al. 2005; Bastarache et al. 2006; Wygrecka et al. 2008). Our previous data showed no significant difference in TATC levels in BALF after paeonol treatment, but demonstrated significantly decreased BALF PAI-1 levels after this treatment (Fu et al. 2012). As shown in Fig. 5, treatment with MCR before or after LPS challenge appears to down-regulate the expression of PAI-1 in BALF. However, this result did not reach statistical significance, suggesting that the anti-fibrinolytic effect of MCR is not as substantial as that in paeonol for treating ALI-induced coagulopathy. Whether the differences between administration route and formula for MCR and paeonol (oral treatment vs. intra-peritoneal injection; crude extracts of herbal medicine vs. ethanol extraction of MCR) causes this result should be studied further in the future. Further experiments are also required to clarify target effects on cells and the causal relationship between the anti-inflammatory and anti-coagulative effects of MCR.

MPO activity is a marker of neutrophil activation (Abraham 2003; Grommes and Soehnlein 2011). In the LPS-induced ALI model, a large amount of PMN is recruited from peripheral blood into the lung, producing a substantial amount of MPO and reactive oxygen derivatives, and finally resulting in a cascade-like response and tissue damage (Razavi et al. 2004; Grommes and Soehnlein 2011). Our results showed phenomena similar to those in proposed theories, and demonstrated that, after LPS was administered through IT, large amounts of pro-inflammatory cytokines were expressed in BALF in rat lung parenchyma with enhanced activity of MPO. MCR treatment before LPS challenge significantly reduced LPS-induced pulmonary parenchymal MPO activity and cytokine expression of IL-1β, MIP-2, and IL-6 in BALF. Furthermore, the number of PMNs in BALF decreased 16 h after treatment, suggesting the mechanism by which MCR attenuates LPS-induced ALI.

In conclusion, the results of the current study demonstrate that MCR reduced lung tissue damage in the LPS-induced ALI rat model. This effect of MCR possibly results from its anti-inflammatory properties. Thus, MCR may be a potential therapeutic reagent that can be used to prevent ALI in the future. Further studies should be implemented to investigate these outcomes.

Conflict of interest

The authors confirm that there are no known conflicts of interest associated with this publication.

Disclosure statement

There was no significant financial support for this work that could have influenced its outcome.

Role of the funding source

None.

Acknowledgments

This study was supported by grants from the China Medical University, Taichung, Taiwan (CMU99-NSC-02 (2/2)) and in part by the Taiwan Department of Health Clinical Trial and Research Center of Excellence (DOH101-TD-B-111-004).

References

Abraham, E., 2000. Coagulation abnormalities in acute lung injury and sepsis. American Journal of Respiratory Cell and Molecular Biology 22, 401–404.

Abraham, E., Carmody, A., Shenkar, R., Arcaroli, J., 2000. Neutrophils as early immunologic effectors in hemorrhage- or endotoxemia-induced acute lung injury. American Journal of Physiology – Lung Cellular and Molecular Physiology 279, L1137–L1145.

Abraham, E., 2003. Neutrophils and acute lung injury. Critical Care Medicine 31, S195–S199.

Balamayooran, G., Batra, S., Fessler, M.B., Happel, K.I., Jeyaseelan, S., 2010. Mechanisms of neutrophil accumulation in the lungs against bacteria. American Journal of Respiratory Cell and Molecular Biology 43, 5–16.

Bastarache, J.A., Ware, L.B., Bernard, G.R., 2006. The role of the coagulation cascade in the continuum of sepsis and acute lung injury and acute respiratory distress syndrome. Seminars in Respiratory and Critical Care Medicine 27, 365–376.

Bauer, T.T., Monton, C., Torres, A., Cabello, H., Fillela, X., Maldonado, A., Nicolas, J.M., Zavala, E., 2000. Comparison of systemic cytokine levels in patients with acute respiratory distress syndrome, severe pneumonia, and controls. Thorax 55, 46–52.

Chae, H.S., Kang, O.H., Lee, Y.S., Choi, J.G., Oh, Y.C., Jang, H.J., Kim, M.S., Kim, J.H., Jeong, S.I., Kwon, D.Y., 2009. Inhibition of LPS-induced iNOS, COX-2 and inflammatory mediator expression by paeonol through the MAPKs inactivation in RAW 264. 7 cells. The American Journal of Chinese Medicine 37, 181–194.

Chignard, M., Balloy, V., 2000. Neutrophil recruitment and increased permeability during acute lung injury induced by lipopolysaccharide. American Journal of Physiology – Lung Cellular and Molecular Physiology 279, L1083–L1090.

Dreyfuss, D., Ricard, J.D., 2005. Acute lung injury and bacterial infection. Clinics In Chest Medicine 26, 105–112.

Grommes, J., Soehnlein, O., 2011. Contribution of neutrophils to acute lung injury. Molecular Medicine 17, 293–307.

Gupta, S., Feng, L., Yoshimura, T., Redick, J., Fu, S.M., Rose Jr., C.E., 1996. Intra-alveolar macrophage-inflammatory peptide 2 induces rapid neutrophil localization in the lung. American Journal of Respiratory Cell and Molecular Biology 15, 656–663.

Hirai, A., Terano, T., Hamazaki, T., Sajiki, J., Saito, H., Tahara, K., Tamura, Y., Kumagai, A., 1983. Studies on the mechanism of antiaggregatory effect of *Moutan Cortex*. Thrombosis Research 31, 29–40.

Hsieh, C.L., Cheng, C.Y., Tsai, T.H., Lin, I.H., Liu, C.H., Chiang, S.Y., Lin, J.G., Lao, C.J., Tang, N.Y., 2006. Paeonol reduced cerebral infarction involving the superoxide anion and microglia activation in ischemia-reperfusion injured rats. Journal of Ethnopharmacology 106, 208–215.

Kim, J., Lee, H., Lee, Y., Oh, B.G., Cho, C., Kim, Y., Shin, M., Hong, M., Jung, S.K., Bae, H., 2007. Inhibition effects of *Moutan Cortex Radicis* on secretion of eotaxin in A549 human epithelial cells and eosinophil migration. Journal of Ethnopharmacology 114, 186–193.

Kinoshita, M., Ono, S., Mochizuki, H., 2000. Neutrophils mediate acute lung injury in rabbits: role of neutrophil elastase. European Surgical Research 32, 337–346.

Kobayashi, A., Hashimoto, S., Kooguchi, K., Kitamura, Y., Onodera, H., Urata, Y., Ashihara, T., 1998. Expression of inducible nitric oxide synthase and inflammatory cytokines in alveolar macrophages of ARDS following sepsis. Chest 113, 1632–1639.

Koo, Y.K., Kim, J.M., Koo, J.Y., Kang, S.S., Bae, K., Kim, Y.S., Chung, J.H., Yun-Choi, H.S., 2010. Platelet anti-aggregatory and blood anti-coagulant effects of compounds isolated from *Paeonia lactiflora* and *Paeonia suffruticosa*. Pharmazie 65, 624–628.

Kristof, A.S., Goldberg, P., Laubach, V., Hussain, S.N., 1998. Role of inducible nitric oxide synthase in endotoxin-induced acute lung injury. American Journal of Respiratory and Critical Care Medicine 158, 1883–1889.

Levi, M., Ten Cate, H., 1999. Disseminated intravascular coagulation. The New England Journal of Medicine 341, 586–592.

Lin, H.C., Ding, H.Y., Ko, F.N., Teng, C.M., Wu, Y.C., 1999. Aggregation inhibitory activity of minor acetophenones from *Paeonia* species. Planta Medica 65, 595–599.

Matthay, M.A., Geiser, T., Matalon, S., Ischiropoulos, H., 1999. Oxidant-mediated lung injury in the acute respiratory distress syndrome. Critical Care Medicine 27, 2028–2030.

Matute-Bello, G., Frevert, C.W., Martin, T.R., 2008. Animal models of acute lung injury. American Journal of Physiology – Lung Cellular and Molecular Physiology 295, L379–L399.

Nizamutdinova, I.T., Oh, H.M., Min, Y.N., Park, S.H., Lee, M.J., Kim, J.S., Yean, M.H., Kang, S.S., Kim, Y.S., Chang, K.C., Kim, H.J., 2007. Paeonol suppresses intercellular adhesion molecule-1 expression in tumor necrosis factor-alpha-stimulated human umbilical vein endothelial cells by blocking p38, ERK and nuclear factor-kappaB signaling pathways. International Immunopharmacology 7, 343–350.

Nys, M., Deby-Dupont, G., Habraken, Y., Legrand-Poels, S., Ledoux, D., Canivet, J.L., Damas, P., Lamy, M., 2002. Bronchoalveolar lavage fluids of patients with lung injury activate the transcription factor nuclear factor-kappaB in an alveolar cell line. Clinical Science (London) 103, 577–585.

Oh, G.S., Pae, H.O., Choi, B.M., Jeong, S., Oh, H., Oh, C.S., Rho, Y.D., Kim, D.H., Shin, M.K., Chung, H.T., 2003. Inhibitory effects of the root cortex of *Paeonia suffruticosa* on interleukin-8 and macrophage chemoattractant protein-1 secretions in U937 cells. Journal of Ethnopharmacology 84, 85–89.

Okubo, T., Nagai, F., Seto, T., Satoh, K., Ushiyama, K., Kano, I., 2000. The inhibition of phenylhydroquinone-induced oxidative DNA cleavage by constituents of *Moutan cortex* and *Paeoniae radix*. Biological & Pharmaceutical Bulletin 23, 199–203.

Olson, T.S., Ley, K., 2002. Chemokines and chemokine receptors in leukocyte trafficking. American Journal of Physiology. Regulatory, Integrative and Comparative Physiology 283, R7–R28.

Pan, L.L., Dai, M., 2009. Paeonol from Paeonia suffruticosa prevents TNF-alpha-induced monocytic cell adhesion to rat aortic endothelial cells by suppression of VCAM-1 expression. Phytomedicine: International Journal of Phytotherapy and Phytopharmacology 16, 1027–1032.

Fu, P.-K., Wu, C.-L., Tsai, T.-H., Hsieh, C.-L., 2012. Anti-inflammatory and anticoagulative effects of paeonol on LPS-induced acute lung injury in rats. Evidence-Based Complementary and Alternative Medicine 2012, 837513. Epub 2012 Feb 21.

Razavi, H.M., Wang le, F., Weicker, S., Rohan, M., Law, C., McCormack, D.G., Mehta, S., 2004. Pulmonary neutrophil infiltration in murine sepsis: role of inducible nitric oxide synthase. American Journal of Respiratory and Critical Care Medicine 170, 227–233.

Reutershan, J., Ley, K., 2004. Bench-to-bedside review: acute respiratory distress syndrome—how neutrophils migrate into the lung. Critical Care 8, 453–461.

Rho, S., Chung, H.S., Kang, M., Lee, E., Cho, C., Kim, H., Park, S., Kim, H.Y., Hong, M., Shin, M., Bae, H., 2005. Inhibition of production of reactive oxygen species and gene expression profile by treatment of ethanol extract of *Moutan Cortex Radicis* in oxidative stressed PC12 cells. Biological & Pharmaceutical Bulletin 28, 661–666.

Sapru, A., Wiemels, J.L., Witte, J.S., Ware, L.B., Matthay, M.A., 2006. Acute lung injury and the coagulation pathway: potential role of gene polymorphisms in the protein C and fibrinolytic pathways. Intensive Care Medicine 32, 1293–1303.

Schultz, M.J., Haitsma, J.J., Zhang, H., Slutsky, A.S., 2006. Pulmonary coagulopathy as a new target in therapeutic studies of acute lung injury or pneumonia—a review. Critical Care Medicine 34, 871–877.

Schutte, H., Lohmeyer, J., Rosseau, S., Ziegler, S., Siebert, C., Kielisch, H., Pralle, H., Grimminger, F., Morr, H., Seeger, W., 1996. Bronchoalveolar and systemic cytokine profiles in patients with ARDS, severe pneumonia and cardiogenic pulmonary oedema. The European Respiratory Journal: Official Journal of the European Society for Clinical Respiratory Physiology 9, 1858–1867.

Sheridan, B.C., McIntyre Jr., R.C., Moore, E.E., Meldrum, D.R., Agrafojo, J., Fullerton, D.A., 1997. Neutrophils mediate pulmonary vasomotor dysfunction in endotoxin-induced acute lung injury. The Journal of Trauma 42, 391–396 (discussion 396–397).

Shinbori, T., Walczak, H., Krammer, P.H., 2004. Activated T killer cells induce apoptosis in lung epithelial cells and the release of pro-inflammatory cytokine TNF-alpha. European Journal of Immunology 34, 1762–1770.

Slofstra, S.H., Groot, A.P., Maris, N.A., Reitsma, P.H., Cate, H.T., Spek, C.A., 2006. Inhalation of activated protein C inhibits endotoxin-induced pulmonary inflammation in mice independent of neutrophil recruitment. British Journal of Pharmacology 149, 740–746.

Strieter, R.M., Kunkel, S.L., 1994. Acute lung injury: the role of cytokines in the elicitation of neutrophils. Journal of Investigative Medicine 42, 640–651.

Tatsumi, S., Mabuchi, T., Abe, T., Xu, L., Minami, T., Ito, S., 2004. Analgesic effect of extracts of Chinese medicinal herbs *Moutan cortex* and *Coicis semen* on neuropathic pain in mice. Neuroscience Letters 370, 130–134.

van Helden, H.P., Kuijpers, W.C., Steenvoorden, D., Go, C., Bruijnzeel, P.L., van Eijk, M., Haagsman, H.P., 1997. Intratracheal aerosolization of endotoxin (LPS) in the rat: a comprehensive animal model to study adult (acute) respiratory distress syndrome. Experimental Lung Research 23, 297–316.

Wang, H.M., Bodenstein, M., Markstaller, K., 2008. Overview of the pathology of three widely used animal models of acute lung injury. European Surgical Research 40, 305–316.

Ware, L.B., Matthay, M.A., 2000. The acute respiratory distress syndrome. The New England Journal of Medicine 342, 1334–1349.

Ware, L.B., Bastarache, J.A., Wang, L., 2005. Coagulation and fibrinolysis in human acute lung injury—new therapeutic targets? The Keio Journal of Medicine 54, 142–149.

Ware, L.B., Camerer, E., Welty-Wolf, K., Schultz, M.J., Matthay, M.A., 2006. Bench to bedside: targeting coagulation and fibrinolysis in acute lung injury. American Journal of Physiology – Lung Cellular and Molecular Physiology 291, L307–L311.

Weijer, S., Schoenmakers, S.H., Florquin, S., Levi, M., Vlasuk, G.P., Rote, W.E., Reitsma, P.H., Spek, C.A., van der Poll, T., 2004. Inhibition of the tissue factor/factor VIIa pathway does not influence the inflammatory or antibacterial response to abdominal sepsis induced by *Escherichia coli* in mice. Journal of Infectious Diseases 189, 2308–2317.

Williams, E.A., Quinlan, G.J., Anning, P.B., Goldstraw, P., Evans, T.W., 1999. Lung injury following pulmonary resection in the isolated, blood-perfused rat lung. The European Respiratory Journal: Official Journal of the European Society for Clinical Respiratory Physiology 14, 745–750.

Wu, C.L., Lin, L.Y., Yang, J.S., Chan, M.C., Hsueh, C.M., 2009a. Attenuation of lipopolysaccharide-induced acute lung injury by treatment with IL-10. Respirology 14, 511–521.

Wu, C.L., Lin, L.Y., Yeh, H.M., Chan, M.C., Yang, C.H., Hsueh, C.M., 2009b. Delay of LPS-induced acute lung injury resolution by soluble immune complexes is neutrophil dependent. Shock 32, 276–285.

Wygrecka, M., Jablonska, E., Guenther, A., Preissner, K.T., Markart, P., 2008. Current view on alveolar coagulation and fibrinolysis in acute inflammatory and chronic interstitial lung diseases. Thrombosis and Haemostasis 99, 494–501.

Yoshikawa, M., Ohta, T., Kawaguchi, A., Matsuda, H., 2000. Bioactive constituents of Chinese natural medicines, V. Radical scavenging effect of *Moutan Cortex*. (1): Absolute stereostructures of two monoterpenes, paeonisuffrone and paeonisuffral. Chemical & Pharmaceutical Bulletin 48, 1327–1331.

Zemans, R.L., Colgan, S.P., Downey, G.P., 2009. Transepithelial migration of neutrophils: mechanisms and implications for acute lung injury. American Journal of Respiratory Cell and Molecular Biology 40, 519–535.

Hindawi Publishing Corporation
Evidence-Based Complementary and Alternative Medicine
Volume 2012, Article ID 837513, 12 pages
doi:10.1155/2012/837513

Research Article

Anti-Inflammatory and Anticoagulative Effects of Paeonol on LPS-Induced Acute Lung Injury in Rats

Pin-Kuei Fu,[1,2,3] Chieh-Liang Wu,[1,3,4] Tung-Hu Tsai,[5] and Ching-Liang Hsieh[6,7,8]

[1] *Division of Critical Care and Respiratory Therapy, Department of Internal Medicine, Taichung Veterans General Hospital, Taichung 407, Taiwan*
[2] *College of Chinese Medicine, Graduate Institute of Chinese Medical Science, China Medical University, Taichung 40402, Taiwan*
[3] *Division of Chest Medicine, Department of Internal Medicine, Taichung Veterans General Hospital, Chiayi Branch, Chiayi 600, Taiwan*
[4] *College of Medicine, School of Medicine, China Medical University, Taichung 40402, Taiwan*
[5] *Institute of Traditional Medicine, School of Medicine, National Yang-Ming University, Taipei, Taiwan*
[6] *Department of Chinese Medicine, China Medical University Hospital, Taichung 40402, Taiwan*
[7] *College of Chinese Medicine, Graduate Institute of Acupuncture Science, China Medical University, Taichung 40402, Taiwan*
[8] *Acupuncture Research Center, China Medical University, Taichung 40402, Taiwan*

Correspondence should be addressed to Ching-Liang Hsieh, clhsieh@mail.cmuh.org.tw

Received 9 August 2011; Revised 27 October 2011; Accepted 27 October 2011

Academic Editor: Angelo Antonio Izzo

Paeonol is an active component of Moutan Cortex Radicis and is widely used as an analgesic, antipyretic, and anti-inflammatory agent in traditional Chinese medicine. We wanted to determine the role of paeonol in treating adult respiratory distress syndrome (ARDS). We established an acute lung injury (ALI) model in Sprague-Dawley rats, which was similar to ARDS in humans, using intratracheal administration of lipopolysaccharide (LPS). The intraperitoneal administration of paeonol successfully reduced histopathological scores and attenuated myeloperoxidase-reactive cells as an index of polymorphonuclear neutrophils infiltration and also reduces inducible nitric oxide synthase expression in the lung tissue, at 16 h after LPS administration. In addition, paeonol reduced proinflammatory cytokines in bronchoalveolar lavage fluid, including tumor-necrosis factor-α, interleukin-1β, interleukin-6, and plasminogen-activated inhibition factor-1. These results indicated that paeonol successfully attenuates inflammatory and coagulation reactions to protect against ALI.

1. Introduction

Acute lung injury (ALI) and acute respiratory distress syndrome (ARDS) are initiated either by direct injury to the lung or by a systemic inflammatory process. Both conditions are characterized by serial pulmonary inflammatory responses of the alveolar-capillary membrane. These responses include polymorphonuclear neutrophils (PMN) accumulation [1, 2], disruption of epithelial integrity, interstitial edema, and leakage of large amounts of protein into the alveolar space [3, 4]. Previous research has used animal models to study the pathophysiologic mechanism of ARDS. The *in vivo* intratracheal (IT) administration of lipopolysaccharide (LPS) has been widely accepted as a clinically relevant animal model of ALI/ARDS [5–7]. The molecular events observed after LPS-induced ALI are local recruitment and activation of PMN [1]; release of proinflammatory cytokines, such as tumor necrosis factor (TNF)-α, Interleukine (IL)-1β, and IL-6 [8]; the formation of reactive oxygen and nitrogen species [9, 10]. Upregulation of inducible nitric oxide synthase (iNOS) that increased nitric oxide (NO) production plays an important role in mediating lung inflammation, a fact that has been well established in both animal models and humans [11–14]. In addition, activated PMN contributes

to an increase in protease activity (such as myeloperoxidase (MPO) and lysozyme activity) and promotes the formation of various oxygen metabolites, finally leading to diffused alveolar matrix damage [2, 15].

High levels of proinflammatory cytokines such as TNF-α, IL-1β, and IL-6 are released, leading to an inflammatory cascade and triggering pulmonary coagulopathy at the same time [5, 16, 17]. These proinflammatory cytokines may activate the coagulation cascade by stimulating tissue factor (TF) expression and attenuating fibrinolysis by stimulating the release of plasminogen activators inhibitors (PAI). The final stage is fibrin deposition in the airspaces and lung microvasculature [16, 18–21]. Studies regarding pulmonary manifestations in patients suffering from ARDS have found enhanced expression of TF, factor VIIa (FVIIa), and TF-dependent factor X (FX) in bronchoalveolar lavage fluid (BALF) [22–25]. In a large multicenter study, higher levels of PAI-1 (the hallmark of impaired fibrinolysis) showed a synergistic association with ALI/ARDS, resulting in higher mortality rates among such patients [26]. Recently, researchers have become increasingly interested in the interplay between coagulation and inflammation in ALI/ARDS. Pulmonary coagulopathy is now accepted as a new target in the treatment of ALI/ARDS [16, 27].

Moutan cortex Radicis (MC), the root cortex of *Paeonia suffruticosa* Andrews, is widely used as an analgesic, antipyretic, and anti-inflammatory agent in traditional Chinese medicine (TCM) [28, 29]. According to ancient Chinese medicine, this herb is used to regulate human sickness such as eliminating heat, promoting blood flow, and removing blood stasis. Paeonol (20-hydroxy-40-methoxyacetophenone), a major phenolic component of MC, improves blood circulation through its inhibitory effects on both platelet aggregation and blood coagulation [30, 31]. Research also indicated that paeonol could inhibit the expression of cell-surface adhesion molecules [32], proinflammatory cytokines such as TNF-α and IL-1β [33, 34], and iNOS-mediated NO [35] and reactive oxygen species production [34, 35]. In addition, paeonol inhibits the generation of proinflammatory cytokine, and increases the production of IL-10 in carrageenan-evoked thermal hyperalgesia rats [36]. However, the effect of paeonol treatment on proinflammatory cytokines (TNF-α, IL-1β, and IL-6), iNOS-mediated NO, and illness severity had not been studied in the LPS-induced ALI rat model prior to our research. Furthermore, we wanted to investigate the effect of paeonol regarding anticoagulation and antifibrinolysis after LPS challenge. We studied the effects of paeonol using intraperitoneal (IP) injection in an experimental rat model of ALI (induced by IT instillation of LPS) *in vivo* and attempted to clarify the mechanism involved.

2. Materials and Methods

2.1. Preparation of Paeonol from MC. The source of paeonol isolated from the root bark of *Paeonia suffruticosa* and extracted with 95% ethanol (1 : 10, w/v) at 50 °C as described Hsieh et al. (2006) [34].

2.2. Establishment of LPS-Induced ALI Animal Model. This study used pathogen-free, adult male Sprague-Dawley (SD) rats, weighing around 250 to 300 g each. The rats were housed in standard iron cages with a twelve-hour light/dark cycle in the animal facility of Taichung Veterans General Hospital (TCVGH). The animal experiments were approved by the Animal Study Protocol Review Board of TCVGH and were conducted according to the principles stated in the "*Guide for the Care and Use of Laboratory Animals*."

The body weight and rectal temperature (RT) of the rats were checked before the LPS challenge was introduced (0 h). The rats were then lightly anesthetized with inhaled 2% isoflurane (Halocarbon Laboratories Div Halocarbon Products Crop, River Edge, NJ, USA) in 0.5 L/min O_2, 16 mg/kg LPS (Escherichia coli 055: B5; Sigma Chemical Co., St Louis, MO, USA), and 0.5 mL of phosphate buffer saline (PBS). This mixture was delivered into the lungs of the experimental rats by a Micro-Sprayer and Laryngoscope (Penn-Century, Philadelphia, PA, USA) as previously described [37, 38]. An equal volume of PBS alone was used for the control group. After IT instillation, the rat was placed in a vertical position and rotated for 30 s to let the instillation distribute evenly throughout the lungs. Sixteen hours after inoculation, the rats' RT was measured again, and they were then killed with CO_2 asphyxiation, as described in our pilot study.

2.3. Grouping. A total of 30 SD rats were randomized on a daily basis to a PBS control group or a treatment group. Treatment groups received paeonol resolved in DMSO. The effective dosage of paeonol resolved in DMSO was tested in the range of 10 mg/kg to 50 mg/kg, according to guidelines presented in previous literature [32, 34, 39–41]. The double dose of the effective dosage was also tested to investigate the dosage effectiveness. All agents were administered in IP bolus injections under light sedation with 2% isoflurane within 10 min after instillation of LPS. Control group rats (LPS-DMSO) received IP administered with the same volume of DMSO. In contrast, the control group (PBS-DMSO) was IT challenged with a PBS solution lacking LPS. At 16 h after inoculation, all rats were sacrificed with CO_2 asphyxiation, and their lungs were removed.

In summary, the rats were randomly divided into five groups comprising 6 rats each, as follows

(1) PBS-DMSO group: IT-challenged PBS and IP DMSO,

(2) PBS-paeonol group: IT PBS and IP paeonol 25 mg/kg,

(3) LPS-DMSO group: IT LPS and IP DMSO,

(4) LPS-paeonol-25 group: IT LPS and IP paeonol 25 mg/kg, and

(5) LPS-paeonol-50 group: IT LPS and IP paeonol 50 mg/kg.

2.4. Assessment of Histopathological Changes in LPS-Induced ALI Rats. The right lung of the rat was fixed with 10% paraformaldehyde by trachea infusion and embedded with paraffin. Hematoxylin and eosin (H&E) staining was conducted with 4 μm tissue slides. The lung injury was assessed

with the modified scoring system described by Kristof et al. [13]. In short, two pulmonologists, who were blind to the treatment, randomly selected 10 fields of lung sections from 3 lobes of right lung tissue per rat and read and scored the damaged levels according to the presence and extent of interstitial cellular infiltration, alveolar protein exudation, and tissue hemorrhage by using microscope at 200x magnification. Normal presentation in each category was scored as 0, and the most severe damaged in each category was scored as 3. If the alveolar space is full with inflammatory cells (such as neutrophils and macrophages), it is denoted as grade 3. Grade 1 reflects just a few inflammatory cell infiltrated. [Less than half of the alveoli are filled denotes as grade 2]. Similarly, the extent of pulmonary infiltration of protein exudation (reddish-stained) and alveolar hemorrhage in the lung is determined by this way. The sum of each category from 10 different microscopic fields is denoted as final damaged score in a rat. The total lung injury score of each rat was determined as the sum of three individual scores of alveolar cellularity, protein exudation, and tissue hemorrhage. If the interpretations of the two physicians are quite different, the slides will be checked by a pathologist.

2.5. Measurement of MPO Activity. The level of lung MPO, a marker of neutrophil infiltration [2, 15], was measured. Right lung tissue (1 gm) was homogenized in 1.5~4.0 N-ethylmaleimide (Sigma) for 30 s on ice, and the homogenate was centrifuged at 12,000 g for 30 min at 4°C. The pellet was re-suspended in 4 mL of potassium phosphate buffer (50 mM pH 6.0) with 0.5% hexadecyltrimethylammonium bromide (HTAB). The sample was sonicated for 30~90 s on ice once more. The sample was then incubated at 60°C for 2 h to deactivate tissue MPO inhibitor and then was centrifuged at 12,000 g for 10 min. The supernatant fluids containing MPO were incubated in a 50 mM potassium phosphate buffer (KH_2PO_4, pH 6.0) buffer containing the substrate H_2O_2 (1.5 M) and o-dianisidine dihydrochloride (167 mg/mL; Sigma-Aldrich, USA) for 30 min. The enzymatic activity was determined spectrophotometrically by measuring the change in absorbance at 460 nm by using a 96-well plate reader.

2.6. Western Blot for the Measurement iNOS. Frozen right lung samples were defrosted and were homogenized with lysis buffer (RIPA with protease inhibitor, with a ratio of lung tissue/lysis buffer equal to 100 mg/400 mL). The homogenate was sonicated and centrifuged at 12,000 ×g for 30 min at 4°C. The supernatant was collected, and its protein concentration was measured by conducting Bradford protein assay (Bio-Rad, Hercules, CA, USA). Aliquots (40 μg) of protein from each lung tissue supernatant were electrophoresed on a sodium dodecyl sulfate-polyacrylamide gel electrophoresis (SDS-PAGE) (7%) for 3 h at 100 V. The protein samples were transferred onto a nitrocellulose membrane (Amersham, USA). The membrane was then probed with polyclonal rabbit anti-mouse iNOS antibody (1 : 500 dilution, GTX213110-01, GeneTex, CA, USA) at 4°C overnight, with appropriate secondary antibodies. After three washes with TPBS, blots enhanced with brown color indicated the expression of iNOS.

2.7. Cell Counting and Measurement of Protein, Pro-Inflammatory Cytokines, and Thrombin-Anti-Thrombin Complexes (TATC), Plasminogen Activator Inhibitor (PAI-1) in BALF in LPS-Induced ALI Rats. The right main bronchus was ligated, and then a cannula was inserted into the left lung through the left main bronchus. The BALF was obtained with three aliquots of 8 mL sterile saline instilled up to a total volume of 24 mL, and withdrawn three times each, with final fluid recovery being around 20 mL. The BALF from each animal was recovered and was then passed through a mesh (200 μm) to remove the mucus, followed by centrifugation (1500 ×g, 4°C) for 15 min. The sediment cells were resuspended in 2 mL PBS. Erythrocytes were lysed using cold water and a hypertonic recovery solution (10x HBSS). The erythrocyte-free cell suspension was then washed once by 1x PBS and was used for total cell count. Finally, 2×10^5 BALF-derived cells were evenly distributed onto a slide by cytospin and then stained with Liu's stain for 2 min, before the neutrophils were counted under the microscope.

The resulting supernatants were stored at −70°C until the analysis stage. Cell counts and protein concentration were measured by Bradford protein assay (Bio-Rad, Hercules, CA, USA).

The proinflammatory cytokines in the BALF, such as TNF-α (BMS622MST, BenderMedsystem), IL-1β (BMS630, BenderMedsystem), IL-6 (BMS625MST, BenderMedsystem), and IL10 (14-8101-62, eBioscience), were measured using commercially available ELISA and in accordance with the manufacturer's protocol (Assay Designs, Inc. MI, USA). Specifically, this entailed pipetting the samples of BALF supernatant (100 μL) and the standards into the cytokine antibody precoated microplate wells. The plates were tapped gently to mix the contents and incubated at 37°C for 60 min. The contents of the wells were removed, and the wells were washed three times with 400 μL of wash solution. Human cytokine antibodies (100 μL) were added into each well and incubated at 37°C for 60 min. We emptied the contents of the wells and again applied 400 μL of wash solution to every well three times. Horseradish peroxidase (100 μL) was added to conjugate the human cytokine antibody. After incubation at 37°C for 30 min, 100 μL of Substrate Solution TMB (tetramethylbenzidine) was added into each well for 15 min at room temperature.

Color development was stopped by adding Stop Solution (100 μL, 1 N solution of hydrochloric acid in water). Colorimetric determination was read at absorbance of 450 nm (Microplate Reader BIO-RAD Laboratories, CA, USA). Serial dilution of each original recombination human cytokine was performed to draw a standard curve with linear range from 0 to 500 pg/mL. Concentrations of BALF cytokines were measured by comparing the absorbance of the standards, and expressed as picograms per milliliter (pg/mL).

TATC was used as a measured of coagulation through the tissue factor pathway; high TATC level reflects the

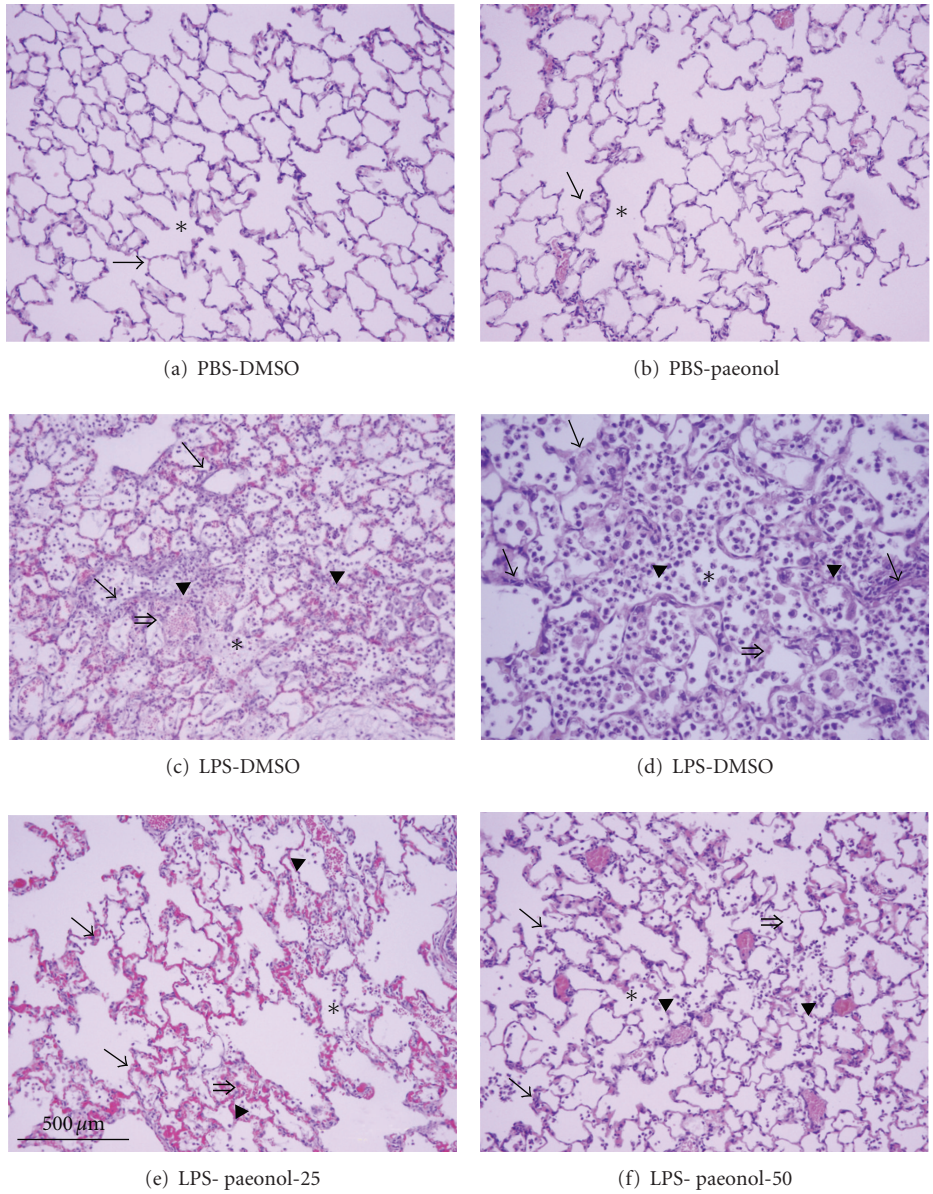

(a) PBS-DMSO (b) PBS-paeonol

(c) LPS-DMSO (d) LPS-DMSO

(e) LPS- paeonol-25 (f) LPS- paeonol-50

Figure 1: Effects of paeonol on LPS-induced histopathological damage in rats. Histopathological damage developed 16 h after intratracheal administration of LPS (16 mg/kg). The alveolar spaces (∗) are filled with a mixed mononuclear/neutrophilic infiltrate (►), red blood cells (⇒), and protein exudation. The alveolar walls (→) are thickened and edematous. Note the presence of cellular debris and proteinaceous material in the air spaces in the lung tissue of the LPS-DMSO group (c) with 200x; (d) with 400x. No prominent neutrophil infiltration, red blood cells or protein exudates were seen in the PBS-DMSO group (a) and PBS-paeonol group (b). The infiltration of neutrophil, red blood cells and protein exudation was reduced in the LPS-paeonol-25 group (e) and LPS-paeonol-50 group (f).

activation of the coagulation system [42, 43]. TATC was measured using the TATC enzyme-linked immunosorbent assay Micrognost kit, in accordance with the manufacturer's instructions (Assay Max human thrombin-antithrombin TAT complex ELISA kit, ET1020-1 Lot no. 1259916R1). The level of PAI-1 antigen in BALF was measured by Rat PAI-1 total antigen assay ELISA kit (Catalog no. RPAIKT-TOT, Molecular Innovations, MI, USA) according to the manufacturer's instructions.

2.8. Measurement of Lung Weight Gain (LWG) in LPS-Induced ALI Rats. The other 24 SD rats were divided into four groups of 6 rats as follows:

(1) PBS-DMSO group,

(2) PBS-Paeonol group,

(3) LPS-DMSO group, and

(4) LPS-Paeonol-50 group.

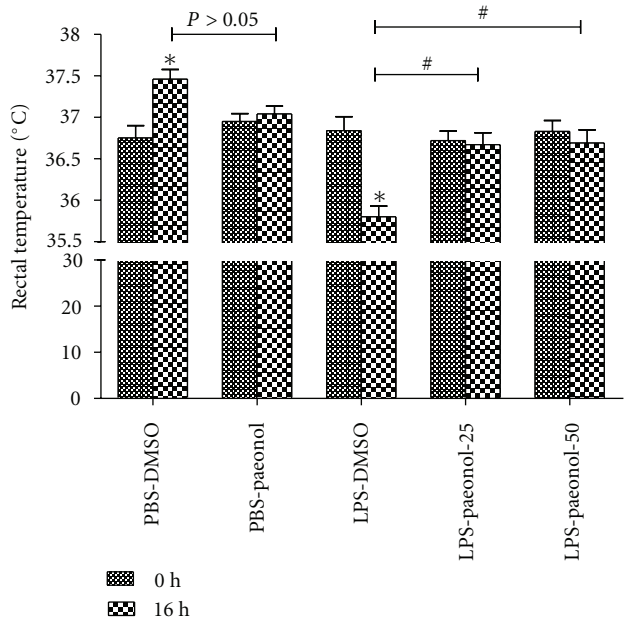

Compared PBS-paeonol with PBS-DMSO, $P > 0.05$
#Compared with LPS-DMSO at 16 h, $P < 0.05$
*Compared 16 h with 0 h in each group, $P < 0.05$

Figure 2: Effect of paeonol on rectal temperature (RT) changes after LPS-induced acute lung injury in rats. In the PBS-DMSO group, RT was greater at 16 h than at 0 h; in the LPS-DMSO group, RT was lower at 16 h than at 0 h. *$P < 0.05$ compared with 0 h. #$P < 0.05$ compared with 16 h.

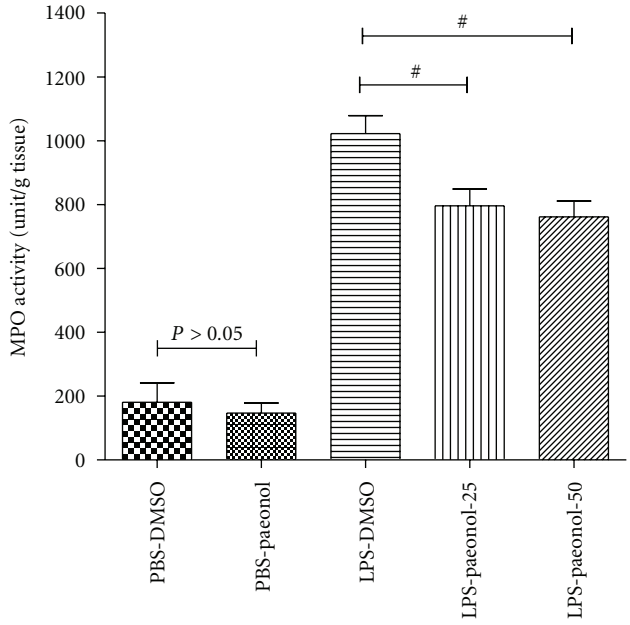

Figure 3: Effect of paeonol on myeloperoxidase (MPO) activity in LPS-induced acute lung injury in rats. The MPO activity was similar between PBS-DMSO and PBS-paeonol groups ($P > 0.05$), whereas the MPO activity was lower in the LPS-paeonol-25 and in the LPS-paeonol-50 groups than LPS-DMSO group. #$P < 0.05$ compared with LPS-DMSO.

The LPS-induced ALI animal model was the same as described above. At 16 h after inoculation, all rats were sacrificed with CO_2 asphyxiation. The total lung (including bilateral trachea) was separated from the chest cavity of the rat, and the body fluid coating the removed lung was wiped gently. The bilateral main bronchus was cut from the hilum area. The residual whole lung was placed on silver paper on an electronic scale, and the weight was recorded as whole lung weight (WLW). The whole lung on the silver paper was placed into an oven at 60°C for 48 h. Then the sample was taken out of the oven and weighed again on an electronic scale, with the weight being recorded as dry lung weight (DLW). The WLW minus the DLW indicated the net lung weight gain (LWG). LWG reflected the net lung edema status after manipulation [44].

2.9. Statistical Analysis. All data were expressed as mean ± SEM, using the data from at 6 rats except iNOS ($n = 4$). Statistical analysis of the data was conducted using Prism 3.02 software (GraphicPad Software Inc. CA, USA), via one-way ANOVA for multiple comparisons (post hoc Tukey test). Results with $P < 0.05$ were considered statistically significant.

3. Results

3.1. Effects of Paeonol on Histopathological Changes of Lung in LPS-Induced ALI Rats. In the PBS-DMSO and PBS-paeonol groups, the alveolar space was not prominent fluid, protein accumulation, and the infiltration of inflammatory cells and red blood cells (Figures 1(a) and 1(b)). In contrast, the alveolar spaced presented with fluid and protein accumulation, large amounts of inflammatory cells, and red blood cell infiltration at 16 h after LPS IT instillation (16 mg/kg) (Figures 1(c) and 1(d)). Paeonol treatment with 25 mg/kg or 50 mg/kg, administered after the LPS challenge, markedly attenuated inflammatory cell infiltration and alveolar wall thickening and diminished alveolar hemorrhage and edema (Figures 1(e) and 1(f)). A semiquantitative analysis of the histopathological scores of the rats' lungs is presented in Table 1.

3.2. Effects of Paeonol on RT in LPS-Induced ALI Rats. The RT in the LPS-DMSO group at 16 h after IT administration was lower than at baseline (0 h), with the difference being statistically significant ($P < 0.05$) (Figure 2). In contrast, for the PBS-paeonol and LPS-paeonol-50 groups, the RT at 16 h was similar to the baseline temperature (both $P > 0.05$) (Figure 2). The RT in the PBS-DMSO group at 16 h after IT administration was higher than at baseline ($P < 0.05$) (Figure 3).

3.3. Effect of Paeonol on MPO Activity and iNOS Expression. The MPO activity of lung tissue was greater in the LPS-DMSO, LPS-paeonol-25, and LPS-Paeonol-50 groups relative to the PBS-DMSO and PBS-paeonol groups, at 16 h after IT administration (all $P < 0.05$) (Figure 3). The MPO activity of lung tissue was lower in the LPS-paeonol-25 and

Table 1: Effect of paeonol on the histopathological scores in lipopolysaccharide-induced acute lung injury.

	Cellularity	Protein exudation	Hemorrhage	Scores
PBS-DMSO	7.2 ± 1.0	3.8 ± 0.6	8.1 ± 1.8	19.0 ± 2.5
PBS-paeonol	4.5 ± 0.2	2.7 ± 0.6	7.8 ± 0.7	14.9 ± 1.2
LPS-DMSO	18.0 ± 0.7	10.9 ± 0.8	16.4 ± 1.0	45.4 ± 1.0
LPS-paeonol-25	10.8 ± 0.9$^{\#}$	4.5 ± 0.8$^{\#}$	11.5 ± 1.5	26.8 ± 2.4$^{\#}$
LPS-paeonol-50	9.1 ± 1.2$^{\#}$	4.1 ± 0.4$^{\#}$	10.5 ± 1.5$^{\#}$	23.7 ± 2.9$^{\#}$

Data are presented as mean ± SEM; PBS-DMSO: PBS-DMSO group; PBS-paeonol: PBS-paeonol group; LPS-DMSO: LPS-DMSO group; LPS-paeonol-25: LPS-paeonol-25 mg/kg group; LPS-paeonol-50: LPS-paeonol-50 mg/kg group; $^{\#}P < 0.05$ compared with LPS-DMSO; $n = 6$.

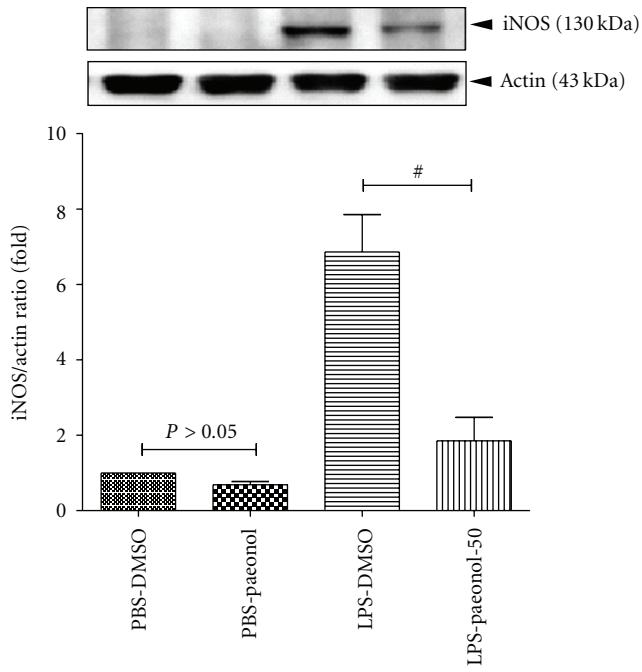

Figure 4: Effect of paeonol on inducible nitric oxide synthase (iNOS) activity in LPS-induced acute lung injury rats. The iNOS expression was similar between PBS-DMSO and PBS-paeonol groups ($P > 0.05$), whereas the iNOS expression was lower in the LPS-paeonol-50 groups than LPS-DMSO group. $^{\#}P < 0.05$ compared with LPS-DMSO.

LPS-paeonol-50 groups relative to the LPS-DMSO group, at 16 h after IT administration (both $P < 0.05$) (Figure 3).

The iNOS expression of lung tissue was greater in the LPS-DMSO group relative to the PBS-DMSO and PBS-paeonol groups, at 16 h (both $P < 0.05$) (Figure 4). The iNOS expression of lung tissue was lower in the LPS-paeonol-50 group than in the LPS-DMSO group at 16 h after IT administration ($P < 0.05$) (Figure 4).

3.4. Effects of Paeonol on Leukocyte Accumulation and Protein Exudation. The total leukocyte counts of BALF were greater in the LPS-DMSO group relative to the PBS-DMSO and PBS-paeonol groups, at 16 h after IT administration (both $P < 0.05$) (Figure 5(a)). The total leukocyte counts of BALF were lower in the PBS-paeonol-25 and PBS-paeonol-50 groups than in the LPS-DMSO group at 16 h (both $P < 0.05$) (Figure 5(a)).

The total PMN counts of BALF were greater in the LPS-DMSO group than in the PBS-DMSO and PBS-paeonol groups, at 16 h after IT administration (both $P < 0.05$) (Figure 5(b)). The total PMN counts of BALF were lower in the LPS-paeonol-25 and LPS-paeonol 50 groups than in the LPS-DMSO group at 16 h (both $P < 0.05$) (Figure 5(b)).

The protein concentration of BALF was greater in the LPS-DMSO group than in the PBS-DMSO and PBS-paeonol groups at 16 h after IT administration (both $P < 0.05$; Figure 5(c)). The protein concentration of BALF was lower in the LPS-paeonol-25 and in the LPS-paeonol-50 groups than these in the LPS-DMSO group at 16 h (both $P < 0.05$; Figure 5(c)).

3.5. Effect of Paeonol on the Expression of Pro-Inflammatory Cytokines of BALF. The TNF-α expression of BALF was greater in the LPS-DMSO group than in the PBS-DMSO and PBS-paeonol groups at 16 h after IT administration (both $P < 0.05$) (Figure 6(a)). The TNF-α expression of BALF was lower in the LPS-paeonol-50 group than in the LPS-DMSO group at 16 h ($P < 0.05$) (Figure 6(a)). However, TNF-α expression in the LPS-DMSO group was similar to that of the LPS-paeonol-25 group ($P > 0.05$) (Figure 6(a)).

The IL-1β expression of BALF was greater in the LPS-DMSO group than in the PBS DMSO and PBS-paeonol groups at 16 h (both $P < 0.05$) (Figure 6(b)). The IL-1β expression of BALF was lower in the LPS-paeonol-25 and the LPS-paeonol-50 groups than in the LPS-DMSO group at 16 h (both $P < 0.05$) (Figure 6(b)).

The IL-6 expression of BALF was greater in the LPS-DMSO group than in the PBS DMSO and PBS-paeonol groups at 16 h (both $P < 0.05$) (Figure 6(c)). The IL-6 expression of BALF was lower in the LPS-paeonol-25 and LPS-paeonol-50 groups than in the LPS-DMSO group at 16 h (both $P < 0.05$; Figure 6(c)).

The IL-10 expression of BALF was greater in the LPS-DMSO group than in the PBS DMSO and PBS-paeonol groups at 16 h (both $P < 0.05$) (Figure 6(c)). The IL-10 expression of BALF was lower in the LPS-paeonol-25 and LPS-paeonol-50 groups than in the LPS-DMSO group at 16 h (both $P < 0.05$; Figure 6(d)).

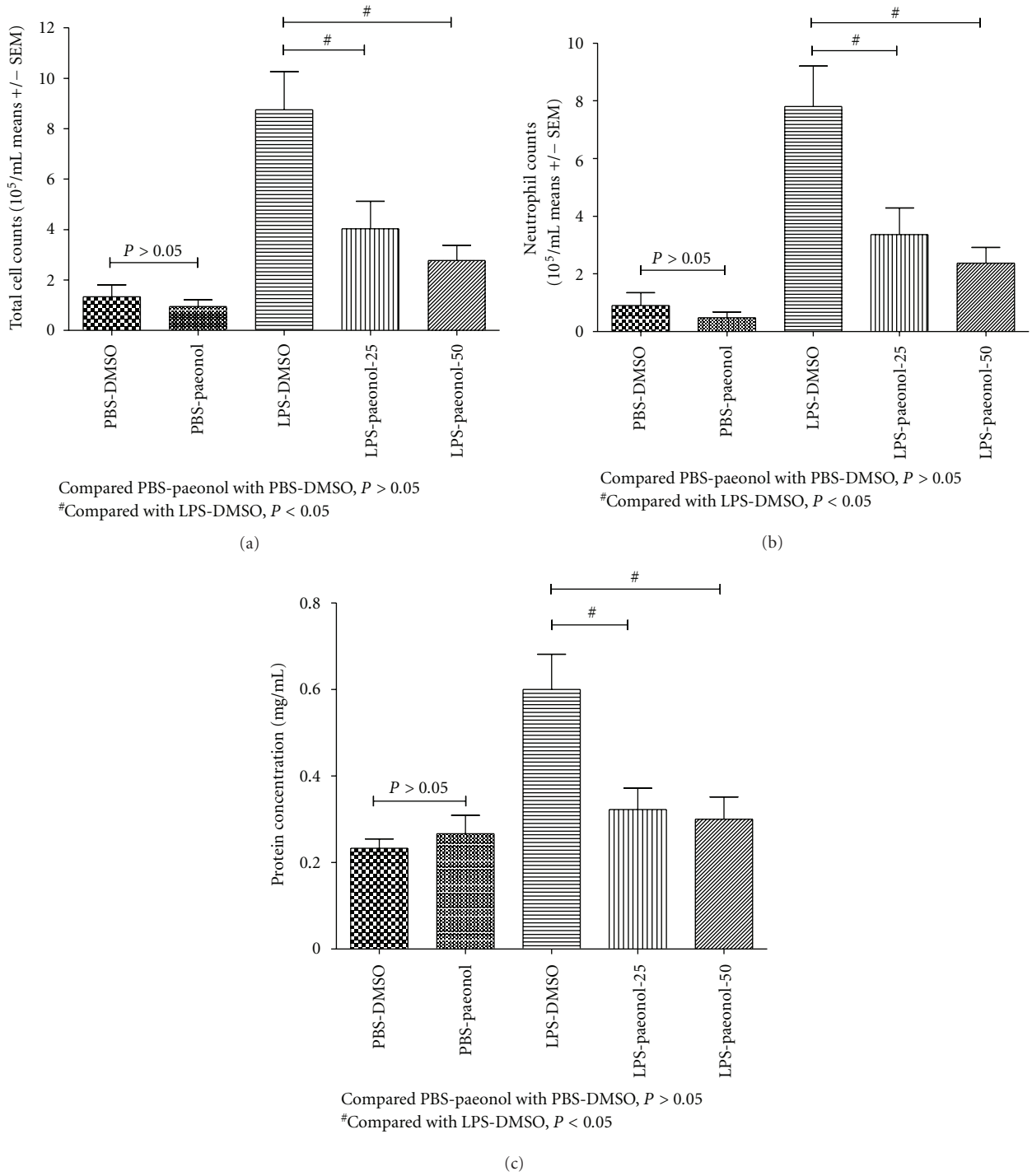

Figure 5: Effect of paeonol on leucocyte cell count and protein exudation of BALF in LPS-induced acute lung injury in rats. The total cell count (a), neutrophil count (b), and protein exudation (c) of BALF was similar between PBS-DMSO and PBS-paeonol groups (all $P > 0.05$), whereas the total cell count, neutrophil count, and protein exudation of BALF was lower in the LPS-paeonol-25 and in the LPS-paeonol-50 groups than LPS-DMSO group. $^{\#}P < 0.05$ compared with LPS-DMSO.

3.6. Effect of Paeonol on the TATC and PAI-1 Concentration of BALF in LPS-Induced ALI Rats. The TATC concentration of BALF in the LPS-DMSO group was similar to that of the PBS-DMSO and PBS-paeonol groups at 16 h after IT administration (both $P > 0.05$) (Figure 7(a)).

The TATC concentration of BALF in the LPS-DMSO group was also similar to that of the LPS-paeonol-25 and LPS-paeonol-50 groups at 16 h (both $P > 0.05$) (Figure 7(a)).

The PAI-1 concentration of BALF was greater in the LPS-DMSO group than in the PBS-DMSO and PBS-paeonol

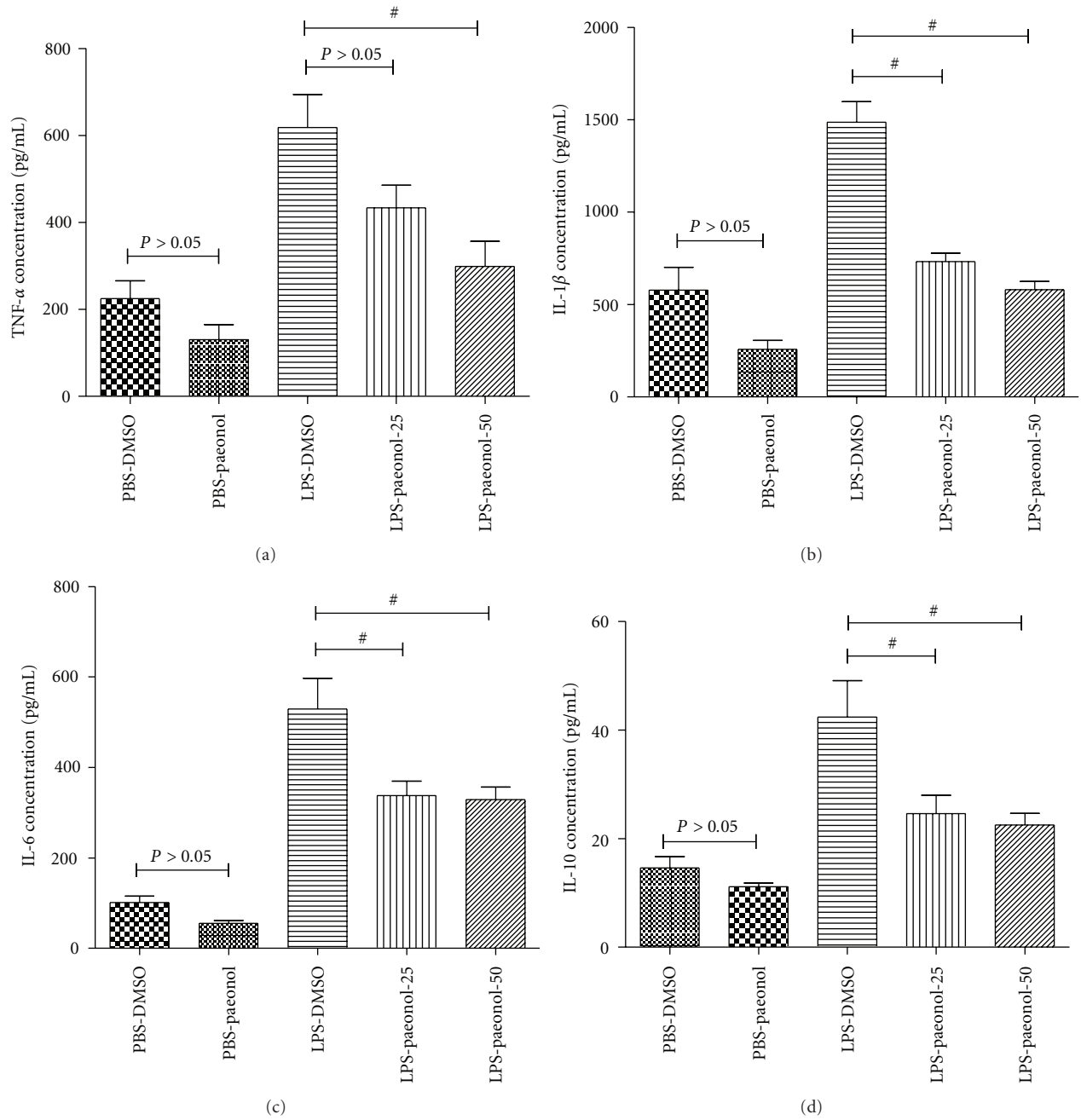

Figure 6: Effect of paeonol on tumor necrosis factor-α (TNF-α), interleukin-1β (IL-1β), IL-6, and IL-10 concentrations of BALF in LPS-induced acute lung injury in rats. The concentrations of TNF-α (a), IL-1β (b), IL-6 (c), and IL-10 of BALF were similar between PBS-DMSO and PBS-paeonol group (all $P > 0.05$), whereas the concentrations of TNF-α, IL-1β, IL-6, and IL-10 of BALF were lower in the LPS-paeonol-25 and in the LPS-paeonol-50 groups than LPS-DMSO group. $^{\#}P < 0.05$ compared with LPS-DMSO.

groups at 16 h (both $P < 0.05$) (Figure 7(b)). The PAI-1 concentration of BALF was lower in the LPS-paeonol-25 and LPS-paeonol-50 groups than in the LPS-DMSO groups at 16 h (both $P < 0.05$) (Figure 7(b)).

3.7. Effects of Paeonol on LWG in LPS-Induced ALI Rats. Lung weight gain was greater in the LPS-DMSO and LPS-paeonol-50 groups compared to the PBS-DMSO group (both $P < 0.05$) at 16 h after LPS IT administration (Figure 8). The LWG in the PBS-paeonol and LPS-paeonol-50 groups was lower than that of the LPS-DMSO group (both $P < 0.05$) (Figure 8).

4. Discussion

Our results indicated that paeonol attenuated histopathological damage scores in the LPS-induced ALI rat model. Paeonol reduced the activity of MPO and the expression

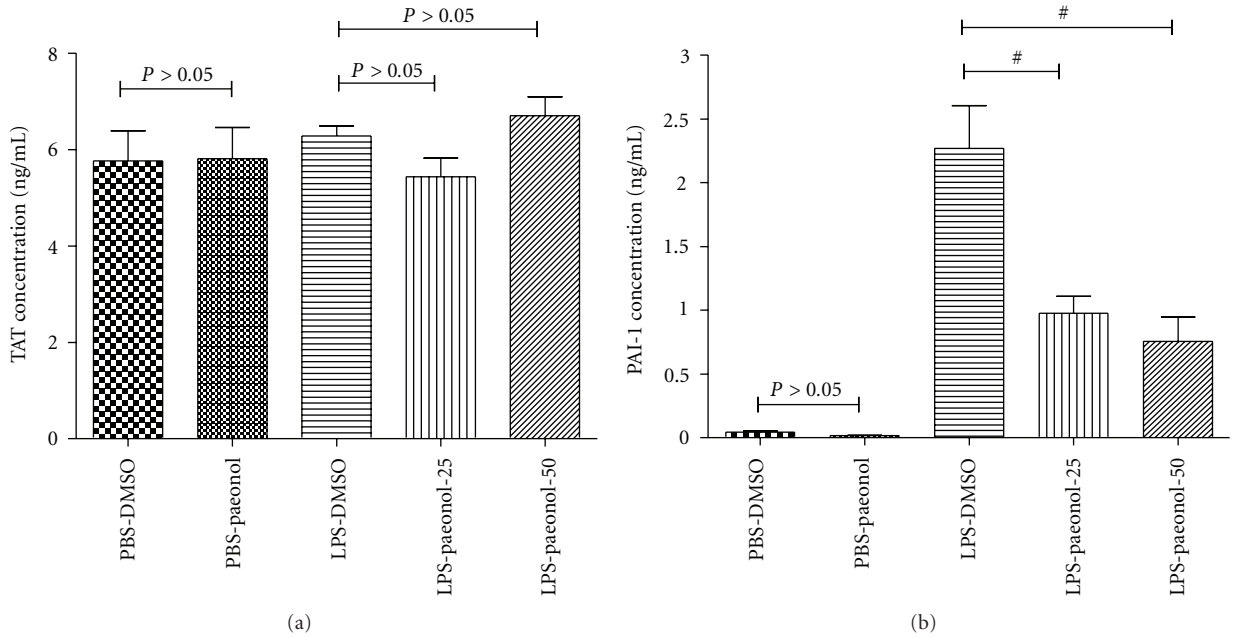

Figure 7: Effect of paeonol on thrombin-anti-thrombin complexes (TATC) and plasminogen activator inhibitor (PAI-1) of BALF in LPS-induced acute lung injury in rats. The concentrations of TATC in BALF were similar between PBS-DMSO and PBS-paeonol groups ($P > 0.05$), between LPS-DMSO and LPS-paeonol-25 groups ($P > 0.05$), and between LPS-DMSO and LPS-paeonol-50 groups ($P > 0.05$) (a); The PAI-1 was similar between PBS-DMSO and PBS-paeonol groups ($P > 0.05$), whereas the PAI-1 was lower in the LPS-paeonol-25 and in the LPS-paeonol-50 groups than LPS-DMSO group. $^{\#}P < 0.05$ compared with LPS-DMSO.

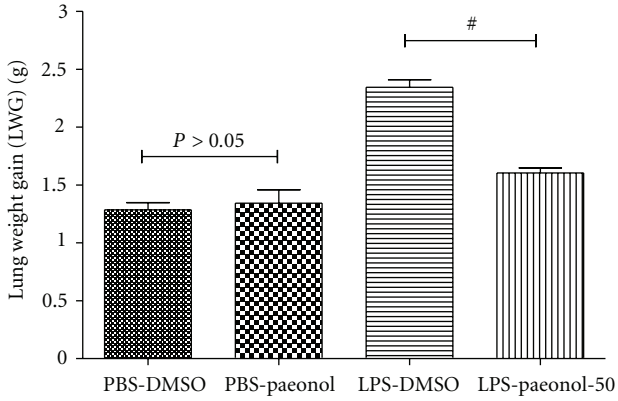

Figure 8: Effect of paeonol on lung weight gain (LWG) in LPS-induced acute lung injury in rats. The LWG was similar between PBS-DMSO and PBS-paeonol groups ($P > 0.05$), whereas the LWG was lower in the LPS-paeonol-50 groups than LPS-DMSO group. $^{\#}P < 0.05$ compared with LPS-DMSO.

of iNOS, and the concentration of PAI-1 in lung tissue, and also reduced LWG. In addition, *Paeonol* reduced TNF-α, IL-1β, IL-6, and PAI-1 concentrations in the BALF. Therefore, we suggest that paeonol protects the lung in LPS-induced ALI rats, and that the effect occurs through the anti-inflammation and anti-coagulation properties of paeonol. MPO activity is a marker of PMN neutrophil [2, 15], whereas iNOS increases NO production and mediates lung inflammation [11–14]. The proinflammatory cytokines TNF-α, IL-1β, and IL-6 mediate the inflammatory cascade [8, 9, 12, 45]. PAI-1 may represent an activation of fibrinolysis [18, 21, 46]. In addition, we used paeonol 25 mg/kg and 50 mg/kg in the present study, if paeonol 100 mg/kg such as Du et al. (2010) [47] whether or not produce greater anti-inflammatory and anti-coagulative effects need further study.

Our results remain one question unanswered that is the levels of IL-10, is an anti-inflammatory cytokine, were lower in the LPS-paeonol-25 and LPS-paeonol-50 groups than these in the LPS-DMSO group were seemly contrast to the results of Chou (2003) [36]. One possible explanation was that the levels of IL-10 reached a peak at 16–24 h [48], whereas the IL-10 was measured at 16 h after LPS administration, therefore, the maximal levels could not obtain in the present study. This explanation needs further study.

Several animal models have been developed to mimic the pathophysiology of ALI-following LPS exposure [5–7]. In the present study, we have produced a constant and reproducible rat model to investigate the treatment effects of paeonol in ALI by delivering LPS directly into airway in our laboratory [37, 38]. The pulmonary histopathological changes of LPS-induced ALI are characterized by PMN accumulation, disruption of epithelial integrity, interstitial edema, and leakage of a large amount of protein into the alveolar spaces [1–4]. The results of the present study indicated that paeonol treatment may reduce the drop in RT, which typically follows LPS challenge. Hypothermia may be

an early phenomenon of sepsis; thus, paeonol might play a critical role in preventing sepsis. In contrast, LWG may indicate the degree of lung edema, which Paeonol may also help reduce in the LPS-induced ALI model.

It has been well documented in both animal models and humans that LPS stimulates iNOS expression and NO overproduction, which damages lung tissue via peroxynitrite formation [12, 14, 46, 49, 50]. One recent report showed that paeonol inhibits LPS-induced iNOS expression through deactivating the mitogen-activated protein kinase (MAPK) in RAW 264.7 macrophage-like cells [35]. However, the effect of paeonol in the ALI rat model remains unclear. In this study, we demonstrated that paeonol significantly attenuates iNOS expression after a rat has been exposed to LPS challenge, suggesting that one anti-inflammatory mechanism of paeonol protects the lung from damage.

High levels of proinflammatory cytokines such as TNF-α, IL-1β, and IL-6 play a central role in the initiation and propagation of the inflammatory cascade [8, 9, 12, 45]. A large amount of PMN is recruited from peripheral blood into the lung, producing large amounts of MPO and reactive oxygen derivatives. The result is a cascade-like response, and tissue damage [2, 15, 49, 51]. In line with these theories, we found that after instilling LPS by IT, large amounts of proinflammatory cytokines were expressed in the BALF in rat lung parenchyma, with enhanced activity of MPO. Paeonol IP injections significantly suppressed the expression of TNF-α, IL-1β, and IL-6 in rat BALF; this also reduced LPS-induced pulmonary parenchymal MPO activity. As expected the number of PMNs in BALF had decreased 16 h after treatment, suggesting a mechanism by which paeonol attenuates the LPS-induced ALI model.

The hallmark of ALI is the deposition of fibrin and platelet plugs, which induce the occlusion of microvasculature of the alveolar space [3, 52]. As excessive fibrin is deposited within the airways, neutrophils and fibroblasts may further be activated. This situation compromises gas exchange and pulmonary endothelial integrity, decreases alveolar fluid clearance, and finally leads to pulmonary microcirculation damage and death [16, 52, 53].

Pulmonary coagulopathy is now accepted as a target in therapeutic studies of acute lung injury or pneumonia [16–18, 21, 27]. The available data suggest that high levels of proinflammatory cytokines (such as TNF, IL-1, and IL-6) may activate the coagulation cascade by stimulating TF expression. High levels of these cytokines may also attenuate fibrinolysis by stimulating the release of PAI [16, 18–21]. Our data showed no significant difference in TATC level of BALF after paeonol treatment. However, the PAI-1 levels in BALF were significantly decreased in the paeonol treatment group, suggesting a strong anti-fibrinolytic effect of paeonol in ALI-induced coagulopathy. Since proinflammatory cytokines serve as potent regulators of macrophage PAI-1 production in ALI, it remains unclear whether the anti-fibrinolysis effect of paeonol occur via inhibiting PAI-1 expression directly, or is perhaps the consequence of anti-proinflammatory cytokines. Further experiments are needed to clarify the target effects on cells, and the causal relationship between anti-inflammation and anti-coagulation effects of paeonol.

In conclusion, the results of the current study demonstrated that paeonol protects against lung tissue damage in the LPS-induced ALI model. This finding suggests that these effects are because of the anti-inflammatory and anti-coagulant properties of paeonol. Thus paeonol may be a potential therapeutic reagent for treating ALI in the future.

Acknowledgment

This study was supported in part by the Taiwan Department of Health Clinical Trial and Research Center of Excellence (DOH101-TD-B-111-004).

References

[1] M. Chignard and V. Balloy, "Neutrophil recruitment and increased permeability during acute lung injury induced by lipopolysaccharide," *American Journal of Physiology—Lung Cellular and Molecular Physiology*, vol. 279, no. 6, pp. L1083–L1090, 2000.

[2] E. Abraham, "Neutrophils and acute lung injury," *Critical Care Medicine*, vol. 31, no. 4, pp. S195–S199, 2003.

[3] L. B. Ware and M. A. Matthay, "The acute respiratory distress syndrome," *The New England Journal of Medicine*, vol. 342, no. 18, pp. 1334–1349, 2000.

[4] D. Dreyfuss and J. D. Ricard, "Acute lung injury and bacterial infection," *Clinics in Chest Medicine*, vol. 26, no. 1, pp. 105–112, 2005.

[5] G. Matute-Bello, C. W. Frevert, and T. R. Martin, "Animal models of acute lung injury," *American Journal of Physiology—Lung Cellular and Molecular Physiology*, vol. 295, no. 3, pp. L379–L399, 2008.

[6] H. M. Wang, M. Bodenstein, and K. Markstaller, "Overview of the pathology of three widely used animal models of acute lung injury," *European Surgical Research*, vol. 40, no. 4, pp. 305–316, 2008.

[7] H. P. M. Van Helden, W. C. Kuijpers, D. Steenvoorden et al., "Intratracheal aerosolization of endotoxin (LPS) in the rat: a comprehensive animal model to study adult (acute) respiratory distress syndrome," *Experimental Lung Research*, vol. 23, no. 4, pp. 297–316, 1997.

[8] T. Shinbori, H. Walczak, and P. H. Krammer, "Activated T killer cells induce apoptosis in lung epithelial cells and the release of pro-inflammatory cytokine TNF-α," *European Journal of Immunology*, vol. 34, no. 6, pp. 1762–1770, 2004.

[9] E. A. Williams, G. J. Quinlan, P. B. Anning, P. Goldstraw, and T. W. Evans, "Lung injury following pulmonary resection in the isolated, blood- perfused rat lung," *European Respiratory Journal*, vol. 14, no. 4, pp. 745–750, 1999.

[10] M. A. Matthay, T. Geiser, S. Matalon, and H. Ischiropoulos, "Oxidant-mediated lung injury in the acute respiratory distress syndrome," *Critical Care Medicine*, vol. 27, no. 9, pp. 2028–2030, 1999.

[11] P. Enkhbaatar, K. Murakami, K. Shimoda et al., "The inducible nitric oxide synthase inhibitor BBS-2 prevents acute lung injury in sheep after burn and smoke inhalation injury," *American Journal of Respiratory and Critical Care Medicine*, vol. 167, no. 7, pp. 1021–1026, 2003.

[12] A. Kobayashi, S. Hashimoto, K. Kooguchi et al., "Expression of inducible nitric oxide synthase and inflammatory cytokines in alveolar macrophages of ARDS following sepsis," *Chest*, vol. 113, no. 6, pp. 1632–1639, 1998.

[13] A. S. Kristof, P. Goldberg, V. Laubach, and S. N. A. Hussain, "Role of inducible nitric oxide synthase in endotoxin-induced acute lung injury," *American Journal of Respiratory and Critical Care Medicine*, vol. 158, no. 6, pp. 1883–1889, 1998.

[14] H. M. Razavi, R. Werhun, J. A. Scott et al., "Effects of inhaled nitric oxide in a mouse model of sepsis-induced acute lung injury," *Critical Care Medicine*, vol. 30, no. 4, pp. 868–873, 2002.

[15] R. L. Zemans, S. P. Colgan, and G. P. Downey, "Transepithelial migration of neutrophils: mechanisms and implications for acute lung injury," *American Journal of Respiratory Cell and Molecular Biology*, vol. 40, no. 5, pp. 519–535, 2009.

[16] M. J. Schultz, J. J. Haitsma, H. Zhang, and A. S. Slutsky, "Pulmonary coagulopathy as a new target in therapeutic studies of acute lung injury or pneumonia—a review," *Critical Care Medicine*, vol. 34, no. 3, pp. 871–877, 2006.

[17] M. Levi and H. Ten Cate, "Disseminated intravascular coagulation," *The New England Journal of Medicine*, vol. 341, no. 8, pp. 586–592, 1999.

[18] E. Abraham, "Coagulation abnormalities in acute lung injury and sepsis," *American Journal of Respiratory Cell and Molecular Biology*, vol. 22, no. 4, pp. 401–404, 2000.

[19] J. A. Bastarache, L. B. Ware, and G. R. Bernard, "The role of the coagulation cascade in the continuum of sepsis and acute lung injury and acute respiratory distress syndrome," *Seminars in Respiratory and Critical Care Medicine*, vol. 27, no. 4, pp. 365–376, 2006.

[20] L. B. Ware, J. A. Bastarache, and L. Wang, "Coagulation and fibrinolysis in human acute lung injury—new therapeutic targets?" *The Keio Journal of Medicine*, vol. 54, no. 3, pp. 142–149, 2005.

[21] M. Wygrecka, E. Jablonska, A. Guenther, K. T. Preissner, and P. Markart, "Current view on alveolar coagulation and fibrinolysis in acute inflammatory and chronic interstitial lung diseases," *Thrombosis and Haemostasis*, vol. 99, no. 3, pp. 494–501, 2008.

[22] A. W. Rijneveld, S. Weijer, P. Bresser et al., "Local activation of the tissue factor-factor VIIa pathway in patients with pneumonia and the effect of inhibition of this pathway in murine pneumococcal pneumonia," *Critical Care Medicine*, vol. 34, no. 6, pp. 1725–1730, 2006.

[23] M. J. Schultz, J. Millo, M. Levi et al., "Local activation of coagulation and inhibition of fibrinolysis in the lung during ventilator associated pneumonia," *Thorax*, vol. 59, no. 2, pp. 130–135, 2004.

[24] T. Fuchs-Buder, P. De Moerloose, B. Ricou et al., "Time course of procoagulant activity and D dimer in bronchoalveolar fluid of patients at risk for or with acute respiratory distress syndrome," *American Journal of Respiratory and Critical Care Medicine*, vol. 153, no. 1, pp. 163–167, 1996.

[25] S. Idell, K. B. Koenig, D. S. Fair, T. R. Martin, J. McLarty, and R. J. Maunder, "Serial abnormalities of fibrin turnover in evolving adult respiratory distress syndrome," *American Journal of Physiology—Lung Cellular and Molecular Physiology*, vol. 261, no. 4, part 1, pp. L240–L248, 1991.

[26] L. B. Ware, M. A. Matthay, P. E. Parsons et al., "Pathogenetic and prognostic significance of altered coagulation and fibrinolysis in acute lung injury/acute respiratory distress syndrome," *Critical Care Medicine*, vol. 35, no. 8, pp. 1821–1828, 2007.

[27] L. B. Ware, E. Camerer, K. Welty-Wolf, M. J. Schultz, and M. A. Matthay, "Bench to bedside: targeting coagulation and fibrinolysis in acute lung injury," *American Journal of Physiology—Lung Cellular and Molecular Physiology*, vol. 291, no. 3, pp. L307–L311, 2006.

[28] H. C. Lin, H. Y. Ding, F. N. Ko, C. M. Teng, and Y. C. Wu, "Aggregation inhibitory activity of minor acetophenones from Paeonia species," *Planta Medica*, vol. 65, no. 7, pp. 595–599, 1999.

[29] S. Tatsumi, T. Mabuchi, T. Abe, L. Xu, T. Minami, and S. Ito, "Analgesic effect of extracts of Chinese medicinal herbs Moutan cortex and Coicis semen on neuropathic pain in mice," *Neuroscience Letters*, vol. 370, no. 2-3, pp. 130–134, 2004.

[30] Y. K. Koo, J. M. Kim, J. Y. Koo et al., "Platelet anti-aggregatory and blood anti-coagulant effects of compounds isolated from Paeonia lactiflora and Paeonia suffruticosa," *Pharmazie*, vol. 65, no. 8, pp. 624–628, 2010.

[31] A. Hirai, T. Terano, and T. Hamazaki, "Studies on the mechanism of antiaggregatory effect of Moutan Cortex," *Thrombosis Research*, vol. 31, no. 1, pp. 29–40, 1983.

[32] I. T. Nizamutdinova, H. M. Oh, Y. N. Min et al., "Paeonol suppresses intercellular adhesion molecule-1 expression in tumor necrosis factor-α-stimulated human umbilical vein endothelial cells by blocking p38, ERK and nuclear factor-κB signaling pathways," *International Immunopharmacology*, vol. 7, no. 3, pp. 343–350, 2007.

[33] L. L. Pan and M. Dai, "Paeonol from Paeonia suffruticosa prevents TNF-α-induced monocytic cell adhesion to rat aortic endothelial cells by suppression of VCAM-1 expression," *Phytomedicine*, vol. 16, no. 11, pp. 1027–1032, 2009.

[34] C. L. Hsieh, C. Y. Cheng, T. H. Tsai et al., "Paeonol reduced cerebral infarction involving the superoxide anion and microglia activation in ischemia-reperfusion injured rats," *Journal of Ethnopharmacology*, vol. 106, no. 2, pp. 208–215, 2006.

[35] H. S. Chae, O. H. Kang, Y. S. Lee et al., "Inhibition of LPS-induced iNOS, COX-2 and inflammatory mediator expression by paeonol through the MAPKs inactivation in RAW 264.7 cells," *American Journal of Chinese Medicine*, vol. 37, no. 1, pp. 181–194, 2009.

[36] T. C. Chou, "Anti-inflammatory and analgesic effects of paeonol in carrageenan-evoked thermal hyperalgesia," *British Journal of Pharmacology*, vol. 139, no. 6, pp. 1146–1152, 2003.

[37] C. L. Wu, L. Y. Lin, H. M. Yeh, M. C. Chan, C. H. Yang, and C. M. Hsueh, "Delay of LPS-induced acute lung injury resolution by soluble immune complexes is neutrophil dependent," *Shock*, vol. 32, no. 3, pp. 276–285, 2009.

[38] C. L. Wu, L. Y. Lin, J. S. Yang, M. C. Chan, and C. M. Hsueh, "Attenuation of lipopolysaccharide-induced acute lung injury by treatment with IL-10," *Respirology*, vol. 14, no. 4, pp. 511–521, 2009.

[39] H. Li, M. Dai, and W. Jia, "Paeonol attenuates high-fat-diet-induced atherosclerosis in rabbits by anti-inflammatory activity," *Planta Medica*, vol. 75, no. 1, pp. 7–11, 2009.

[40] K. Ishiguro, T. Ando, O. Maeda et al., "Paeonol attenuates TNBS-induced colitis by inhibiting NF-κB and STAT1 transactivation," *Toxicology and Applied Pharmacology*, vol. 217, no. 1, pp. 35–42, 2006.

[41] S. H. Kim, S. A. Kim, M. K. Park et al., "Paeonol inhibits anaphylactic reaction by regulating histamine and TNF-α," *International Immunopharmacology*, vol. 4, no. 2, pp. 279–287, 2004.

[42] S. Weijer, S. H. H. F. Schoenmakers, S. Florcpin et al., "Inhibition of the tissue factor/factor VIIa pathway does not influence the inflammatory or antibacterial response to

abdominal sepsis induced by Escherichia coli in mice," *Journal of Infectious Diseases*, vol. 189, no. 12, pp. 2308–2317, 2004.

[43] S. H. Slofstra, A. P. Groot, N. A. Maris, P. H. Reitsma, H. Ten Cate, and C. A. Spek, "Inhalation of activated protein C inhibits endotoxin-induced pulmonary inflammation in mice independent of neutrophil recruitment," *British Journal of Pharmacology*, vol. 149, no. 6, pp. 740–746, 2006.

[44] C. H. Chu, D. David Liu, Y. H. Hsu, K. C. Lee, and H. I. Chen, "Propofol exerts protective effects on the acute lung injury induced by endotoxin in rats," *Pulmonary Pharmacology and Therapeutics*, vol. 20, no. 5, pp. 503–512, 2007.

[45] R. M. Strieter and S. L. Kunkel, "Acute lung injury: the role of cytokines in the elicitation of neutrophils," *Journal of Investigative Medicine*, vol. 42, no. 4, pp. 640–651, 1994.

[46] C. F. Su, F. L. Yang, and H. I. Chen, "Inhibition of inducible nitric oxide synthase attenuates acute endotoxin-induced lung injury in rats," *Clinical and Experimental Pharmacology and Physiology*, vol. 34, no. 4, pp. 339–346, 2007.

[47] Q. Du, G. Z. Feng, L. Shen, J. Cui, and J. K. Cai, "Paeonol attenuates airway inflammation and hyperresponsiveness in a murine model of ovalbumin-induced asthma," *Canadian Journal of Physiology and Pharmacology*, vol. 88, no. 10, pp. 1010–1016, 2010.

[48] C. L. Wu, L. Y. Lin, J. S. Yang, M. C. Chan, and C. M. Hsueh, "Attenuation of lipopolysaccharide-induced acute lung injury by treatment with IL-10," *Respirology*, vol. 14, no. 4, pp. 511–521, 2009.

[49] H. M. Razavi, F. W. Le, S. Weicker et al., "Pulmonary neutrophil infiltration in murine sepsis: role of inducible nitric oxide synthase," *American Journal of Respiratory and Critical Care Medicine*, vol. 170, no. 3, pp. 227–233, 2004.

[50] D. Wang, J. Wei, K. Hsu et al., "Effects of nitric oxide synthase inhibitors on systemic hypotension, cytokines and inducible nitric oxide synthase expression and lung injury following endotoxin administration in rats," *Journal of Biomedical Science*, vol. 6, no. 1, pp. 28–35, 1999.

[51] E. Abraham, A. Carmody, R. Shenkar, and J. Arcaroli, "Neutrophils as early immunologic effectors in hemorrhage- or endotoxemia-induced acute lung injury," *American Journal of Physiology—Lung Cellular and Molecular Physiology*, vol. 279, no. 6, pp. L1137–L1145, 2000.

[52] A. Günther, P. Mosavi, S. Heinemann et al., "Alveolar fibrin formation caused by enhanced procoagulant and depressed fibrinolytic capacities in severe pneumonia: comparison with the acute respiratory distress syndrome," *American Journal of Respiratory and Critical Care Medicine*, vol. 161, no. 2 I, pp. 454–462, 2000.

[53] A. Sapru, J. L. Wiemels, J. S. Witte, L. B. Ware, and M. A. Matthay, "Acute lung injury and the coagulation pathway: potential role of gene polymorphisms in the protein C and fibrinolytic pathways," *Intensive Care Medicine*, vol. 32, no. 9, pp. 1293–1303, 2006.